STRAIN-DEPENDENT VARIATION IN DEVELOPMENTAL TGFβ1 KNOCKOUT PHENOTYPES.

Sarah Anne Buchanan Rusholme,
Department of Medical Genetics,
University of Glasgow.

A thesis submitted for the degree of PhD to the University of Glasgow, February 1997.

ProQuest LLC.
789 East Eisenhower Parkway
P.O. Box 1346
Ann Arbor, MI 48106 – 1346

ABSTRACT.

The transforming growth factors Beta (TGFβ) comprise three closely-related polypeptides with non-overlapping functions *in vivo*. On a mixed genetic background, a proportion of mice homozygous null and heterozygous for a targeted disruption in their TGFβ1 gene die pre-natally with defects in yolk sac haematopoiesis and vasculogenesis (Dickson *et al.*, 1995). In this project, the variable penetrance of lethality in TGFβ1 knockouts was investigated. The TGFβ1 null allele was bred to 93.75% purity in different inbred strains of mice, and the gross morphology and histology of TGFβ1+/- intercross litters from these backgrounds was examined at different pre- and post-natal stages. Molecular aspects of the abnormal mid-gestation phenotype were analysed.

The lethal phenotype of the TGFβ1 knockout was clearly strain-dependent - and the variable expressivity and penetrance of the observed phenotypes in TGFβ1+/- and TGFβ1-/- conceptuses suggested three critical stages when TGFβ1 is essential: a) pre-organogenesis; b) in the establishment of a stable extra-embryonic vasculature and during haemoglobinisation of primitive erythroid precursors; c) post-natally as an immunomodulator. This study shows that a combination of genetic and environmental factors interact to produce the TGFβ1 knockout phenotypes.

DECLARATION.

I certify that this thesis does not contain material previously published or written by any other person, except where referred to in the text, and that the results in this thesis have not been submitted for any other degree or diploma.

Sarah A. B. Rusholme.

ACKNOWLEDGEMENTS.

I am indebted to Dr. Rosemary Akhurst for her guidance, patience and wisdom whilst supervising this project, and to Drs. Marion Dickson and Alison Trainer, without whom this work would not have been completed.

Dennis Duggan and Francis Cousins made this project possible with their good humour and 'expert technical assistance' above and beyond the call of duty; and I could not have got achieved anything without the expertise of Betty, Liz, Anne, Hazel, Alison C. and the long suffering staff of Yorkhill Pathology and Veterinary Haematology.

I would like to thank everyone else in the Duncan Guthrie Institute, mainly my colleagues in Dev. Gen and PGR; namely Patricia, Eunice, Reza, Guity, Li-Ming and Jane. Iam grateful to Sarah J. for her good humour, good advice and spotting my split infinitives; Pete, for missing his vocation with BSM and making me look industrious; Julie for the hangovers; Alison C. and Mort. for the primers, the taq, the dNTPs, the ladder etc. etc. etc; Francis for being the designated driver; Dennis for being the designated drinker; Shaban for the running commentaries; Hazel for the walks; Alison T. for her strongly-held views on haircare; Betty and Travis for keeping my feet warm; and Adam, Al, Blaithin, Gran, Gerry, Lee and Rae for the cigarettes and coffee.

Finally; I need to thank my family for their unquestioning support and belief and, most importantly, my beloved husband Stephen, without whom I would be lost.

SUMMARY.

The transforming growth factors type Beta (TGFβ) are proteins with widespread and well-documented expression patterns *in vivo*. There are three isoforms of TGFβ found in vertebrates; TGFβs 1, 2 and 3. *in vitro*, the TGFβs have been reported to be both growth inhibitory and stimulatory, depending on the target cell type. All three isoforms are expressed in the developing embryo, and are thought to play important roles during embryogenesis.

Two groups have generated transgenic mice with a targeted disruption of the TGFβ1 gene (Shull *et al.*, 1992 & Kulkarni *et al.*, 1993). The cause of death of the homozygous TGFβ1 null animals was characterised by Dickson *et al.* (1995), working on a mixed genetic background (50% NIH/ Ola, 37.5% C57BL/ 6J/ Ola, 12.5% 129/ Sv): Dr. Dickson found that 50% of TGFβ1-/- and 25% of TGFβ1+/- embryos died *in utero* due to defective extra-embryonic haematopoiesis and vasculogenesis. This is in concordance with previous reports that in the murine embryo, TGFβ1 RNA expression is first detected in the haemangioblasts of the yolk sac at approximately 7.0dpc (Akhurst *et al.*, 1990). The haemangioblasts are located in the blood islands and give rise to vascular endothelial and primitive haematopoietic cells. TGFβ1 expression persists in the descendant cells of these lineages (Akhurst *et al.*, 1990). All TGFβ1-/- animals which survived to birth died at around three weeks of age due to a wasting syndrome involving a multifocal, mixed inflammatory cell response and tissue necrosis.

This project was undertaken in order to characterise any strain-specific differences in the onset and manifestation of the abnormal TGFβ1 knockout phenotype. The TGFβ1 null allele was bred to 93.75% purity on inbred NIH/ Ola (NIH), 129/ Sv/ Ola (129) and C57BL/ 6J/ Ola (C57) genetic backgrounds. Defined intercrosses of these strains; i.e. F1 (reciprocal NIH x C57) and F2 (F1 x F1), were also used in this study. In order to objectively and accurately assess the gross morphology of conceptuses at 8.0-10.5dpc, a scoring system was developed to specifically and precisely stage the embryo and yolk sac using developmental landmarks. This system also incorporated a means of quantifying the abnormalities typically found in mid-gestation TGFβ1 knockout conceptuses; and therefore enabled the comparison of the precise developmental age and severity of defects observed in conceptuses of different genotypes from different genetic backgrounds. Thus, in the course of this project; >100, 9.5dpc and 11.5dpc conceptuses from TGFβ1+/- intercross litters of each strain were morphologically scored and genotyped by

PCR. In addition, the genotype ratios of animals generated from reciprocal TGFβ1+/- x TGFβ1+/+, and TGFβ1+/- intercrosses at 3 weeks of age and 1 day old were studied.

It was found that 89% of C57 TGFβ1-/- embryos died before 9.5dpc due to an unknown cause. The majority of NIH TGFβ1-/- animals survived to birth, but died at around 3 weeks of age with a multi-focal immune reaction. The majority of F1, F2 and 129 animals died during mid-gestation (10.5dpc-12.0dpc) with defects of the extra-embryonic vascular system. This phenotype typically comprised a combination of the following abnormalities: An inadequate or disorganised yolk sac vasculature, yolk sac anaemia, haemmorhages in the yolk sac or embryo, defects of the allantois and/ or chorion. Thus, the TGFβ1 knockout phenotype was shown to have a strain-specific expressivity and penetrance.

A number of histological and molecular aspects of the TGFβ1 knockout phenotype were investigated at mid-gestation. When examined histologically, the yolk sac from abnormal TGFβ1 knockout conceptuses appeared to have weak contacts between the endoderm and mesothelium, leading to the shearing of tissue layers, dilated endothelial tubes and exovasation of primitive erythroid cells. Immunohistochemistry revealed a down-regulation in the number of perivascular pericytes in the affected yolk sacs. The apparent anaemia of some mutant yolk sacs may have been due to defective haemoglobinisation of the primitive red blood cells, assessed in this study using May-Grunwald Giemsa staining of yolk sac blood smears; however, haemorrhages observed in the yolk sac and/ or embryo could also have contributed to the anaemic phenotype.

The effect of the parental origin of alleles of the TGFβ1 modifier gene (Bonyadi *et al.*, 1997) upon death *in utero* was studied in >260 F2 conceptuses at 9.5dpc using a PCR marker polymorphic for the chromosomal location of the modifier gene between NIH and C57-derived alleles. TGFβ1+/- and -/- embryos with two C57-derived modifier gene alleles were more likely to die in early/ mid-gestation, compared to littermates. Interestingly, it was found that an NIH allele at this locus could contribute to the survival of C57 TGFβ1-/- embryos to 9.5dpc.

Thus, it appears that TGFβ1 is crucial for three stages of murine development: Prior to 9.5dpc; during the establishment of a functional extra-embryonic circulatory system at mid-gestation; and as an immunomodulator at around 3 weeks of age. A variety of genetic and environmental factors interact to produce the observed TGFβ1 knockout phenotype.

ABBREVIATIONS.

Units.

aa = amino acid
bp = base pairs
°C = degrees Celsius
cm = centimetre
cpm = counts per minute
dpc = days post coitum
dpp = days post partum
g = gram
kb = Kilobase
kDa = kiloDalton
L = litre
M = molar
mg = milligram
ml = millilitre
mM = millimolar
ng = nanogram
nm = nanometre
OD = optical density
rpm = revolutions per minute
V = volts
µCi = microCurie
µg = microgram
µl = microlitre
µm = micrometre

Chemicals and Reagents.

BSA = bovine serum albumin
cDNA = complementary DNA
DAB = 3,3'- diaminobenzidine
DEPC = diethylpyrocarbonate
DIG = digoxigenin
DNA = deoxyribonucleic acid
dNTP = deoxynucleoide triphosphates
DTT = dithiothreitol
EDTA = ethylenediaminine tetra acetic acid
ET = Embryo Transfer Freezing medium
EtBr = ethidium bromide
mRNA = messenger RNA
PBS = phosphate buffered saline
PFA = paraformaldehyde
RNA = ribonucleic acid
SDS = sodium dodecyl sulphate
TE = Tris-EDTA
TESPA = 3-amino propyltriethoxysilane
UTP = Uridine 5'- Triphosphate

Proteins.

β-LAP = TGFβ latency associated peptide
BMP = bone morphogenetic protein
CDMP = cartilidge-derived morphogenetic protein
dpp = *decapentaplegic*
DVR = *decapentaplegic* -*Vg*-related group

Proteins (continued).

ECM = extracellular matrix
EGF = epidermal growth factor
FGF = fibroblast growth factor
FN = fibronectin
FSH = follicle stimulating hormone
GDF-9 = growth/ differentiation factor 9
GDNF = glial-derived neurotrophic factor
LTBP = latency associated TGFβ binding protein
MIS = Müllerian inhibitory substance
TGFβ = transforming growth factor type Beta
VEGF = vascular endothelial growth factor
Vg-1 = vegetal-1
Vgr-1 =*Vg*-1 related

Other

C57 = C57BL/ 6J/ Ola
EC = endothelial cells
F1 = Generated by reciprocal C57 x NIH intercrosses.
F2 = Generated by F1 intercrosses.
HSC = haematopoietic stem cells
NIH = NIH/ Ola
PCR = polymerase chain reaction
RFC = microvascular endothelial cells
RFLP = restriction fragment length polymorphism
UV = ultraviolet
+/+ = homozygous wild type
+/- = heterozygous
-/- = homozygous null
129 = 129/ Sv/ Ola

CONTENTS.

Chapter 2 MATERIALS AND METHODS.

FIGURES.

TABLES.

GRAPHS.

Chapter 1

INTRODUCTION.

1.1 Cellular Interactions and Pattern Formation in Embryogenesis.

Mammalian prenatal development has been studied for centuries. Prior to the advent of molecular biology a variety of elegant descriptive and grafting studies enabled the postulation of key theories regarding cell fate, morphogen gradients and the inductive ability of certain tissues. However, it is only due to investigations on a molecular level that the precise mechanism of some of the interactions observed during embryogenesis have been elucidated.

In the last few decades a multitude of proteins which are active during mammalian embryogenesis have been identified. The sequences of many of the genes which encode these proteins are highly conserved across divergent species, indicating common evolutionary origins. This has proved to be a useful tool in the investigation of the structural and functional homology and analogy of many developmental systems.

Genes and gene products are typically classified by their degree of relatedness to each other on various structural levels. The transforming growth factor type Beta (TGFβ) superfamily is one such discrete group of highly conserved proteins with disparate functions. The TGFβ superfamily is reviewed below.

1.2 The Transforming Growth Factor Beta Superfamily.

The TGFβ superfamily comprises a large family of secreted signalling proteins which have many different functions *in vivo* and *in vitro*. All are known to play a role or roles during developmental processes. Members of the superfamily are found in a wide variety

of species including *Drosophila*, *C. elegans* and man, and exhibit between approximately 40-80% homology at the amino acid (aa) level. All of the family members are initially synthesised as a large precursor protein which must be cleaved at an R-X-X-R site (where R = arginine and X can be any amino acid) to release a mature peptide. The mechanisms of this process are covered in detail later in this chapter. It is the structure of the mature region which is the most highly conserved within the superfamily; there is up to 100% aa identity of this region between homologues of different species.

Cysteine residues in the mature peptide are conserved between all superfamily members. One of these residues is involved in an intermolecular disulphide bond linking the biologically active homo- or hetero-dimeric form of the molecule, the others are involved in the formation of an intramolecular 'cysteine knot', a common structural motif within the superfamily (McDonald & Hendrickson, 1992).

The TGFβ superfamily can be subdivided into smaller, more related groups: The TGFβs, the activins and the DVR (*decapentaplegic Vg*-related) group. Other newer unclassifiable superfamily members also exist; for example *lefty* (Meno *et al.*, 1996 & Colligton *et al.*, 1996). The superfamily members described in detail below may share receptors. For an overview of the degree of relatedness between the members of the TGFβ superfamily, see Figure 1.

1.2.1 The Transforming Growth Factors Beta.

The first member of the TGFβ superfamily to be identified was human TGFβ1 (Assoian *et al.*, 1983; Frolick *et al.*, 1983 & Roberts *et al.*, 1983). It was cloned in 1985 by Derynck *et al.* Further biochemical purification and molecular cloning has led to the identification of three distinct TGFβs in mammals, designated TGFβ1, TGFβ2 and TGFβ3. Work done *in vitro* and *in vivo* on all 3 TGFβ isoforms has revealed a great diversity of function. They are able to stimulate or inhibit cell proliferation and differentiation or alter the cellular phenotype. The potency of each isoform depends upon the cell type and environment (Miyazono, 1993; Akhurst, 1994 & Cui & Akhurst, 1996 for review articles).

All three TGFβ genes share common structural features: All contain 7 exons, with conserved splice site junctions. The proteins are synthesized as pre-pro-TGFβs; the length of which varies between isoforms, i.e. TGFβ1 is 390 aa and TGFβs 2 and 3 are 412aa. These are large precursor molecules with a short N-terminal signal peptide, the

latter enables the protein to be released from the cell (see Figure 2). The precursor proteins usually exist as homodimers bound by disulphide bonds, however, heterodimers between TGFβs 1 and 2 (Cheiftez *et al*, 1988), and TGFβs 2 and 3 (Ogawa *et al*, 1992) have been characterised. The mature bioactive form of TGFβ is released by proteolytic cleavage of the pre-pro TGFβ at an arginine - rich sequence 112aa from the C-terminal. However, the N-terminal fragment remains non-covalently associated with the mature dimer and is termed the latency-associated peptide (β-LAP). The β-LAP maintains the TGFβ in a latent state, forming the small latent complex.

Although certain features of the β-LAPs of the different TGFβ isoforms are conserved for functional and structural reasons; the sequence of the β-LAPs is dissimilar. β2-LAP lacks an RGD integrin-binding motif, which β1 and β3 β-LAPs possess. This has been postulated to provide a functional distinction for TGFβ2. All 3 β-LAPS are capable of binding to each of the mature isoform homodimers and in most biological assays each isoform is interchangeable (Roberts & Sporn, 1990). Thus, although the β-LAP may not be directly responsible for functional differences between TGFβ2 and TGFβs 1 and 3, it may play a part in modulating the affinity of the latent TGFβ2 complex for the extra-cellular matrix (ECM).

In humans, little similarity has been found between the promoters characterised for each TGFβ gene (Kim *et al.*, 1989; Lafyatis *et al.*, 1990; Noma *et al.*, 1991). Each has distinct regulatory elements, suggesting, as expected, that each isoform can be independently regulated in response to diverse stimuli. With the gene promoters, as with the mature TGFβs, there is a high degree of interspecies homology. This is consistent with observation that the localisation and function of the TGFβ isoforms is comparable across a variety of species. For example, mature human TGFβ1 is identical to mature avian, bovine, simian and porcine TGFβ1 (Derynck *et al.*, 1985, 1987; Sharples *et al.*, 1987; van Obberghen-Schilling *et al.*, 1987 & Jakowlew *et al.*, 1988) and differs from murine TGFβ1 by one amino acid (Derynck *et al.*, 1986). However, there may be different inter-specific roles for the regulation and function of TGFβ isoforms during embryogenesis. Evidence presented by Potts and Runyan shows that TGFβ3 plays a key role in avian heart development (Runyan *et al.*, 1992). Work done on murine cardiac development (Millan *et al.*, 1991 & Dickson *et al.*, 1993) suggests that TGFβ2 may replace it in the developing mouse heart.

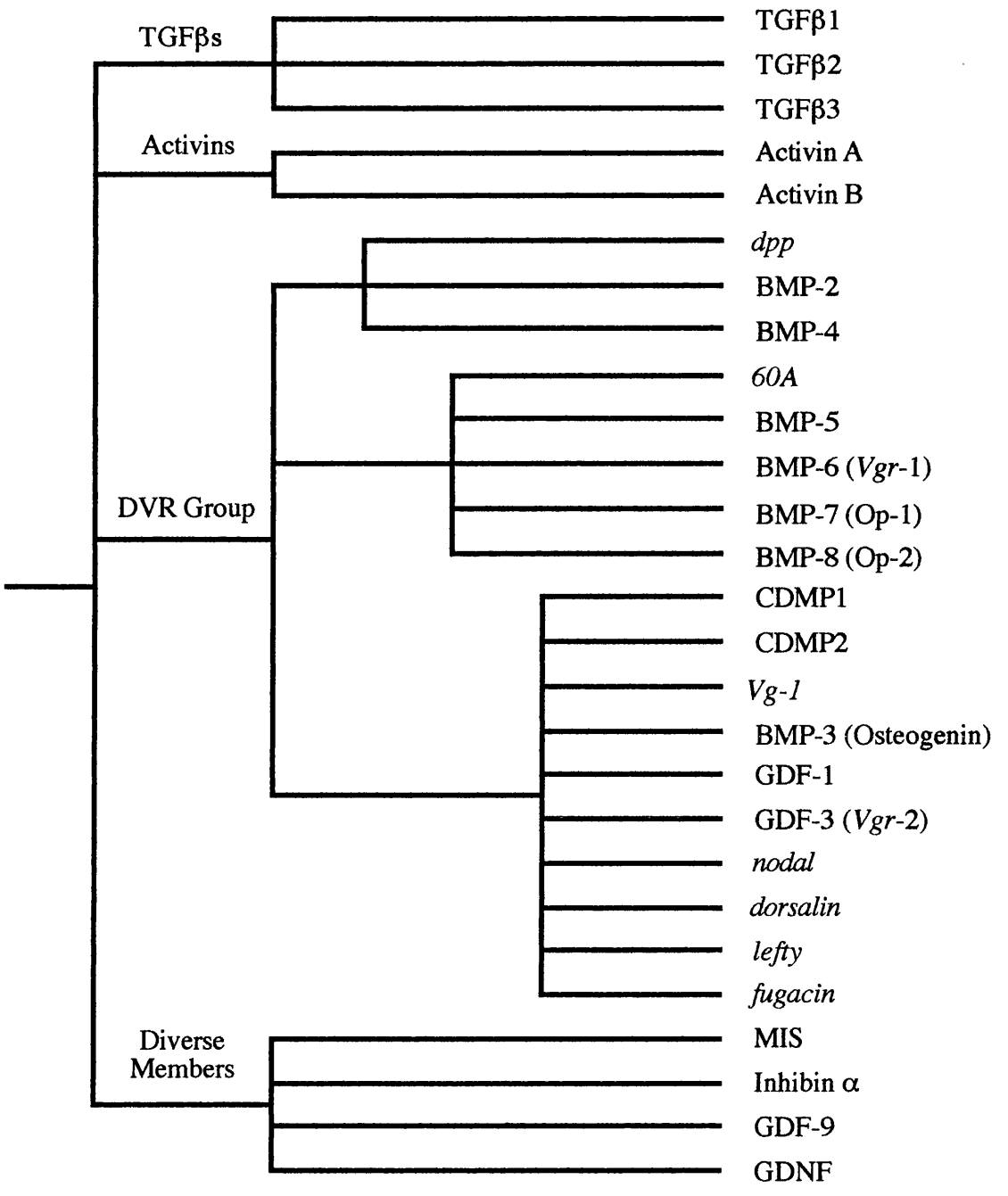

Figure 1. The Transforming Growth Factor Beta Superfamily.

The diagram shows the inter-relationship of the members of the TGFβ, Activin, DVR and unclassified subgroups of the TGFβ superfamily. Length of the branches does not indicate the degree of inter-relatedness.

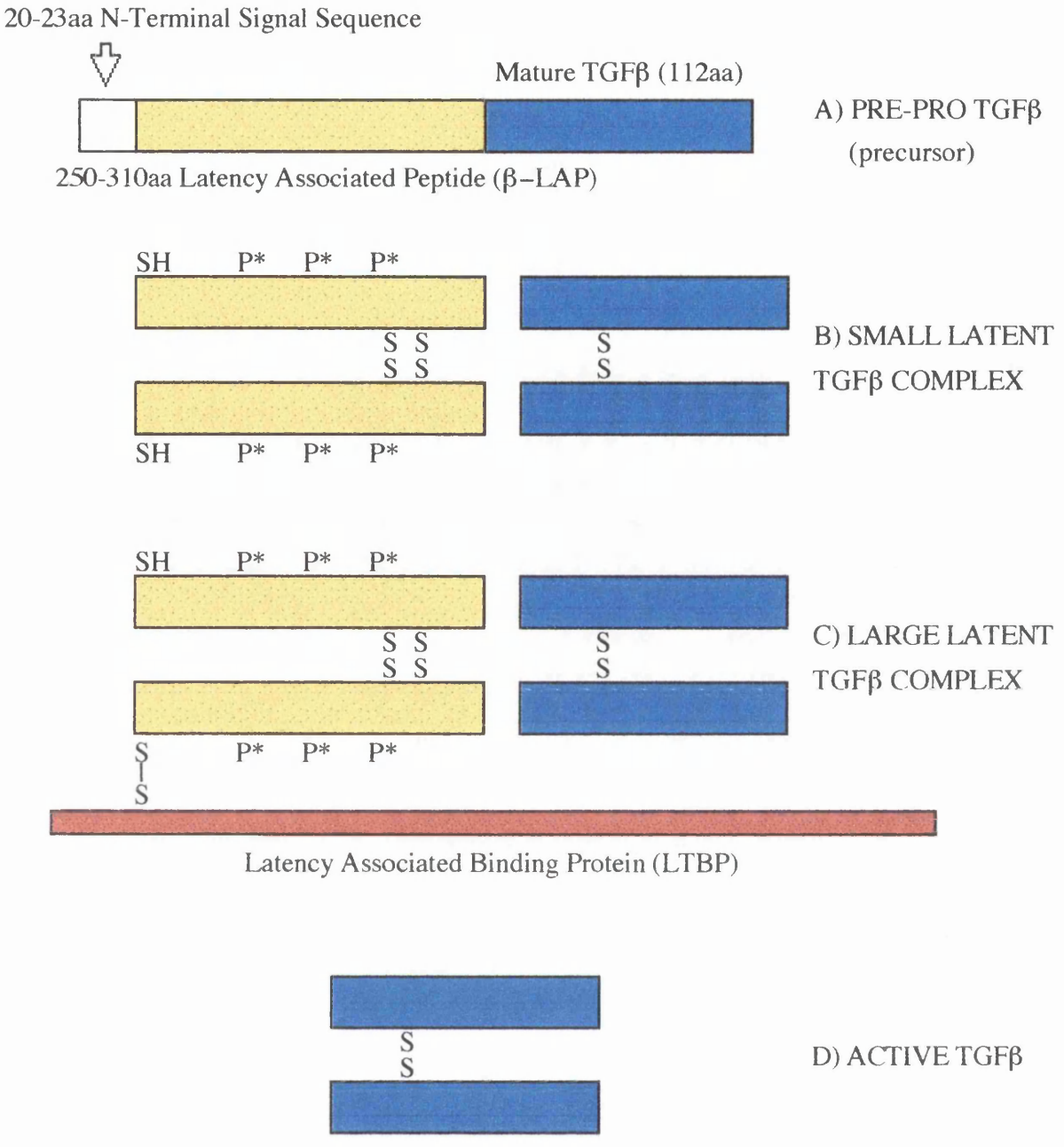

Figure 2. Diagrammatic Representation of the Different Forms of TGFβ.

TGFβ is translated into a precursor molecule, known as pre-pro TGFβ (A). Two of these monomers associate via disulphide bonds (S) and the mature dimeric TGFβ is formed by proteolytic cleavage at an arginine-rich region; i.e. the mature regions of the molecules are separated from their latency associated peptides (β–LAP). The cleaved β–LAP can remain covalently associated with the TGFβ dimer and, by this, will continue to confer latency. This is called the small latent TGFβ complex (B). The large latent complex (C) contains the small latent complex plus the latency associated binding protein (LTBP). The LTBP binds to the β–LAP via disulphide bonds. The mature form of TGFβ is activated only on release from the β–LAP (D). The activation process of TGFβ may involve the interaction of mannose-6-phosphate (P*) with the cell surface and plasmin.

1.2.2 The Activins.

Activins function as dimers, of which there are 2 distinct monomeric forms: β_a and β_b. The β_b subunit also forms part of the inhibin heterodimer. Thus, 3 types of activin have been isolated, activin A ($\beta_a\beta_a$), activin B ($\beta_b\beta_b$) and activin AB ($\beta_a\beta_b$). All are capable of inducing mesoderm in animal cap explants from the *Xenopus* embryo (Nakamura *et al.*, 1992) and inducing the release of follicle stimulating hormone (FSH) (Mason *et al.*, 1985). Extensive studies in the mouse have shown that both activin subunits are expressed zygotically before implantation (Albano *et al.*, 1993) and expressed in several tissue types during post-implantation development. During gastrulation and early post-implantation development the activins are expressed exclusively in the decidua. By 10.5 days post conception (dpc), activin A has localised in mesenchymal tissues of the embryo and activin B is expressed in the central nervous system as well as the gastric epithelium. β_a and β_b subunits are coincidentally expressed in, among other tissues, the blood vessels and intervertebral disc anlagen (Feijen *et al.*, 1994).

Knockout mice, i.e. animals lacking the activin genes, have been generated. Animals without the β_b subunit developed to term and only exhibited defects in eyelid formation and female reproductive ability, thus proving that activin B is not essential for mesoderm formation (Vassalli *et al.*, 1994). It must be remembered that mutants involving the activin β_b subunit also affect the formation of inhibin. β_a homozygous null mutations die within 24 hours of birth with severe craniofacial malformations, however, the mesoderm had developed normally (Matzuk *et al.*, 1995a). Mice lacking both activin subunits exhibit the sum of defects from the individual mutants (Matzuk *et al.*, 1995b).

Since these phenoytypes do not involve gross disturbances in mesoderm formation, it has been postulated that maternal decidual activin plays a role in rescuing the homozygous null conceptuses (Smith, 1995). Letterio *et al.*, (1994) showed that TGFβ1 protein can cross the placenta. However, since the activin A knockout is lethal it would be impossible to test this theory properly for the activins without using inducible knockouts (see Introduction 1.5.3).

A number of activin receptors have been cloned and characterised. All are serine/threonine kinase receptors and fall into two classes, type I or type II. These receptors form a heterodimeric complex to signal. To date, only the knockout of

activin receptor IIA (ActRcIIA) has been published. Surprisingly, the majority of homozygous mutants developed normally, although some exhibited skeletal abnormalities. General defects included a decrease in the level of FSH and reduced reproductive capabilities (Matzuk *et al.*, 1995b). This result suggests that there are several activin type II receptors mediating different cellular responses i.e. ActRcIIA governs activin's role in FSH induction, but not mesoderm induction. Preliminary reports of activin type IA and IB receptor knockouts show early post implantation loss in both mutants, as do double knockouts for ActRcIIA and ActRcIIB (Gu *et al.*, 1996; Oh *et al.*, 1996). The data suggests a complex interaction of combinations of receptors and ligands necessary for the multifarious effects of activin.

1.2.3 The *Decapentaplegic*-Vg Related Group (DVR group).

The DVR subfamily are classified together because they are more similar to one another than to the TGFβs and activins (see Figure 1). The group comprises the *Xenopus* gene *Vg-1* and its mammalian homologue *Vgr-1,* the *Drosophila* gene *decapentaplegic* (*dpp*) and the bone morphogenetic proteins (BMPs). This subgroup is rapidly expanding.

The details of the *dpp* signalling pathway are emerging: one, type II and two, type I serine/threonine kinase receptors have been characterised; *punt*, *saxophone* and *thick veins* respectively. Both receptor types are required for *dpp*-related signalling (Ruberte *et al.*, 1995). Downstream signalling elements in the TGFβ signalling pathway will be discussed later in this chapter.

1.2.3.1 The Bone Morphogenetic Proteins (BMPs).

The BMPs were first described by Urist in 1965. Urist found that by implanting extracts of demineralised bone into ectopic sites in rodents, new bone formed. The inductive proteinacious factor(s) involved were named bone morphogenetic protein (BMP). Subsequently, a family of BMPs have been cloned which fall into a number of subfamilies. BMP-1 is not a member of the TGFβ superfamily and closely resembles the *Drosophila tolloid* protein. Mature BMPs 2 and 4 are classified with *dpp*. BMP-3 and BMPs 5-8 are also in distinct subgroups (see Reddi, 1992 for a review article) (see Figure 1).

In vertebrates, BMPs are expressed in many embryonic tissues and organs. This is reflected in the variety of phenotypes reported in the knockouts of BMPs which have been characterised: The majority of BMP-4 homozygous mutants die at the egg cylinder stage. The conceptuses which survive to mid-gestation are developmentally retarded and die with truncated posterior structures and a haematopoietic deficiency in the yolk sac (Winnier *et al.*, 1995). BMP-2 mutants die at 9.5dpc with defects of cardiac and amnion/ chorion formation (Zhang & Bradley, 1996) and BMP-7 homozygous mutants die shortly after birth with renal failure. They also suffer micropthalmia and polydactyly (Dudley *et al.*, 1995).

Recent work suggests that different members of the BMP family interact with their receptors using different mechanisms to those utilised by the rest of the TGFβ superfamily, and that a number of BMP receptors remain unidentified (Neuhaus *et al.*, 1996). Binding studies have shown that the type I activin-like kinase receptor 3 (ALK-3) and ALK-6 can bind BMPs 2, 4 and 7, thus they have been designated BMPR-1A and BMPR-1B respectively (ten Dijke *et al.*, 1994). Interestingly, BMPR-1A deficient embryos die at gastrulation without forming any mesoderm (Mishina *et al*, 1995). A type II receptor, BMPR-II has been cloned (Rosenweig *et al.*, 1995).

1.3 Activation and Signalling of the TGFβs.

1.3.1 TGFβ Latency.

As previously described, the TGFβs are synthesised as large pre-pro (precursor) molecules which are proteolytically cleaved to give the mature peptide and a β-LAP fragment. The β-LAP remains non-covalently associated with the mature peptide, forming the small latent complex (see Figure 2). Thus, all 3 TGFβ isoforms are secreted as biologically inactive complexes which must be activated in order to interact with TGFβ receptors.

Fractions of latent TGFβ have been found to contain additional high molecular weight proteins, which are associated with the β-LAP. The best characterised of these is latent TGFβ binding protein (LTBP), which is found bound to the β-LAP by a disulphide bond (Miyazono *et al.*, 1988). Binding studies have shown that the LTBP cannot confer latency alone; in fact, the β-LAP is sufficient to confer TGFβ latency and thereby control the bioactvity of TGFβ (Kanzaki *et al.*, 1990 & Miyazono *et al.*, 1993)

(see Figure 2). A second LTBP, LTBP-2 has also been described (Moren *et al.*, 1994).

The LTBP amino acid (aa) sequence contains repeat motifs which are present in fibrillin, an ECM protein. It also contains an RGD motif and a potential β2-laminin binding domain (Kanzaki *et al.*, 1990 & Maslen *et al.*, 1991). Protein studies have confirmed that LTBP-1-associated TGFβ is found in the ECM of fibroblasts and can be released by the addition of plasmin (Taipale *et al.*, 1994). More recently, Ghosh & Brauer (1995) showed that latent TGFβ is present in much of the embryonic cardiac ECM, whilst the distribution of active TGFβ is much more restricted. Thus, the role of the LTBP appears to be to direct the latent TGFβ to the cell surface where it can either be stored, or processed to the active form. Dallas *et al.* (1995) have also proposed a role for LTBP-1 as means of storing latent TGFβ in the ECM of bone where LTBP-1 may be involved in the formation of the ECM of bone. This work also supported previous assertions that plasmin was the key regulator of both free and matrix-bound latent TGFβ activation.

1.3.2 TGFβ Receptors.

The nomenclature of the TGFβ receptors is based upon their sizes as elucidated in chemical crosslinking studies using radio-iodinated TGFβ. Thus, Type I receptors are approximately 53 kDa, Type II receptors between 70-85 kDa and Type III receptors between 200-400 kDa . The first TGFβ superfamily receptor to be cloned was an activin type II receptor, ActRIIA (Matthews and Vale, 1993) (see Massague *et al.*, 1993 & Kingsley *et al.*, 1994, for review articles).

Sequence comparison between the TGFβ superfamily type I and II receptors cloned subsequently showed that these receptors represent subfamilies of novel serine/ threonine kinase signalling molecules. Each comprises an extracellular domain, a transmembrane region and an intracellular kinase domain. Type II receptors contain a serine/ threonine- rich C-terminal tail not present in type I receptors. Unique to the type I receptors is a 30 aa conserved region; namely, the GS domain, which is located immediately N-terminal to the kinase domain. This region is involved in type I receptor activation (Wrana *et al.*, 1994a, b) (see Massague *et al.*, 1992 & Kingsley *et al.*, 1994 for review articles).

In a pattern echoed throughout the TGFβ superfamily, a number of receptors have been cloned for TGFβ: One type II receptor; TβR-II (Lin *et al.*, 1992) and two type I receptors; TβR-I and TSR-1 also known as ALKs 5 and 1 respectively (Franzen *et al.*, 1993 & Bassing *et al.*, 1994). TβR-1 appears to be a definitive TGFβ type I receptor whereas TSR-1 interacts with both activin and TGFβ type II receptors (Carcamo *et al.*, 1994). Thus, the initiation of the TGFβ signal is complex. It involves a system which has the ability to induce an array of diverse cellular effects using receptors which may overlap with other TGFβ superfamily signal pathways.

TβR-II is a constitutively active serine/ threonine kinase whose activity is not increased by ligand binding. Ligand binding to TβR-II induces recruitment of TβR-I into a stable complex and, once this complex is formed, TβR-II phosphorylates TβR-I at serine/ threonine residues in the GS domain and a signal is induced (Wrana *et al.*, 1994a). This heteromeric complex is required for a TGFβ signal i.e. the kinase activity of both TβR-II and TβR-I is necessary for TGFβ signalling, and a constitutively active TβRI can generate certain cellular responses in the absence of TβR-II (Weiser *et al.*, 1995 & Carcamo *et al.*, 1995). Thus TβR-I is effectively a cell-surface component of the downstream TGFβ signalling pathway. Naturally-occuring kinase-deficient receptor Is can compensate for their defects by dimerising in complex with a TβR-II and co-operatively interact in the induction of a TGFβ signal (Weis-Garcia *et al.*, 1996). This may provide a means of producing the diverse cellular effects induced by TGFβ. Indeed, there is other evidence that members of the TGFβ superfamily can form homo- and hetero-dimers and it may be these different combinations which drive the formation of specific receptor combinations and elicit different cellular responses (Kingsley, 1994).

Both type III receptors; betaglycan and endoglin, are thought to play a role in the presentation of TGFβ to TβR-II. Transient complexes between TβR-II and TβR-III have been detected on the cell-surface after the addition of TGFβ (Lopez-Castillas *et al.*, 1993 & Zhang *et al.*, 1996). Betaglycan is a membrane-bound proteoglycan with a short cytoplasmic tail and no apparent signalling motif (Lopez-Castillas *et al.*, 1991 & Wang *et al.*, 1991). It is found in many cell-types excluding haematopoietic and endothelial cells (Ohta *et al.*, 1987) and also exists in a free-floating form. This can still bind TGFβ, but cannot present it to the receptors (Lopez-Castillas *et al.*, 1994). Thus, betaglycan may play a role in controlling excess ligand. Endoglin is a 180 kDa homodimeric membrane glycoprotein. It is only found on vascular endothelial cells and erythroid precursors (Buhring *et al.*, 1991) and does not exist in a free-floating

form (Cheifetz *et al.*, 1992). The type III receptors also exhibit different binding affinities for the TGFβ isoforms. Betaglycan can bind all 3 TGFβ isoforms with varying affinities (Mitchell *et al.*, 1992), whereas endoglin only binds TGFβ1 and 3 (Cheifetz *et al.*, 1992).

Thus, the variations of affinity in ligand-receptor interaction may assist in the modulation of the effects of the different TGFβs: TGFβs 1 and 3 bind TβR-II with high affinity, however, TGFβ2 does not bind well to either TβR-II or TβR-I, despite all 3 isoforms having similar effectiveness. However, TβR-II has been shown to be necessary for TGFβ2 function (Wrana *et al.*, 1992). It appears that type III receptors may control the cell's responsiveness to TGFβ2. Endoglin binds TGFβ2 with a lower affinity than it binds TGFβ1 and 3, which may be why certain types of haematopoietic and endothelial cells are less responsive to TGFβ2 (Ohta *et al.*, 1987; Ottman & Pelus., 1988; Merwin *et al.*, 1991 & Qian *et al.*, 1992).

It is possible that betaglycan acts as a modulator of TGFβ2. TGFβ2 will not bind to TβR-II when the receptor exists in a free, soluble form; whereas at the cell-surface, in transfected COS cells the binding of TGFβ2 to TβR-II was increased 10-100 fold by the presence of betaglycan (Lin *et al.*, 1995). It has been observed that a small subset of TGFβ receptors display a similar affinity for all TGFβ isoforms (Cheifetz *et al.*, 1990 & Zhou *et al.*, 1995). It is not known whether these molecules are acting in concert with binding proteins, such as a type III receptor or a similar molecule, or if they represent a unique, unknown type of TGFβ receptor.

1.3.3 TGFβ Receptor Signalling.

The TGFβ family transduce their signals via a heteromeric complex of a type I and a type II serine/ threonine kinase receptors. This is generally the same throughout the TGFβ superfamily: Activins, BMPs and TGFβs have all been shown to require both receptor types in order to signal. However, there are differences in receptor-ligand interaction between the subgroups. Whereas in the TGFβ and activin signalling pathway only the type II receptor binds ligand and recruits a type I receptor into a stable heteromeric complex, all BMP receptors show weak binding of ligand, however, a high affinity binding of BMP is observed when both receptor types are present. There is also a degree of type I receptor subunit promiscuity within the TGFβ superfamily; i.e. the type II receptors are able to interact with a number of type I receptors, for example, TSR-1 has been reported to bind both activin and TGFβ and

ActR-I can signal with both BMP-7 and activin (ten Dijke *et al.*, 1996 for a reveiw article).

Several molecules thought to play downstream roles in TGFβ receptor activation and signalling have been identified. FKBP-12 and farnesyl protein transferase A were both isolated using a yeast two-hybrid system with an intracellular TGFβ type I receptor as "bait". The exact function of these molecules is unknown. Both fail to interact with a kinase-defective type I receptor, although no ligand dependence has been demonstrated in the ability of either to phosphorylate or associate with the receptor (Wang *et al.*, 1994 & Kawabata *et al.*, 1995). Using a TβR-II intracellular domain as "bait", TβR interacting protein-1 (TRIP-1) was isolated. The interaction and phosphorylation of TRIP-1 is dependent on TβR-II kinase activity, but independent of ligand and TβR-I (Chen *et al.*, 1995). Similarly, the exact function of TRIP-1 is unknown.

As previously mentioned, the *Drosophila* type I and II receptors are *saxophone*, *thick veins* and *punt*. They interact with the *Drosophila* BMP-2 and 4 homologue *dpp*. A genetic screen for enhancers of weak *dpp* alleles led to the identification and characterisation of *mothers against decapentaplegic* (*mad*), a downstream component required for *dpp* signalling (Raftery *et al.*, 1995 & Sekelsky *et al.*, 1995).

In *C. elegans, daf-4* has been characterised as a serine/ threonine kinase BMP receptor homologue, able to bind ligand and signal without interacting with a receptor I (Estevez et al., 1993). The *sma-2, 3* and *4* genes were identified as downstream elements in the *daf-4* pathway and found to be structurally related to the *Drosophila mad* gene (Savage *et al.*, 1996). Thus far, four vertebrate homolgues of *mad* have been identified; these have been named *Smad-1* to *Smad-4* (Zhang *et al.*, 1996). *Smads* from different species show a high level of sequence conservation; for example, human and *Xenopus Smad-1* are 95% identical.

Experimental evidence has shown that different *Smads* can induce different intracellular responses, and overexpression of specific *Smads* can mimic the effect of different TGFβ superfamily ligands. For example, overexpresion of *Smad-1* induces BMP-2 and 4 effects, *Smad-2* induces activin-like effects and *Smad-3* induces TGFβ-like effects (Graff *et al.*, 1996; Liu *et al.*, 1995; Thomsen *et al.*, 1996 & Zhang *et al.*, 1996). *Smad-4* is different in structure to the other *Smads*, and may be involved co-operatively in signal transduction. Thus, overexpression of a truncated *Smad-3* and

Smad-4 but not *Smad-2*, inhibits a TGFβ intracellular response (Zhang *et al.*, 1996). Hence, it has been postulated that the signal from a TGFβ superfamily receptor I can be transmitted via a single *Smad* and this process may involve functional interactions with *Smad-4*.

The precise roles of the *Smad* family remain unclear, but they may be involved in the transcriptional upregulation or activation of other downstream genes in the TGFβ family signalling pathways. Vertebrate homologues of the *Drosophila* transcription factors *schnurri, sal* and *salr* which act downstream from *dpp*, may be involved in this interaction (Arora *et al.*, 1995; Greider *et al.*, 1995 & de Celis *et al.*, 1996).

1.4 TGFβ1 and Embryogenesis.

The distribution of TGFβ1 RNA and protein throughout murine embryogenesis has been well documented. Transcripts are found from the 4-cell embryo stage onwards by reverse transcription PCR, but are undetectable by in-situ hybridisation until 7.5dpc when they are found in the developing blood islands (Rappolee *et al.*, 1988). Thereafter, TGFβ1 localises to the developing endothelial and haematopoietic cells in the yolk sac, allantois and embryo proper, the pro-angiogenic progenitors of the cardiogenic mesoderm and the endocardium (Lenhert & Akhurst, 1988 & Akhurst *et al.*, 1990).

1.4.1 TGFβ and Preimplantation Development.

Spatial and temporal patterns of TGFβ during preimplantation development suggest that it may play a role in implantation, decidualization and placentation. Successful implantation requires a series of complex co-ordinated interactions between the maternal and embryonic tissues involving many cellular processes. Maternal tolerance to the conceptus must be established to prevent rejection of the developing embryo. Cell migration, proliferation and differentiation, ECM remodelling and neo-vascularisation must also take place to create a suitable environment for gestation.

TGFβ1 RNA and protein studies have shown that during the preimplantation period TGFβ1 is localised intracellularly in the maternal uterine luminal and glandular epithelium. It is diffusely expressed extracellularly throughout the decidualizing uterine stroma after the initiation of implantation at 4.5dpc (Tamada *et al.*, 1990). This

pattern continues in the deciduum through mid-gestation with the highest level of TGFβ1 expression occurring proximal to the uterine wall (Akhurst *et al.*, 1990).

During the preimplantation period TGFβ2 is localised in the maternal uterine luminal and glandular epithelium, the myometrium and vascular smooth muscle. Post-implantation, TGFβ2 immunoreactivity is observed in the deciduum as well as the myometrium and epithelium (Das *et al.*, 1992). TGFβ3 protein is found in the myometrium and vascular smooth muscle at the peri-implantation stage (Das *et al.*, 1992).

Type I and II TGFβ receptors and TSR-1 are present in the uterine and decidual tissue (Roelen *et al.*, 1994). Thus, these tissues can respond to TGFβ in an autocrine manner.

All three TGFβ isoforms have been detected in the 1-cell, then the 4-cell embryo suggesting that the embryo begins to produce TGFβ as soon as the genome is activated (Rappolee *et al.*, 1988 & Paria *et al.*, 1992). It is not known precisely whether preimplanation embryos can respond to TGFβ. *In vitro* culture of individual 2-cell embryos to blastocyst stage is significantly enhanced by the addition of TGFβ1 (Paria & Dey, 1990). In addition, specific binding of radiolabelled TGFβ1 and 2 to blastocysts has been demonstrated, and distinct roles for TGFβ isoforms in blastocyst dormancy and activation proposed (Paria *et al.*, 1992). However, Roelen *et al.*, (1994) presented data that the TGFβ type I and II receptors were undetectable in the embryo until after gastrulation and therefore concluded that embryonic TGFβ acts in a paracrine fashion upon maternal tissue, regulating implantation and maintaining pregnancy. Thus, there may be specific, as yet undetected TGFβ receptors functioning in early embryogenesis.

1.4.2 TGFβ and Yolk-Sac Development.

1.4.2.1 Normal Development of Extra-Embryonic Tissue.

During murine embryogenesis; the extra-embryonic tissues serve several essential functions. They provide a well-regulated environment for embryonic development prior to the formation of the chorio-allantoic junction at around 10.0dpc and protect the developing embryo. The extra-embryonic tissues are consituted of; the placenta - derived from trophoblast, mesoderm and endoderm; the parietal yolk sac - derived

from parietal endoderm and trophoblast; the visceral yolk sac - derived from visceral endoderm and mesoderm; and the amnion which is derived from mesoderm and ectoderm.

The visceral yolk sac, hereafter referred to as the yolk sac, starts to form as the inner cell mass (ICM) of the blastocyst differentiates into layers of primitive ectoderm and endoderm. The primitive endoderm does not contribute to the definitive endoderm of the adult mouse but only to the visceral and parietal extraembryonic endoderm. Cells from the primitive endoderm migrate along the inner surface of the trophectoderm. This layer becomes the parietal endoderm and secretes the Reichert's membrane which is thought to act as a passive filter between the maternal and foetal environment.

The remainder of the endoderm forms a visceral endoderm layer wrapped around the egg cylinder. As gestation progresses mesodermal cells generated from the posterior primitive streak of the embryo migrate onto the inner surface of the visceral endoderm and the yolk sac is formed from regions where mesoderm is adjacent to the visceral endoderm. It is these mesodermal cells which give rise to the first haematopoietic tissue, i.e. the blood islands of the yolk sac.

The amnion begins as a roof over the primitive, unturned 8-8.5dpc embryo. It expands rapidly with the turning of the embryo and, by 9.5dpc exists as a thin membrane lying between the embryo and the yolk sac

The allantois is a major component of the maternal and foetal relationship during gestation. At 8.0-8.5dpc the allantois is a finger-like projection of mesodermal cells from the posterior margin of the embryonic ectoderm which expands upwards from the amniotic cavity into the exocoelomic cavity. Between 8.5 and 8.75dpc the allantois begins to fuse with the chorion. The chorion lies in direct contact with the ectoplacental cone and is covered by a layer of mesodermal cells which contribute to the placenta. By 9.0dpc, a primitive placenta has been formed as a result of the fusion of the allantois, chorion and ectoplacental cone. The primitive vasculature of the allantois connects with the vasculature in the chorion and the umbilical vessels appear. At around 10.0dpc the ectoplacental cone becomes the labyrinthine part of the placenta and the embryo begins to receive nutrients from the mother. Prior to this, the embryo was reliant upon the yolk sac for nourishment. (Yang *et al.*, 1995).

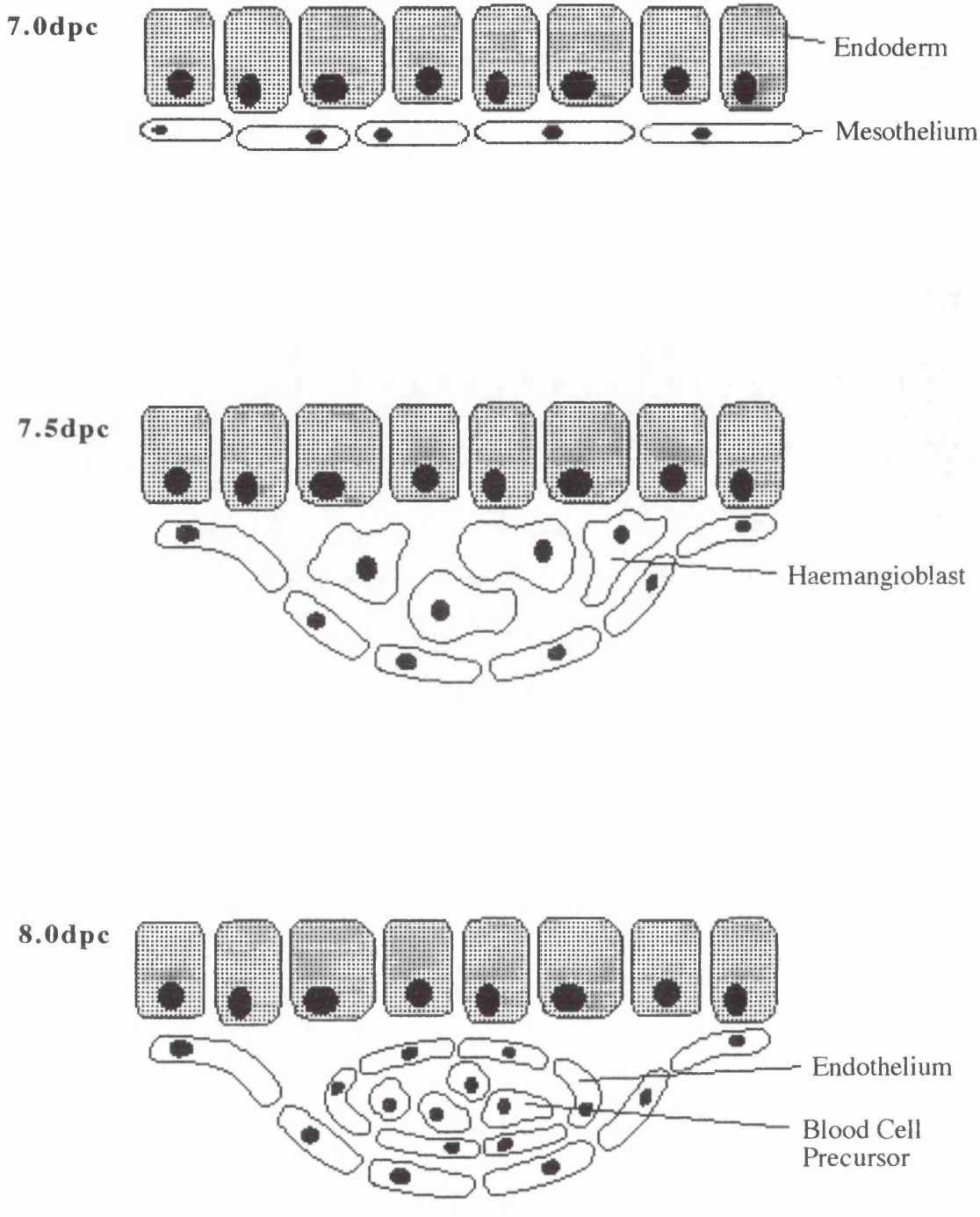

Figure 3. A Diagrammatic Representation of Blood Island Formation in the Murine Yolk Sac.

Between 7.0 and 8.0dpc, the blood islands develop in the yolk sac. They are distinct regions of mesodermal proliferation induced by the endoderm. The blood islands contain the haemangioblast progenitor cells which give rise to both the endothelial and haematopoietic cell lineages in the yolk sac. By 8.0dpc, the outermost haemangioblasts have flattened and become a layer of endothelial cells. The inner haemangioblasts remain rounded and form erythroid precursors. Between 8.5 and 9.0dpc, the endothelial cells begin to anastomose, forming the basis of the developing vascular plexus in the yolk sac (Martin *et al.*, 1995).

See Slack, 1983 and Hogan *et al.*, 1994 for a detailed overview of murine development.

1.4.2.2 The Role of TGFβ in Yolk-Sac Development.

At 7.0-8.0dpc in the murine yolk sac, the blood islands are induced by the endoderm. The blood islands are functionally distinct regions of mesodermal proliferation which contain the haemangioblasts, the progenitors of endothelial and haematopoietic cell lineages (Miura & Wilt, 1969; Pardanaud *et al.*, 1989 & Martin *et al.*, 1995). The first expression of TGFβ1 mRNA occurs in the blood islands of the 7.5dpc conceptus (Akhurst *et al.*, 1990). In the blood islands, outer haemangioblasts differentiate into a layer of endothelial cells which anastamose to form blood vessels during vasculogenesis. The primitive erythroid cells are generated from the inner haemangioblasts (see Figure 3). The TGFβ1 gene continues to be expressed in both lineages in the yolk sac and allantois as the extra-embryonic vascular plexus develops (Akhurst *et al.*, 1990).

The vascular plexus is formed by a combination of the distinct processes of vasculogenesis and angiogenesis. The former is defined as the the *in situ* differentiation of mesodermally-derived precursors and the assembly of these differentiating endothelial cells into discrete blood vessels, and only occurs during early embryogenesis: Whereas the latter is the sprouting of new vessels by the proliferation and migration of endothelial cells from pre-existing blood vessels, and is essential throughout embryogenesis as well as adulthood. Vasculogenesis results in the formation of the primordia of the heart and large vessels, as well as the capillary network found throughout the yolk sac and embryo during development (Suri *et al.*, 1996).

It is generally thought that TGFβ is growth inhibitory to endothelial cells in culture (Heimark *et al.*, 1986 & Muller *et al.*, 1987). *In vitro* studies have been used to examine the effect of TGFβ on vascular endothelial cells. Both TGFβs 1 and 2 inhibit the proliferation and migration of bovine vascular endothelial cells in culture, although TGFβ1 is almost 100 times as potent as TGFβ2 (Baird & Durkin, 1986; Frater-Schroder *et al.*, 1986 & Jennings *et al.*, 1988). When microvascular endothelial cells (RFCs) are seeded within a 2D collagen gel, TGFβ1 inhibits cell proliferation and induces α smooth-muscle actin expression. However, when RFCs are seeded into a

3D collagen gel, TGFβ1 induces the formation of capilliary tubes and the upregulation of cell adhesion molecules, ECM proteins and receptors. The cells no longer express α smooth-muscle actin. Interestingly, in the 3D culture system, cells could not be inhibited by TGFβ1 (Madri *et al.*, 1988; Merwin *et al.*, 1990 & Madri *et al.*, 1992).

α smooth-muscle actin is known to be a marker for perivascular pericytes (Herman *et al.*, 1985). Pericytes are found in close association with endothelial cells (EC) within the microvascular basement membrane but their exact function is unclear. They have been attributed roles in the maintenance of microvascular integrity and the regulation of the growth, migration and differentiation of EC during angiogenesis. These effects are mediated by TGFβ1 *in vitro* (Sato & Rifkin, 1989 & Antonelli-Orlidge *et al.*, 1989). TGFβ1 is reported to induce the expression of α smooth-muscle actin in pericytes in culture (Verbeek *et al.*, 1994). Latent TGFβ1 is produced by both endothelial cells and pericytes *in vitro,* however, it only becomes activated when EC and pericytes are cocultured. The group also found that removing TGFβ1 with antibodies inhibits EC migration (Sato & Rifkin, 1989).

Thus, in the light of the defective extra-embryonic vascular phenotype of the mid-gestation TGFβ1-/- conceptuses, TGFβ1 has been proposed to play an autocrine role in the vasculogenesis and angiogenesis of the yolk sac (Dickson *et al.*, 1995).

1.4.3 TGFβ and Haematopoiesis.

1.4.3.1 Normal Haematopoiesis in Development.

Blood is comprised of cells of many lineages i.e. erythrocytes, neutrophils, monocytes/ macrophages, platelets, mast cells, B-lymphoid and T-lymphoid cells. These are all derived from haematopoietic stem cells (HSCs). Each lineage is produced continuously throughout the lifespan of the individual and relies upon the proliferative expansion of progenitor cells and the progressive commitment of progenitors to single lineage differentiation (for an overview, see Dzierzak & Medvinsky, 1995; Orkin, 1995).

Haematopoiesis occurs in waves. In murine embryogenesis, primitive haematopoiesis begins in the yolk-sac from precursors initially observed at 7dpc (Moore & Metcalf, 1970). By 8.0dpc, the first blood cells to arise, that is, nucleated, primitive red blood cells are visible in the yolk sac. However, these cells do not enter the primitive

circulation until 8.5dpc. At 8.5-9.0dpc definitive haematopoiesis begins, and HSCs are detectable in the aortic/ gonadal/ mesonephros (AGM) region of the embryo proper. Until recently, the foetal liver was presumed to be the site of initiation of definitive murine haematopoiesis. However; mature, progenitor and stem-cell haematopoietic activity is only detectable in the foetal liver after 10.5dpc; and this may be directly related to the earlier onset of haematopoietic activity in the yolk sac and AGM region. Therefore, it is probable that the HSCs of mice (and possibly man) which populate the adult, arise in the AGM region (Medvinsky *et al.*, 1993). Yolk sac HSCs may contribute transiently to embryonic haematopoiesis, but their exact role is unclear (Godin *et al.*, 1995). It has been shown that primitive and definitive erythrocytes arise from different types of precursor cells which have distinct morphological and biochemical characteristics. By 14.0dpc erythroid cells from definitive precurors comprise the majority of circulating red blood cells (Nakano *et al.*, 1996). In adults, definitive haematopoiesis is maintained in the spleen and bone marrow.

There are clear molecular and developmental distinctions between primitive and definitive haematopoiesis. Gene-targeted c-myb-/- mice and mice deficient in the retinoblastoma (Rb-/-) gene die with anaemia at 15.0-16.0dpc during definitive haematopoiesis.These mice exhibit normal primitive haematopoiesis in the yolk-sac, but are severely anaemic by 15.0dpc. This is due to a proliferative defect of definitive haematopoietic progenitors in c-myb-/- embryos and abnormalities in the haematopoietic microenvironment in Rb-/- embryos (Mucenski *et al.*, 1991 & Clarke *et al.*, 1992). GATA-2 knock out mice die at 10.5-11.5dpc with severe anaemia due to defects in primitive haematopoiesis (Tsai *et al.*, 1994). It was inferred that GATA-2 controls the proliferation and/or maintenance of early progenitors or stem cells.

1.4.3.2 The Role of TGFβ in Haematopoiesis.

The initial embryonic localization of TGFβ1 RNA transcripts is within the blood-islands of the yolk-sac. The blood-islands contain mesodermal haemangioblasts, the progenitors of the endothelial and haematopoietic lineages (Sabin, 1920; Wilt, 1965; Miura & Wilt, 1969) (see Figure 3). The cellular descendants of both of these lineages have been shown to express TGFβ1 RNA and protein (Akhurst *et al.*, 1990). Later in development, during definitive haematopoieis, TGFβ1 RNA is detectable in foetal blood cells in the developing liver.

TGFβ1 has been reported as having many and varied effects on haematopoietic cell lines in culture and *in vivo*. It appears to be bi-functional, ie. either growth stimulatory or inhibitory depending on the target cells and the cytokines present. In general, the sensitivity of progenitor cells to the inhibitory effects of TGFβ1 is thought to be inversely correlated with maturity, i.e. immature progenitors are profoundly inhibited by TGFβ whereas more mature progenitors may be stimulated by TGFβ1 (Ohta *et al.*, 1987; Keller *et al.*, 1990; Sing *et al.*, 1988 & Keller *et al.*, 1991). For example, repeated injections of TGFβ1 given to adult mice resulted in a reversible 95% reduction in red cell counts and a 50-400% increase in circulating white cells. The reduction in erythroid production was due to suppression of differentiation of early erythroid precursors, not the lysis of existing cells (Carlino *et al.*, 1992). TGFβ1 can also induce the accumulation of haemoglobin in K-562 cells, a multipotential human haematopoietic cell line (Chen *et al.*, 1989).

It is not known precisely what the relevance of these results is in terms of murine primitive haematopoiesis. Directly, it is possible that growth inhibition of erythroid precursors may mask less profound effects. Indirectly, it may also be the case that ablation of TGFβ1 causes specific abnormalities in the correct formation of the blood-islands which result in defective haematopoiesis.

1.4.4 TGFβ and the Extra-Cellular Matrix (ECM).

The ECM provides a complex and dynamic support for tissue structure. It is required in cell migration which is essential during the processes of vasculogenesis, angiogeneis and haematopoiesis.

TGFβ is known to modulate ECM deposition by promoting its formation and controlling its degradation. TGFβ is known to stimulate the deposition of, among others: Fibronectins, collagens I, II, IV and V, thrombospondin, chondroitin/ dermatin sulphate proteoglycans, laminin and tenascin. Tenascin distribution is restricted in the embryo, and correlates with the expression of TGFβ1. TGFβ1 is known to activate the transcription of tenascin, and may play a role in its induction (Chiquet-Ehrismann *et al.*, 1988 & Akhurst, 1990). TGFβ also decreases the synthesis and secretion of several ECM-degrading proteases such as plasminogen activator (PA), elastase and collagenase. However, this process is controlled by the upregulation of a number of protease inhibitors by TGFβ; plasminogen activator

inhibitor-1 (PAI-I) and tissue inhibitor of metalloproteinases (TIMP) (see Roberts & Sporn, 1990).

Specifically, TGFβ1 has been shown to induce the expression of fibronectin by microvascular endothelial cells in 2D and 3D culture systems. Interestingly, the synthesis of PAI-1 and PA were both increased but only briefly, early in the angiogenic process in 3D culture (Sankar *et al.*, 1996). The seemingly contradictory nature of TGFβ1 function in the ECM may be attributable to the culture conditions, differention state of the cells and the cell types used.

TGFβs 1 and 2 are able to selectively upregulate the expression of integrins. Integrins are the cell-surface receptors of ECM proteins; thus TGFβ1 can regulate cellular phenotype and behaviour by modulating the interaction of the cell with the ECM (Ignotz & Massague, 1987 & Roberts *et al.*, 1988), as well as by altering the composition of the ECM.

1.4.5 TGFβ and the Immune System.

The *in vitro* and *in vivo* response of cells to TGFβ have shown that it acts as a potent modulator of the immune system, generally functioning as an immunosupressor (for review articles see Roberts & Sporn, 1990; Cui & Akhurst, 1996). Interestingly, all TGFβ1-/- mice which survive to birth die at around 3 weeks of age due to a massive multi-focal immune disorder (see Introduction 1.6.1).

During inflammation TGFβ acts as a chemoattractant, stimulating monocyte migration and macrophage production (Wahl *et al.*, 1987). At higher concentrations TGFβ can induce monocyte cytokine expression (McCartney-Francis, 1989). TGFβ can also modulate macrophage function - by inhibiting the cells' ability to release hydrogen peroxide it removes their capacity to kill cells, whilst retaining the cells' ability to produce growth factors (Tsunawaki *et al.*, 1988). After initiation of an inflammatory response, TGFβ exhibits inhibitory effects by preventing the adhesion of neutrophils and T-lymphocytes to the endothelium (Gamble & Vadas, 1991).

Analysis of the immunomodulatory properties of the structure of TGFβ isoforms has lead to the conclusion that each isoform has a distinct influence on the immune response. Based on 3D protein analysis, it has been postulated that TGFβ1 would possess an immunosuppressive and stimulative ability, whereas TGFβ2 would be a

strong immunosuppressor and TGFβ3 would be immunostimulative (Weiczorek *et al.*, 1995). For example, TGFβ1 has been suggested as a potential immunosupressor in the therapy of the human autoimmune disease multiple schlerosis (MS): The administration of TGFβ1 to mice with experimental allergic encephalomyelitis (EAE), a mouse model of MS, has been found to ameliorate the symptoms and reduce nervous system damage (Racke *et al.*, 1991). TGFβ2 has been cited as an immunosupressor in glioblastoma tumourigenesis (De Martin *et al.*, 1987).

1.4.6 TGFβ and Cardiogenesis.

Cardiogenesis is an extremely complex morphogenetic process: In the mouse; progenitor, cardiac mesoderm cells arise at gastrulation. The primitive, layered heart tube is formed at 7-7.5dpc by the rapid spread of angiogenic and promyogenic clusters located in the mesoderm. The heart tube consists of an acellular jelly separating 2 concentric tubes of endocardium and myocardium. Between 7.5-11.0dpc septation and valve formation take place and a recognisable 4-chambered contractile organ is formed.

In *in vitro* studies of cardiac culture systems, in contrast to the usual growth inhibitory effects, TGFβs 1 and 2 are both able to induce differentiation of cardiac muscle (Parker *et al.*, 1991 & Muslin & Williams, 1991). The addition of TGFβ1 or 2 to ES cells in culture can induce the formation of cardiac and skeletal muscle. TGFβ2 can also increase the beating rate of the cardiac muscle (Slager *et al.*, 1992).

As previously described, expression studies have shown that TGFβs 1 and 2 RNA are both detectable in the developing murine cardiac mesoderm from 7.0dpc onwards. By 8.0dpc TGFβ1 expression has localised to the endocardium, while TGFβ2 is detected in the myocardium. This distinct pattern continues, but by 8.5-9.5dpc the expression of both isoforms is restricted to the outflow tract (OFT) and atrioventricular (AV) regions. This is the period when endothelial cells from the AV canal and OFT become capable of mesenchymal transformation and migrate into the underlying cardiac jelly leading to septation and formation of valves (Akhurst *et al.*, 1990; Dickson *et al.*, 1993). It has been postulated that TGFβs 1 and 2 form a co-operative signal which induces the formation of cushion tissue: Autocrine TGFβ1 modulates the ECM to allow migration of enothelial cells into the cardiac jelly forming cardiac cushion tissue; whilst a paracrine TGFβ2 signal emanates from the myocardium and induces an endothelial-mesenchymal transition in the cardiac cushion tissue, enabling valve

formation and septation (Runyan & Markwald, 1983; Akhurst *et al.*, 1990 & Dickson *et al.*, 1993).

Expression of all 3 TGFβ isoforms becomes restricted later in cardiac development. TGFβ3 is expressed transiently at the base of the valves at 14.5-16.5dpc in mesenchymal condensations (Millan *et al.*, 1991). TGFβ2 is undetectable in the heart after 17.5dpc whereas TGFβ1 continues to be expressed in the endocardium until 7 days post partum (dpp) (Pelton *et al.*, 1991 & Millan *et al.*, 1991). In the adult mouse, TGFβ1 is expressed in the myocardium and can control the expression of a number of cardiac-specific genes (Roberts *et al.*, 1981 & Parker *et al.*, 1990). The expression of TGFβ1 is upregulated in response to mechanical load, infarction and adrenergic agonists (Thompson *et al.*, 1988, 1989 & Bhambi & Eghbali, 1991). Thus, all 3 isoforms of TGFβ appear to be involved in many aspects of cardiogenesis, however TGFβ1 also has a key role in the maintenance of the normal adult heart.

1.5 Generation of Mutants in the Analysis of Gene Function.

1.5.1 Introduction.

Despite a wealth of information regarding the distribution of a protein and/ or its mRNA during development and during different situations in the adult animal, the exact function of a gene can only be assumed. However, the relative ease of genetic manipulation of the mouse allows the researcher to modify the genome by ablating or modifying target genes. The production of single, then double and triple knock-outs (as well as 'knock-ups'; whereby the expression level of a gene is upregulated, and 'knock-ins'; when the targeted sequence of a gene is replaced by that of another) and the advent of tissue-specific and inducible mutations are powerful tools in the study of mammalian gene expression and can provide a complementary approach to more longstanding molecular techniques (see Brown & Jones, 1996; Barinager 1994 & Takahashi *et al.*, 1994 for review articles).

The mouse was the mammal of choice studied by early geneticists because of its small size, ease of maintenance, resistance to infection, large litter size and rapid generation time. Also, natural variants and mice with spontaneous mutations mainly affecting coat-colour and behaviour were well-characterised and readily available from mouse breeders. Examples of these; the *albino* and *pink-eyed dilute* mutants, were used in the

first experiments demonstrating Mendelian inheritance and linkage by J.B.S. Haldane and his contemporaries in the early twentieth century. These spontaneous mutants and variants also proved valuable in more recent studies. For example, the *Dominant white spotting* (*W*) and *Steel* (*Sl*) pigmentation mutants were found to be caused by mutations in genes encoding a transmembrane tyrosine kinase receptor, *c-kit* (Chabot *et al.*, 1988 & Geissler *et al.*, 1988) and its ligand, Steel factor (Anderson *et al.*, 1990 & Zsebo *et al.*, 1990), respectively. These proteins play a major role in the growth and survival of melanocytes, primordial germ cells and haematopoietic cells.

1.5.2 The Use of 'Forward Genetics'.

More recently, geneticists have employed artificial means of generating murine mutants for research. Large numbers of mice are subjected to a mutagenesis study i.e. systematically exposed to potent mutagens such as x-rays and chlorambucil, both known to produce large deletions; or to the alkylating agent N-ethyl-N-nitrosourea (ENU) best for producing point mutations. The mice and their progeny are then screened for interesting phenotypic defects and the causative lesions examined. This process is known as 'forward genetics' i.e. working from phenotype to gene.

An example of a successful ENU mutagenesis project is the investigation of the circadian rhythm '*Clock*' mutation in mice (Vitaterna, *et al.*, 1994). Over 300 C57BL/6J mice were treated with ENU and their wheel-running patterns analysed. Normal mice have a set circadian pattern of exercise. One mouse which exhibited abnormal wheel-running patterns was isolated and analysed. From the homozygous mutant progeny of this founder, it was clear that the mutation regulated the length of the circadian period and the persistence of circadian rhythm. The *Clock* mutation was rapidly mapped by linkage analysis.

1.5.3 The Use of 'Reverse Genetics'.

The relative ease with which the mouse genome can be manipulated has permitted the use of transgenic animals as a means of studying gene expression: That is, transmissable mutations can be produced in the mouse genome by the replacement of a gene of choice with a segment of exogenous DNA. The DNA introduced into the genome may be an entire cloned gene, a cDNA, or a region of a gene which has been mutated *in vitro*. The biological consequences of these induced mutations are of great

interest to the researcher; thus 'reverse genetics', working from the targeted mutation of a gene to the resulting phenotype, has become commonplace within the last six years.

Since the TGFβ1 knockout mice used in this project were generated by gene transfer into embryonic stem (ES) cells this method of gene manipulation *in vivo* will be described in detail below:

ES cells are totipotent. They are derived from the inner cell mass (ICM) of the blastocyst and can re-integrate into the ICM of another blastocyst. ES cells can be maintained in an undifferentiated state *in vitro*, hence, while in culture, modified DNA can be transfected into the cells. Once genetically modified, the ES cell is injected into the ICM of another blastocyst which is then transferred to the uterus of a pseudo-pregnant host mother and allowed to develop to term. If the exogenous DNA has integrated into the genome, the resulting offspring will be chimeric, and, if the chimeras contain the mutation in their germ line, the mutation will be transmitted to the next generation. The phenotype of heterozygous and homozygous mutant progeny should provide evidence for the function of the gene *in vivo*. Also, where questions of functional redundancy between co-expressed proteins have arisen, the problem can be addressed by intercrossing single knockouts to create double and triple knockouts (see Melton, 1994 & Hogan *et al.*, 1994 for an overview of transgenic mouse production).

Random integration of the exogenous DNA into the genome in transgenic mouse production may cause additional unquantifiable phenotypic effects, thus a process of gene targeting via homologous recombination is employed. However, the incidence of random integration is still very high. To identify recombinants, a neo cassette is included in the targeted cDNA. This will provide resistance to neomycin to any cell with intergration and expression of the transgene. To differentiate between random and homologous recombination events, the herpes simplex virus thymidine kinase (HSV-TK) gene is placed at one or both ends of the targeted cDNA construct. The HSV-TK gene is removed if the cDNA integrates at its homologous site, and therefore is continuously expressed if the construct has integrated randomly. HSV-TK makes the cell sensitive to the drug gancyclovir; thus, only homologous recombinants will survive exposure to gancyclovir (Frohmann & Martin, 1989) (see Figure 4 for a schematic example).

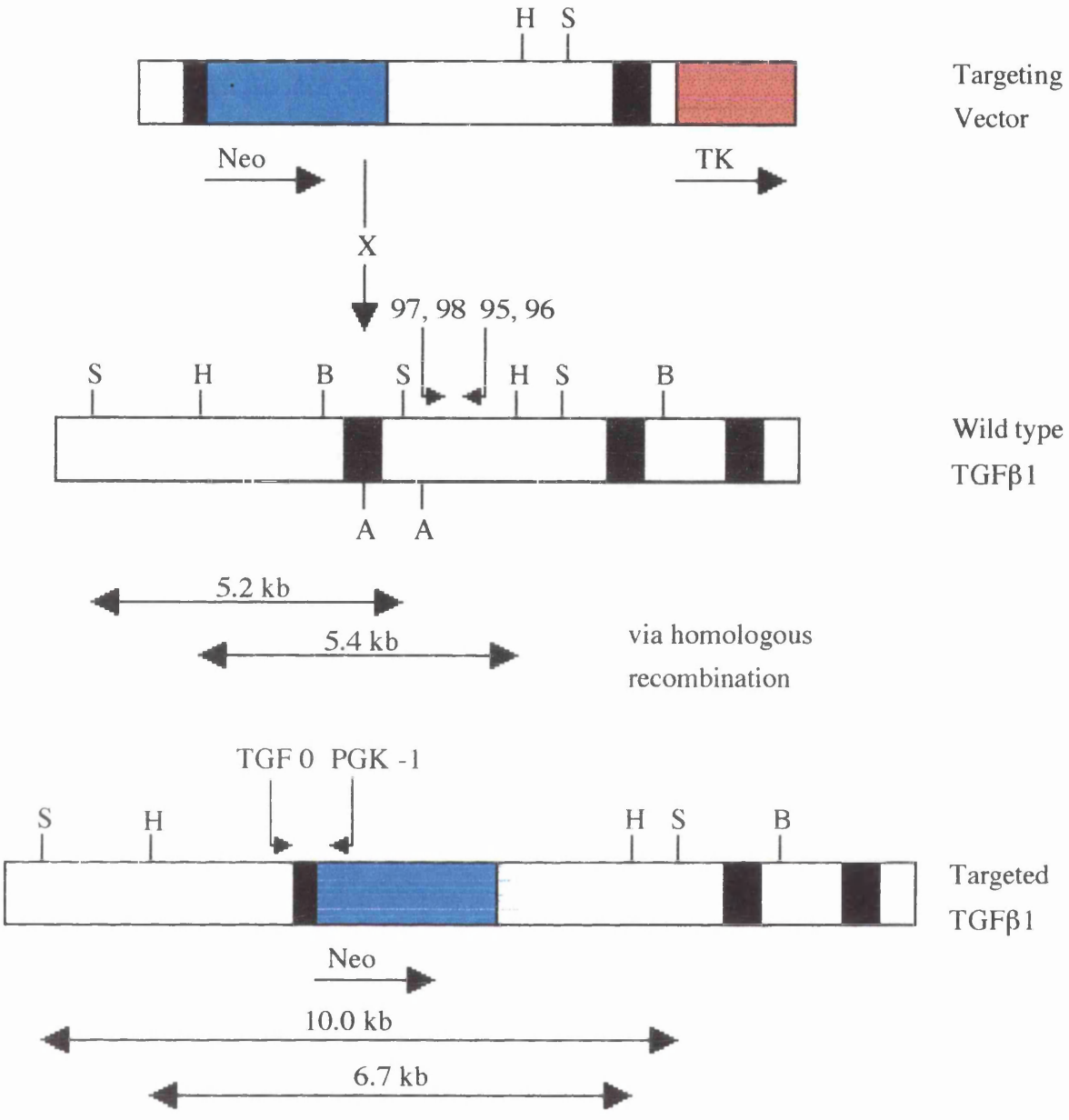

Figure 4. Targeted Disruption of Exon 1 of the TGFβ Gene.

A schematic representation of the targeting vector, the wild type TGFβ1 allele and the predicted disrupted TGFβ1 allele are shown above. The black boxes show exons, the open boxes indicate introns and promoterless regions. The neomycin (Neo) resistance/ HSV-TK (TK) sensitivity selection system was used to isolate the ES cells which contained the transgene in the desired selection site (see Introduction 1.5.3).

95, 96, 97 and 98 indicate the nested set of PCR primers used routinely to amplify the TGFβ1 wild-type allele, whereas TGF 0 and PGK -1 are the PCR primers used to amplify the TGFβ1 null allele. Their annealing sites are indicated by arrows. The difference in the size of the *Sac* I (S) and *Hind* III (H) fragments in the wild type and targeted alleles are shown by double-headed arrows.

A major disadvantage of creating knockout mice in the above manner is that the protein is removed completely from the animal from the outset of development. If the mutation is lethal any study of the knockout at later stages of development is precluded. Thus, methods for controlled expression of transgenes have been developed. For example, if transgenic mice carrying the P1 bacteriophage Cre recombinase under the control of a tissue-specific regulatory element are crossed with a line of mice in which *lox*P recombination sites have been inserted in the genome; such as either side of the targeted gene. The Cre lines up the *lox*P sites and removes the intervening DNA leaving one *lox*P site behind (Lasko *et al.*, 1992)(see Figure 5). Lasko *et al.* (1992) generated mice which carried a lens-specific αA-crystallin promoter followed by a stop codon flanked with *lox*P sites, this was followed by a SV40 T antigen coding sequence. When these animals were mated with Cre mice, the stop codon was excised and the dormant T antigen was activated, resulting in mice with lens tumours. A similar method involving yeast FLP recombinase which recognises FRP sites has also been described (O'Gorman *et al.*, 1991).

Both the Cre/ *lox*P and the FLP/ FRP systems are useful in creating tissue-specific mutations. However, there is no temporal control over the expression of the modified gene. A system has been developed whereby a transgene may be switched on throughout the animal at any developmental stage for a controlled period. The exogenous DNA is introduced into the mouse genome under the control of the repressor of the tetracycline -resistance operon from *E. coli* (*tet*). The *tet* transgenic is mated with a mouse containing the activating domain of viral protein VP16 of herpes simplex virus tetracycline-controlled tetracycline trans-activator protein (tTa). In the resulting double transgenics, the tTa binds to the *tet* operator sequences in the absence of tetracycline, thereby activating transcription of the gene. However, transcription is not permitted in the presence of tetracycline since, in this circumstance, the tTa does not bind to the *tet* operator sequence (Furth *et al.*, 1994). Thus tetracycline must be routinely administered to the double transgenics in order to repress transcription of the exogenous sequence. Tetracycline is not toxic at the concentration required for control of transcription, but may require titration to adequately repress the expression of the transgene (G. O'Neill, pers. comm.). Therefore, the use of a tetracycline-responsive binary system, either systemically, or with a Cre/ *lox*P or FLP/ FRP tissue-specific system could answer many of the unanswered questions of mouse genetics.

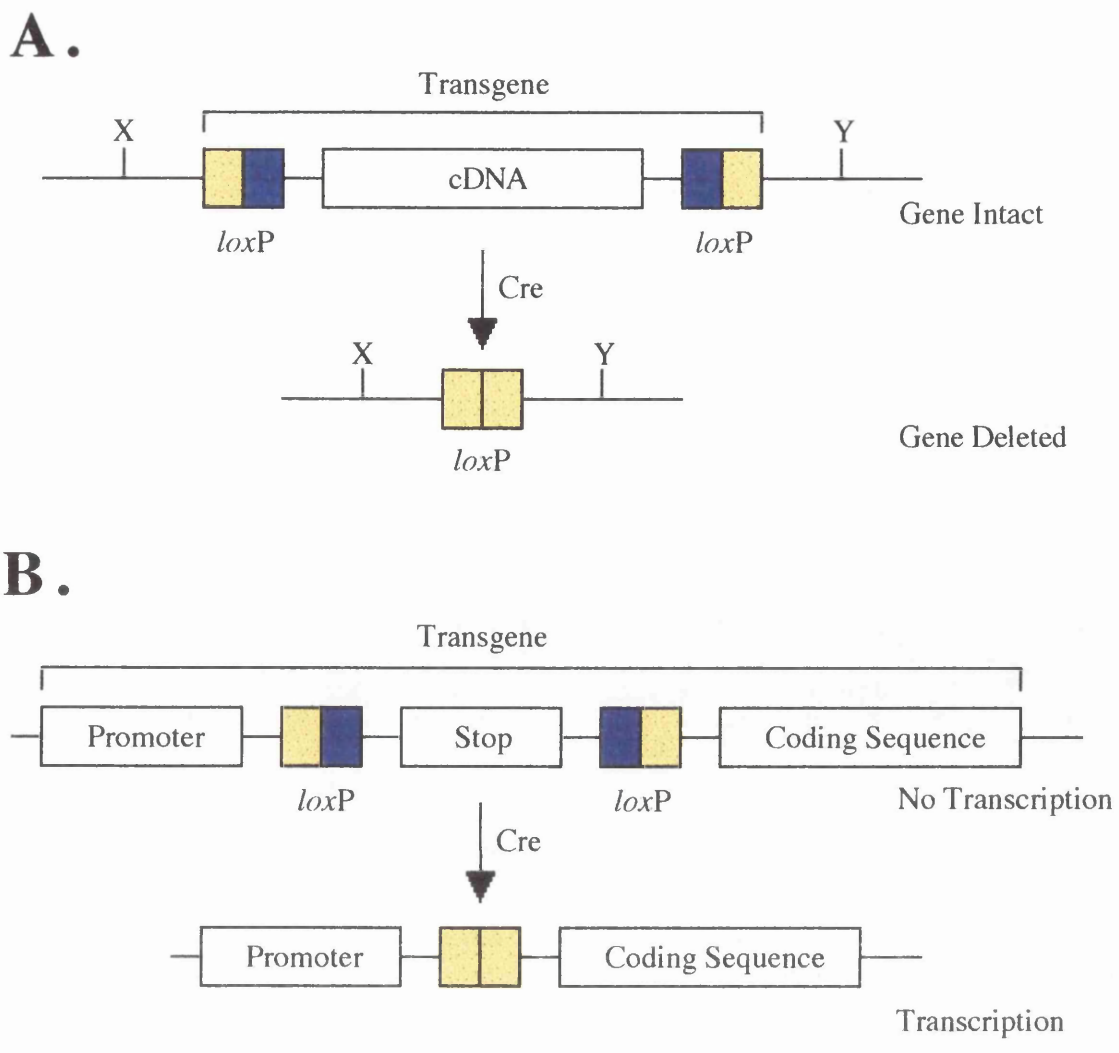

Figure 5 - A Schematic Representation of the Use of the Cre/*lox*P System in Transgenic Mice.

Cre is a recombinase from *E. coli* which recognises *lox*P sites in the genome. By mating transgenic mice which carry the Cre gene with mice that have *lox*P sequences, the Cre/*lox*P system can be used as a control switch in gene induction and ablation. A) shows an example of Cre being used to excise a *lox*P-flanked sequence from the genome. In B) expression of the gene is permitted by the excision of the stop codon via the Cre/*lox*P system.

X and Y are random sites within the genome.

1.6 TGFβ Knockout Mice.

1.6.1 TGFβ1 Knockout Mice.

Two independent groups have generated TGFβ1 knockout mice. The endogenous TGFβ gene was disrupted by the insertion of a neo-cassette into exon 6 (Shull *et al.*, 1992), and exon 1 (Kulkarni *et al.*, 1993) (see Figure 4). Lines of mice able to transmit a copy of the TGFβ1 knockout allele were bred from chimeric founder animals. Both groups reported that a proportion of TGFβ homozygous null (TGFβ1 -/-) animals were born and survived to 3 weeks of age. These animals were indistinguishable from their littermates until 10-14 days post-partum (dpp), whereafter they became noticeably runted and displayed a hunched posture and dishevelled coat. 1-2 weeks later these mice were severely wasted and died. Post-mortem investigations revealed no major malformations. However, Shull *et al.* (1992) reported that the TGFβ1-/- animals had fewer Peyer's patches and smaller spleens compared to TGFβ1+/+ littermates. Histological analysis by both groups revealed that the cause of death appeared to be an infiltration of lymphocytes and macrophages resulting in secondary necrosis in many organs, including the heart, lungs and stomach. Since no evidence was found of pathogens it was concluded that death resulted from an autoimmune disorder. This was in concordance with previous work which had suggested that TGFβ1 was a negative regulator of the immune system (Racke *et al.*, 1991).

Further investigation (Geiser *et al.*, 1993) showed that there was an increase in major histocompatability (MHC) Type II gene expression in infiltrated TGFβ1-/- tissues prior to the inflammatory response. MHC Type II molecules are expressed on a limited number of cells involved in antigen presention to T-helper cells. In autoimmune diseases immune activity is directed against cells inappropriately expressing MHC class II molecules. These results suggest that TGFβ1 may downregulate the expression of MHC Type II molecules *in vivo*.

Dickson *et al.* (1995), described the TGFβ1 knockout phenotype at mid-gestation. The knockout allele (Kulkarni *et al.*, 1993) was bred onto a mixed genetic background (12.5% 129/Sv/ Ola, 33.5% C57BL/6J/ Ola, 50% NIH/ Ola) and the resulting embryonic phenotype characterised. The results were as follows: All of the severe abnormalities observed in TGFβ1+/- and TGFβ1-/- conceptuses at 9.5dpc were

restricted to extra-embryonic tissue and involved defects of vasculogenesis and/or haematopoiesis. Any embryonic defects observed were thought to be secondary effects of the yolk sac phenotype. Genotype and phenotype analysis at different developmental stages led to the conclusion that 50% TGFβ1-/- and 25% TGFβ1+/- embryos died at around 10.5dpc as a result of yolk sac insufficiency. All of the TGFβ1-/- animals which survived to birth died at 3 weeks post-partum due to a massive inflammatory reaction. Reciprocal TGFβ1+/- x TGFβ1+/+ crosses showed a statistically significant 20% loss of TGFβ1+/- pups when the mother was TGFβ1+/-. However, this loss was rectified when 2-cell stage preimplantation embryos from TGFβ1+/- intercrosses were transferred into wild-type pseudo-pregnant females. It was therefore concluded that the maternal genotype influenced the ability of a TGFβ1 knockout conceptus to survive *in utero* (Dickson *et al.*, 1996).

Further evidence that the maternal environment influences the TGFβ1-/- phenotype exists. It is known that murine maternal circulating TGFβ1 can cross the placenta, and is also detectable in milk. Letterio *et al.* (1994) reported that TGFβ1 protein was detectable by immunohistochemistry in TGFβ1-/- embryos from TGFβ1+/- intercrosses *in utero*, but was not present in TGFβ1-/- conceptuses from a TGFβ1-/- mother. Thus, on some genetic backgrounds maternal sources of TGFβ1 are sufficient to support the TGFβ1-/- animal through development to weaning. In the 2 reported cases of a litter being born to a surviving TGFβ1-/- mother (crossed with a TGFβ1+/- stud), the resulting TGFβ1-/- phenotype increased in penetrance and severity (Letterio *et al.*, 1994 & Dickson *et al.*,1995). The embryos died at around 9.5dpc with cardiac as well as extraembryonic defects. It is unclear whether the reported cardiac abnormalities were a primary effect of a reduction in TGFβ1, or a secondary effect of yolk-sac insufficiency.

1.6.2 TGFβ3 Knockout Mice.

Two independent groups have generated TGFβ3 knockout mice by the targeted disruption of exon 6 of the gene (Proetzel *et al.*, 1995 & Kaartinen *et al.*, 1995). Both groups report that the expected numbers of TGFβ3-/- animals were born. These pups were noted to be unable to suckle at 4 hours post-partum. They rapidly become cyanotic and dehydrated and died within 24 hours of birth. Post-mortem analysis revealed the cause of death to be defective development of the palate and delayed pulmonary development. Proetzel *et al.* (1995) also presented evidence that there was a variable expressivity of the cleft palate phenotype in the three inbred strains studied.

The most severe cleft palate phenotypes were observed on a C57BL/6J genetic background.

Mammalian palatogenesis occurs between 14.5 and 18.5dpc. The developing palatal shelves must elevate and the medial edge epithelium (MEE) of both adhere. The resulting epithelial seam is eliminated forming a seamless mesenchymal shelf separating the oral and nasal cavities (Ferguson, 1988). Previously, expression studies have suggested a crucial role for TGFβ3 during palatogenesis, specifically in the MEE (Fitzpatrick et al., 1990 & Pelton et al., 1990). *In vitro* organ culture studies have shown that TGFβs 1 and 2 accelerate palatal shelf fusion, but antibodies to TGFβ3 block the fusion process altogether (Brunet et al., 1995). The defects seen in the TGFβ3-/- neonates appears to be due to inadequate fusion between the palatal shelves. However it is not known whether this is due insufficient expression of ECM molecules or defects in epithelial-mesenchymal transition. It is noteworthy that the phenotypes of the TGFβ1 and TGFβ3 knockout animals indicate no overlap in their essential function.

1.6.3 TβR-II Knockout Mice.

Recently, Oshima *et al.*, (1996) reported the phenotype of TβR-II knockout mice on an unspecified genetic background. A truncation mutation was introduced by homologous recombination upstream of the TβR-II cytoplasmic serine/ threonine kinase domain. This design allowed normal ligand-binding, but prevented signal transduction.

When TβR-II+/- mice were intercrossed, no TβR-II-/- pups survived to birth. No TβR-II+/- conceptuses were affected. Upon gross morphological inspection, 8.5dpc TβR-II-/- conceptuses were identical to their littermates, however, by 9.5dpc the TβR-II-/- yolk sacs exhibited severe anaemia. No live TβR-II-/- embryos were observed at 13.5dpc. Histological analysis of the 9.5dpc TβR-II-/- yolk sacs revealed detatchment of tissue layers resulting in distended capilliary vessel formation. This was noted to be similar to the vascular phenotype seen by histology in TGFβ1 knockout conceptuses at 9.5dpc by Dickson *et al.*, 1995.

In order to assess the developmental potential of TβR-II cells, Oshima *et al.* (1996) also generated eight chimeric mice from a TβR-II-/- ES cell line. The extent of chimerism was estimated by coat colour contribution and thought to be <5%,

suggesting that high-contribution chimeras died *in utero*. The chimeras were indistinguishable from normal littermates at birth, but exhibited a severe wasting phenotype at 2 weeks post-partum similar to TGFβ1-/- animals which survive to birth (Shull *et al.*, 1991; Kulkarni *et al.*, 1992). A number of different congenital abnormalities were observed i.e. anopthalmia, cystic kidney, and hydrocephalus, however, it was impossible to determine the cell lineages to which the TβR-II-/- cells had contributed.

Unexpectedly, the phenotype of the TβR-II-/- embryos is strikingly similar to the reported TGFβ1 knockout phenotype. This implies that the earliest developmental stage where signalling via TβR-II is essential is 8.5-9.0dpc for haematopoiesis and vasculogenesis. Inducible TGFβ and TβR-I and II knockouts as well as an investigation of the phenotype of TβR-II-/- mice on other pure inbred strains are required to fully eludcidate the role of each TGFβ1 isoform and receptor in development.

1.7 Inbred Mouse Strains.

An inbred strain of mice is defined as one which has been maintained for more than 20 generations of brother-to-sister matings and is essentially homozygous at all genetic loci, except for mutations arising spontaneously (Altman & Katz 1979 & Morse, 1981). There are more than 400 inbred strains available today and most can be obtained commercially. A standardised nomenclature refers to strain, substrain and history and the different characteristics of each strain such as littersize and tumour-susceptibility are well documented.

Inbred mouse strains have rapidly become an important tool in the elucidation and mapping of modifier genes in disease models. Previously, several groups have noted strain-specific differences in severity and penetrance of mutant phenotypes (see Discussion for a detailed appraisal); for example, the TGFβ3 knockout (Introduction 1.6.2). Sufficient differences exist between inbred strains to enable the researcher to use mapping resources such as RFLPs and microsatellites in concert with statistical tools to investigate inter-strain polymorphisms with respect to specific knockout phenotypes and thus begin to dissect the genetic and environmental components of strain-specific phenotypes, for example, to identify modifier genes (Bonyadi *et al.*, 1997).

1.8 Project Aims.

1.8.1 A Strain-Specific Phenotype in TGFβ1-/- Mice?

Previously, this group had characterised the phenotype of mixed genetic background TGFβ1 knockout mice and identified the cause of pre-natal lethality as defects in extra-embryonic vasculogenesis and haematopoiesis (Kulkarni *et al.*, 1993 & Dickson *et al.*, 1995). Since the penetrance of the pre-natal lethal phenotype reported in this study was at odds with that published initially (Shull *et al.*, 1992 & Kulkarni *et al.*, 1993), the primary aim of this project was to analyse the expressivity and penetrance of the pre-natal phenotype associated with the TGFβ1 null allele on defined genetic backgrounds. To this end the TGFβ1 null allele was bred through 4 generations of mice onto 3 different genetic backgrounds ie. NIH/ Ola (NIH), C57BL/6J/Ola (C57) and 129/ Sv/ Ola (129) by F. Cousins. Defined intercrosses of those backgrounds i.e. F1 (reciprocal NIH x C57) and F2 (F1 x F1) were used as tools to better define the genetic and epigenetic factors acting.

In order to clarify the onset of pre-natal lethality; embryos from TGFβ1+/- intercrosses were scored at 9.5 and 11.5dpc using an objective scoring system and genotyped by PCR. The relationship between genotype and phenotype on each genetic background was analysed statistically and put in context with genotype data collected from neonates and mice at weaning. Histological, molecular and immunohistochemical attempts to define the cause of pre-natal death were made.

1.8.2 The Role of a Strain-Specific TGFβ1 Modifier in Pre-Natal Lethality.

Bonyadi *et al* (1997, in press) have shown that around 80% of the genetic variation seen between NIH and C57 mice in the TGFβ1 knockout phenotype is due to the action of a strain-specific modifier gene. That is, TGFβ1-/- animals homozygous for NIH derived alleles at this locus tend to survive to 3 weeks of age, whereas TGFβ1-/- embryos homozygous for C57 derived alleles at this locus die pre-natally. Since the data used in this study was generated using post-natal TGFβ1-/- animals, it was decided to investigate the associations between phenotype, genotype and strain-specific alleles of the modifier gene at 9.5dpc.

>260 9.5dpc F2 conceptuses were objectively morphologically scored, TGFβ1 genotyped by PCR and screened for the origin of the modifier gene alleles (C57 and/ or NIH) using microsatellite-based PCR primers. If there was no association between TGFβ1 genotype, the modifier genotype and severity of phenotype, there would be no deviation from the expected 1 : 2 : 1 ratio of normal embryos when the TGFβ1 genotype ratio and screening data were correlated and analysed using a χ^2 'goodness of fit' statistical test.

Chapter 2

MATERIALS AND METHODS.

All solutions used in the preparation and manipulation of nucleic acids were made using deionised water purified by a Millipore Milli-Q reagent grade water purification system then autoclaved. Glassware and plasticware for use with DNA was washed and autoclaved. Gloves were worn at all times. Sterile, disposable microfuge tubes and pipette tips were used in all experiments.

All glassware for handling RNA was washed thoroughly, rinsed in Milli-Q water and baked for a minimum of four hours at 180°C. Plasticware was submerged in Milli-Q water, treated with 0.01% Diethylpyrocarbonate (DEPC) in water for a minimum of 4 hours then autoclaved. Solutions for use with RNA were made exclusively for this purpose. They, with the exception of organic solvents and Tris based solutions, were Millipore-filtered and treated with 0.01% DEPC for a minimum of four hours, then sterilised by autoclaving.

2.1 Mouse Husbandry.

2.1.1 Introduction.

The TGFβ1 null allele was originally generated on a 129/Sv/Ev background (Kulkarni *et al.*, 1993). Previously, the TGFβ1 knockout mice were bred by this group to produce a mixed genetic background (50% NIH/Ola, 37.5% C57BL/6J/Ola, 12.5% 129/Sv/Ola) (Dickson *et al.*, 1995). For the purposes of this study the TGFβ1 knockout allele had been bred through four generations, i.e. to 93.75% purity onto either inbred NIH/ Ola (NIH), inbred C57BL/ 6J/ Ola (C57), or inbred 129/ Sv/ Ola (129) strains. All mice were obtained from Harlan Olac Ltd. UK.

F1 mice were generated by reciprocal intercrossing of NIH and C57 mice heterozygous for the TGFβ1 knockout allele. F2 mice were generated by intercrossing F1 mice heterozygous for the TGFβ1 null allele.

2.1.2 Collection of Embryos.

Embryos were harvested from natural timed pregnancies. Noon on the day of the vaginal plug was regarded as 0.5dpc. Pregnant females were sacrificed by cervical dislocation. A ventral incision in the body wall was made and the uterus dissected out into chilled Embryo Transfer Freezing (ET) Medium (Gibco BRL) by either D. Duggan, F. Cousins or S. Rusholme. Embryos for scoring, and those used for whole mount in-situ hybridisation, were dissected from the uterus and decidua in ET medium using watchmakers forceps and assessed using a modified version of Brown and Fabros' morphological scoring system (1981); see Tables 1 and 2. Embryos for genotyping were washed in fresh ET Medium to remove any residual maternal tissue. Genotyping was performed by PCR using genomic DNA extracted from a whole conceptus or halved embryo. Embryos genotyped by radioactive in-situ hybridisation were dissected free of the uterus only.

2.1.3 Collection and Screening of Pups.

Pups were harvested on the day of birth and sacrificed by decapitation by D. Duggan. Genotyping was done by PCR using genomic DNA extracted from washed tail tissue.

2.1.4 Screening Adult Animals.

Tail biopsies were performed on anaesthetised 3 week old mice at weaning by D. Duggan and F. Cousins. 0.5cm of tail tissue was removed using a hot, sterile scalpel blade. Genomic DNA was isolated for the purpose of genotyping by PCR.

Tables 1 and 2. An Objective Morphological Scoring system for Mid-Gestation Conceptuses.

These tables detail a modified version of a morphological scoring system devised by Brown and Fabro (1981). It has been expanded specifically in the range of 0-41 somites in order to characterise fully and as objectively as possible the variation of the precise developmental stage of 9.5dpc conceptuses used in this study. Scoring using Table 1 provides 'score 1', a detailed analysis of key features, and therefore should enable the user to gauge accurately the precise developmental stage of a conceptus. Table 2 was devised as a means to objectively and quantitatively assess the range of defects commonly occurring in TGFβ1 knockout mice, and provides 'score 2'. Defects noted not encompassed by Table 2 were also recorded. Prior to genotyping, representative conceptuses from each litter were photographed. Scores 1 and 2 were used as a tool to compare the relative developmental stage and phenotype of all conceptuses studied (see Results).

Table 2.

	0	1B	2B	3B
YS VESSELS	NORMAL	MAIN VESSELS PRESENT BUT NO BRANCHING	INADEQUATE MAIN VESSELS AND /OR PERSISTENT BLOOD ISLANDS	AVASCULAR YOLK SAC
ANAEMIA	NORMAL	EMBRYO ANAEMIC +/++/+++	YOLK SAC ANAEMIC +/++/+++	EMBRYO AND YOLK SAC TOTALLY ANAEMIC +/++/+++
BLOOD LEAKAGE	NORMAL	FAINT LEAK IN YOLK SAC OR EMBRYO	HAEMORRHAGE IN YOLK SAC OR EMBRYO	HAEMORRHAGE IN YOLK SAC AND EMBRYO
ALLANTOIS	NORMAL	ALLANTOIS EMPTY, OR CONTAINING CLOTS OR LUMPS	ALLANTOIS ABNORMAL AND /OR CHORION SWOLLEN	FAILURE TO MAKE A CHORIO-ALLANTOIC CONNECTION
NECROSIS	NORMAL	EMBRYONIC HEART NOT BEATING	EMBRYO STARTING TO APPEAR NECROTIC	EMBRYO AND YOLK SAC DISINTEGRATING
IMMATURITY	NORMAL	0.25 DPC RETARDED	0.5DPC RETARDED	0.75DPC+ RETARDED
HEART DEFECTS	NORMAL	PERICARDIUM SWOLLEN	PERICARDIAL HAEMORRHAGE	PERICARDIUM SWOLLEN WITH HAEMORRHAGE

Table 1.

	0	1A	2A	3A	4A	5A
YOLK SAC CIRCULATION	NO VISIBLE, OR SCATTERED BLOOD ISLANDS	CORONA OF BLOOD ISLANDS WITHOUT ANASTAMOSES	CORONA OF BLOOD ISLANDS WITH ANASTAMOSES	VITELLINE VESSELS WITH FEW YS VESSELS	FULL PLEXUS OF YS VESSELS	YOLK STALK OBLITER-ATED, VITELLINE VESSELS SEPARATED
FLEXION	VENTRALLY CONVEX	BEGINNING TO TURN	MID-TURN	END OF TURN	DORSALLY CONVEX	DORSALLY CONVEX WITH A SPIRAL TORSION
HEART	ENDOCARDIAL RUDIMENT NOT VISIBLE, OR VISIBLE AND NOT BEATING	BEATING 'S' SHAPED CARDIAC TUBE	CONVOLUTED CARDIAC TUBE	BULBUS CORDIS, ATRIAL AND VENTRICULAR COMMUNIS	SEPTUM DIVIDING ATRIAL COMMUNE	
BRANCHIAL BARS	NONE VISIBLE	I VISIBLE	I AND II VISIBLE	I, II AND III VISIBLE	II OVERGROWING AND OBSCURING III	
ALLANTOIS	PRIMARY ALLANTOIS FREE IN EXOCOELOM	MIDSIZED ALLANTOIS FREE IN EXOCOELOM	LARGE ALLANTOIS FREE IN EXOCOELOM	ALLANTOIS FUSED WITH CHORION	UMBILICAL VESSELS	SEPARATE AORTIC ORIGINS OF UMBILICAL AND AORTIC VESSELS
FORELIMB BUD	NO SIGN OF FORELIMB BUD	NO SIGN OF FORELIMB BUD	DISTINCT EVAGINATION AT LEVEL OF SOMITES 7-11	FORELIMB BUD	PADDLE-SHAPED FORELIMB BUD	DISTINCT APICAL RIDGE ON FORELIMB BUD
SOMITE NUMBER	0-6	7-13	14-20	21-27	26-34	35-41
CAUDAL NEURAL TUBE	NEURAL PLATE OR FOLDS	CLOSING UNFUSED NEURAL FOLDS	NEURAL FOLDS FUSED AT SOMITES 4/ 5	POSTERIOR NEUROPORE OPEN	POSTERIOR NEUROPORE CLOSING	POSTERIOR NEUROPORE CLOSED
OPTIC SYSTEM	NO OPTIC DEVELOP-MENT	SULCUS OPTICUS	ELONGATED OPTIC PRIMORDIUM	PRIMARY OPTIC VESICLE WITH OPEN OPTIC STALK	INDENTED LENS PLATE	LENS POCKET OR LENS VESICLE

2.2 General DNA and RNA Methods.

2.2.1 Ethanol Precipitation of DNA and RNA.

Both DNA and RNA samples were precipitated by the addition of sodium acetate pH5.5 to a final concentration of 3mM plus 2 volumes of 100% ethanol for DNA, 3 volumes for RNA. Tubes were shaken and left at -20°C for at least 1 hour or incubated on dry ice for 20 minutes. The nucleic acid was pelleted by centrifugation in a benchtop microfuge for 20 minutes. The pellet was washed twice in 70% Ethanol and air-dried, then completely resuspended in a suitable volume of Tris-EDTA (TE) (10mM Tris HCL pH 8.0, 1mM EDTA).

2.2.2 Agarose Gel Electrophoresis.

A 0.8-2.0% agarose solution was made up in 1 x TAE buffer (0.04M Tris-acetate, 1mM EDTA pH 8.0) and dissolved in a microwave; Ethidium Bromide (EtBr) was added to a final concentration of 0.5μg/ml. The agarose mixture was poured into a horizontal gel mould and allowed to set at room temperature in a fume hood. DNA samples were mixed with 10% volume of gel-loading buffer (50% glycerol, 1% bromophenol blue, 10mM sodium phosphate pH7.0) and loaded into wells. Gels were run at approximately 7V/ cm inter-electrode distance in TAE buffer containing 0.5μg/ml EtBr. An appropriate size marker (Gibco) was run alongside the PCR samples, the bands were visualised on a UV transilluminator and photographed.

2.2.3 Intermediate Melting Temperature Agarose Gel Electrophoresis.

A high-resolution gel was required to distinguish between products from the screening PCR for *D5Mit268*. 4% Metaphor (Flowgen) intermediate melting point agarose was added to an appropriate volume of chilled 1 x TAE buffer whilst the solution was stirred. The mixture was tared on a balance then heated at 70% power in a microwave for several 20 second bursts. The solution was mixed gently between bursts. Once the agarose was completely melted and the solution cooled to approximately 60°C, hot distilled water was added to return the mixture to its initial weight. 0.5μg/ml EtBr was added and the agarose solution poured into a gel casting kit to a depth of 3-5mm. The gel was allowed to set at room temperature, then chilled at 4°C for a minimum of 30 minutes.

Gels were run in 1 x TAE buffer containing 0.5μg/ml EtBr at a 6V/ cm interelectrode distance until the loading buffer dye front had travelled at least 60% of the gel.

2.2.4 Restriction Endonuclease Digests of Plasmid DNA.

An appropriate amount of DNA, not exceeding 200μg/ml, was incubated with the required restriction enzyme(s) (Pharmacia) and OnePhorAll buffer (Pharmacia) at a concentration of at least 2 units/μg DNA according to the manufacturer's instructions. An aliquot of the completed digest was analysed with respect to an uncut sample by agarose gel electrophoresis, as previously described. 1μg/ml 1Kb ladder was run alongside the samples to confirm the band sizes.

2.2.5 Spectrophotometric Quantitation of DNA.

1μl of DNA solution was placed in a cuvette containing 999μl ddH_2O and the absorbance measured at a wavelength of 260nm. The machine was first zeroed with a ddH_2O blank.

The following were used to calculate the concentration of DNA in the sample: A solution containing 50μg/ml of double stranded DNA has an absorbance of 1 at a wavelength of 260nm. The optical density of a pure preparation of DNA has a E_{260}/E_{280} ratio $\geq$ 1.8. Oligonucleotide solutions have an absorbance of 1 corresponding to 33μg/ml at 260nm.

2.3 Isolation of DNA.

2.3.1 Transfection of Plasmid into Bacterial Cells.

100μl competent DH5α *E.Coli* cells (Stratagene) were transfected by the addition of 20-50ng plasmid DNA in a 1.5 ml Eppendorf tube. The mixture was incubated on ice for 30 minutes, then heat-shocked for 3 minutes at 42°C. The cells were allowed to recover for 5 minutes at room temperature before adding 800μl L-broth (1% bactotryptone, 0.5% yeast extract (Difco) and 0.5% NaCl in water at pH 7.5) and incubating at 37°C for 45 minutes. The cells were then briefly pelleted for 20 seconds in a microfuge, and all but 100μl of the supernatant poured off. The pellet was resuspended in the residual amount of L-broth and spread evenly onto L-agar plates (1.5% agar in L-broth) containing 50mg/ml ampicillin (Sigma) and allowed to dry. The plates were inverted and incubated at 37°C overnight.

2.3.2 Small Scale Extraction of Plasmid DNA.

A single bacterial colony was picked using sterile technique and used to inoculate 5 ml of L-Broth containing 50mg/ml ampicillin. This was cultured overnight at 37°C in an orbital shaker at 225 rpm. 1.5 ml of the overnight culture was microcentrifuged for 5 minutes, the supernatant discarded and the pellet resuspended in 100µl of Solution 1 (50mM glucose, 25mM Tris-HCl, 10mM EDTA pH8.0). 200ml of fresh Solution 2 (0.4M NaOH, 1%SDS) was added and inverted gently until the mixture cleared. The lysed cells were incubated on ice for 5 minutes. The solution was neutralised by the addition of 150ml Solution 3 (3M KOAc pH4.8), the tubes mixed gently, and then placed on ice for 30 minutes to precipitate the protein. The samples were microcentrifuged for 2-3 minutes before removing and retaining the supernatant. An equal volume of isopropanol was added to the solution and the tubes vortexed, then centrifuged at 14,000 rpm to precipitate and pellet the DNA. The supernatant was removed and the pellet resuspended in 50µl TE plus 50µg/ml RNase A. This was incubated at 37°C. After 30 minutes an equal volume of Tris-equilibrated phenol pH8.0 was added to the sample, mixed thoroughly and centrifuged for 5 minutes in a microcentrifuge. The aqueous phase was retained and added to an equal volume of 49 : 1 chloroform : isoamyl alcohol. This was mixed and microcentrifuged for 5 minutes and the aqueous phase removed to a fresh tube and ethanol precipitated as previously described.

The DNA was checked by a diagnostic restriction enzyme digest and its concentration was assessed using spectrophotometry.

2.3.3 Large Scale Preparation of Plasmid DNA.

Large scale extraction of plasmid DNA was carried out by a modifed alkali-lysis method as described in Sambrook *et al.*, 1989.

The bacteria containing the plasmid of interest was used to inoculate a subculture, i.e. 5ml of L-broth containing 50mg/ml ampicillin. This was cultured overnight at 37°C with orbital shaking at 225 rpm. The 5ml culture was used to inoculate 500 ml of L-broth in a 2 litre flask with 50mg/ ml ampicillin. The large scale culture was incubated overnight at 37°C with vigorous shaking (225rpm).

Mature bacterial cells were harvested by centrifugation (3,000 rpm, 10 minutes at 4°C) in a Sorvall RC-5B centrifuge with a GS-3 rotor. The supernatant was discarded and the pellet resuspended gently in Solution 1 (2ml/50ml culture) containing 10mg/ml freshly added

lysozyme (Sigma). The cell suspension was vortexed and incubated on ice for 5 minutes. Fresh Solution 2 was added (4ml/50ml culture) and inverted gently until the mixture cleared. The lysed cells were incubated on ice for 5 minutes. The solution was neutralised by the addition of Solution 3 (6ml/50ml culture) and the mixture inverted gently until a heavy white precipitate was formed, then incubated on ice for 30 minutes. This was centrifuged at 3,000 rpm for 10 minutes at 4°C to pellet the precipitated bacterial chromosomal DNA and protein. The supernatant was filtered through sterile gauze into a fresh 50ml screw-capped Sorvall polypropylene tube and the plasmid DNA was precipitated by the addition of 0.6 volumes of isopropanol. The sample was mixed thoroughly and the DNA was pelleted by centrifugation (Sorvall RC-5B centrifuge in a GSA rotor) at 10,000 rpm for 10 minutes at room temperature. The supernatant was discarded and the DNA resuspended in 10 ml 1 x TE; 50µg/ml RNAse A was added and the samples incubated at 37°C for 30 minutes. The DNA was phenol-chloroform, then chloroform extracted and preciptated with ethanol, as previously described.

The pellet was resuspended in 500µl 1 x TE and the concentration determined by spectrophotometry. Diagnostic restriction digests were used to confirm the identity of the plasmid and insert.

2.3.4 Extraction of Genomic DNA from Tail Biopsies.

Tail tissue was placed in 200µl Tail Lysis Buffer (100mM Tris-HCl pH8.5, 0.2% SDS, 5mM EDTA, 200mM NaCl) with 100µg/ml proteinase K (Sigma) and incubated at 55°C until the tissue was fully digested. Tubes were shaken and centrifuged for 10 minutes in a bench-top microcentrifuge to pellet the tail debris. The cell lysate was poured off into 1 volume of isopropanol, inverted and allowed to stand at room temperature for 15 minutes. Precipitated DNA was picked up using a clean pippette tip and placed in a fresh tube. The DNA was air dried and completely resuspended in 50µl of TE (10mM Tris pH8.0, 1mM EDTA).

The DNA solution was heated to 94°C for 10 minutes then chilled on ice and stored at 4°C before genotyping by PCR.

2.3.5 Extraction of Genomic DNA from Conceptuses.

Conceptus tissue was placed in 200µl Tail Lysis Buffer with 100µg/ml proteinase K and incubated at 55°C until the tissue was fully digested. Tubes were shaken and an equal

volume of phenol (Sigma) was added and mixed. This was microcentifuged in a bench-top centrifuge for 10 minutes whereupon the upper phase was removed to a fresh tube and an equal volume of 49 : 1 chloroform : isoamyl alcohol added and the mixture vortexed for 10 seconds. This was centrifuged for 5 minutes prior to the transfer of the upper phase to a fresh tube. The DNA was ethanol precipitated.

Genomic DNA from tails, pups and embryos was resuspended in 50µl sterile TE.

2.4 Genotyping and Screening by PCR.

2.4.1 Genotyping by PCR.

The genotype of embyos, pups and adult mice was determined by PCR analysis. All DNA used for PCR had previously been heated to 94°C for 10 minutes then chilled on ice and stored at 4°C before genotyping and/or screening.

3 pairs of primers were used simultaneously: Nested primers; 95, 96, 97 and 98 complementary to the first exon and the first intron of the TGFβ1 genomic sequence amplified the wild-type TGFβ1 allele; and 2 oligonucleotide primers; TGF 0 and PGK-1 complementary to the deleted portion of the first exon of the TGFβ1 and the Neomycin cassette amplified the null TGFβ1 allele (see Table 3 and Figure 6). Oligonucleotide primers were manufactured on an Applied Biosystems 391 DNA Synthesizer by E.O'Hare.

150-200µg of DNA and 1 unit *Tfl* (taq) polymerase (Cambio) were added to 25µl of premix containing 1 x PCR buffer (Cambio), 1.5mM $MgCl_2$ (Cambio) and 5mM dNTPs (Boehringer Mannheim). A layer of mineral oil (Sigma) was placed over the top of the reaction to prevent evaporation. PCR was carried out on a Perkin Elmer Cetus DNA Thermocycler. The protocol used consisted of cycles of the following sequential steps: Denaturation (95°C for 1 minute), annealing (61°C for 1.5 minutes), elongation (72°C for 2 minutes). An additional elongation step (72°C for 15 minutes) was implemented after completion of 28-33 cycles. 15µl of each PCR reaction was analysed by agarose gel electrophoresis on a 1.5% gel.

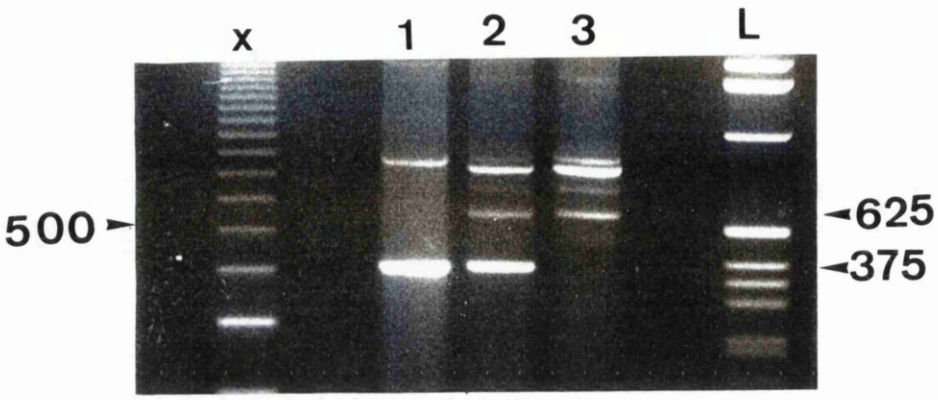

Figure 6 - Genotype Analysis of TGFβ1 Knockout Animals by PCR.

DNA extracted from TGFβ1 knockout embryos or tails was genotyped by PCR. Lanes 1, 2 and 3 each represent a separate PCR reaction. The premix used for TGFβ1 genotyping contained 6 primers; a nested set of 4 to amplify the TGFβ1 wild type allele (625bp), and a pair of primers to amplify the null allele (375bp). Thus, in the above panel, lane 1 is a sample from a TGFβ1-/-, lane 2 from a TGFβ1+/- and lane 3 from a TGFβ1+/+ animal. In all genotyping PCR reactions a negative (no DNA) and positive (non-transgenic DNA) control was assessed alongside the experimental PCR reactions.

L = 1 kb ladder.
X = 50 bp ladder

95	5'-GAG AGT AAG CCC ACT AGA G-3'
96	5'-CGT GCG CCT GTC GCT TTC TG-3'
97	5'-GCG GAC TAC TAT GCT AAA G-3'
98	5'-GGT CAC CCG CGT GCT AAT GG-3'
TGF 0	5'-AGG GAG CTG GTG AAA CGG AA-3'
PGK-1	5'-TCC ATC TGC ACG AGA CTA GT-3'

Table 3. Oligonucleotides for Genotyping TGFβ1 Transgenic Mice by PCR.

In order to genotype TGFβ1+/+, +/- and -/- animals by PCR, genomic DNA from whole conceptuses, half-embryos or tail biopsies was isolated and diagnostic fragments were amplified using a premix containing the above primers as detailed in Materials and Methods. Primers 95, 96, 97 and 98 comprise a nested set which amplify the wild type TGFβ1 allele (625bp). TGF 0 and PGK-1 amplify the null allele (375bp) (see Figure 6).

2.4.2 Screening for *D5Mit268* Alleles by PCR.

Genomic DNA from scored F2 embryos was analysed by PCR for the presence of either a C57 and/or NIH polymorphic allele using microsatellite *D5Mit268* primers (obtained from Research Genetics or synthesised in-house on an Applied Biosystems 391 DNA synthesiser by E. O'Hare). The PCR protocol used consisted of 33 cycles of the following sequential steps: Denaturation (95°C for 1 minute), annealing (55°C for 1.5 minutes), elongation (72°C for 1 minute). An additional elongation step (72°C for 15 minutes) was implemented after completion of 33 cycles. 5µl of the PCR reaction was analysed by electrophoresis. However, since the size differential between the NIH and C57 polymorphisms was only 20 nucleotides the PCR results were analysed on a 4% Metaphor intermediate melting temperature gel (see Figure 7).

2.5 Histochemistry.

2.5.1 Preparation of TESPA Coated Slides.

Sterile microscope slides for use in tissue sectioning were immersed for 30 seconds in 70% Ethanol, 10% HCl followed by sterile Milli-Q water, then 95% Ethanol. The slides were then baked at 150°C for at least 2 hours and allowed to cool before being dipped in a fresh 2% TESPA (3-aminopropyltriethoxysilane) (Sigma)/acetone solution, followed by four washes in 100% acetone and two washes in sterile Milli-Q water. The slides were dried at 42°C overnight and stored in dust-free boxes before use.

2.5.2 Preparation of Tissue for Embedding.

Conceptuses were dissected free of the uterus and fixed in ice-cold, fresh, filtered 4% paraformaldehyde (PFA) in phosphate buffered saline (PBS) for 6-20 hours. Fixation was carried out at 4°C with continuous rotation. Tissue was washed at 4°C in cold PBS (1 tablet/ 100 ml (Unipath) for 30 minutes, 0.85% saline for 30 minutes, 70% ethanol : 0.85% saline for 15 minutes, 100% ethanol : 0.85% saline twice for 15 minutes then 70% ethanol twice for 15 minutes. The tissue could be stored at this stage for an indefinite period. The conceptuses were processed through a Shandon Citadel automatic processor on a 24 hour cycle. This cycle comprised 100% ethanol, five washes in methanol, 100% ethanol, 50% ethanol : 50% chloroform, two washes in chloroform, one in xylene and finally two washes in paraffin wax. The embryos were embedded in paraffin wax in a known orientation and stored at 4°C.

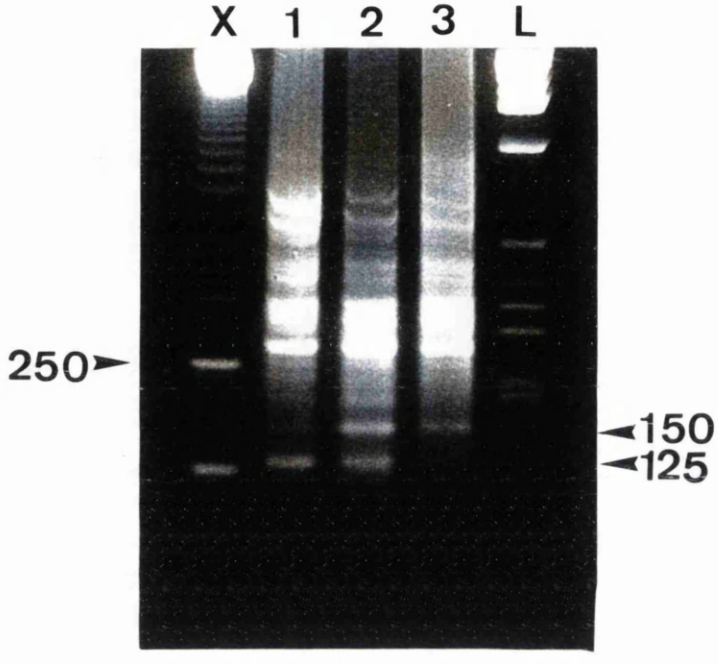

Figure 7 - Screening F2 TGFβ1 Knockout Mice for NIH and C57-Derived Alleles at *D5Mit268*.

DNA extracted from TGFβ1+/- and -/- embryos at 9.5dpc was screened for the presence of polymorphic NIH (150bp) and/ or C57 (125bp) -derived alleles at the chromosomal locus *D5Mit268* by PCR. Due to the small size differential, the PCR products were analysed on a 4% intermediate melting point agarose gel. Lane 1 shows the PCR result from a homozygous C57 (CC) embryo; lane 2 shows the PCR result from a heterozygous NIH/ C57 (NC) embryo and lane 3 shows the PCR result from a homozygous NIH (NN) embryo. In all screening PCR reactions a negative (no DNA) and positive (pure-bred C57 and NIH non-transgenic DNA) control was assessed alongside the experimental PCR reactions.

L = 1 kb ladder.
X = 50 bp ladder

2.5.3 Cutting Tissue Sections.

All tissue embedded in paraffin wax was placed in a microtome and 6μm serial sections cut. These were transferred as intact strips onto a clean microscope slide and floated on a 30% ethanol solution. Once the strip had fully extended it was carefully transferred to a water bath containing fresh Milli-Q water at 42°C. Sections were picked up using a clean non-TESPA coated microscope slide and checked using a stereo microscope. Suitable sections were re-floated and picked up with TESPA coated microscope slides and left to dry on a 42°C hot plate for at least four hours. Slides were stored at 4°C with dessicant in dust-free boxes.

2.5.4 Haematoxylin and Eosin Staining.

Slides were dewaxed twice in Histoclear^{TM} for 5 minutes then rehydrated in two, x 2 minute washes of 100% ethanol, followed by 2 minute immersions in an ethanol series comprising 90%, 80%, 70%, 50% and 30% ethanol in Milli-Q water. Sections were stained in filtered Harris' haematoxylin (Gurr) for 30 seconds, rinsed in running tap water for 1 minute. The stain was fixed in Scott's Tap water (20g $MgSO_4$, 20g $NaHCO_3$/ litre of water) and the slides rinsed in running water for 1 minute. Sections were stained in filtered eosin (5g yellowish eosin (Gurr), 50 ml saturated acetic picric acid, 400 ml water, 2.5g potassium dichromate, 50 ml 100% ethanol added in this order for a 500 ml stock solution; the stock was diluted 1 in 4.5 with water for a working concentration) for 30 seconds, then rinsed briefly in running water. The slides were immediately rehydrated and prepared for mounting as described in Materials and Methods 2.5.6).

2.5.5 May-Grunwald Geimsa Staining.

9.5dpc conceptuses were dissected free of maternal tissue using sterile watchmakers forceps and morphologically scored. The yolk sac was carefully torn and half the embryo removed for genotyping. The remains of the conceptus was used to generate blood smears, by gently daubing the open yolk sac and cut embryo onto a clean TESPA slide. The blood smears were quickly dried onto the slides using a fan, then fixed in methanol for 5 minutes. The slides were immersed in filtered May-Grunwald stain (BDH) (freshly diluted to 50% with buffered distilled water) for 6 minutes then transferred into Geimsa stain (BDH) (freshly diluted to 7.5% with buffered distilled water) for 8 minutes. This step was repeated and the slides washed rapidly in buffered distilled water (pH6.8) three times. The slides were then

allowed to stand in buffered distilled water for 1 minute to allow differentiation to take place. Slides were dried rapidly using a fan.

2.5.6 Preparation and Mounting of Slides.

After staining, the sections were dehydrated through an ethanol series in Milli-Q water (30%, 50%, 70%, 90%, 100%, 100%, 2 minutes each) then incubated in two baths of Histoclear^{TM}, 5 minutes each. Coverslips were attached in a fumehood using DPX mountant (Gurr). The mounted slides were left to dry overnight.

2.6 Immunohistochemistry

2.6.1 α Smooth-Muscle Actin Antibody Staining.

Tissue was sectioned and mounted onto TESPA-coated slides as described in Materials and Methods 2.5. The sections were dewaxed by immersion in Histoclear^{TM} twice for 10 minutes, then rehydrated in a descending series of washes; firstly 100% Ethanol twice for 5 minutes, then 2 minutes each in 90, 80 and 70% ethanol in Milli-Q water. Endogenous peroxidase activity was inhibited by a 15 minute immersion in methanol containing 4% H_2O_2, then the slides were washed three times in PBS. All washes were 5 minutes long unless otherwise stated. Non-specific binding of the antibody to the section was prevented by blocking the tissue for 30 minutes with 0.1% gelatin, 0.1% BSA (bovine serum albumin) (both Sigma) plus 2.5% sheep serum, 2.5% mouse serum (both Seralab) in PBS. Meanwhile, the primary (mouse anti-human α smooth-muscle actin monoclonal antibody) (Sigma A2547) and secondary (sheep anti-mouse) (Amersham RPN1001) antibodies were pre-blocked together at a ratio of 1 : 3 in 400ml PBS containing 0.1% mouse serum. This process took place at room-temperature with rotation for 90 minutes.

The pre-blocked antibody complex was applied to the tissue sections and incubated for 60-90 minutes at room-temperature in a moist chamber. The slides were washed three times in PBS and a presorbed avidin-biotin complex (Dako, ABC kit) was applied to the tissue. After a 30 minute incubation period, the slides were washed twice in PBS and incubated for 10 minutes in a solution of 3-3' Diaminobenzidene (DAB) (Sigma) (1 tablet dissolved per 15ml PBS, filtered and activated by the addition of 15ml H_2O_2 imediately prior to use). Finally, the slides were washed briefly in PBS, then running water for 10 minutes. The tissue is counter-stained lightly with haematoxylin for visualisation, and the slides are dehydrated and mounted (see Materials and Methods 2.5).

2.7. In Situ Hybridisation.

Table 4. Antisense Probes.

Mouse cDNA	Plasmid	Linearised by:	RNA polymerase	Probe length
ζ globin (Dickson *et al.*, 1995)	pGEM 3	*Eco* RI	Sp6	360bp
full-length TGFβ1 (Derynck *et al.*, 1986)	Bluescribe$^+$	*Hind* III	Sp6	1,254bp

Table 5. Sense Probes.

Mouse cDNA	Plasmid	Linearised by:	RNA polymerase	Probe length
ζ globin (Dickson *et al.*, 1995)	pGEM 3	*Bam* HI	T7	360bp
full-length TGFβ2 (Millan *et al.*, 1991)	Bluescribe$^+$	*Hind* III	T7	1,245bp

Tables 4 and 5. A Summary of Templates and Probes used for Whole-mount and Radioactive In Situ Hybridisation During this Project.

2.7.1 Radioactive In Situ Hybridisation.

2.7.1.1 Radioactive Riboprobe Synthesis.

In order to generate a ^{35}S-labelled riboprobe, the plasmid containing the insert of choice was linearised using appropriate restriction enzymes with respect to the T7, T3 and/or SP6 promoters (see Tables 4 and 5), ethanol precipitated and resuspended in clean 1 x TE at a known concentration. 1µg DNA template in 1µl TE was incubated at 37°C for 1.5-3 hours with the appropriate polymerase and reaction buffer (0.04M Tris-HCl pH 8.0, 8mM $MgCl_2$, 1 mM spermidine, 0.025M NaCl) (Gibco BRL) and 0.1mM DTT, 1mM ATP, CTP and GTP, 7.5mM UTP-S, 0.3mg/ml BSA (RNase and DNase free) (all Pharmacia) and 75µCi S^{35}UTP (Amersham) (dried into a RNase-free 1.5 ml eppendorf tube), 30 units RNAguard™ (Pharmacia) in a total volume of 20µl with DEPC water. The reaction was terminated by incubation with 0.15 units DNase1 in 1xDNase buffer (0.1M NaOAc pH 5.0, 5mM MgCl2, 10mM DTT (added fresh), 50 units RNAguard™ and 0.05mg polyA. The reaction mix was separated through a G50 sephadex nick-column (Pharmacia). The column was firstly equilibrated with 3 ml column buffer (0.3M NaOAc pH5.0, 10mM Tris-HCl pH 7.5, 1 mM EDTA pH 8.0. 0.1% SDS, 10 mM DTT (added fresh). The probe mixture was eluted through the column with 2 volumes column buffer and the final fraction retained. An equal volume of phenol pH 5.0 was added, mixed and microcentrifuged for 10 minutes. The aqueous phase was retained and extracted with an equal volume of chloroform : isoamyl alcohol (49 : 1). Three volumes of ethanol were added to precipitate the riboprobe. The RNA was pelleted by microcentrifugation for 15 minutes and the pellet washed twice in 70% ethanol in DEPC water. The riboprobe was resuspended in 100ml alkali digestion buffer (40 mM $NaHCO_3$ pH 10.2, 60mM Na_2CO_3, 10mM DTT (added fresh)) and alkali-digested for a predetermined time at 60°C.

The length of alkali-digestion is governed by the following equation (Cox *et al.*, 1984):

$$\text{Incubation time (minutes)} = (Lo - Li) / (0.11 \times Lo \times Li)$$

where Lo = Original length of riboprobe (Kb)
and Li = Required length of riboprobe (Kb)

The alkali digested probe was quenched on ice and 10µl 0.1M NaOAc pH 6.0, 0.05mg PolyA added before the sample was separated using a G50 sephadex nick column

(Pharmacia) as before. The eluted sample was extracted as before with phenol pH 5.0 and 49 : 1 chloroform : isoamyl alcohol before ethanol precipitation.

The pellet was resuspended in an appropriate volume of 50mM DTT calculated so that a 1 in 10 final dilution would result in a solution at 3 x 10^4 cpm/ µl . The 10 x stock solution of riboprobe was stored at -20°C for up to 14 days before use.

2.7.1.2 Pretreatment of Tissue Sections.

All pre and post-hybridiastion washes were performed using 250 ml glass troughs (Solmedia). Slides were held in a glass microscope slide carrier. All washes took place at room temperature unless otherwise stated.

Slides were dewaxed twice in Histoclear™ for 10 minutes then rehydrated in three, 2 minute washes of 100% ethanol, followed by 2 minute immersions in an ethanol series comprising 90%, 80%, 70%, 50% then 30% ethanol in Milli-Q water. The slides were equilibrated in 0.85% saline for 5 minutes and then immersed in PBS for 5 minutes. The tissue was refixed in fresh 4% PFA/ PBS for 20 minutes then washed twice in PBS for 5 minutes. The sections were incubated with 40µg/ml proteinase K in PKB (50 mM Tris-HCl pH 7.5, 5mM EDTA pH 8.0) for 7.5 minutes then washed for 3 minutes in PBS. This was followed by further fixation in 4% PFA/ PBS for 5 minutes. The tissue was acetylated in 0.1M triethanolamine with freshly added 0.2% acetic anhydride for 10 minutes then washed for 5 minutes in PBS followed by 0.85% NaCl. The sections were dehydrated by 2 minute washes in an ascending ethanol in Milli-Q water series (30%, 50%, 70%, 80%, 90% then 100%). The slides were left to air dry under cover at room temperature.

2.7.1.3 Hybridisation of Probe to Tissue Sections.

The riboprobe was applied to selected tissue sections at a 1 in 10 dilution (3 x 10^4 cpm/ µl) in a freshly made hybridisation mix comprising 0.3M NaCl, 10mM Tris-HCl pH 8.0, 5mM EDTA, 10mM NaPO4 pH 6.8, 10% dextran sulphate, 1 x Denhardts, 0.5 mg/ml tRNA, 0.5 mg/ml PolyA, 50 mM DTT. The hybridisation mixture and probe were mixed and heated to 80°C for 3 minutes and quenched on ice. 3-7µl of the riboprobe mixture was carefully pipetted onto individual tissue sections then covered with a coverslip. Coverslips were cut using a diamond pen in order to fit individual tissue sections. They were placed

carefully onto the sections to prevent air bubble formation and to protect the tissue. The slides were placed in a humid chamber containing a tissue soaked in 4 x SSC, 50% formamide and sealed with tape for hybridisation overnight at 55°C.

2.7.1.4 Post Hybridisation Washes.

Slides were transferred quickly to a glass slide holder, then washed sequentially in the following: 5 x SSC, 0.1% 2-mercaptoethanol for 15 minutes at 50°C; 2 x SSC, 50% formamide, 1% 2-mercaptoethanol for 20 minutes at 65°C; four, 10 minute washes at 37°C in RNase buffer (10mM Tris-HCl pH 8.0, 5mM EDTA, 0.5M NaCl) followed by a 30 minute incubation in RNase buffer plus 20μg/ml RNase A at 37°C then a 15 minute wash in RNase buffer; followed by 2 x SSC, 50% formamide, 1% 2-mercaptoethanol at 65°C for 20 minutes; 2 x SSC at 50°C for 15 minutes; then 0.1 x SSC at 50°C for 15 minutes. The sections were dehydrated in an ethanol series in Milli-Q water (50%, 70%, 90%, 100%) for 2 minutes each. The slides were allowed to dry in a dust-free environment then dipped for 10 seconds in a 0.1% gelatin, 0.01% chrome alum solution and allowed to dry before emulsion (Ilford) was applied.

2.7.1.5 Autoradiography.

All autoradiograpic procedures were carried out in darkroom conditions illuminated with Kodak 904 filtered light. Slides were dipped in a 45°C, 50% solution of Ilford K5 emulsion/ 1% glycerol. The emulsion was allowed to dry for 1.5-2 hours in a light-tight environment. Dry slides were stored in light-tight boxes with dessicant at 4°C prior to developing. The period of storage (7-14 days) was governed by the expression levels of the mRNA under investigation.

After the sections had been exposed for an appropriate period of time they were developed at room temperature by agitation in 20% Phenisol (Ilford) for 3 minutes, followed by 30 seconds in 1% acetic acid, then 30 seconds in Milli-Q water and fixed in a fresh 30% solution of sodium thiosulphate for 5 minutes. The developed slides were washed in cold running water for a minimun of 1 hour before staining.

2.7.1.6 Staining Radioactive In Situ Slides.

Slides were stained in filtered Harris' haematoxylin (Gurr) for 30 seconds, rinsed in running tap water for 1 minute. The stain was fixed in Scott's Tap water (20g $MgSO_4$, 20g

$NaHCO_3$/ litre of water) and the slides rinsed in runnng water for 1 minute. The slides were then prepared for mounting, see Materials and Methods 2.6.6.

2.7.2 Whole-Mount In Situ Hybridisation.

2.7.2.1 Preparation of Embryo Powder.

14.5dpc embryos were dissected free of maternal and extraembryonic tissue and rinsed in clean PBS. Using sterile forceps the embryos were cut into several pieces and transferred to an autoclaved homogeniser. The tissue was homogenised, and 4 volumes of ice-cold acetone were added. The homogenate was mixed and left on ice for 30 minutes. The mixture was aliquoted into 1.5 ml eppendorf tubes and microcentrifuged for 10 minutes at room temperature. The supernatant was removed, the pellet washed in ice-cold acetone and centrifuged again to re-pellet the tissue. The liquid was completely removed by careful pipetting, and the pellet lifted out onto a disc of filter paper. The pellet was then spread between 2 filter discs and allowed to dry at room temperature overnight. The dried flakes were ground to a fine powder with a sterile pestle and mortar.

The embryo powder could be stored at 4°C indefinitely.

2.7.2.2 Preparation of DIG-Labelled Riboprobe.

A template of the probe of interest was prepared by linearisation of the appropriate plasmid, using a suitable restriction enzyme (see Tables 4 and 5) and incubated, as follows with the appropriate RNA polymerase in the following synthesis mixture: 13µl sterile distilled water, 2µl 10 x transcription buffer (0.04M Tris-HCl pH 8.0, 8mM $MgCl_2$, 1 mM spermidine, 0.025M NaCl) (Gibco BRL), 0.2mM DTT (Gibco BRL), 1mM ATP, 1mM CTP, 1mM GTP, 0.65mM UTP, 0.35mM digoxigenin-UTP, pH8.0 (Boehringer Mannheim), 1µl linearised plasmid DNA at a concentration of 1µg/µl, 50 units RNAguard™ (Pharmacia) and 10 units T7 or SP6 RNA polymerase (Boehringer Mannheim) were added sequentially to an RNAse-free 1.5ml eppendorf and carefully mixed. The synthesis mixture was microcentrifuged for 10 seconds and incubated at 37°C for 2 hours, whereupon a 1µl aliquot was removed and run on a 1% agarose gel containing 0.5µg/ml EtBr. If an appropriately sized, discrete RNA probe band at approximately 10 times the intensity of the residual template band was clearly visible then the protocol was continued. This indicated that approximately 10µg RNA probe had been synthesised.

The RNA was precipitated by the addition of 100µl 1 x TE, 10µl 3M NaOAc and 300µl ethanol. The tube was inverted gently 10 times and incubated at -20°C for 30-60 minutes. The RNA was pelleted by centrifugation in a bench-top microfuge at 4°C for 10 minutes. The pellet was washed twice in 70% ethanol/ sterile water then air-dried for a minimum time in a fume hood.

The probe was resuspended in sterile 1 x TE at approximately 0.1µg/ml and stored at -20°C. If an unduly long period elapsed between probe synthesis and use, the integrity of the probe was reassessed by agarose gel electrophoresis.

2.7.2.3 Preparation and Prehybridisation of Tissue.

Embryos for use in whole-mount in-situ hybridisation were dissected free from the maternal tissue using sterile watchmakers forceps. The conceptuses were washed in chilled ET medium and fixed overnight at 4°C by rotation in fresh 4% PFA.

All washes were undertaken with constant rotation in sterile 5 ml bijous (Sterilin) at room-temperature unless otherwise stated. Washes were removed using sterile pasteur pipettes.

Post-fixation the embryos were dehydrated by washing twice in PTW (PBS, 0.1% Tween-20) at 4°C followed by 5 minutes each in 1 : 3, 1 : 1 and then 3 : 1 methanol/ PTW, then twice with 100% methanol. They were rehydrated by being taken through this series in reverse and then washed three times in PTW. In order to increase the accessability of the target RNA, the tissue was treated with 10µg/ml proteinase K in PTW for 10 minutes. The embryos were not rocked during this stage to prevent tissue damage. They were then washed in a 2mg/ml freshly prepared glycine (Sigma) solution in PTW and refixed using fresh 0.2% glutaraldehyde (Sigma)/4% PFA in PTW for 20 minutes. The embryos were then washed twice for 5 minutes with PTW. The PTW was replaced with two washes of 1 ml prehybridisation mix (50% formamide, 5 x SSC pH5.0, 50µg/ml yeast RNA, 1%SDS, 50µg/ml heparin (both Sigma)) with the second wash containing the riboprobe at 1µg/ ml. The embryos were incubated thus at 60°C for 3-16 hours.

Post-hybridisation embryos were stored at -20°C indefinitely.

2.7.2.4 Post Hybridisation Washes.

Post-hybridisation, the embryos were washed in the following to remove unbound probe: Twice in solution 1 (50% formamide, 5 x SSC pH5.0, 1% SDS) for 30 minutes at 60°C, twice in 1 : 1 solution 1 : solution 2 (0.5M NaCl, 10mM Tris-HCl pH 7.5, 0.1% Tween-20) for 10 minutes at 60°C, three times in solution 2 for 5 minutes at 37°C and twice in 20µl/ml ribonuclease A in solution 2 for 30 minutes at 37°C. Then the embryos were washed with solution 2, then solution 3 (50% formamide, 2 x SSC pH5.0) at room-temperature for 5 minutes, followed by 2 washes of solution 3 for 30 minutes at 65°C. Finally the embryos were washed 3 times for 5 minutes in TBST (0.14M NaCl, 2.7mM KCl , 25mM Tris-HCl pH 7.5, 0.1% Tween-20).

2.7.2.5 Immunocytochemical Detection of Probe.

The embryos were preblocked in 10% heat-inactivated sheep serum in TBST for 60-90 minutes. During this period, the antibody was presorbed as follows: 3mg of embryo powder, 0.5ml TBST, 5µl sheep serum and 1µl anti-digoxigenin antibody coupled to alkaline phosphatase (Boehringer Mannheim) were placed in a clean 1.5 ml Eppendorf tube and rotated at 4°C for 60 minutes. The antibody mixture was microcentrifuged for 1 minute and the supernatant recovered. The supernatant was diluted to 2 ml with 1% sheep serum in TBST and used to replace the 10% serum preblocking the embryos. This was rocked overnight at 4°C.

The following day the embryos were washed three times for 5 minutes, then five times for 1 hour in TBST. This was followed by three, 10 minute washes in fresh NTMT (100mM NaCl, 100mM Tris-HCl pH 9.5, 50mM $MgCl_2$, 0.1% Tween-20). In order to detect the signal the embryos were incubated in a light-tight box with NTMT contaning freshly-added 4.5µl NBT (Nitro Blue Tetrazolium salt) and 3.5µl BCIP (5-bromo-4-chloro-3-indoyl phosphate) (both Boehringer Mannheim) per ml of NTMT. The embryos were rocked for the first 20 minutes.

When the colour had developed to the desired extent, the embryos were washed twice in fresh NTMT then stored for a short time in the dark in PTW until the conceptuses had been photographed. If necessary, the level of background could be reduced by washing the embryos in methanol for 10 minutes, isopropanol for 15 minutes then Histoclear™ for 15 minutes. Embryos were placed in a 70% glycerol/ PBT solution for photography. They were not fixed as this was found to reduce the sensitivity of the TGFβ1 genotyping PCR.

2.8. Statistical Methods.

2.8.1 Null Hypothesis.

In a project where data will be analysed statistically, it is important to define a null hypothesis. A null hypothesis allows groups of data to be compared; under the assumption that they are from the same population, and therefore do not differ. Having assumed this, the correct conclusions can be drawn from any statistical analyses undertaken. In this study, the genotypic ratios of offspring from TGFβ1+/- intercrosses and reciprocal crosses between TGFβ1+/+ and TGFβ1+/- animals were ascertained by PCR of genomic DNA. Since each TGFβ1 allele is expected to assort independently, a Chi-squared (χ^2) 'goodness of fit' statistical test was used to determine whether the observed data differed significantly from the expected data (provided the smallest expected data class was not ≤ 5).

The null hypothesis used in this case assumed that there were no factors affecting the observed ratios of offspring. Using Mendelian principles, a ratio of 1 : 2 : 1 TGFβ1+/+ : TGFβ1+/- : TGFβ1-/- is expected in animals generated by TGFβ1+/- intercrosses. A 1 : 1 TGFβ1+/+ : TGFβ1+/- ratio is expected in animals generated by reciprocal TGFβ1+/- x TGFβ1+/+ crosses. Deviations from these expected ratios implies that another factor is contributing to the result, and would therefore lead to the rejection of the null hypothesis and the formulation of an alternative hypothesis. This is the process used throughout this project.

All of the conceptuses examined in this study were scored using an objective scoring system. Using a null hypothesis, statistical analysis of this data was executed under the assumption that no factors were contributing to the observed ratios. Thus, it was expected that any observed defects should be random and segregate evenly throughout all members of a litter regardless of genotypic class.

2.8.2 The Chi-Squared (χ^2)'Goodness of Fit' Statistical Test.

In order to assess whether an observed set of data represents a chance deviation from the values predicted by a null hypothesis, the results can be evaluated using a χ^2 test.

Where:-

$$\chi^2 = \Sigma \frac{(\text{observed} - \text{expected})^2}{\text{expected}}$$

The $\chi 2$ value is inversely related to the goodness-of -fit between the experimental results and the null hypothesis under test. By placing the $\chi 2$ value in context with the appropriate degrees of freedom (dof) for the calculation (dof = number of classes of data analysed - 1); probability (p) can be calculated. p is the probability that the observed set of data could have occured by chance. In this project p values of ≤ 0.05 were taken as significant. This implied that there was a 5% or less chance that the observed results were the same as the expected results.

$\chi 2$ cannot be applied to small data sets i.e. those with an expected outcome ≥ 5 in any individual class.

2.8.3 Student's t Test.

Throughout this project the Student's t test was used to test whether or not two samples of data come from the same, or different populations when both samples contained less than thirty pieces of data. The Students's t test compares the standard error of the difference of the means between the samples in terms of the t distribution. The t distribution is symmetrical about a mean of zero, and varies according to the size of a sample i.e. the smaller the sample, the greater the difference required by the t test for a significant result.

Where:-

$$s = \frac{\Sigma_1 (x - \text{mean}_1)^2 + \Sigma_2 (x - \text{mean}_2)^2}{n_1 + n_2 - 2}$$

$$t = \frac{\text{mean}_1 - \text{mean}_2}{s \sqrt{\frac{1}{n_1} + \frac{1}{n_2}}}$$

x is any piece of data from a sample, n = the number of pieces of data in a sample. s is the standard deviation here shown calculated for a two-sample t test, where the samples contain an unequal number of members.

The found t value is used to find the probability (p) value of the two samples tested coming from the same population. In this project p-values of ≤ 0.05 were taken as significant.The number of degrees of freedom is calculated as follows:

Degrees of freedom = $n_1 + n_2 - 2$

Chapter 3

RESULTS.

INTRODUCTION.

The pre- and post-natal phenotypic effects of the TGFβ1 null allele have been characterised by several groups on a number of ill-defined genetic backgrounds (Shull *et al.*, 1992, Kulkarni *et al.*, 1993 & Dickson *et al.*, 1995) (see Introduction). For the purposes of this project, the TGFβ1 null allele was bred to 93.75% purity on inbred NIH/ Ola (NIH), inbred C57BL/ 6J/ Ola (C57) and inbred129/ Sv/ Ola (129) genetic backgrounds by F. Cousins. Therefore, the aim of this project was to investigate the onset and penetrance of the pre- and post-natal phenotypes of TGFβ1 knockout mice in each of these strains.

Defined intercrosses were also used in this study: F1 mice were produced by intercrossing C57 and NIH mice; F2 mice were produced by intercrossing F1 mice (see Materials and Methods).

3.1 Survival of TGFβ1+/- and -/- Mice to Weaning on Different Genetic Backgrounds.

3.1.1 TGFβ1 Heterozygous Intercrosses.

The original characterisation of the TGFβ1 knockout phenotype identified the cause of post-natal death of 50% TGFβ1-/- mice to be a multi-focal inflammatory disorder occurring at roughly 3-4 weeks of age (Shull *et al.*, 1992 & Kulkarni *et al.*, 1993). TGFβ1-/- mice appeared to be healthy until approximately 12-14 days of age whereupon they develop a progressive wasting syndrome. Thereafter they became distinguishable from their littermates due to their significant lack of body weight and

typically hunched posture (Kulkarni *et al.*,1993). These observations were replicated by Dickson *et al.*, (1995) using a mixed genetic background.

Genotype data accrued by the PCR of tail genomic DNA (see Figure 6) of mice at weaning (approximately 3 weeks of age), from TGFβ1+/- intercrosses on NIH, C57 and 129 backgrounds was compared to the expected 1 : 2 : 1 TGFβ1 +/+ : +/- : -/- ratio of genotypes using χ^2. As predicted, the results show a loss of TGFβ1-/- animals on each background (see Graph 1; Tables 6 and 7). In each case the observed ratio of genotypes differs significantly from the expected 1 : 2 : 1 ratio.

There is a range in the number of surviving TGFβ1-/- animals on each background, with the NIH homozygous null mice appearing to have a greater ability to survive to weaning relative to 129 and C57 strains. No C57 -/- animals were observed to survive to weaning. All of the surviving null pups were noted by F. Cousins/ D. Duggan as having a severely runted appearance, as did a number of TGFβ1+/- offspring on each genetic background. In this experiment, animals classified as runts were those expected by F. Cousins/ D. Duggan to die imminently.

A χ^2 analysis of the number of 'normal' mice i.e. total numbers of mice of each genotype minus the runts of that genotype (see Table 7; Graph 2) shows that the abnormalities noted in each genetic background do not segregate randomly, but are associated with the presence of a TGFβ1 null allele. Also, a 1 : 2 TGFβ1+/+ : +/- ratio should be occuring in each strain despite the loss of TGFβ1-/- animals, if the TGFβ1 allele has no effect on the TGFβ1+/- animals. This was assessed in each cross using a χ^2 test. It was found that there had been no significant loss of NIH TGFβ1+/- animals; however, on both C57 and 129 backgrounds a significant loss of TGFβ1+/- offspring had occured by 3 weeks of age.

Therefore, it can be concluded that the TGFβ1 null allele is a major contributory factor in the death of a significant number of conceptuses on NIH, 129 and C57 genetic backgrounds by 3 weeks of age. As expected from previous reports, the majority of TGFβ1-/- conceptuses were dead or dying by this time point. However, there is a strain-specific difference in the survival to 3 weeks post-partum of TGFβ1-/- animals: It appears that TGFβ1+/- and -/- animals bred onto an NIH background may be less prone to death prior to 3 weeks post-partum than those on a C57 and 129 genetic background. However, further work is required to pin-point the onset of lethality.

Graph 1. TGFβ1 +/+ : +/- : -/- 1 : 2 : 1 Ratios at Weaning.

The expected ratio of TGFβ1+/+ : +/- : -/- animals generated by TGFβ1+/- intercrosses at any developmental stage is 1 : 2 : 1. Graph 1 shows the observed genotype ratios of NIH, C57 and 129 animals at weaning (around 3 weeks of age). In the calculation of ratios, the number of TGFβ1+/+ animals was taken as '1'. There is clearly a strain-dependent difference in the ability of TGFβ1+/- and -/- animals to survive to weaning.

Graph 2. Observed Percentage of Phenotypic TGFβ1 Knockout Animals at Weaning in Each Genotypic Class.

The post-natal TGFβ1 knockout phenotype is lethal and invariably affects all TGFβ1-/- and a proportion of the TGFβ1+/- animals which survive to birth. Graph 2 shows the percentage of animals in each genotypic class in NIH, C57 and 129 mice which were noted (D. Duggan, & F. Cousins) to be exhibiting signs of the TGFβ1 knockout phenotype at weaning. In the C57 strain, no TGFβ1-/- mice survived to birth; this is represented as a 100% abnormality.

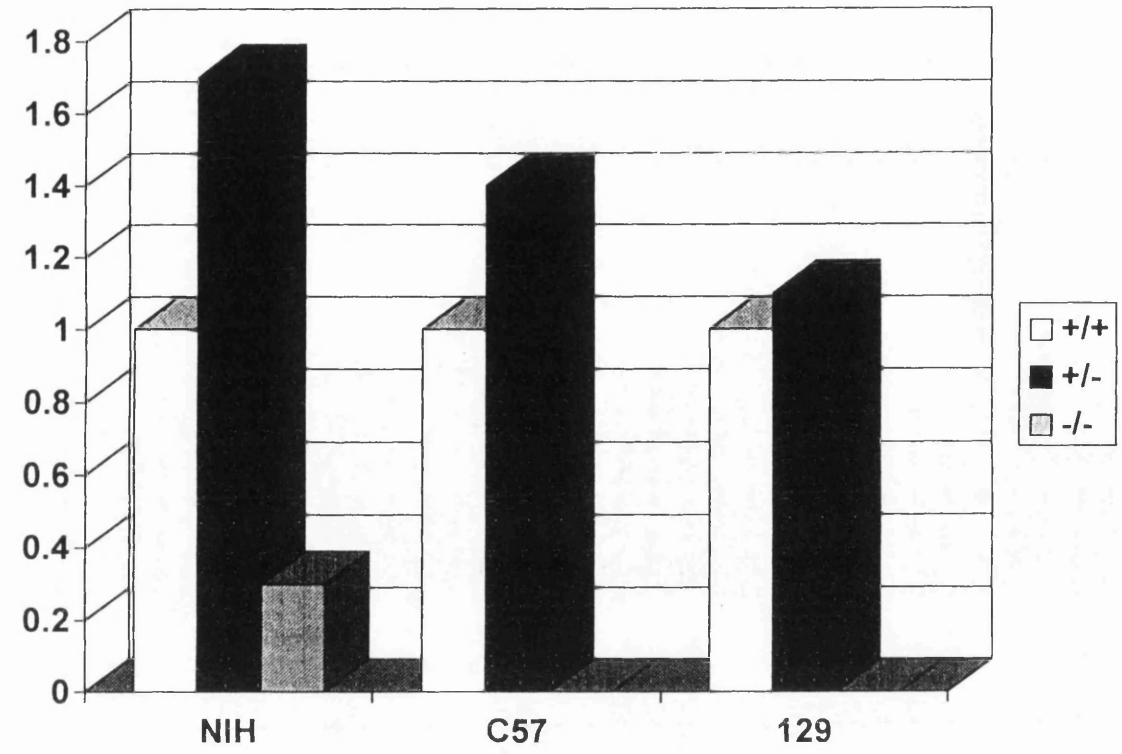
1.8
1.6
1.4
1.2
1
0.8
0.6
0.4
0.2
0
NIH
C57
129
+/+
+/-
-/-

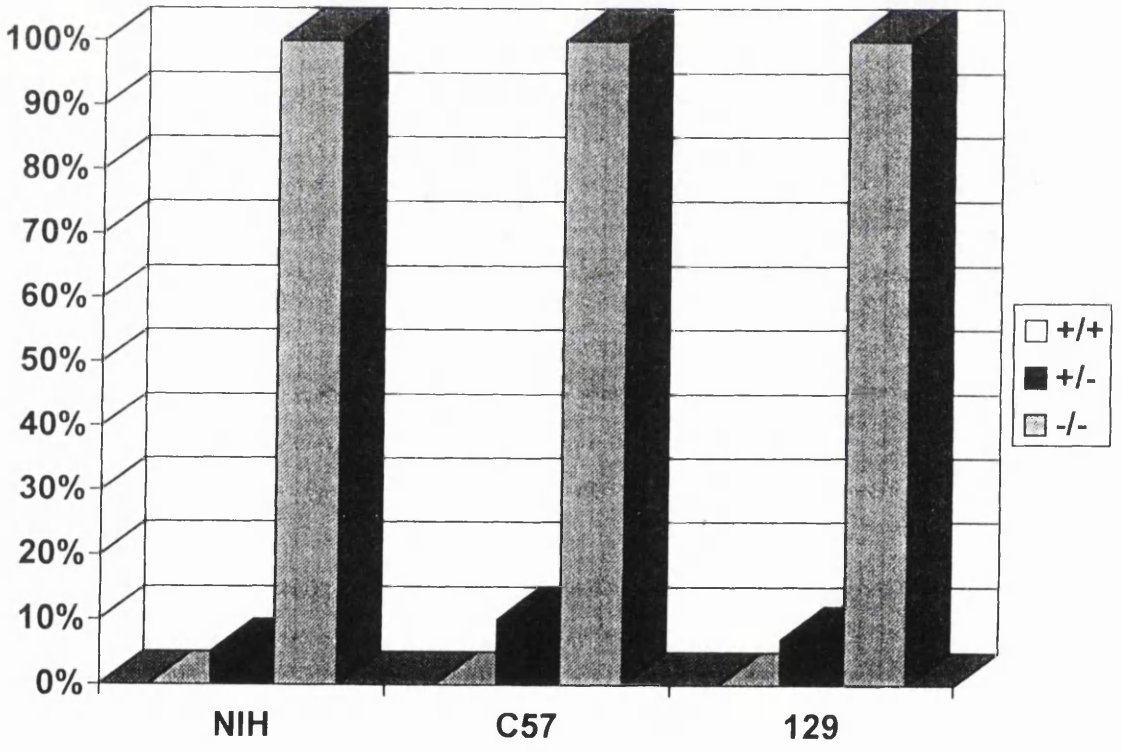
100%
90%
80%
70%
60%
50%
40%
30%
20%
10%
0%
NIH
C57
129
+/+
+/-
-/-

Table 6.

Strain	+/+	+/-	-/-	Dead	Total	+/+ : +/- : -/- Ratio
NIH	66 [0]	110 [5]	15 [15]	27	218	1:1.7:0.3
C57	124 [0]	179 [10]	0	15	318	1:1.4:0
129	58 [0]	66 [4]	2 [2]	5	131	1:1.1:0

Table 7.

Strain	1 : 2 : 1 TGFβ1+/+ : +/- : -/- Total Animals	1 : 2 : 1 TGFβ1+/+ : +/- : -/- Normal Animals	1 : 2 TGFβ1+/+ : +/- Total Animals
NIH	p=<0.01	p=<0.01	p=0.24
C57	p=<0.01	p=<0.01	p=<0.01
129	p=<0.01	p=<0.01	p=<0.01

Tables 6 and 7. Genotype Ratios of NIH, C57 and 129 Mice at 3 Weeks of Age from TGFβ1+/- Intercrosses.

Genomic DNA was isolated from tail biopsies taken at weaning from mice derived from TGFβ1+/- intercrosses and used to ascertain TGFβ1 genotype by PCR (see Materials and Methods). The numbers in square brackets represent the number of notably runted animals, i.e. those expected to die, in each genotypic class. Genotype ratios were tested for significant deviation from the expected 1 : 2 : 1 TGFβ1+/+ : +/- : -/- and 1 : 2 TGFβ1+/+ : +/- ratios using χ^2 tests. Totals of 'normal' animals were calculated by the subtraction of runts from the total number in each genotypic class.

3.1.2 TGFβ1+/- x TGFβ1+/+ Reciprocal Crosses.

The investigations of Dickson *et al* (1995) showed that, in TGFβ1+/- intercrosses on a mixed genetic background, a 25% loss of TGFβ1+/- animals occured *in utero*. It was also reported that a significant 20% loss of TGFβ1+/- embryos occured in TGFβ1+/- x TGFβ1+/+ crosses when the mother was TGFβ1+/-. Paternal yolk-sac imprinting was excluded, and it was postulated that factors such as maternal environment and litter size may compromise the development of TGFβ1+/- conceptuses *in utero*.

In order to ascertain whether or not there was a directional loss of TGFβ1+/- animals prior to 3 weeks post-partum, mice generated by reciprocal TGFβ1+/+ x TGFβ1+/- crosses on NIH, C57 and 129 strains were genotyped at 3 weeks of age by the PCR of genomic tail DNA (see Tables 8 and 9). If factors such as maternal environment were acting on these genetic backgrounds a significant deviation from the expected 1 : 1 TGFβ1+/+ : +/- ratio would result only when the mother was TGFβ1+/-. Since a 20% loss of TGFβ1+/- conceptuses born to a TGFβ1+/- mother has been reported previously (Dickson *et al.*, 1995); each set of data was subjected to two χ^2 'goodness of fit' tests: Firstly, was the data comparable to, or significantly different from the expected 1 : 1 TGFβ1+/+ : TGFβ1+/- ratio? Secondly, was the data also comparable to, or significantly different from a 20% loss of TGFβ1+/- pups? i.e. was $p \leq 0.05$ when the data was compared to a 1 : 0.8 TGFβ1+/+ : TGFβ1+/- ratio? (Table 9).

Given the small predicted loss of heterozygotes, any significant effects acting on the mice used in this experiment may be masked due to the relatively small data sets genotyped in each genetic background. It is notable that the ratio of +/+ : +/- mice generated on C57 and NIH backgrounds by crossing TGFβ1+/- female mice with TGFβ1+/+ male mice drops in both cases from 1 : 1 to 1 : 0.7 and 1 : 0.8 respectively when compared to the reciprocal cross, whereas the 129 ratio is unaffected by direction. However, the data did not differ significantly from 1 : 1 TGFβ1+/+ : +/-, hence, it was important to use two χ^2 'goodness of fit' tests in order to check if the data was consistent with both no loss of TGFβ1+/- conceptuses and a 20% loss of TGFβ1+/- conceptuses.

When the results for male TGFβ1+/- x female TGFβ1+/+ mice, shown in Table 8, are analysed using a $\chi 2$ 'goodness of fit' test for the expected ratio of 1 : 0.8 TGFβ1+/+ : +/- pups; the only significant difference found was in the 129 strain ($p=0.04$). A probability value nearing significance was also seen on the NIH background ($p=0.06$) - suggesting that there is no loss of TGFβ1+/- conceptuses in 129 and NIH animals in this cross,

when the father is TGFβ1+/-. This is consistent with the results of Dickson *et al.* (1995). When the data for male TGFβ1+/+ x female TGFβ1+/- mice, shown in Table 9, is analysed by $\chi 2$, no significant differences from the expected ratios are found. However, the p value for C57 animals born to a TGFβ1+/- mother is very small (p=0.06) when the data is compared to a 1 : 1 TGFβ1+/+ : TGFβ1+/- ratio, conversely, the p value for a 1 : 0.8 TGFβ1+/+ : TGFβ1+/- is 0.51, i.e. highly consistent with a 20% loss of heterozygous animals, but the sample size was too small to make this a significant result.

In general, these results are neither consistent with a 20% loss or with no loss of TGFβ1+/- embryos in both directions of the cross, due to a lack of data. In an attempt to circumvent this effect, the samples from each individual strain was pooled and analysed statistically. Again, the ratio of TGFβ1+/+ : +/- dropped from 1 : 1, to 1 : 0.8 when a TGFβ1+/- animal was the mother. The data was significantly different from a 20% loss of TGFβ1+/- animals when the mother was TGFβ1+/+: However, when the mother was TGFβ1+/-, the data was consistent with a 20% loss of TGFβ1+/- animals (p>0.90) - and with a 1 : 1 TGFβ1+/+ : +/- ratio (p=0.09), although the probability of this result occurring by chance was substantially lower.

Although the genotype ratios are highly suggestive of a small heterozygous loss occurring when a TGFβ1+/- animal is the mother, these results show that if there is any directional effect on the production of TGFβ1+/- mice from reciprocal TGFβ1+/+ and +/- crosses, it is very small, i.e. ≤20%. Therefore, samples of a much greater size would be required to demonstrate this loss on any specific genetic background. A loss of TGFβ1+/- animals when the mother is TGFβ1+/-, would probably be due to the effect of reduced levels of circulating TGFβ1 in TGFβ1+/- mothers as opposed to wild type mothers. It is notable that there appears to be an absence of a directional effect on the 129 genetic background (see Discussion 4.4).

Table 8. Genotype Ratios of NIH, C57 and 129 Mice at 3 Weeks of Age from Female TGFβ1+/+ x Male TGFβ1+/- Crosses.

Strain	+/+	+/-	Total	TGFβ1 +/+:+/- Ratio	1:1 p value	1:0.8 p value
NIH	141	141	282	1 : 1	>0.90	0.06
C57	68	67	135	1 : 1	0.85	0.22
129	68	76	144	1 : 1.1	0.51	0.04
TOTAL	277	284	561	1 : 1	0.85	<0.01

Table 9. Genotype Ratios of NIH, C57 and 129 Mice at 3 Weeks of Age from Female TGFβ1 +/- x Male TGFβ1+/+ Crosses.

Strain	+/+	+/-	Total	TGFβ1 +/+:+/- Ratio	1:1 p value	1:0.8 p value
NIH	56	48	104	1:0.8	0.43	0.73
C57	55	37	92	1:0.7	0.06	0.51
129	49	48	97	1:1	>0.90	0.31
TOTAL	160	133	293	1:0.8	0.09	>0.90

Tables 8 and 9. No Directional Effect on the Observed Genotype Ratio Generated By TGFβ1+/+ and TGFβ1+/- Reciprocal Crosses.

These tables show data detailing TGFβ1 genotype ratios from TGFβ1+/+ x +/- reciprocal crosses at weaning of NIH, C57 and 129 inbred strains of mice. Using a χ^2 'goodness of fit' test the probability of the ratios of surviving mice differing significantly from 1 : 1 and 1 : 0.8 was assessed.

3.2 Analysis of the Genotype Ratio at Birth of Pups from TGFβ1+/- Intercrosses.

The genotype ratios of NIH, C57, F1 litters from TGFβ1+/- intercrosses at birth were characterised by Bonyadi *et al.* (1997) concomitant to this study. This information is central to the present study, and is therefore tabulated in Table 10. For the purposes of this study the genotypic ratio at birth of pups from TGFβ1+/- intercrosses on a 129 background was also of interest (Table 10). In each experiment genomic DNA from one day-old pups was genotyped by PCR and the results compared to expected 1 : 2 : 1 TGFβ1+/+ : +/- : -/-, 1 : 1 TGFβ1+/+ : -/- and 1 : 2 TGFβ1+/+ : -/- ratios using χ^2 'goodness of fit ' tests. By birth, a significant loss of TGFβ1-/- pups had occured in each genetic background.

An overview of TGFβ1 genotype ratios at birth of pups from all genetic backgrounds is presented in Graph 3.

There is an extreme variation in the percentage of prenatal death in TGFβ1+/- and -/- animals. Percentages were calculated as follows: Firstly, heterozygotes; the total number of surviving TGFβ1+/- pups was halved, divided by the number of TGFβ1+/+ animals genotyped, then multiplied by 100; secondly homozygous nulls - the total of surviving TGFβ1-/- pups was divided by the number of TGFβ1+/+ pups, then multiplied by 100. The results show that pups from an NIH background are the least affected, with an approximate 28% loss of TGFβ1+/- and an 18% loss of TGFβ1-/- conceptuses *in utero*. On the 129 genetic background, 29% of TGFβ1+/- animals die before birth. 74% of the 129 TGFβ1-/- animals are lost *in utero*. All C57 TGFβ1-/- animals are lost before birth. In the F1 reciprocal NIH x C57 intercross 70% of TGFβ1-/- conceptuses died pre-natally. Around 12% of TGFβ1+/- conceptuses on the C57, and reciprocal F1 genetic backgrounds died *in utero*.

Thus, by birth, the TGFβ1 null allele has had a strong influence on the loss of pups on each of the genetic backgrounds studied in this project. There is a striking variation in the degree of lethality suffered by TGFβ1+/- and TGFβ1-/- conceptuses between the genetic backgrounds studied. Thus, it can be concluded that there are a number of differences between the inbred strains used in this project which may have a direct or indirect effect on the penetrance of the TGFβ1 knockout phenotype. These differences may be genetic or epigenetic, or involve a combination of factors.

Strain	+/+	+/-	-/-	Total	Ratio	1 : 2 : 1 TGFβ1 +/+ : +/- : -/-	1 : 2 TGFβ1 +/+ : +/-	1 : 1 TGFβ1 +/+ : -/-
NIH	89	129	73	291	1 : 1.4 : 0.8	p=0.07	p=0.01	p=0.21
C57	68	122	0	190	1 : 1.8 : 0	p=<0.01	p=0.46	p=<0.01
NIH x C57	50	90	15	155	1 : 1.8 : 0.3	p=<0.01	p=0.50	p=<0.01
C57 x NIH	29	50	9	88	1 : 1.7 : 0.3	p=<0.01	p=0.48	p=<0.01
129	39	55	10	104	1 : 1.4 : 0.3	p=<0.01	p=0.05	p=<0.01

Table 10. A Strain-Specific Loss of TGFβ1+/- and -/- Pups Occurs *in utero* .

>100 pups from TGFβ1+/- intercrosses were sacrificed on the day of birth and genotyped by PCR using genomic tail DNA. The results were compared to the expected 1 : 2 : 1 TGFβ1+/+ : +/- : -/- and 1 : 2 TGFβ1+/+ : +/- and TGFβ1+/+ : -/- genotype ratios using a χ^2 'goodness of fit' test. p values are shown above. The data shown above for C57, NIH and reciprocal F1 intercrosses are from Bonyadi *et al.*, 1997.

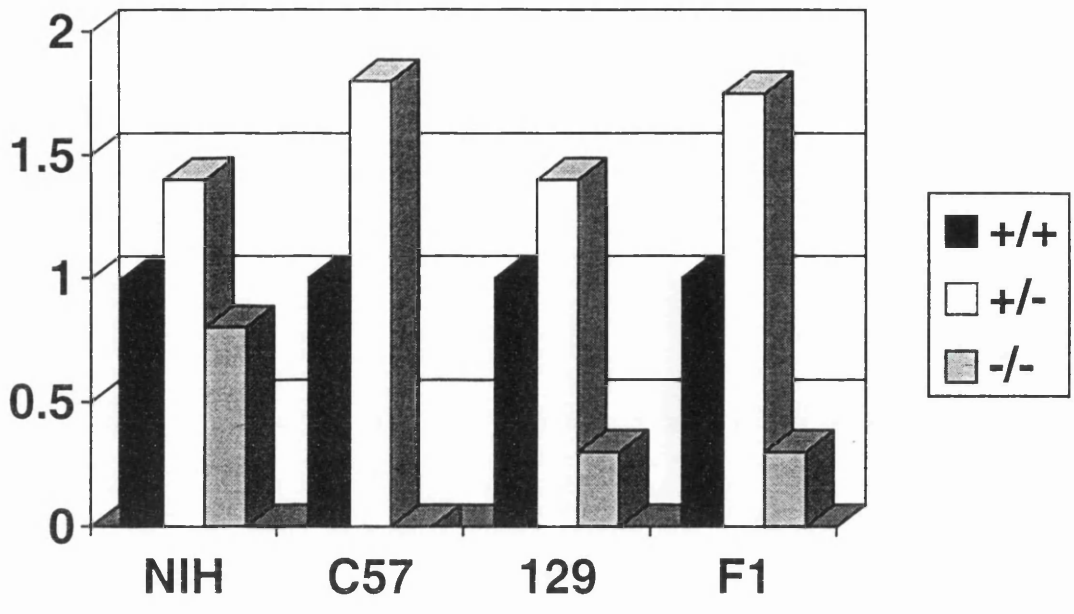

Graph 3. TGFβ1 +/+ : +/- : -/- 1 : 2 : 1 Ratios at Birth.

The expected ratio of TGFβ1+/+ : +/- : -/- animals generated by TGFβ1+/- intercrosses at any developmental stage is 1 : 2 : 1. Graph 3 shows the observed genotype ratios of NIH, C57, 129 and F1 animals at birth (Bonyadi *et al.*, 1997). In the calculation of ratios, the number of TGFβ1+/+ animals was taken as '1'. There is clearly a strain-dependent difference in the ability of TGFβ1+/- and -/- animals to survive to birth.

3.3 Analysis of 9.5dpc Embryos.

Work done on TGFβ1 knockout mice at birth and 3 weeks post-partum had shown that a variable lethality due to the TGFβ1 knockout allele occurs *in utero* on each genetic background studied. Therefore, it was decided to investigate the developmental stage and cause of lethality in each strain and in the defined F1 intercross.

3.3.1 Comparison of Developmental Staging for Wild Type NIH, C57 and 129 Embryos.

In order to ascertain the range of developmental variations in wild type embryos on NIH, C57, 129 and F1 genetic backgrounds, a control panel of >75 embryos from TGFβ1+/+ intercrosses from each strain was morphologically scored using the modified version of Brown and Fabros' scoring system (see Materials and Methods) (Table 11). This scoring system provides an objective, additive analysis of key developmental landmarks at 9.5dpc, and therefore facilitates the comparison of morphological scores between strains. This study was undertaken to provide a baseline for future scoring before a long-term morphological study of TGFβ1+/- intercross litters at 9.5dpc was undertaken.

The rate of total resorptions in the wild type intercrosses was 8-10% at 9.5dpc in each strain studied. Resorptions were defined as a decidual mass containing a dead embryo, at any stage of necrosis. Other abnormalities in conceptuses occured at a rate of around 10%. Upon analysis, these abnormalities were found to comprise embryos developmentally delayed by 0.75-1.0dpc and conceptuses found to be dying for unidentified reasons rather than specific morphological abnormalities. Interestingly, there was a clear strain-specific difference in the typical littersizes of these strains; on average, NIH litters contained 11 conceptuses; F1, 9 conceptuses and C57 and 129 litters, 8 conceptuses. There was a strain-specific difference in the average morphological score; but, as the standard deviations indicate, there was still a considerable spread in the range of scores for each strain. Thus, despite the larger littersizes, it appears that in general, NIH and F1 conceptuses develop more efficiently than 129 and C57 conceptuses. These observations are consistent with the characteristics of the NIH, C57 and 129 inbred strains published in *Mouse Genome* (Festing, 1993).

Strain	Total	Resorptions	Average Litter Size	Average Morph. Score
NIH	92 [5=5%]	7 (8%)	11	31.0 ± 2.2
C57	94 [7=7%]	8 (8.5%)	8	26.0 ± 3.8
129	70 [7=10%]	7 (10%)	8	27.5 ± 2.9
F1	112 [9=8%]	10 (9%)	9	29.0 ± 2.8

Table 11: Analysis of Resorption and Abnormality Rate in TGFβ1+/+ Intercrosses on Different Genetic Backgrounds.

70-120, 9.5dpc wild type embryos from NIH, C57, 129 and F1 genetic backgrounds were generated using TGFβ1+/+ parents. The conceptuses were dissected free from maternal tissue and assessed using a modified version of Brown and Fabros' scoring system (see Materials and Methods) to give a morphological score. Resorptions were defined as any decidual mass containing a necrotic embryo.

3.3.2 Analysis of Genotype and Phenotype Ratios of Embryos from TGFβ1+/- Intercrosses at 9.5dpc.

In order to ascertain the onset and cause of pre-natal death of TGFβ1-/- embryos, litters generated by C57, NIH, 129 and F1 (C57 x NIH reciprocal crosses) TGFβ1+/- intercrosses were morphologically scored and TGFβ1 genotyped by PCR using a whole clean conceptus or half-embryo. >100 conceptuses from each genetic background were scored and classified as TGFβ1+/+, +/-, -/- or unknown genotype. The latter class comprised conceptuses either partially or totally resorbed for an unknown reason.

Each TGFβ1+/- intercross genotyped at 9.5dpc should have resulted in a 1 : 2 : 1 TGFβ1+/+ : +/- : -/- ratio of embryos if being homozygous for the TGFβ1 null allele did not result in pre-organogenesis death (see Graph 4). Likewise, if the TGFβ1 null allele had no affect on mid-gestation development, there should be few conceptuses with an identifiable abnormal phenotype, and the observed phenotype should not segregate with genotype (see Graph 5). In order to analyse these two hypotheses, the data in Table 12 was subjected to two χ^2 'goodness of fit' tests: Firstly, to ascertain whether there was a significant deviation from the expected 1 : 2 : 1 total genotype ratio on each genetic background (see Table 13). The p values for each strain are all >0.05, except C57 (p=<0.01), this suggests that there is a significant loss of TGFβ1-/- embryos in this strain before 9.5dpc. TGFβ1-/- conceptuses on this background appear to be extremely compromised, and only 11% survive to 9.5dpc, at which point 4/ 5 were severely abnormal. Since there is no significant loss of any other class of conceptus on any other genetic background prior to 9.5dpc, this appears to be a strain-specific phenotype, leading to the death of the majority of C57 TGFβ1-/- conceptuses prior to 9.5dpc. A χ^2 test for C57 1 : 2 +/+ : +/- ratio gives a p value of 0.35, showing no significant loss of TGFβ1+/- conceptuses prior to this stage of gestation (see Table 13). No TGFβ1+/- conceptuses had been lost on any of the other strains studied.

Secondly, a χ^2 'goodness of fit' test was used to ascertain whether or not the severe abnormalities recorded among conceptuses from these genetic backgrounds were segregating randomly, or with a specific genotype. Observed totals of normal conceptuses were calculated by subtracting the number of severely abnormal conceptuses from the total number of conceptuses scored in each class. Severely abnormal conceptuses were defined as those whose specific defect or combination of defects would probably prove lethal during mid-gestation. On every genetic

background studied except NIH (p=0.08) the number of normal conceptuses deviated significantly from an expected 1 : 2 : 1 TGFβ1+/+ : +/- : -/- ratio (see Table 13). Therefore, the identified phenotype is not randomly segregating with genotype - it is notable that no severely phenotypic conceptuses were genotyped as TGFβ1+/+.

Thus, the data implies that there are 3 key stages where TGFβ1 is vital to normal development: Pre organogenesis, mid-gestation and 2-3 weeks post-partum.
89% of C57 TGFβ1-/- animals are lost prior to 9.5dpc, whereas the TGFβ1 null allele on a 129 and reciprocal F1 genetic background leads to an increased chance of developing a severe mid-gestation phenotype. There is no significant occurrence of a mid-gestation phenotype on the NIH genetic background. However, the relatively small sample size may be affecting the statistical significance of the segregation of the NIH TGFβ1 null allele with the phenotype. Data presented in Results 3.2 and 3.1 show that 80% of NIH TGFβ1-/- conceptuses are born but die at around 3 weeks post-partum.

Graph 4. TGFβ1 +/+ : +/- : -/- 1 : 2 : 1 Ratios at 9.5dpc.

The expected ratio of TGFβ1+/+ : +/- : -/- animals generated by TGFβ1+/- intercrosses at any developmental stage is 1 : 2 : 1. Graph 4 shows the observed genotype ratios of NIH, C57, 129, reciprocal and total F1 conceptuses at 9.5dpc. There is no significant directional difference in the F1 TGFβ1+/- intercross. In the calculation of ratios, the number of TGFβ1+/+ animals was taken as '1'. Notably, there has been a striking loss of C57 TGFβ1 -/- conceptuses prior to 9.5dpc.

Graph 5. Observed Percentage of Severely Abnormal TGFβ1 Knockout Conceptuses at 9.5dpc in Each Genotypic Class.

Upon dissection each TGFβ1 knockout conceptus was morphologically scored. Graph 5 shows the percentage of animals in each genotypic class in NIH, C57, 129, reciprocal and total F1 conceptuses which were scored as being severely abnormal. There is no significant directional difference on the prevalence of the TGFβ1 knockout mid-gestation phenotype in F1 conceptuses. A strain-dependent percentage of the total TGFβ1+/- and -/- embryos scored in each genotypic class were scored as severely abnormal.

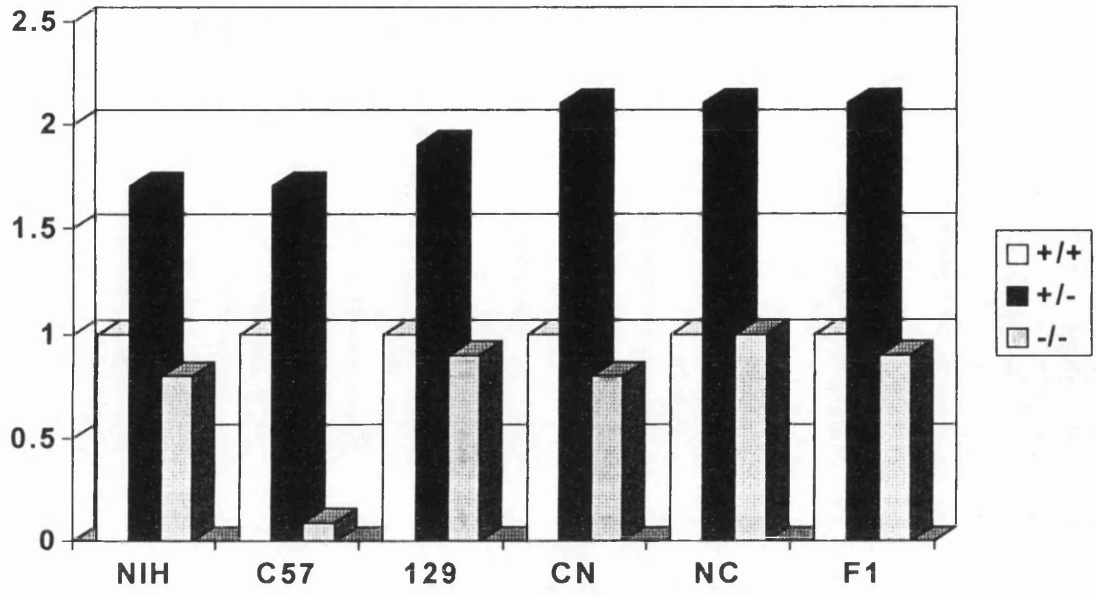
2.5
2
1.5
1
0.5
0
NIH
C57
129
CN
NC
F1
+/+
+/-
-/-

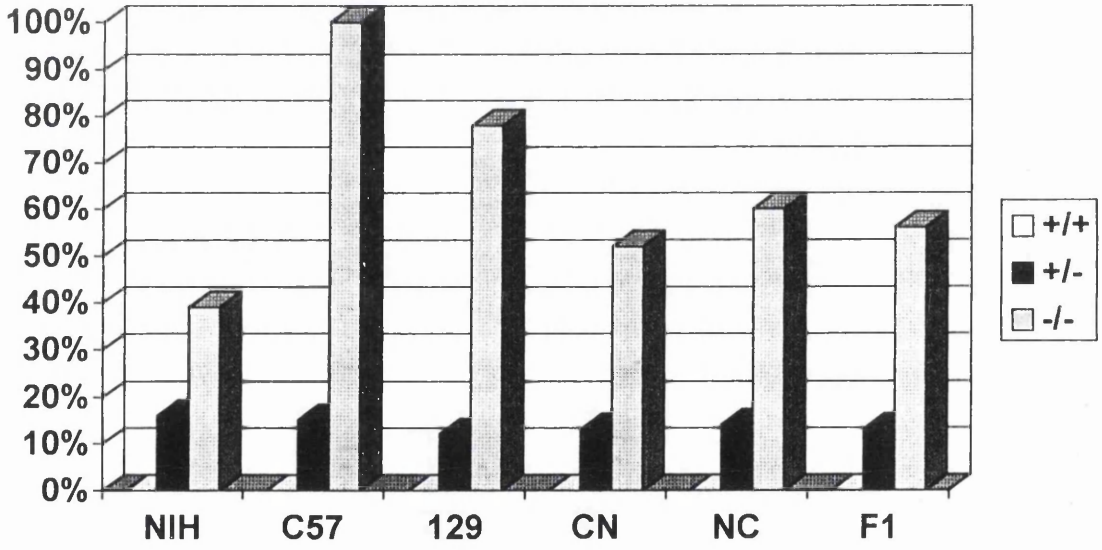
100%
90%
80%
70%
60%
50%
40%
30%
20%
10%
0%
NIH
C57
129
CN
NC
F1
+/+
+/-
-/-

Strain	+/+	+/-	-/-	Dead	Total	Ratio
NIH	29 [0]	49 [8=16%]	23 [9=39%]	5	106	1:1.7:0.8
C57	44 [0]	74 [11=15%]	5 [4=80%]	10	133	1:1.7:0.09
129	26 [0]	49 [6=12%]	23 [18=78%]	5	106	1:1.9:0.9
F1 (C57 x NIH)	30 [0]	62 [8=13%]	23 [12=52%]	8	123	1:2.1:0.8
F1 (NIH x C57)	27 [0]	57 [8=14%]	27 [16=60%]	7	118	1:2.1:1
F1 Total	57 [0]	119 [16=13%]	50 [28=56%]	15	241	1:2.1:0.9

Table 12. Genotype and Phenotype Ratios of NIH, C57, 129 and Reciprocal F1 Embryos at 9.5dpc from TGFβ1+/- Intercrosses.

The table shows the total number of conceptuses scored and genotyped by PCR on each genetic background studied at 9.5dpc. The total numbers are expressed as 4 classes ie. TGFβ1+/+, +/-, -/- or dead (unknown genotype). Conceptuses of an unknown genotype were either totally or partially resorbed. The numbers in square brackets represent the number of severely phenotypic animals of each genotypic class; this number is expressed as a percentage of the total number of animals of each genotypic class.

Strain	1 : 2 : 1 TGFβ1 +/+ : +/- : -/- Total animals	1 : 2 TGFβ1 +/+ : +/- Total animals	1 : 1 TGFβ1 +/+ : -/- Total animals	1 : 2 : 1 TGFβ1 +/+ : +/- : -/- Normal animals
NIH	p=0.61	not determined	p=0.40	p=0.09
C57	p=<0.01	p=0.35	p=<0.01	p=<0.01
129	p=0.68	not determined	p=0.65	p=<0.01
F1 (C57 x NIH)	p=0.37	not determined	p=0.34	p=0.01
F1 (NIH x C57)	p=0.75	not determined	p=>0.90	p=0.03
F1 Total	p=0.36	not determined	p=0.56	p=<0.01

Table 13. Statistical Analysis of Genotype and Phenotype Ratios of NIH, C57, 129 and Reciprocal F1 Embryos at 9.5dpc from TGFβ1+/-Intercrosses.

Genotype ratios of observed and expected total and normal embryos were compared using χ^2 'goodness of fit' tests. The number of normal conceptuses was calculated by the subtraction of those identified as severely phenotypic from the total number of conceptuses in each genotypic class.

3.3.3 Definition of the Abnormal Mid-Gestation Phenotype Observed in TGFβ1+/- and -/- Conceptuses.

In a previous study Dickson *et al.*, 1995 characterised the TGFβ1 knockout phenotype on a mixed genetic background and found that the primary defects were restricted to extra-embryonic tissue, namely the yolk-sac vasculature and haematopoietic system. One aim of this study was to identify any strain-specific differences in the manifestation of the TGFβ1 knockout phenotype. By using a morphological scoring system modified for use between 8.5 and 10.5dpc (see Materials and Methods) an objective and quantitative assessment of the TGFβ1 knockout phenotype on the genetic backgrounds studied could be made.

The embryos were scored using a dual system. Firstly the exact developmental stage of a number of landmark characteristics was assessed and scored (score 1). This was used additively as an indicator of the exact developmental age of the conceptus. Secondly, each conceptus was scored on an abnormality scale (score 2). Abnormalities of any embryonic feature were quantified using a standard system. This score reflected the severity and number of defects suffered by the conceptus. Since the conceptuses scored tended to exhibit different combinations and extremities of defects, these scores are not strictly additive. However, when presented together they can provide a basic indication of the divergence between the three genotypic classes on each genetic background.

The range of scores 1 and 2 for TGFβ1+/+, +/- and -/- conceptuses on C57, NIH, 129 and reciprocal F1 genetic backgrounds are presented as box-plots (Graphs 6a-10b, presented in Appendix 1) . The graphs show that for score 1, although there is a slight developmental delay in TGFβ1+/- and -/- compared to TGFβ1+/+ conceptuses, the scores vary only slightly between the different genotypes in each strain. Conversely, when score 2 is compared between genotypes, it is obvious that whereas TGFβ1+/+ conceptuses tend to be developmentally normal; TGFβ1+/-, and especially TGFβ1-/- conceptuses have suffered a range of developmental defects by 9.5dpc.

A closer analysis of the data shows that regardless of genetic background, the severe gross abnormalities observed at 9.5dpc associated with the TGFβ1 null allele mainly affect extra-embryonic structures and the haematopoietic system. For the purposes of this study these defects can be broken down into several categories: Inadequate/ complete lack of yolk sac vasculature, severe yolk sac anaemia; defects of the allantois

and chorion, i.e. the allantois contains blood clots, appears blocked or, as in several severe cases, fails to form an adequate chorio-allantoic junction; haemorrhage(s) in the embryo and/ or yolk sac; a swollen pericardium; necrosis, or the yolk sac and/or embryo retarded by >0.5dpc. Occasionally other combinations of severe abmormalities were observed and recorded.

By 9.5dpc, the embryonic circulation is normally connected to the extra-embryonic circulation via the allantois and the umbilical vessels as well as the vitelline vessels. The vitelline vein and artery are the first major vessels to appear in the yolk sac and form the basis of the branching plexus of blood vessels containing haemoglobinised red blood cells typically seen in the murine yolk sac at 9.5dpc. However, the most common defect of the vascular system identified in this study was a yolk sac with a reduced number of small, inadequately branching vessels with delicate connections. Usually this phenotype manifested itself as the appearance of an unbranched vitelline vein and artery in the absence of any other vessels. This was sometimes accompanied by areas of aberrant capilliary network development in the yolk sac. Occasionally haemorrhages of blood were observed between the endodermal and mesothelial layers of inadequately vascularised intact yolk sacs. The most severe manifestation of the vascular phenotype noted was an apparently complete failure of yolk sac vasculogenesis in the presence of persistent anastamosing blood islands (see Figures 8 and 9 for photographic examples of the TGFβ1 knockout yolk sac phenotype).

Defects in the allantois and chorion were common in the TGFβ1+/- and -/- conceptuses. The typical abnormalities scored were either a completely empty umbilical artery/ vein, the appearance of blood clots and/ or 'lumps' in the umbilical artery/ vein or a chorion distended with blood (see Figure 11). In a few extreme cases there had been a failure of the allantois to make a connection with the chorion.

Anaemia was observed in severely abnormal TGFβ1-/-and +/- intact yolk sacs. This aspect of the phenotype was observed independently, or in association with vascular defects, i.e. well vascularised intact yolk sacs could appear pale and conversely, yolk sacs with severe vascular defects could contain red blood cells. The degree of anaemia seen was variable; from a yolk sac appearing pallid in comparison to its littermates, to the presence of completely non-haemoglobinised blood in the vessels of the yolk sac (see Figures 8 and 9).

Figure 8 - Morphological Analysis of Dissected TGFβ1 Knockout Conceptuses at 9.5dpc.

9.5dpc conceptuses generated by TGFβ1+/- intercrosses were dissected free from the maternal tissue, morphologically scored and genotyped by the PCR of genomic DNA. (A) and (B) show a normal TGFβ1+/+ conceptus with well-developed extra-embryonic vasculature containing haemoglobinised blood. (C), (D), (E) and (F) are all TGFβ1-/- conceptuses with abnormal vasculature. (C) exhibits minimal branching of the major yolk sac vessels. There is a total absence of any major branching vessels in (D), and the embryo appears necrotic. (E) and (F) show a blood lake between the extra-embryonic tissue layers, despite the well-vascularised appearance of the yolk sac.

Scale bar = 600μm.
bv = blood vessel, ec = ectoplacental cone, h = haemmorhage, ys = yolk sac.

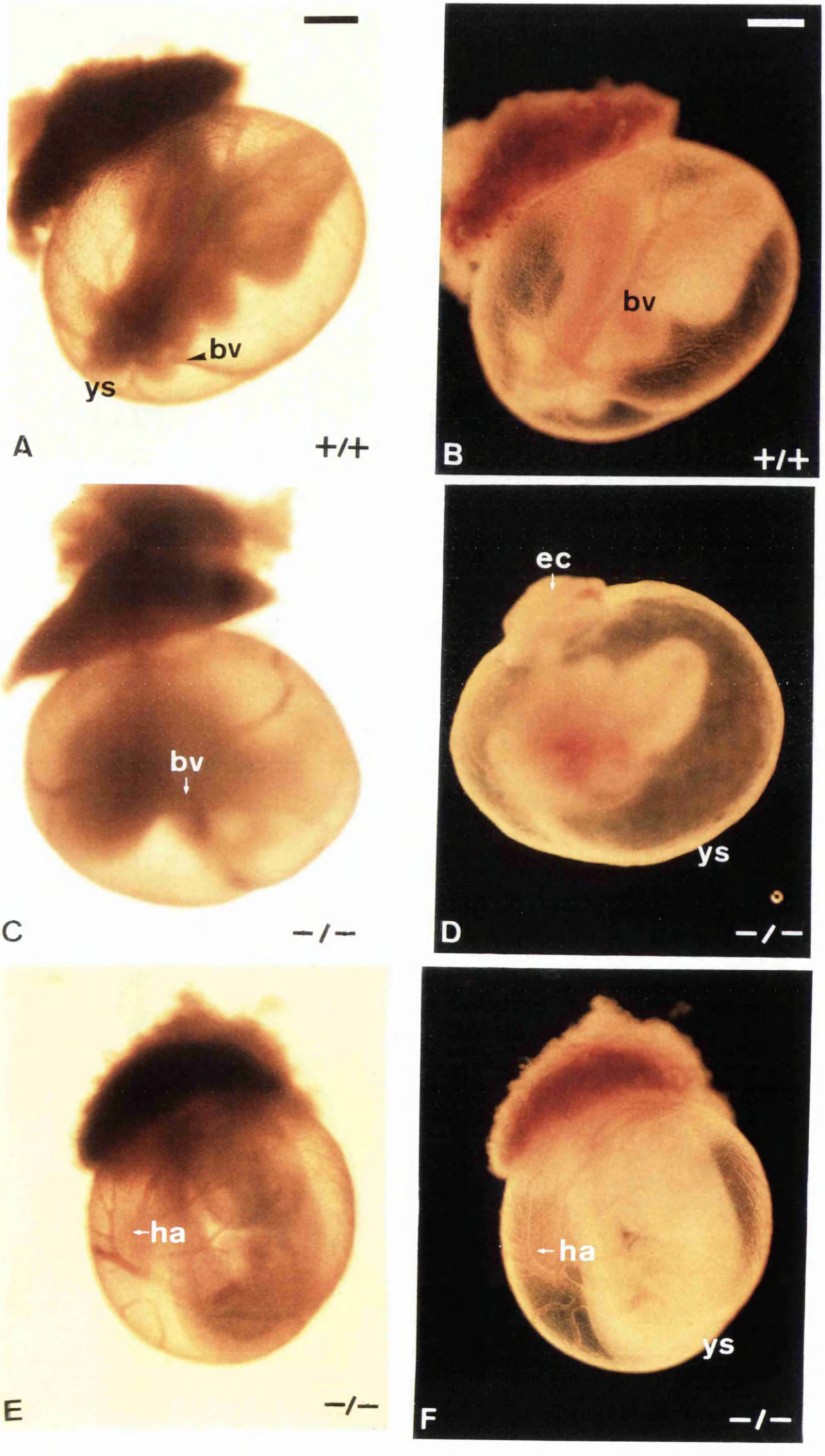
bv
ys
A
+/+
B
bv
+/+
bv
C
−/−
ec
ys
D
−/−
ha
E
−/−
ha
ys
F
−/−

Figure 9 - Morphological Analysis of Dissected TGFβ1 Knockout Conceptuses at 9.5dpc (2).

(A) - (E) all have characteristics of the TGFβ1 knockout mid-gestation phenotype. (A) and (B) show a TGFβ1-/- embryo in an avascular yolk sac. Both (C) and (D) exhibit yolk sac anaemia, despite having an apparently well-formed vasculature. Persistent blood islands in (E) demonstrate severe developmental delay. The embryo has arrested at around 8.0-8.5dpc and is extremely abnormal.

Scale bar (A) - (D) = 600μm. (E) = 225μm
bi = blood island, bv = blood vessel, hf = head fold, ys = yolk sac.

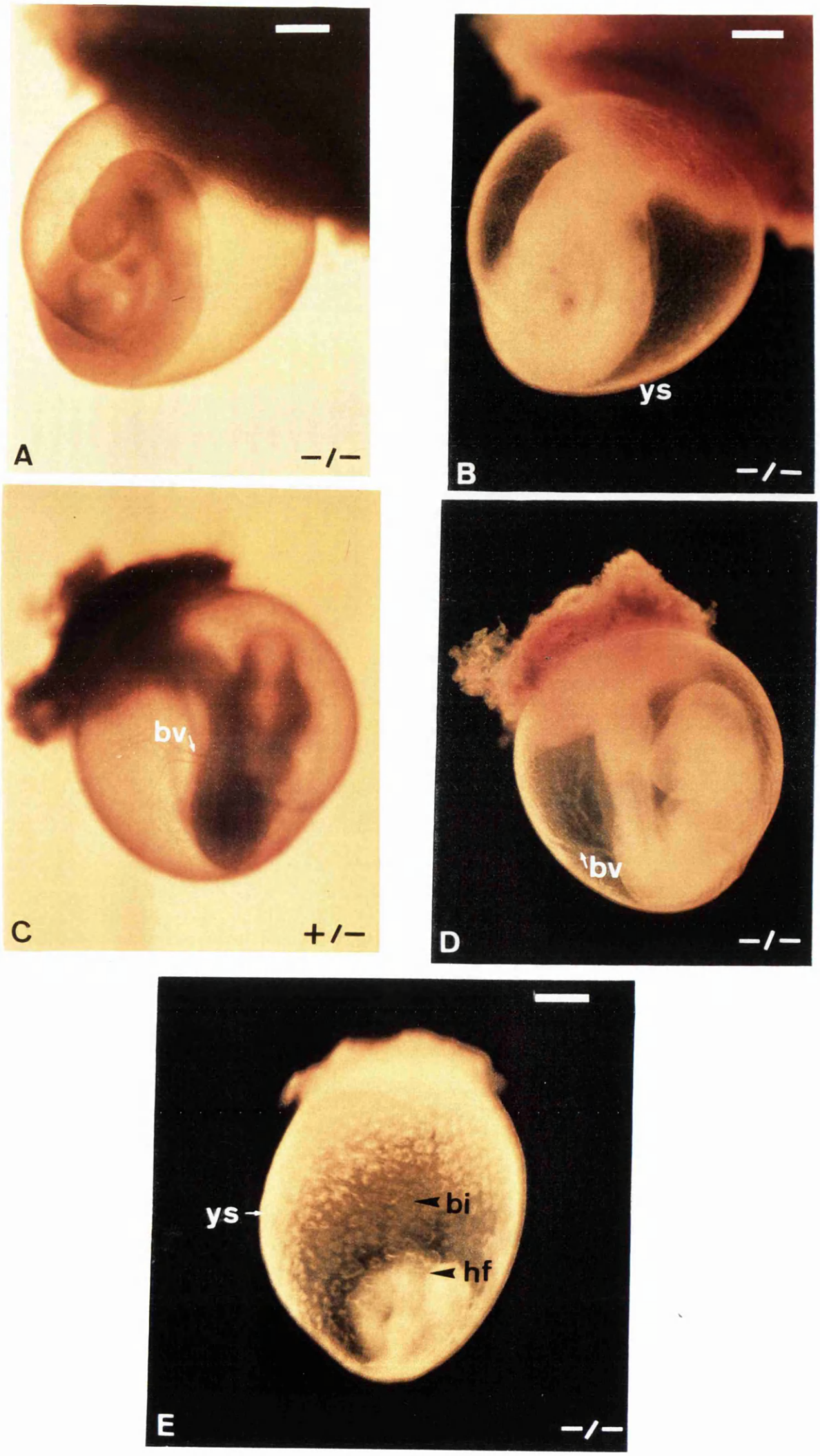
A
−/−
B
ys
−/−
C
bv
+/−
D
bv
−/−
E
ys
bi
hf
−/−

Figure 10 - Morphological Analysis of Dissected TGFβ1 Knockout Embryos at 9.5dpc.

TGFβ1 embryos generated by TGFβ1+/- intercrosses were dissected free from the yolk sac and morphologically assessed. (A) and (B) shows both aspects of a normal TGFβ1+/+ embryo at 9.5dpc, whereas TGFβ1-/- embryos (C) and (D) both have severe abnormalities. (C) has hydrocephaly. (D) has severe oedema; the heart is swollen and a haemmorhage has occurred in the cardiac region.

Scale bar = 375μm.
bb = branchial bars, in (A) numbered 1-3, da = dorsal aorta, h = heart, lb = limb bud, me = mesencephalon, op = otic pit, ov = optic vesicle.

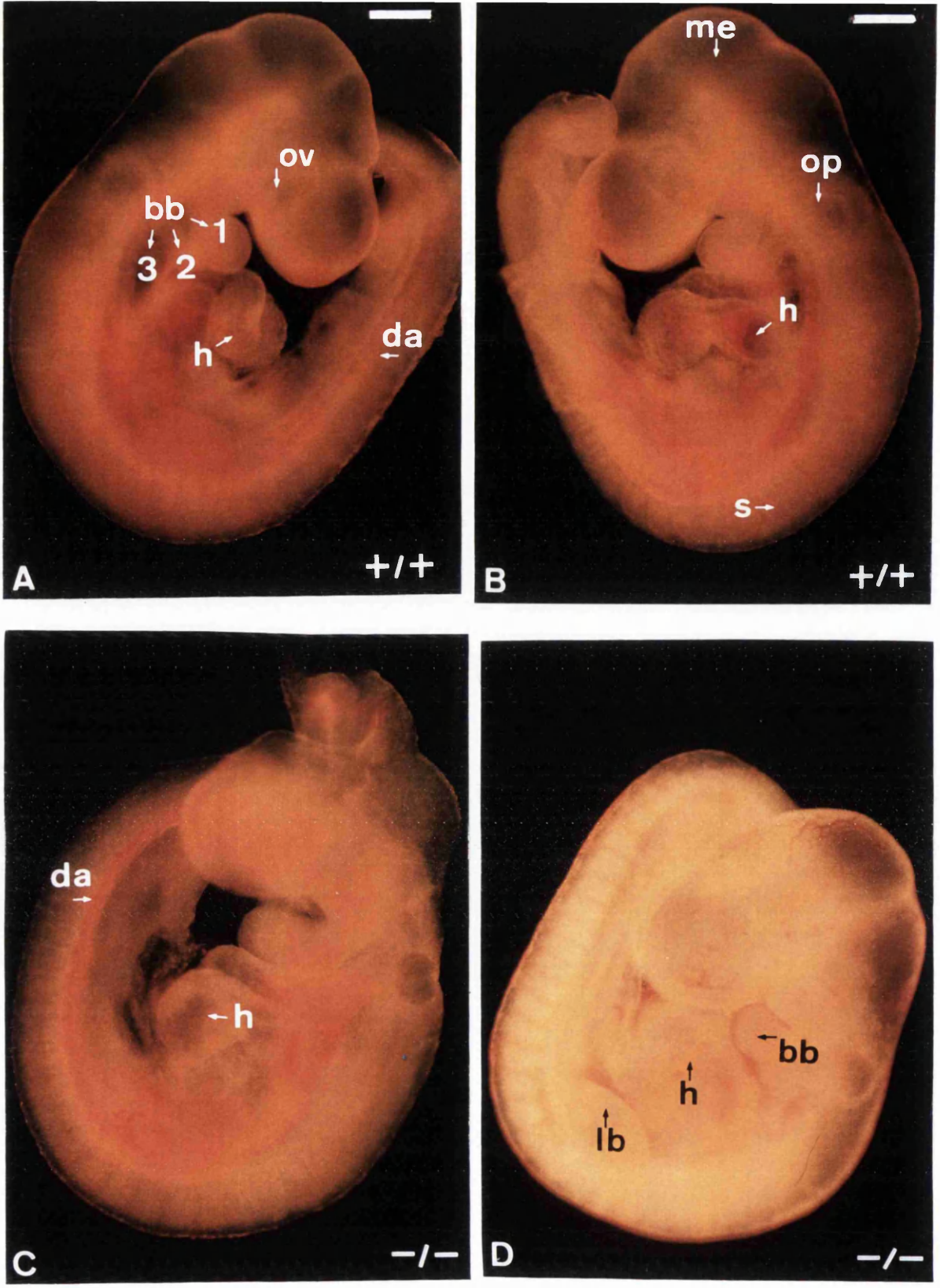
ov
bb
1
3
2
h
da
A
+/+
me
op
h
s
B
+/+
da
h
C
−/−
bb
h
lb
D
−/−

Figure 11 - Defects Observed in the Circulatory System of TGFβ1-/- Embryos at 9.5dpc.

Photographs (A), (B) and (C) illustrate defects observed in the TGFβ1 knockout mid-gestation phenotype. In a wild type conceptus, the umbilical artery and vein are both clearly visible, discrete and continuously full of haemoglobinised blood. The umbilical vessels fuse with a visible developing plexus of vessels in the chorion. However, (A) shows a distended umbilical vessel only half-full of blood. Embryo (B) has clots or 'lumps' lining its umbilical vessels. There is also a collection of blood in the chorion. (C) exemplifies the pericardiac swelling observed in abnormal TGFβ1 knockout mice. Additionally, a small haemmorhage has occurred around the heart.

am = amnion, bb = branchial bars, ch = chorion, h = heart, lb = limb bud, pe = pericardium, um = umbilical vessels, ys = yolk sac.

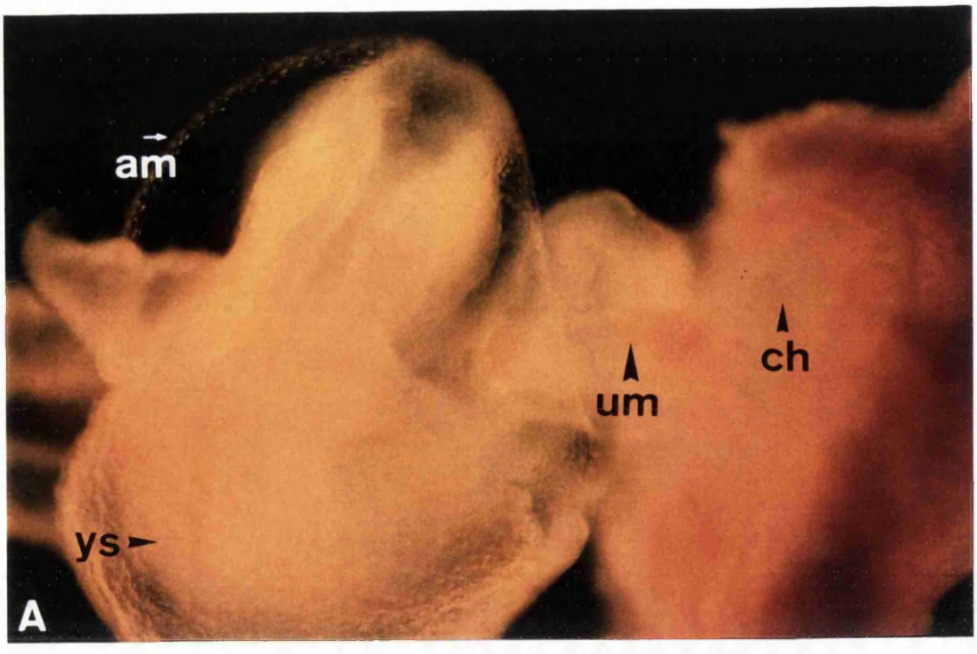
am
ch
um
ys
A

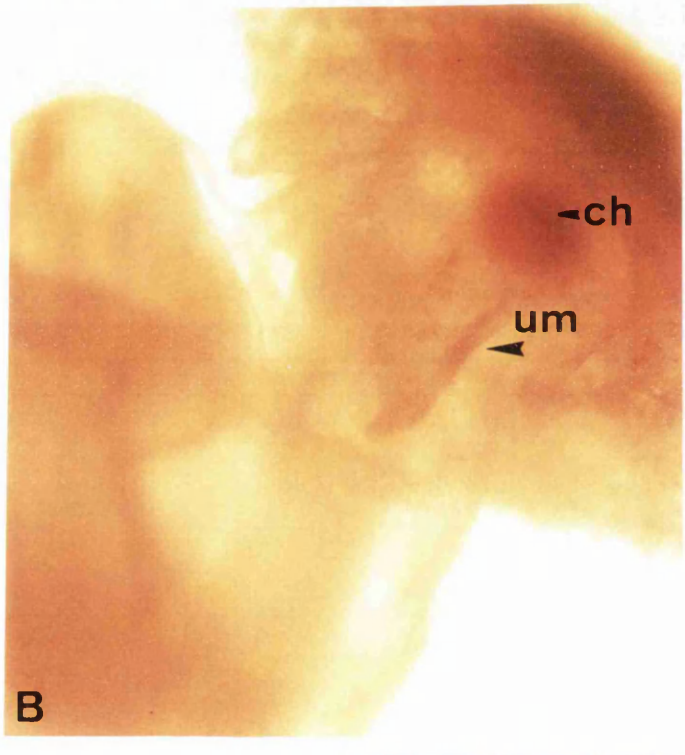
ch
um
B

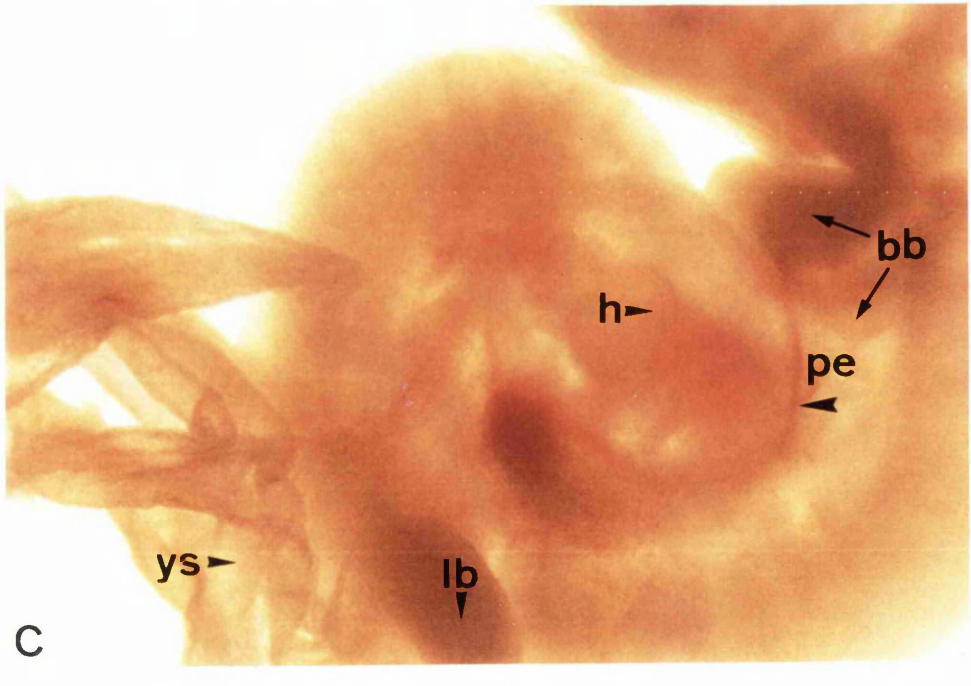
bb
h
pe
ys
lb
C

The embryo *per se* in all conceptuses studied appeared grossly normal. However, a number of embryos contained haemorrhages, either around the heart or dorsal aorta. Several phenotypic conceptuses also appeared to have grossly swollen pericardia, a secondary defect normally associated with the cessation of blood-flow in the yolk sac plexus. A very small number of embryos from the study exhibited hydrocephaly. Photographic examples of these defects are shown in Figures 10 and 11.

In conclusion, there does not appear to be any strain-specific difference in the manifestation of the TGFβ1 mid-gestation phenotype as analysed here using gross morphological means. On all genetic backgrounds studied the defining attributes of the TGFβ1 knockout phenotype were aberrant yolk sac vasculogenesis, defective chorio-allantoic development and yolk sac anaemia. The defective haematopoiesis and vasculogenesis occur both independently of one another and together. Other defects included blood pools in the yolk sac and embryo and extreme swelling of the pericardium. These findings are comparable with those characterised by Dickson *et al.*, 1995.

3.4. Analysis of Embryos at 11.5dpc.

3.4.1 Severe Defects in Vasculogenesis and Haematopoiesis Lead to Death at 10.5-12.0dpc.

Previous accounts of the mid-gestation phenotype in TGFβ1+/- and -/- embryos report that severely abnormal embryos were lost prior to 11.5dpc secondary to defective yolk sac development (Dickson *et al.*, 1995). In this project, an analysis of genotype and phenoype ratios of NIH, 129 and F1 conceptuses at 11.5dpc was undertaken for a number of reasons. Firstly, to check the efficacy of the morphological scoring system in assessing the potential lethality of the phenotype; and secondly, to pinpoint precisely the developmental age of death of embryos on each of the genetic backgrounds studied.

>100 conceptuses from TGFβ1+/- intercrosses on NIH, 129 and F1 backgrounds were examined and scored (Table 14; Graph 11). Those found to be phenotypic and/ or dead or dying were scored with respect to the severity of the phenotype. At 11.5dpc the yolk sac is fully vascularised. A well-defined branching plexus of vessels extends completely around the yolk sac, and it should be easy to separate the vitelline artery and vein. In this study, a severe phenotype was defined as an avascular yolk sac, or

the absence of a full yolk sac plexus but the presence of inadequate/ disorganised vessels. This was typified by yolk sacs which exhibited only an unbranching vitelline artery and vein. A yolk sac with delicate vessels sustaining a normally developing conceptus was scored as a minor phenotype. In each of the conceptuses examined, the embryo *per se* was either normal, in a normal or mildly phenotypic yolk sac or dead/ dying in a severly abnormal yolk sac. Photographic comparison of severely phenotypic and non-phenotypic conceptuses is shown in Figures 12 and 13 .

The results show that no TGFβ1+/+ conceptuses in each strain studied had severe defects at 11.5dpc. Only conceptuses which possessed a TGFβ1 null allele had become severely phenotypic at mid-gestation. However, the percentage of TGFβ1+/- and -/- conceptuses judged to be severely abnormal varied greatly between genetic backgrounds (Graph 12). Again, the least affected background at mid-gestation was NIH. Using a χ^2 'goodness of fit' statistical test it was found that like at 9.5dpc, the ratios of total embryos on a 129 and F1 genetic background did not deviate significantly from the expected 1 : 2 : 1 TGFβ1+/+ : +/-: -/- ratio ($p=<0.06$ in each case), whereas, on an NIH background $p=>0.40$ (Table 15).

In a TGFβ1+/- intercross, the number of TGFβ1+/+ conceptuses should equal the number of TGFβ1-/- conceptuses at any developmental age if there is no other factor(s) acting to affect this ratio. Thus, any significant loss of TGFβ1-/- conceptuses can be identified by comparing the ratio of observed TGFβ1+/+ : TGFβ1-/- to the expected 1 : 1 ratio using a χ^2 'goodness of fit' test. The results show that a significant loss of TGFβ1-/- conceptuses had occured by 11.5dpc on both the 129 and F1 genetic backgrounds ($p=<0.01$ and $p=0.03$ respectively) but not the NIH genetic background ($p=0.30$). Therefore a significant proportion of affected 129 and F1 TGFβ1-/- embryos had already been resorbed or were too degraded to genotype by PCR by 11.5dpc.

Calculations to ascertain ratios of normal embryos in each genotype again show that a significant proportion of 129 and F1 TGFβ1+/- and -/- conceptuses are severely phenotypic at 11.5dpc ($p<0.01$), whereas on an NIH background $p=0.09$. Numbers of normal conceptuses were calculated by the subtraction of the number identified as severely phenotypic from the total in each genotypic class.

Loss of TGFβ1+/- conceptuses and the occurrence of a severe phenotype in TGFβ1+/- conceptuses was analysed statistically (see Table 15). No significant

deviation from an expected 1 : 2 +/+ : +/- ratio of total or normal conceptuses was seen on any genetic background. However, the probability of deviation from the expected number of normal TGFβ1+/- conceptuses was 0.07 on a 129 background, whereas p=>0.30 in NIH and F1 strains, implying that use of larger data sets might have produced statistically distinct results.

Thus it would appear that the defective yolk sac phenotype of the TGFβ1-/- embryos mid-gestation phenotype is not variable between strains, and always occurs between 10.5 and 12.0dpc, as previously reported (Dickson *et al.*, 1995). However, there is a strain-specific penetrance of the severe mid-gestation TGFβ1 knockout phenotype, illustrated by a lower prevalence of the phenotype on a NIH genetic background compared to 129 and F1 strains.

Any significant loss of heterozygous embryos, or occurence of a severe phenotype at 11.5dpc in the TGFβ1+/- embryos is unclear; certainly - a number of severely abnormal TGFβ1+/- conceptuses were identified on all genetic backgrounds at 9.5 and 11.5dpc. The p values indicate that 129 TGFβ1+/- conceptuses are more prone to developing a severe mid-gestation phenotype than those from F1 and NIH genetic backgrounds. Previous work suggests that a small sub-set of TGFβ1+/- animals may be affected in each strain (Dickson *et al.*, 1995), thus, the use of relatively small sample sizes may be masking any strain-specific contributions to onset and severity of the mid-gestation TGFβ1 knockout phenotype in TGFβ1+/- conceptuses.

To summarize, this data is comparable with the results shown in Table 12, i.e. the genotype and phenotype ratios of TGFβ1+/- intercrosses analysed at 9.5dpc: It also closely reflects data of observed genotype ratios of pups at birth from TGFβ1+/- intercrosses on NIH, 129 and reciprocal F1 genetic backgrounds (Bonyadi *et al.*, 1997). There is a strain-specific difference in the penetrance of the TGFβ1 knockout mid-gestation phenotype: NIH conceptuses are least affected, whereas a significant loss of F1 and 129 TGFβ1-/-conceptuses had occurred by 11.5dpc. Severely affected embryos die between 10.5 and 12.0dpc as a result of yolk sac insufficiency.

Table 14.

Strain	+/+	+/-	-/-	Unknown	Total	Ratio
NIH	34 [0]	62 [6=10%]	26 [8=31%]	10	132	1:1.8:0.8
129	37 [0]	55 [4=8%]	10 [4=40%]	13	115	1:1.5:0.3
F1	29 [0]	57 [7=12%]	14 [9=64%]	8	108	1:2:0.5

Table 15.

Strain	1 : 2 : 1 TGFβ1 +/+ : +/- : -/- Total Embryos	1 : 2 TGFβ1 +/+ : +/- Total Embryos	1 : 1 TGFβ1 +/+ : -/- Total Embryos	1 : 2 TGFβ1 +/+ : +/- Normal Embryos	1 : 2 : 1 TGFβ1 +/+ : +/- : -/- Normal Embryos
NIH	p=0.42	p=0.65	p=0.30	p=0.37	p=0.09
129	p=0.01	p=0.16	p=<0.01	p=0.07	p=<0.01
F1	p=0.02	p=>0.90	p=0.03	p=0.52	p=<0.01

Tables 14 and 15. Genotype and Phenotype Ratios of NIH, 129 and F1 Conceptuses from TGFβ1+/- Intercrosses at 11.5dpc.

>100 conceptuses from TGFβ1+/- intercrosses on NIH, 129 and F1 genetic backgrounds at 11.5dpc were dissected from maternal tissue and morphologically scored, then genotyped by PCR using genomic DNA. Numbers in square brackets indicate conceptuses scored in each genotypic class as having a severe phenotype, dead or dying - but not yet resorbed; these figures are also expressed as a percentage of the genotypic class. The data was analysed using χ^2 'goodness of fit' tests. Numbers of normal conceptuses were calculated by subtracting the total of severley phenotypic conceptuses from the total in each genotypic class.

Graph 11. TGFβ1 +/+ : +/- : -/- 1 : 2 : 1 Ratios at 11.5dpc.

The expected ratio of TGFβ1+/+ : +/- : -/- animals generated by TGFβ1+/- intercrosses at any developmental stage is 1 : 2 : 1. Graph 11 shows the observed genotype ratios of NIH, 129 and total F1 conceptuses at 11.5dpc. In the calculation of ratios, the number of TGFβ1+/+ animals was taken as '1'. The apparent loss of TGFβ1+/- animals on the 129 genetic background is statistically insignificant.

Graph 12. Observed Percentage of Severely Abnormal TGFβ1 Knockout Conceptuses at 11.5dpc in Each Genotypic Class.

Upon dissection each TGFβ1 knockout conceptus was morphologically assessed. Graph 12 shows the percentage of animals in each genotypic class in NIH, 129 and total F1 conceptuses which were severely abnormal, and therefore judged to be unable to survive through mid-gestation. Thus, a strain-dependent percentage of the total surviving TGFβ1+/- and -/- embryos in each genotypic class were observed to be severely abnormal.

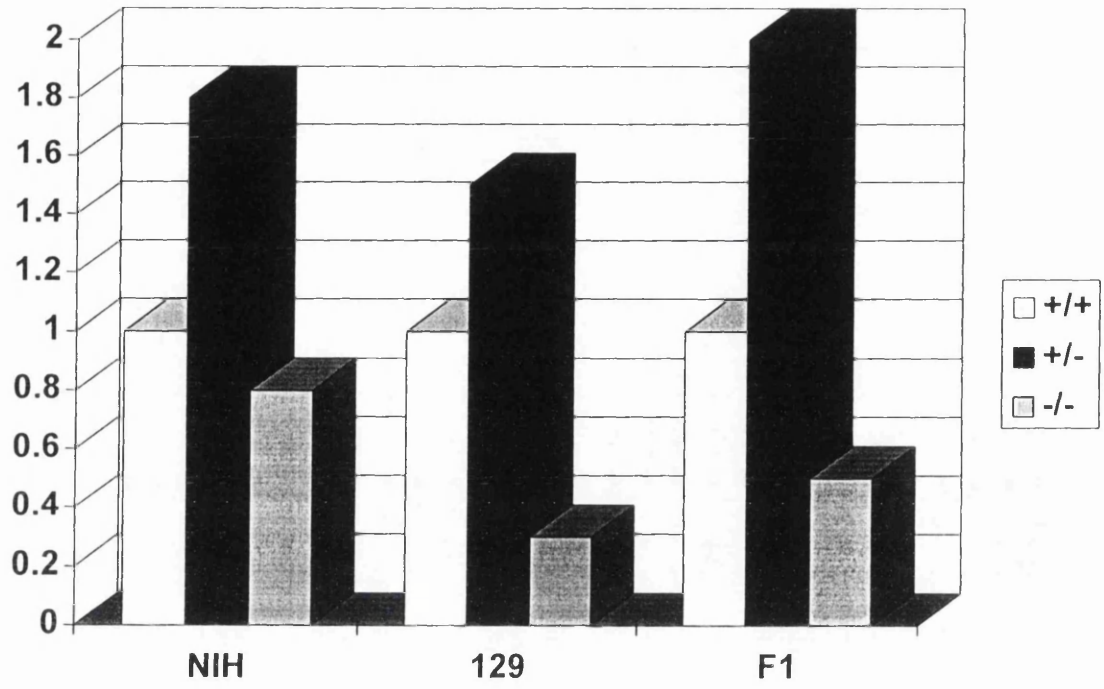
2
1.8
1.6
1.4
1.2
1
0.8
0.6
0.4
0.2
0
NIH
129
F1
+/+
+/-
-/-

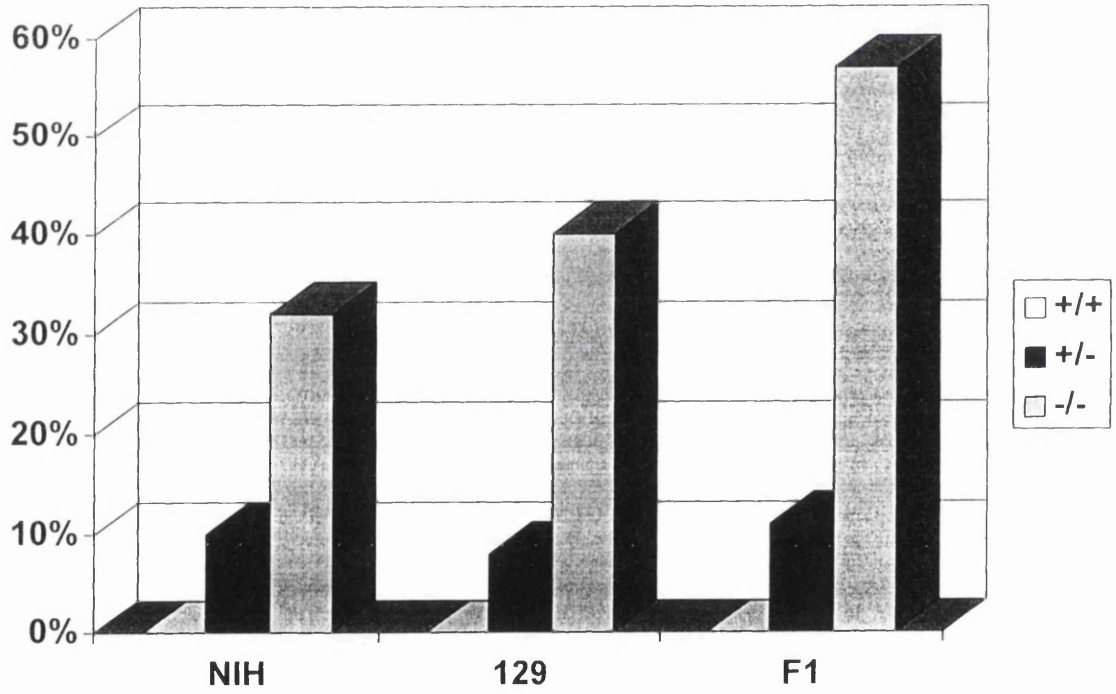
60%
50%
40%
30%
20%
10%
0%
NIH
129
F1
+/+
+/-
-/-

Figure 12 - Morphological Analysis of TGFβ1 Knockout Conceptuses at 11.5dpc.

Conceptuses generated by TGFβ1+/- intercrosses were dissected free from the maternal tissue, morphologically assessed and genotyped by PCR of genomic DNA. A normal TGFβ1+/+ conceptus at 11.5dpc (A), (B) has a full, branching plexus of yolk sac vessels containing haemoglobinised blood. (C) shows a healthy TGFβ1+/+ embryo, whereas (D) illustrates a typical dead embryo dissected from a necrotic yolk sac. Note the developmental delay.

Scale bars (A), (B) = 850μm (C), (D) = 675μm.
bb = branchial bars, bv = blood vessel, h = heart, lb = limb bud, pe = pericardium, s = somite, vv = vitelline vessels.

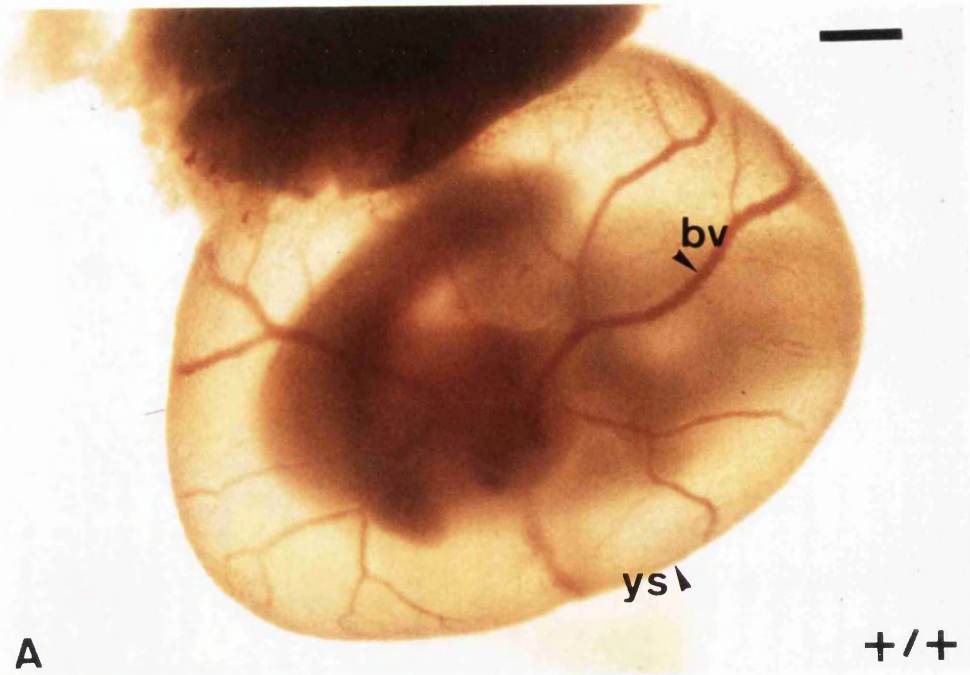
bv
ys
A
+/+

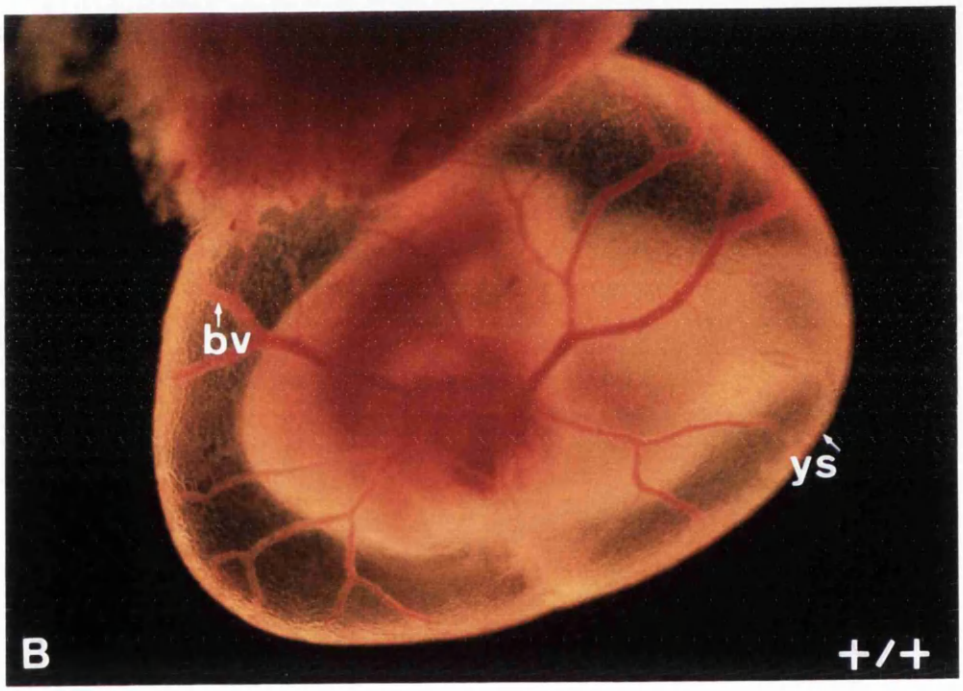
bv
ys
B
+/+

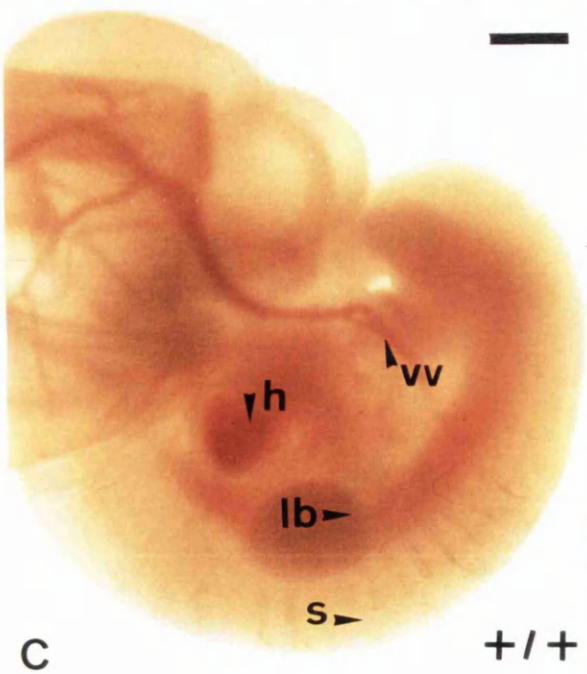
vv
h
lb
s
C
+/+

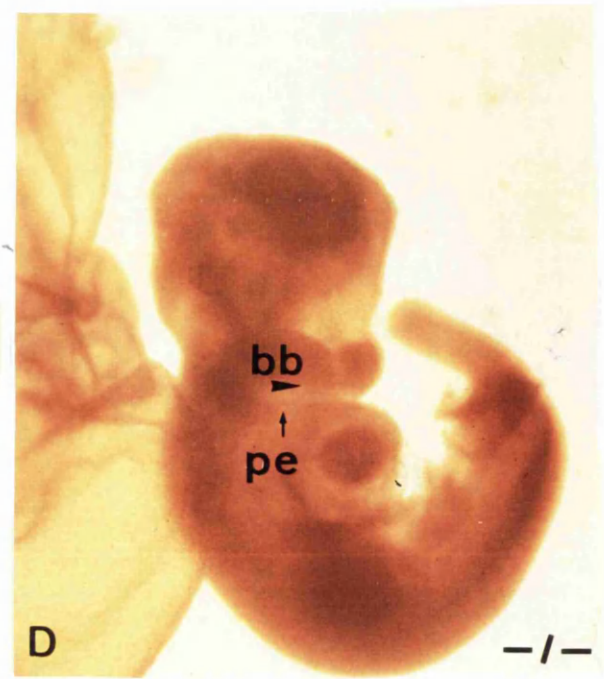
bb
pe
D
−/−

Figure 13 - Morphological Analysis of TGFβ1 Knockout Conceptuses at 11.5dpc.

Compared to (A) and (B) (Figure 12), conceptuses (A), (B) and (C) displayed here all have defects of the extra-embryonic vasculature. (A) has a delicate, relatively unbranched yolk sac plexus. Some vessels appear anaemic and a large haemmorhage has occurred in the region of the embryonic heart. The yolk sac vessels in (B) also appear delicate, and have pronounced extra-embryonic anaemia. Yolk sac (C) shows a striking example of inadequate branching in the major yolk sac vessels. A small amount of haemoglobinised blood is present. The embryo in the yolk sac was found to be dead.

Scale bars = 850μm.
bv = blood vessel, ha = haemmorhage, ys = yolk sac.

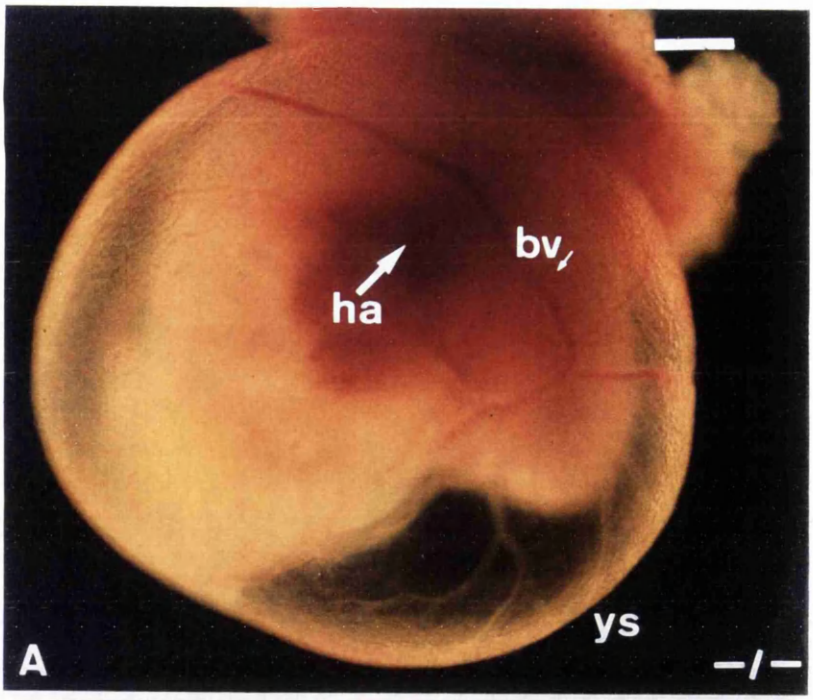
ha
bv
ys
A
−/−

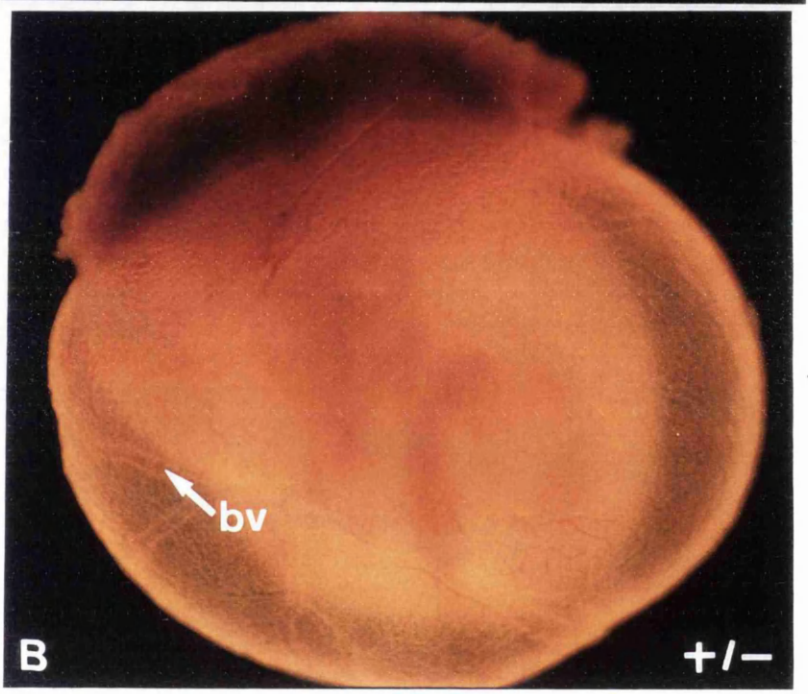
bv
B
+/−

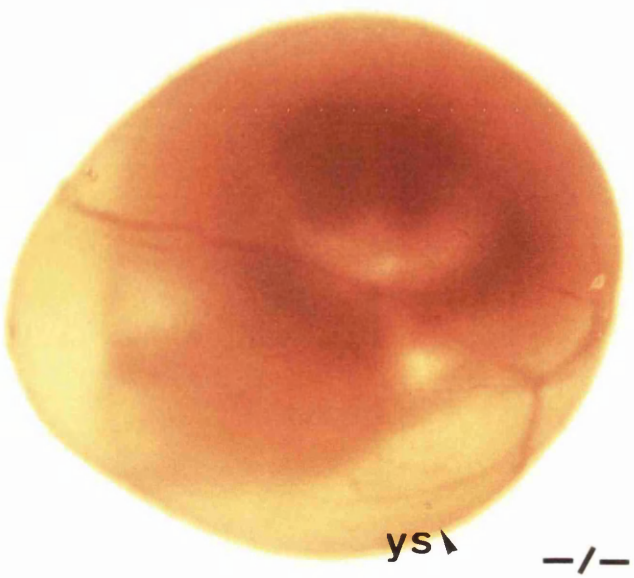
ys
C
−/−

3.5 Analysis of Anaemia in TGFβ1 Knockout Mid-Gestation Conceptuses.

3.5.1 No Variation in the Expression of ζ-Globin mRNA is Seen In 8.5dpc F1 Conceptuses from TGFβ1+/- Intercrosses.

Analysis of the gross anaemic phenotype of the TGFβ1 knockout mice is problematic; the observed vascular phenotype may have made an direct or indirect contribution to the apparently anaemic state of the yolk sac. Thus, the anaemic appearance of yolk sacs carrying a TGFβ1 null allele may be due either to a specific defect in the haemoglobinisation process, or to a reduction in the absolute number of circulating erythroid cells, or both. A reduction in circulating erythroid cells could be a secondary effect of the TGFβ1 knockout vascular phenotype, since the proper development of the blood islands is required for the differentiation of haematopoietic precursors (see Introduction).

In an attempt to address this problem, 30, F1 conceptuses from four TGFβ1+/- intercross litters at 8.0-8.5dpc were dissected free from the maternal tissue, and fixed overnight in 4% PFA. Thereafter, they were hybridised by whole-mount in situ hybridisation with an antisense ζ-globin mRNA probe, as described in Materials and Methods 2.8. A number of control embryos were hybridised using a sense ζ–globin mRNA probe.

At 8.0-8.5dpc, the blood islands form an anastomosing corona around the top of the murine yolk sac. This spreads towards the base of the yolk sac as other blood islands in the yolk sac anastomose to form primitive blood vessels and by 9.0-9.5dpc, the vascular plexus of the yolk sac has begun to develop. During this period the vitelline artery and vein have started to branch, and other yolk sac vessels are formed. Haemoglobinised blood is visible in the yolk sac circulation.

	+/+	+/-	-/-
0	0	0	0
+	1 =12.5%	3 =20%	1 =14%
++	4 =50%	6 =40%	3 =43%
+++	3 =37.5%	6 =40%	3 =43%
Total	8 = 100%	15 = 100%	7 = 100%

Table 16. There is No Difference in the Level of Hybridisation of a ζ-Globin Antisense mRNA Probe on 8-8.5dpc F1 Conceptuses from TGFβ1+/- Intercrosses.

30 F1 conceptuses from TGFβ1+/- intercrosses were hybridised with an antisense mRNA ζ-globin probe by whole-mount in situ hybridisation. The intensity of signal was scored; 0, +, ++, +++, and the conceptus was photographed and genotyped by PCR.

Figure 14 - ζ-globin Whole Mount In Situ Hybridisation on TGFβ1+/- Intercross Litters at 8.5dpc.

>30 8.0-8.5dpc TGFβ1 knockout conceptuses were subjected to whole mount in situ hybridisation using an anti-sense ζ-globin mRNA probe. The degree of positive staining was scored, and each embryo genotyped. Photographs (A), (B) and (C) show that there is no striking difference in the level of ζ-globin mRNA expression regardless of TGFβ1 genotype at around 8.5dpc. The positive stain above corresponds to the anastomosing corona of blood islands seen in the developing yolk sac.

Scale bar = 150μm.
bi = blood islands, hf = head folds, ht = heart, ys = yolk sac.

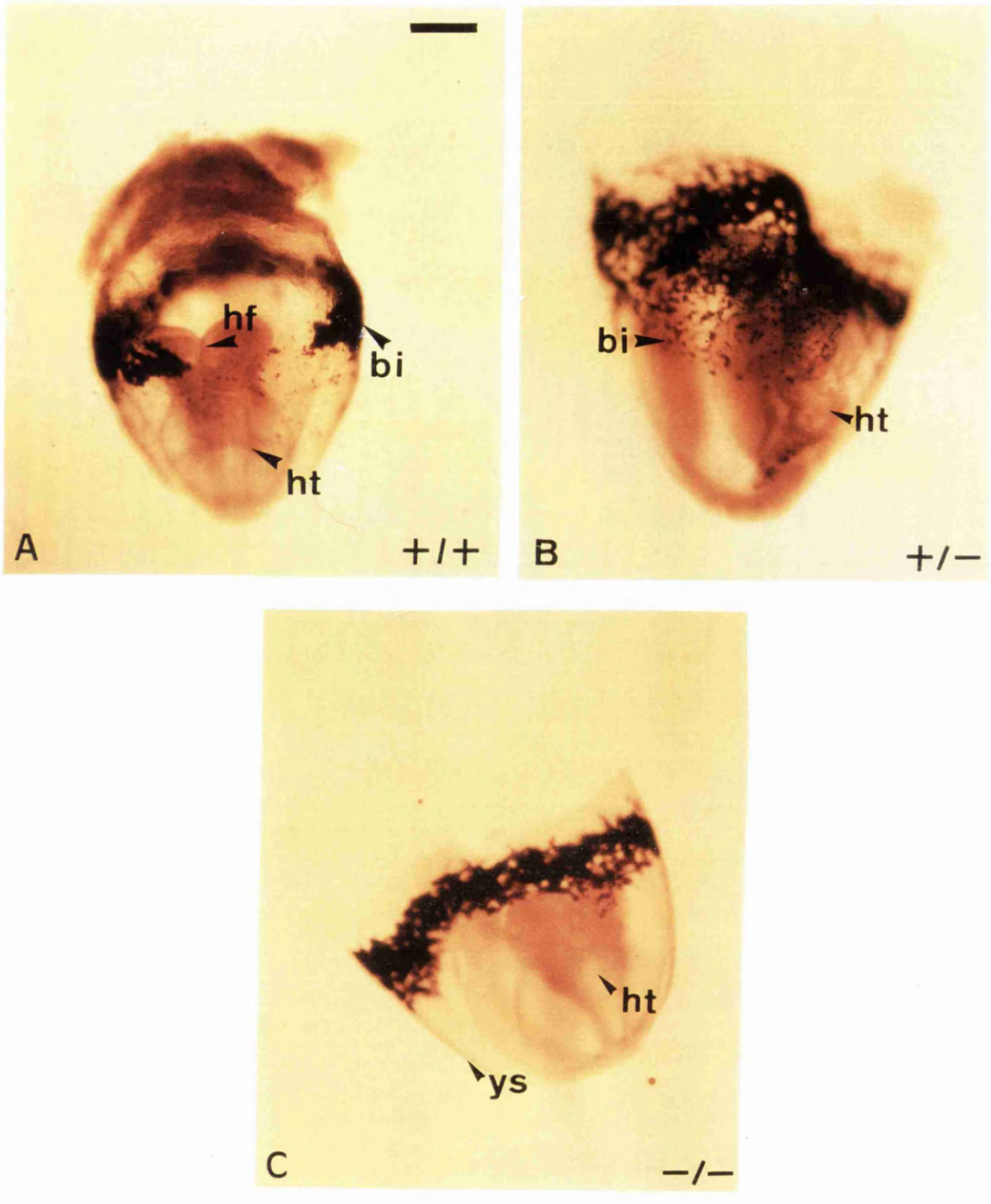
hf
bi
ht
A
+/+
bi
ht
B
+/−
ht
ys
C
−/−

In this experiment, the resulting level of ζ-globin hybridisation was scored as 0, +, ++, or +++ depending on signal intensity. Assessment of several landmark developmental features ensured that the conceptuses scored were of comparable developmental ages. Then the conceptuses were photographed and retrospectively genotyped by PCR (see Materials and Methods). As shown in Table 16, there is no obvious genotypic relationship to the level of expression of ζ-globin mRNA at 8.0-8.5dpc in F1 conceptuses (see Figure 14).

Thus at 8.5dpc in F1 conceptuses there is no clear genotype-specific difference in the expression level of ζ-globin mRNA. This is in concordance with the findings of Dickson *et al.* (1995), working on a mixed genetic background. Dickson et al. (1995) also reported that by 9.5dpc there was an obvious downregulation of ζ-globin mRNA positive cells in TGFβ1 mutant yolk sacs.

3.5.2 May-Grunwald Giemsa Staining Can Be Used to Identify Anaemia in F1 TGFβ1+/- Intercross Litters.

One of the defining characteristics of the TGFβ1 knockout phenotype is the occurrence of anaemia in the yolk sacs of TGFβ1+/- and -/- conceptuses. At 8.0-8.5dpc the level of ζ-globin mRNA expression in TGFβ1+/+ and -/- yolk sacs is comparable. However, by 9.0-9.5dpc, the two genotypic classes are easily distinguishable. Dickson *et al.*, 1995 postulated that this was due to an overall reduction in the number of circulating erythroid cells, not a specific defect in the haemoglobinisation process. This experiment can address the latter, but not the former, aspect of the TGFβ1 knockout anaemic phenotype.

In order to investigate further the anaemic mid-gestation phenotype of the F1 TGFβ1 knockout conceptuses, the level of haemoglobinisation in erythroid cells was analysed histologically. Blood smears were made from the opened yolk sacs of the four litters of F1 conceptuses used in Results 3.5.3, and stained with May-Grunwald Giemsa stain (see Materials and Methods). The littermates were dissected and morphologically scored at 9.5dpc and half of the embryo was retained for isolation of genomic DNA for genotyping by PCR. 29 slides were scored.

	+/+	+/-	-/-	Non-Phenotypic	Phenotypic
Mean Proportion of Haemaglobinised Cells	0.43 ± 0.09	0.36 ± 0.10	0.25 ± 0.09	0.41 ±0.08	0.25 ±0.08
Mean Proportion of Dead/ Damaged Cells	0.15 ±0.04	0.14 ±0.05	0.17 ±0.03	0.15 ±0.04	0.17 ±0.04
Number of Samples	9	14	6	20	9

Table 17. Assessment of Haemoglobinisation in F1 Conceptuses from TGFβ1+/- Intercrosses at 9.5dpc.

The table shows figures derived from 29 informative blood smears from 9.5dpc littermates. Three, x 40 fields of view each containing >100 cells were counted and the proportion of haemoglobinised and dead/ damaged primitive erythroid cells for each conceptus calculated as a proportion of the total cells counted. On average, the total number of cells counted per conceptus was >500. Student's t test was used to compare the different genotypic and phenotypic classes of data.

Graph 13a. The Mean Proportion of Haemoglobinised Cells (score 1) Observed in Blood Smears from TGFβ1+/- Intercross Litters in Each Genotypic Class.

Blood smears were made from morphologically scored littermates from TGFβ1+/- intercrosses. The graph shows the mean proportion of haemoglobinised cells (score 1) counted in blood smears from yolk sacs of genotypes 1 (TGFβ1+/+), 2 (TGFβ1+/-) and 3 (TGFβ1-/-). There is a significant difference between the mean proportion of haemoglobinised cells observed in TGFβ1+/+ and -/- conceptuses.

Graph 13b. The Mean Proportion of Haemoglobinised Cells (score 1) Observed in Blood Smears from TGFβ1+/- Intercross Litters from Normal and Abnormal Yolk Sacs.

Blood smears were made from morphologically scored littermates from TGFβ1+/- intercrosses. The graph shows the mean proportion of haemoglobinised cells (score 1) counted in blood smears from conceptuses scored upon dissection as anaemic (p) or normal (/). There is a significant difference between the mean proportion of haemoglobinised cells observed in conceptuses scored as anaemic and normal.

Box and Whisker Plots: The data is presented as follows; the box represents the 1st to 3rd quartiles, the line in the centre of the box is the median value and the whiskers cover the remaining data. Stars represent individual pieces of outlying data.

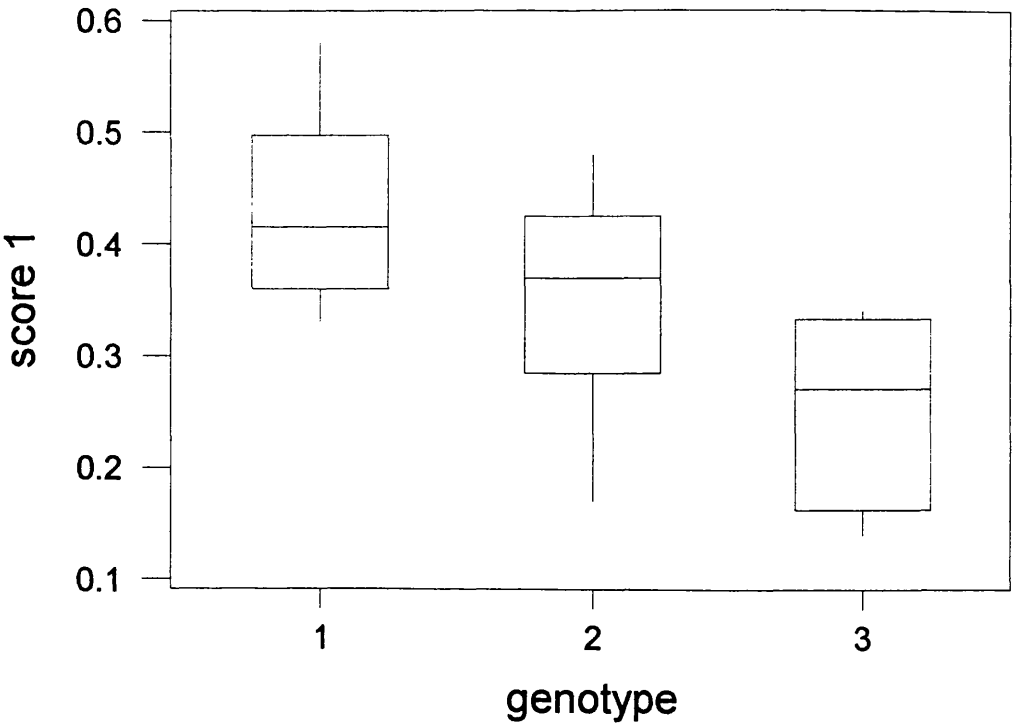
0.6
0.5
0.4
0.3
0.2
0.1
score 1
1
2
3
genotype

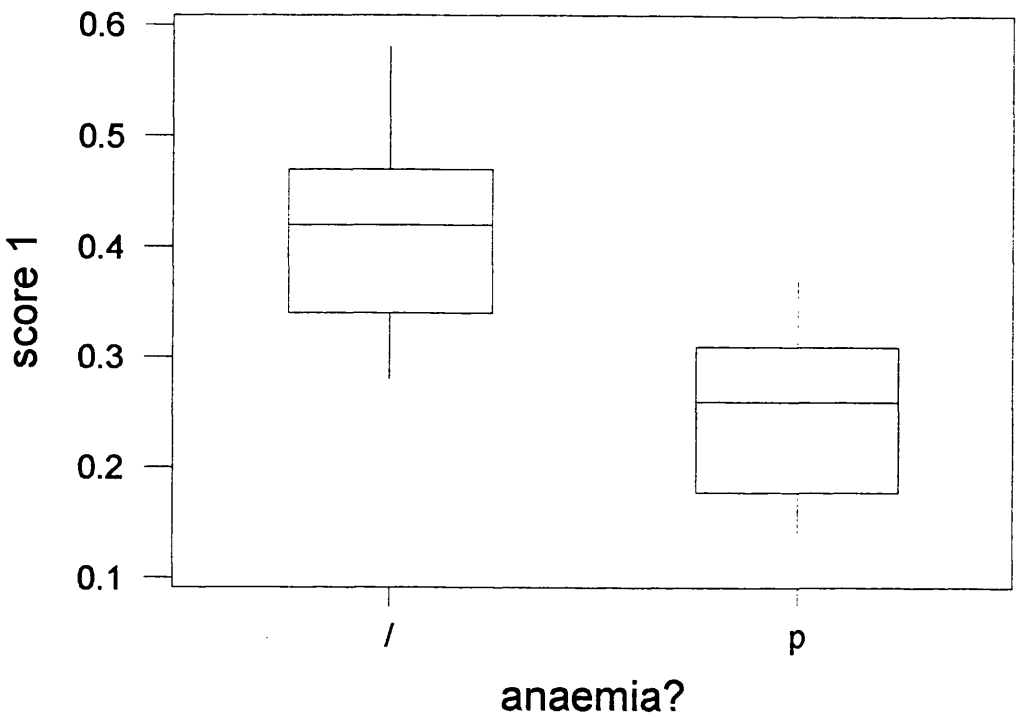
0.6
0.5
0.4
0.3
0.2
0.1
score 1
/
p
anaemia?

Graph 14a. The Mean Proportion of Dead/ Dying Cells (score 2) Observed in Blood Smears from TGFβ1+/- Intercross Litters in Each Genotypic Class.

Blood smears were made from morphologically scored littermates from TGFβ1+/- intercrosses. The graph shows the mean proportion of dead/ dying cells (score 2) counted in blood smears from yolk sacs of genotypes 1 (TGFβ1+/+), 2 (TGFβ1+/-) and 3 (TGFβ1-/-). There is no significant difference between the mean proportion of dead/ dying cells observed in TGFβ1+/+ and -/- conceptuses.

Graph 14b. The Mean Proportion of Dead/ Dying Cells (score 2) Observed in Blood Smears from TGFβ1+/- Intercross Litters from Normal and Abnormal Yolk Sacs.

Blood smears were made from morphologically scored littermates from TGFβ1+/- intercrosses. The graph shows the mean proportion of dead/ dying cells (score 2) counted in blood smears from conceptuses scored upon dissection as anaemic (p) or normal (/). There is no significant difference between the mean proportion of dead/ dying cells observed in conceptuses scored as anaemic and normal on dissection.

Box and Whisker Plots: The data is presented as follows; the box represents the 1st to 3rd quartiles, the line in the centre of the box is the median value and the whiskers cover the remaining data. Stars represent individual pieces of outlying data.

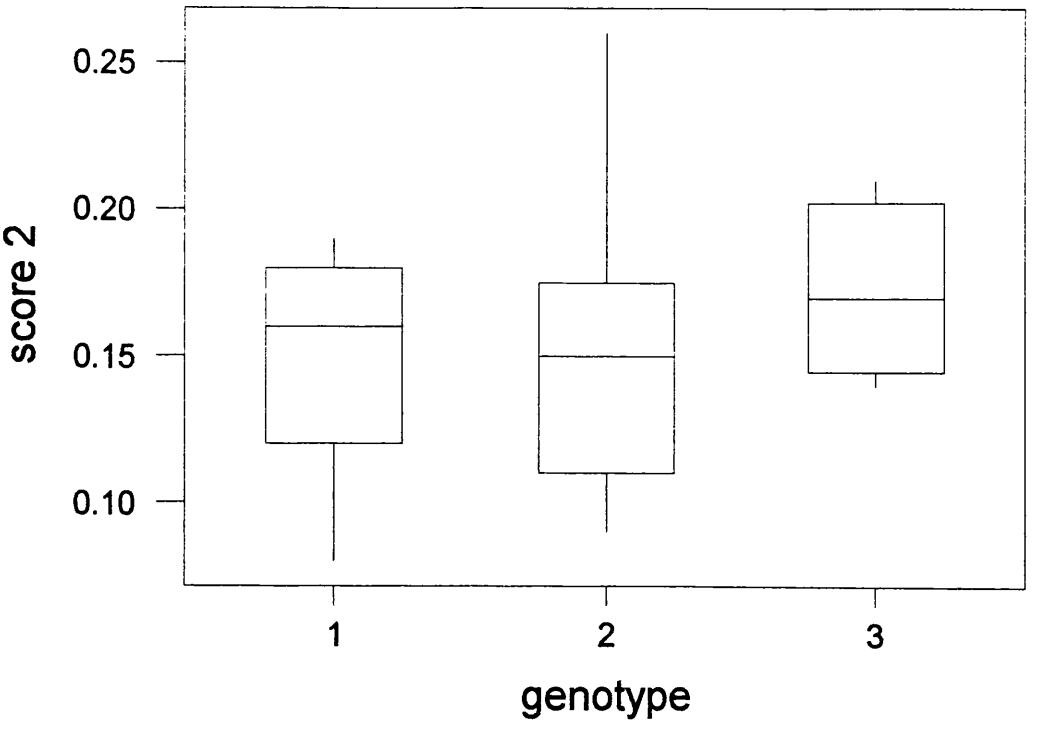
0.25
0.20
0.15
0.10
score 2
1
2
3
genotype

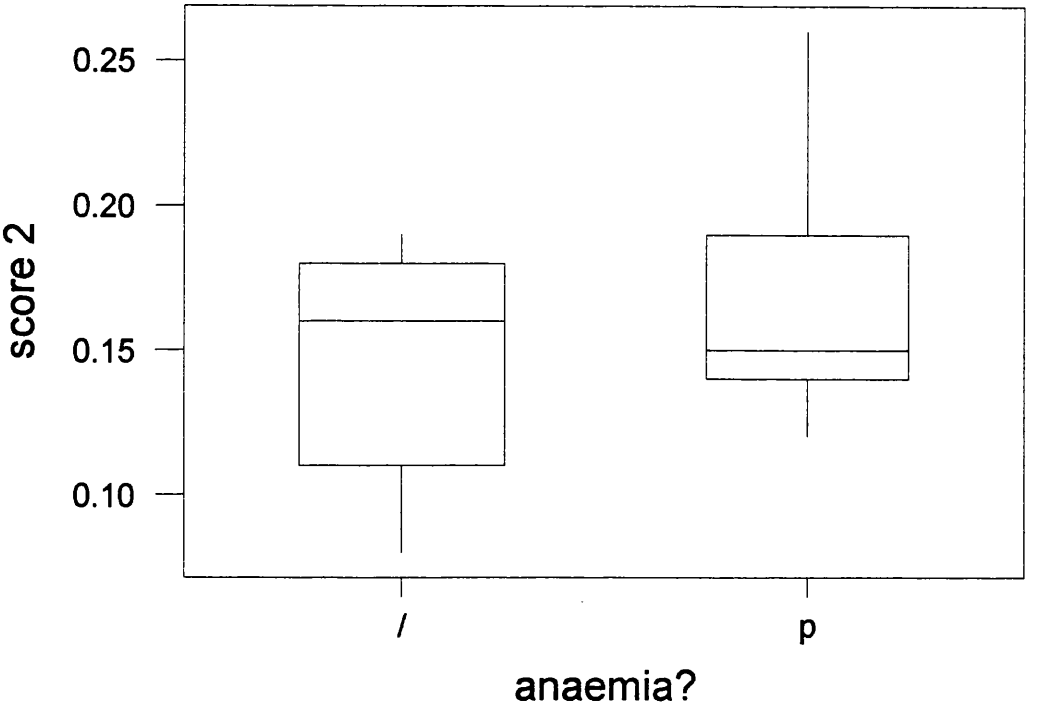
0.25
0.20
0.15
0.10
score 2
/
p
anaemia?

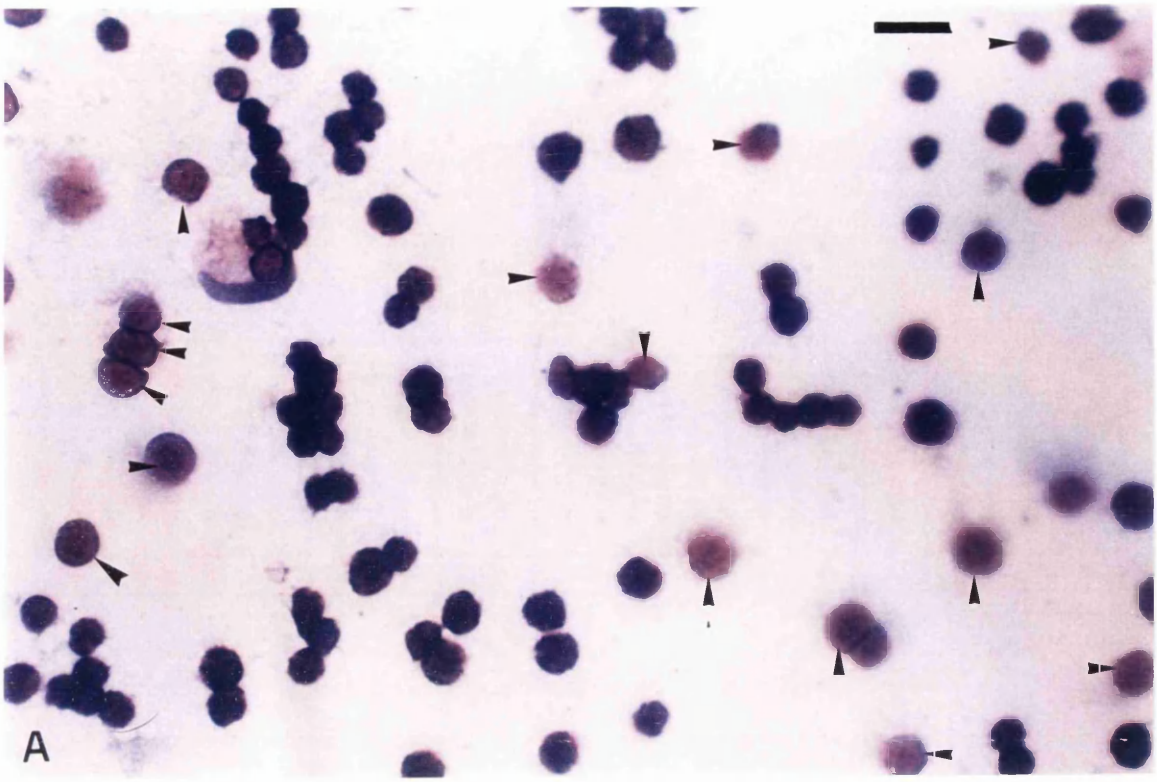

Figure 15 - Assessment of the Proportion of Haemoglobinised Cells from TGFβ1 Knockout Conceptuses at 9.5dpc.

Blood smears were made from dissected and morphologically scored yolk sacs (Materials and Methods 2.5.5). The blood was subjected to May-Grunwald Geimsa staining and the proportion of haemoglobinised and dead/ dying cells calculated. On average a total exceeding 500 cells from 3 fields of view were counted per smear. Pinkish cells were counted as haemoglobinised (examples here indicated by arrowheads). The results suggested a significant reduction in the proportion of haemoglobinised cells present in TGFβ1-/- and anaemic yolk sacs compared to normal littermates. The proportion of cells scored as dead/ dying did not alter with respect to genotype/ phenotype.

Scale bar = 12μm.

Blood cells were counted thus: Total cells in three, x 40 magnification fields of view were counted on each slide and the number of cells judged to be haemoglobinised and the number appearing to be dead/ damaged recorded. Each field of view counted contained >100 cells - on average, the number of primitive erythroid cells counted per conceptus exceeded 500. A pinkish hue identified the onset of haemoglobinisation of these cells (Weiss *et al.*, 1994) (Figure 15). The total proportion of haemaglobinised and dead/ damaged cells was calculated for each yolk sac (Table 17). This data is also presented in box-plots (Graphs 13 and 14). Clearly there is a striking difference in the proportion of haemoglobinised cells counted between TGFβ1+/+ and -/- conceptuses ($p=<0.01$), also between conceptuses scored as anaemic and non-anaemic at dissection ($p=<0.01$). However, the proportion of dead/ dying erythroid cells appears to be indistinguishable between genotypic and phenotypic classes ($p=>0.05$). This observation was validated by statistical comparison of these data sets using Student's t test.

Thus, there appears to be a delay/ specific defect in the process of haemogloginisation of blood cells in TGFβ1 knockout yolk sacs, rather than an illusion of anaemia created by blood loss from defective vessels. However, the latter may contribute to the anaemic phenotype and to the overall reduction in circulating erythroid cells as reported by Dickson *et al.* (1995).

3.6 Histological Analysis of the TGFβ1 Knockout Mid-Gestation Phenotype.

3.6.1 Specific Abnormalities in Dissected Yolk Sacs from F1 TGFβ1+/- Intercross Litters.

In a normal yolk sac the mesothelial and endodermal cell layers are closely apposed except in the regions where they are separated by blood vessels. However, reports of the mixed genetic background TGFβ1 and TβR-II (Dickson et al., 1995) (Oshima *et al.*, 1996) knockout mice mid-gestation phenotypes both demonstate specific abnormalities of yolk sac integrity.

In order to assess the yolk sac phenotype of TGFβ1 knockout mice, four litters of F1 conceptuses were dissected and morphologically scored at 9.5dpc. Half of the embryo was used for isolation of genomic DNA for genotyping by PCR; and the rest of the

conceptus was placed into a vial of fresh 4% PFA and fixed overnight prior to embedding and sectioning (see Materials and Methods).

Sections of yolk sac from each conceptus were examined histologically. Three sections from each of the 32 conceptuses were scored for abnormalities, and scored on a scale of 1-8. There were two main defects identified: Firstly, the degree of buckling i.e. the 'looped out' appearance of the yolk sac endoderm relative to the endothelial and mesothelial layers; and secondly, the amount of shearing i.e. the separation of contacts along the plane of the endothelial cells or dilation of endothelial tubes (see Figure 16 for photographic examples). In both cases a score of 1-4 denoted a normal yolk sac, a score of 5-6 was counted as mildly affected and a score of 7-8 was counted as severely affected. These results are shown in Table 18 and Graph 15.

The results imply that the presence of a TGFβ1 null allele has either directly or indirectly reduced the level of cell-cell adhesion in the F1 yolk sacs in this study. This has resulted in an increased incidence of shearing and and buckling between the endothelial layers in TGFβ1-/- and TGFβ1+/- yolk sacs. It is plausible also that the act of tearing the yolk sac, making blood smears and the retrieval of half the embryo for genotyping as well as the fixation proccess have contributed to an accentuated result.

These findings comply with those of Dickson *et al.* (1995) working on a mixed genetic background. TGFβ1 is known to modulate both the formation of the ECM, and the proliferation of endothelial cells (see Introduction). Dickson *et al.* reported no difference in either the overall number of endothelial and mesothelial cells, nor in the levels of Bromodeoxyuridine (BrdU) incorporation into the nuclei of yolk sac endothelial and mesothelial cells between TGFβ1+/+ and -/- conceptuses. Therefore, endothelial hyperplasia was excluded as a cause of the observed defects. However, a reduction in the expression levels of *flk*-1, a molecular marker of embryonic endothelial cells was identified in TGFβ1-/- yolk sacs (Dickson *et al.*, 1995) which implies a possible defect of maturation/ differentiation in the endothelial cells in TGFβ1 knockout yolk sacs.

Score	+/+	+/-	-/-
1-4 =Normal yolk sac	5 (1)	8 (2)[1]	0
5-6 =Mild defects	1	10 (4)[1]	5 (2)[2]
7-8 =Severe defects	0	1 (1)[0]	1
Total number of yolk sacs scored	6 (1)[0]	20 (7)[2]	6 (2)[2]
Mean	3.7 ± 0.7	4.9 ± 1.2	5.7 ± 0.7

Table 18. Histological Assessment of Yolk Sac Buckling and Shearing in F1 Conceptuses from TGFβ1+/- Intercrosses at 9.5dpc.

Conceptuses from four F1 litters were morphologically scored, genotyped by PCR and the opened yolk sacs embedded and analysed histologically for shearing and buckling. Three sections from each conceptus were examined and a quantitative score assigned for each attribute. Numbers in parenthesis indicate those conceptuses which were scored as slightly phenotypic upon dissection, that is the yolk sac vasculature was developing, but may have appeared delicate or been slightly developmentally delayed. The numbers in square brackets indicate the conceptuses which were scored as severely phenotypic. These conceptuses had major defects of the extra-embryonic vasculature, ranging from a lack of branching and major vessel formation to a completely avascular yolk sac. Data was tested for statistical significance using the Student's t test.

Graph 15a. Abnormalities Observed via Histology in Dissected Yolk Sacs from TGFβ1+/- Intercross Litters

The graph shows the mean score from opened, embedded yolk sacs of genotypes 1 (TGFβ1+/+), 2 (TGFβ1+/-) and 3 (TGFβ1-/-). Sections of each yolk sac were assessed for the degree of endodermal buckling and shearing between the tissue layers, on a scale of 1-8, where 8 represented the most severe defect. There is a significant difference between the mean scores of TGFβ1+/+ and -/- conceptuses.

Graph 15b. Abnormalities Observed via Histology in Dissected Yolk Sacs from TGFβ1+/- Intercross Litters, Expressed as a Function of Phenotype.

Tissue sections were made from the opened, embedded yolk sacs of morphologically scored littermates from TGFβ1+/- intercrosses. These were assessed for the degree of endodermal buckling and shearing between the tissue layers, on a scale of 1-8, where 8 represented the most severe defects. The graph shows the mean scores from conceptuses which, upon dissection had a defective extra-embryonic vasculature (p) or were normal (/). There is no significant difference between the mean scores for conceptuses scored as phenotypic and normal on dissection due to the observed range of phenotypic severity.

Box and Whisker Plots: The data is presented as follows; the box represents the 1st to 3rd quartiles, the line in the centre of the box is the median value and the whiskers cover the remaining data. Stars represent individual pieces of outlying data.

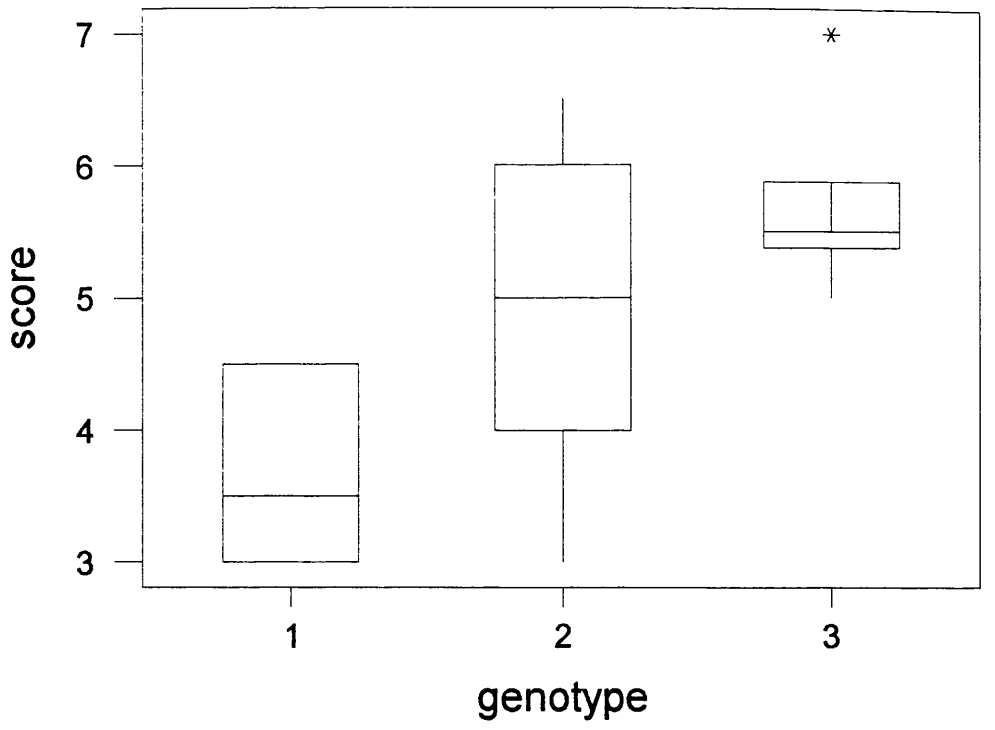
7
6
5
4
3
score
1
2
3
genotype

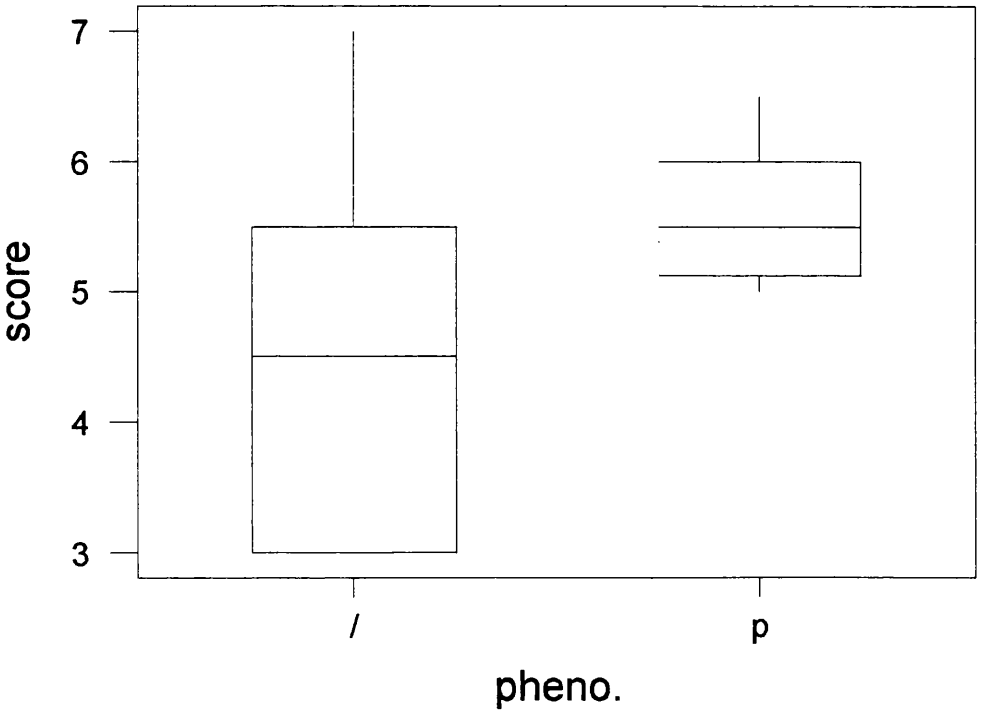
7
6
5
4
3
score
/
p
pheno.

Figure 16 - Histological Analysis of Dissected TGFβ1 Knockout Yolk Sacs at 9.5dpc.

Yolk sacs from embryos generated by TGFβ1+/- intercrosses were dissected free from the maternal tissue and morphologically scored. Half of the embryo was retained for genotyping by PCR. Sections from the opened, embedded yolk sacs were examined histologically. Each yolk sac was scored for endodermal buckling and shearing of the tissue layers in the plane of the endothelial cells. (A) shows a normal TGFβ1+/+ yolk sac. The vessels are discrete and contain blood cells. (B) shows an abnormal yolk sac from a TGFβ1-/- embryo. There is minimal association between the tissue layers, which has resulted in the formation of dilated endothelial tubes.

Scale bar = 45μm.
bc = blood cell, di = dilated endothelial tube, en = endothelium, n = endoderm, v = vessel. Arrowheads indicate regions where cell - cell adhesion has been disrupted.

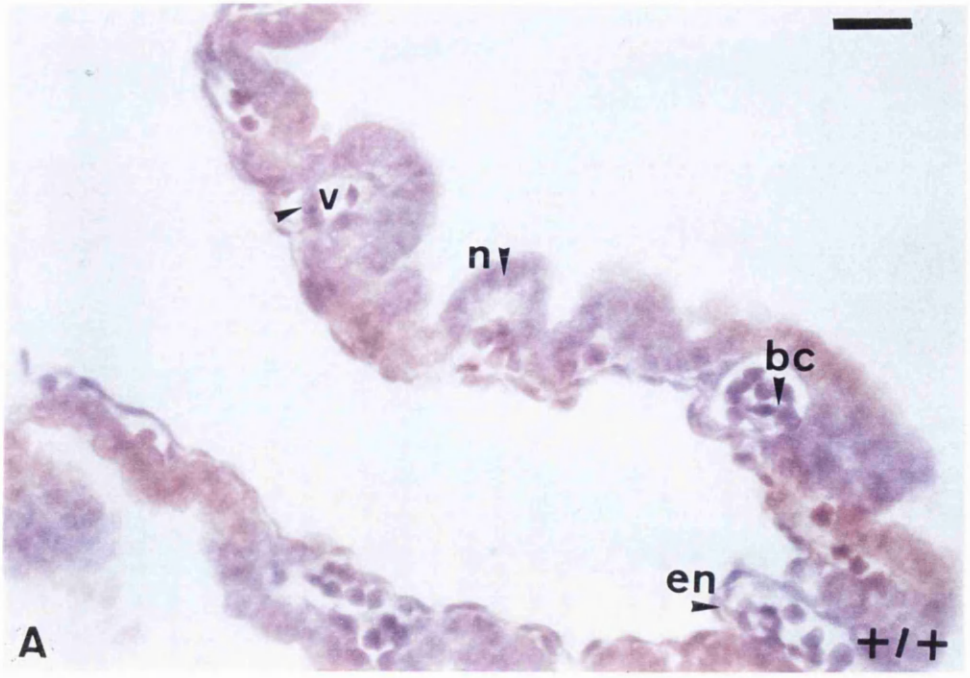
v
n
bc
en
A
+/+

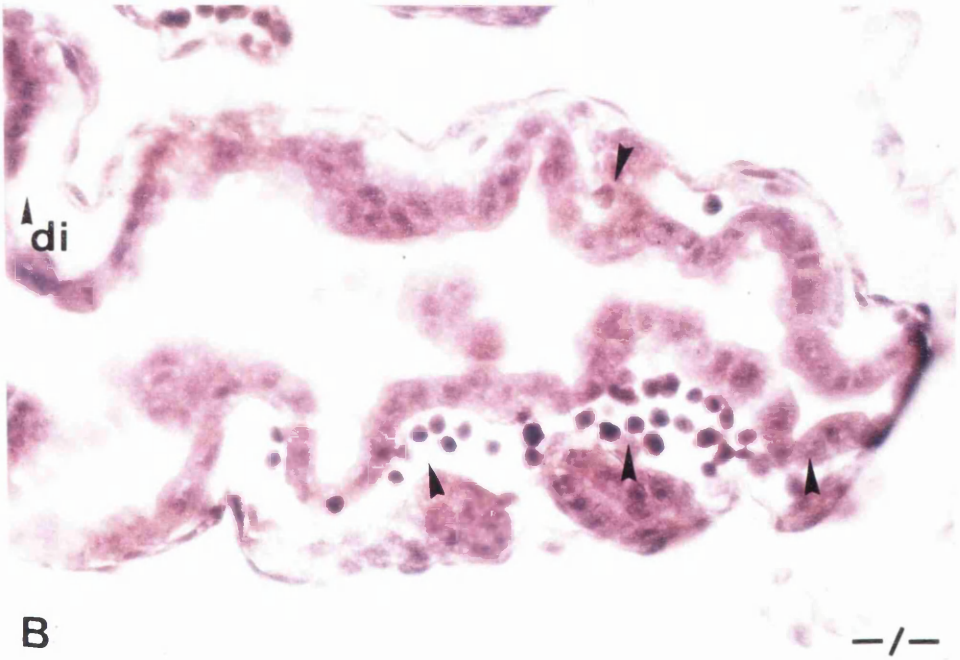
di
B
−/−

3.6.2 Analysis of Unperturbed TGFβ1 Knockout Conceptuses *in utero* by Radioactive In Situ Hybridisation.

The gross yolk sac defects seen in TGFβ1 null animals at 9.5dpc are evident when the yolk sac is sectioned and examined histologically. However, in these cases the yolk sac is opened prior to embedding to facilitate excision of half of the embryo for genotyping by PCR. Consequentially, the mechanical pressures exerted upon the yolk sac during dissection and fixation may have an effect on the typical shearing and buckling defects identified in mutant yolk sacs. It is also impossible to draw conclusions about leaks of blood cells from defective yolk sac vasculature in yolk sacs processed in this manner.

In order to examine and compare yolk sacs from TGFβ1+/- intercrosses whilst minimising secondary effects on the phenotype, two F1 and one NIH litter at 9.5dpc were dissected free of the uterus only and embedded while still in the decidual tissue. The conceptual masses were fixed overnight in 4% PFA, embedded and sectioned (Materials and Methods). To genotype the embryos with minimal disruption to the conceptus, sections were selected for the presence of optimal tissue for genotyping by radioactive in situ hybridisation using an antisense mRNA 1.2kb TGFβ1 probe (Materials and Methods 2.7). TGFβ1 is known to be expressed in the endocardium, endothelial cells of the embryo and allantois at 9.5dpc. Control sections were hybridised with a sense mRNA 1.2kb TGFβ2 probe.

The resulting sections were scored for probe signal intensity (see Table 19) in the relevant tissues and therefore classified either as TGFβ1(+/+ or +/-), or TGFβ1-/-. Hereafter the former class of conceptuses will be referred to a Class (i) - and the latter class of conceptuses referred to as Class (ii). Since TGFβ1 is known to be strongly expressed in the deciduum at 9.5dpc, this was used as a positive experimental control. That is, if an embryo had a low TGFβ1 signal intensity, yet a cell-specific, positive signal in the deciduum it was interpreted that the in-situ hybridisation was successful and that the embryo was TGFβ1-/- (see Figure 17).

To summarise; Out of 23 conceptuses scored, 18 were scored as positive; i.e. 13 with a weak signal and 5 as strongly positive. These might comprise the TGFβ1+/- and TGFβ1+/+ conceptuses respectively. More importantly, 5 were clearly scored as TGFβ1-/-, i.e. the percentage of the total number of conceptuses estimated to be TGFβ1-/- was close to the expected 25% of the total number scored.

	Class (i).		Class (ii).		
Strain	**Strong TGFβ1 Signal**	**Intermediate TGFβ1 Signal**	**No TGFβ1 Signal**	**Total**	**Litters**
NIH	2	5 (1) [2]	1 (1)	8	1
F1	3 (1)	8 (2) [1]	4 (1) [2]	15	2
Total	5 (1)	13 (3) [3]	5 (2) [2]	23	3

Table 19. Estimation of Genotype of Conceptuses from TGFβ1+/- Intercrosses at 9.5dpc by Radioactive In Situ Hybridisation.

Certain sections from NIH and F1 conceptuses at 9.5dpc from TGFβ1+/- intercrosses were subjected to radioactive in situ hybridisation using a full length TGFβ1 antisense mRNA probe. The level of intensity of the resulting signal was scored and classified as TGFβ1(+/+/ +/-) i.e. Class (i); or TGFβ1-/- i.e. Class (ii). Parallel sections to those used for radioactive in-situ hybridisation were examined histologically. Sections were scored on a number of criteria i.e. yolk sac integrity and the development of the embryo. Each conceptus was classified as normal, mildly phenotypic or severely phenotypic. In each genotypic class, the numbers in parenthesis represent conceptuses scored as mildly affected and numbers in square brackets show the number of conceptuses judged to be severely phenotypic.

Figure 17 - Estimation of the Genotype of Intact TGFβ1 Knockout Conceptuses at 9.5dpc Using Radioactive In Situ Hybridisation.

Suitable sections from TGFβ1+/- intercross litters were subjected to radioactive in situ hybridisation using a full-length TGFβ1 antisense mRNA probe. (A), (C), (E) and (G) show the corresponding darkfield images to those shown in (B), (D), (F) and (H). (A) and (B) show an embryo and decidua which were strongly positive for TGFβ1. This conceptus was thus classified as class (i). (C), (D), (E) and (F) illustrate examples of conceptuses which contained an embryo which was negative for TGFβ1, whereas the decidua was positive for TGFβ1. These conceptuses were classified as class (ii). A sense TGFβ1 mRNA probe was used as a negative control (G), (H).

Scale bar = 750μm.
d = decidua, h = heart, hf = head folds, nt = neural tube.

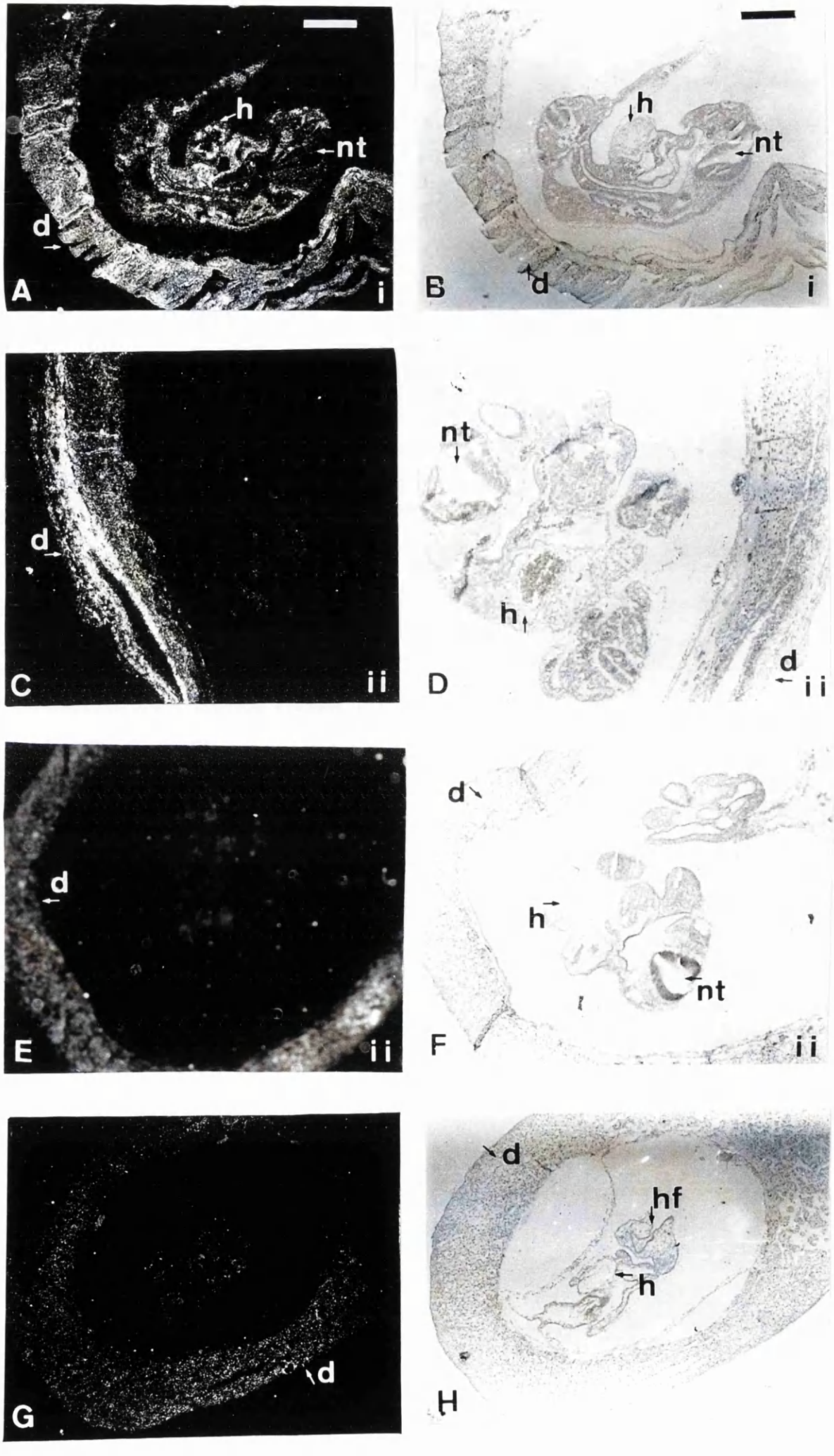
h
nt
d
A
i
h
nt
B
d
i
d
C
ii
nt
h
D
d
ii
d
E
ii
d
h
nt
F
ii
d
G
d
hf
h
H

3.6.3 Identification of Conceptuses with the TGFβ1 Knockout Phenotype at 9.5dpc.

Neighbouring sections to those used in Results 3.6.1 were used for histological analysis. This strategy allowed the histological examination of the yolk sac in the closest approximation possible of its *in vivo* state. By embedding and sectioning the conceptuses without removing the decidual tissue, the mechanical stresses on the yolk sacs were minimised. Selected sections were subjected to haematoxylin and eosin staining, then examined for defects of the embryo and extra-embryonic tissue. Conceptuses used were all embedded and sectioned in the same orientation.

It was found that defining phenotypic attributes fell into the following categories: i) shearing of the yolk sac along the plane of the endothelial cells, typically resulting in the appearance of greatly extended endothelial tube and exovasation of erythroid cells into the yolk sac cavity; ii) oedema and necrosis of the embryo and iii) developmental retardation; iv) two conceptuses exhibited specific defects of the developing placenta. The yolk sac, developing placenta and embryo proper in each conceptus were all scored as either being normal, having a mild defect, or having severe defects (see Figure 18).

As shown in Table 19, 4/ 5 of the conceptuses scored as having no signal when hybridised with a full-length TGFβ1 riboprobe were also judged to be phenotypic. Conversely, 1/ 5 conceptuses scored as having a strong TGFβ1 signal after radioactive in situ hybridisation was found to have defects of the extra-embryonic tissue. 6/ 13 of the conceptuses scored as being weakly positive for TGFβ1 signal exhibited histological traits of the TGFβ1 knockout phenotype. These results are in concordance with the data reported in Results 3.3; i.e. the TGFβ1 knockout phenotype shows incomplete penetrance at mid-gestation on the NIH and F1 genetic backgrounds; and, a proportion of TGFβ1+/- conceptuses have been identified as severely phenotypic at 9.5 and 11.5dpc on both genetic backgrounds.

The main abnormality occurring in all strains studied at mid-gestation is a defect of cell-cell adhesion in the yolk sac manifested as shearing of tissue layers along the plane of the endothelial cells (see Figure 20). Since no buckling was seen in these complete yolk sacs compared to the opened yolk sacs examined in Results 3. 5. 2, it is likely that buckling is a secondary effect of the dissection, fixation and embedding process in opened yolk sacs. The varying degrees of leakage of blood cells into the

yolk sac cavity seen in these conceptuses is probably a secondary effect of the vascular aspect of the TGFβ1 knockout phenotype. This may have been a contributory factor in the anaemic appearance of some whole conceptuses with the TGFβ1 knockout phenotype, also the finding by Dickson *et al.* (1995) that whole-mounted 9.5dpc TGFβ1-/- yolk sacs had a 90% reduction in the number of circulating erythroid cells.

The embryo *per se* in each conceptus was assessed; in particular, the cardiovascular system was examined. No specific abnormalities were seen. However, one embryo, scored after radioactive in situ as having an intermediate amount of TGFβ1 signal, exhibited signs of necrosis; and one, scored after radioactive in situ as having no signal, was developmentally retarded (see Figure 19). These defects are possibly the secondary consequence of yolk sac insufficiency.

The developing placenta was examined in the region of the chorio-allantoic connection. Gross morpholgical scoring of littermates from TGFβ1+/- intercrosses at 9.5dpc revealed defects of the chorio-allantoic connection in a number of conceptuses on all genetic backgrounds. These fell into a number of classes; either the chorion was distended with blood, the umbilical vessels contained blood clots or the umbilical artery and /or vein appeared to be empty. In extreme cases there had been failure to make a successful chorio-allantoic connection. Unfortunately, it was impossible to score accurately the allantois' in these conceptuses for malformations as had been planned. All conceptuses used had been embedded in the same orientation, however the angle of the umbilical vessels remained unpredictable and resulted in uninformative sections. In this study, 2 conceptuses assessed as having a severe abnormal phenotype were also scored as possibly having a reduced or flattened spongiotrophoblast layer (Figure 19). It is unknown whether this defect was a primary or secondary effect of the knockout.

The employment of this strategy has allowed an appraisal of whole NIH and F1 conceptuses from TGFβ1+/- intercrosses whilst causing minimal disruption to the yolk sac structure. The TGFβ1 knockout yolk sac phenotype, identified by gross morphological scoring, has been characterised histologically, i.e. shearing between the endothelial layers, dilation of the endothelial tubes and exovasation of erythroid cells into the yolk sac cavity. In this limited survey there does not appear to be any disparity in the manifestation of the mid-gestation phenotype with respect to genetic background. However, a far larger and more detailed study would be required to confirm this.

Figure 18 - Histological Assessment of Intact TGFβ1 Knockout Conceptuses at 9.5dpc (1).

Sections parallel to those shown in Figure 17 were selected for histological assessment of the TGFβ1 knockout mid-gestation phenotype. In particular the embryonic cardiovascular system, the yolk sac, the allantois and the placenta were inspected. (A) shows a class (i) conceptus whereas (B) and (C) are class (ii). Note the developmental delay of approximately 1.0-1.5 days suffered by conceptus (C).

Scale bar = 300μm.
h = heart, hf = head folds, nt = neural tube, p = placenta, ys = yolk sac.

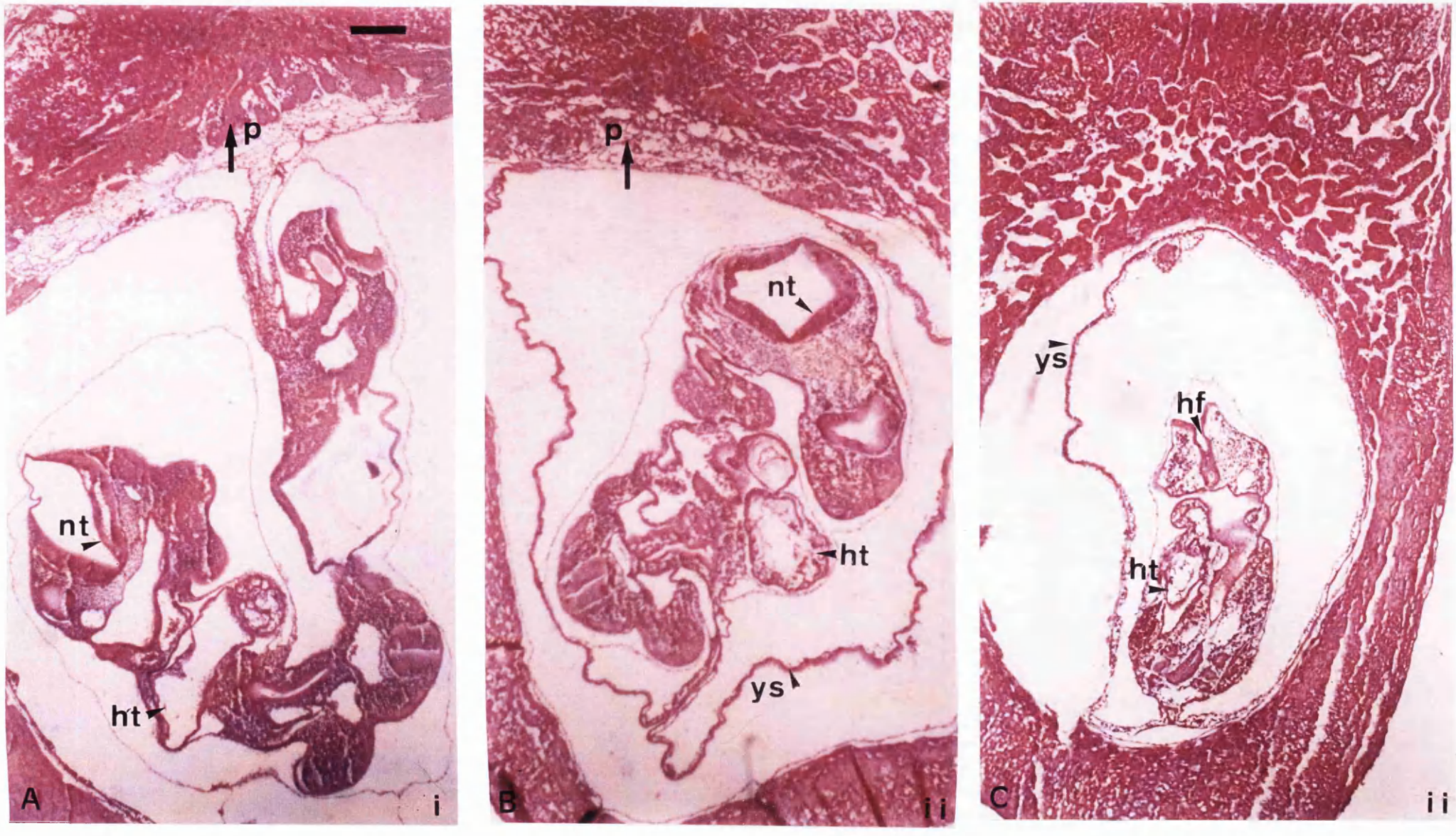
p
nt
ht
A
i
p
nt
ht
ys
B
i i
ys
hf
ht
C
i i

Figure 19 - Histological Assessment of Intact TGFβ1 Knockout Conceptuses at 9.5dpc (2).

Photographs (A) and (B) are higher magnifications of the yolk sacs of embryos (A) and (B) (Figure 18). Photographs (C) and (D) are higher magnifications of sections (A) and (B) respectively. (A) and (C) illustrate normal TGFβ1+/+ yolk sac structure. The vessels are discrete and contain blood cells. Reduced cell-cell adhesion has resulted in dilated endothelial tubes and exovasation of blood cells in photos (B) and (D). Arrowheads indicate obvious areas of disruption of cell-cell contacts.

Scale bar = (A), (B) 50μm (C), (D) 25μm.
bc = blood cell, di = dilated endothelial tube, en = endothelium, n = endoderm, v = vessel. Arrowheads indicate regions where cell - cell adhesion has been disrupted.

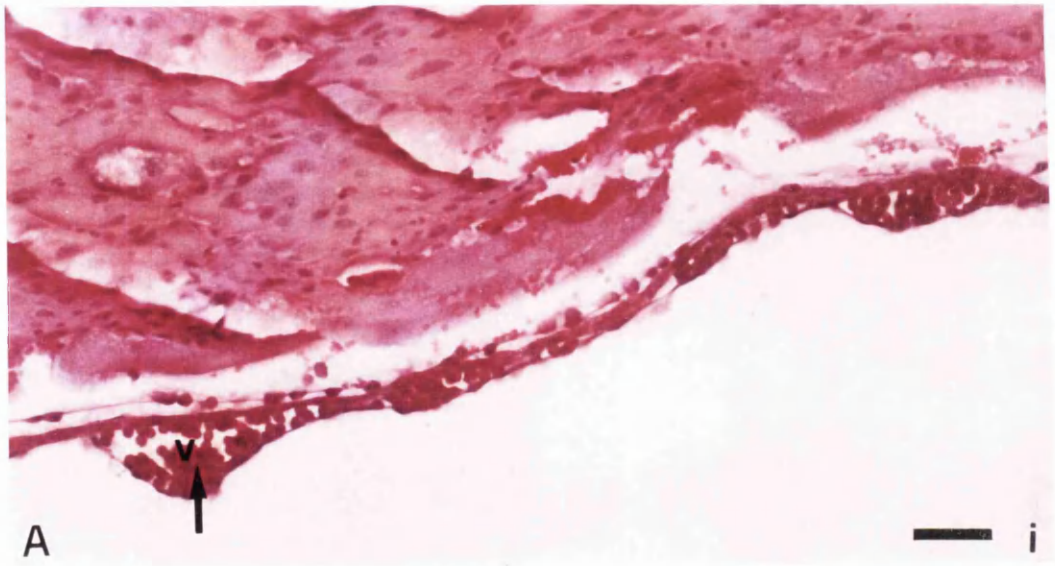
v
A
i

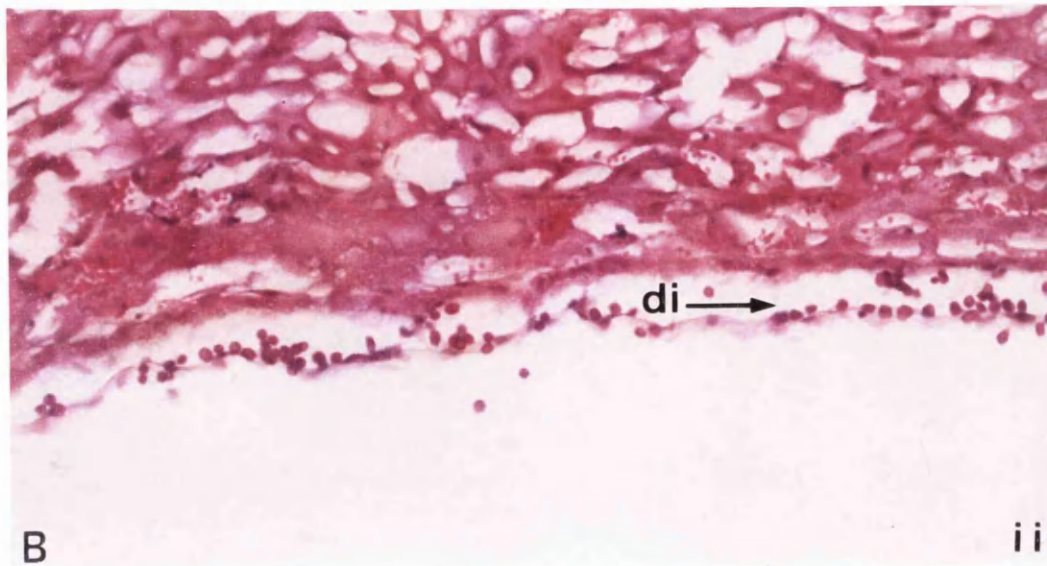
di
B
ii

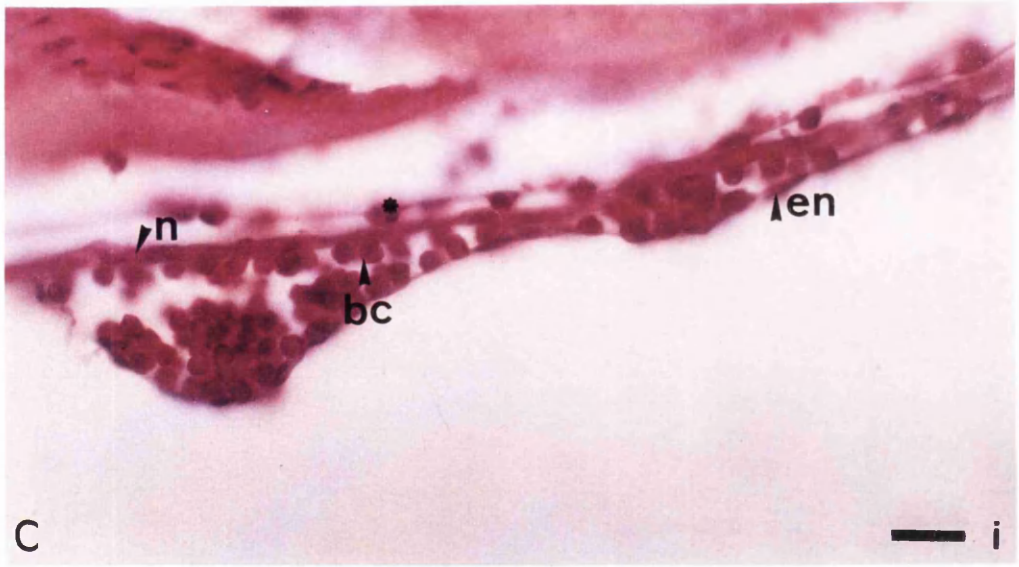
n
bc
en
C
i

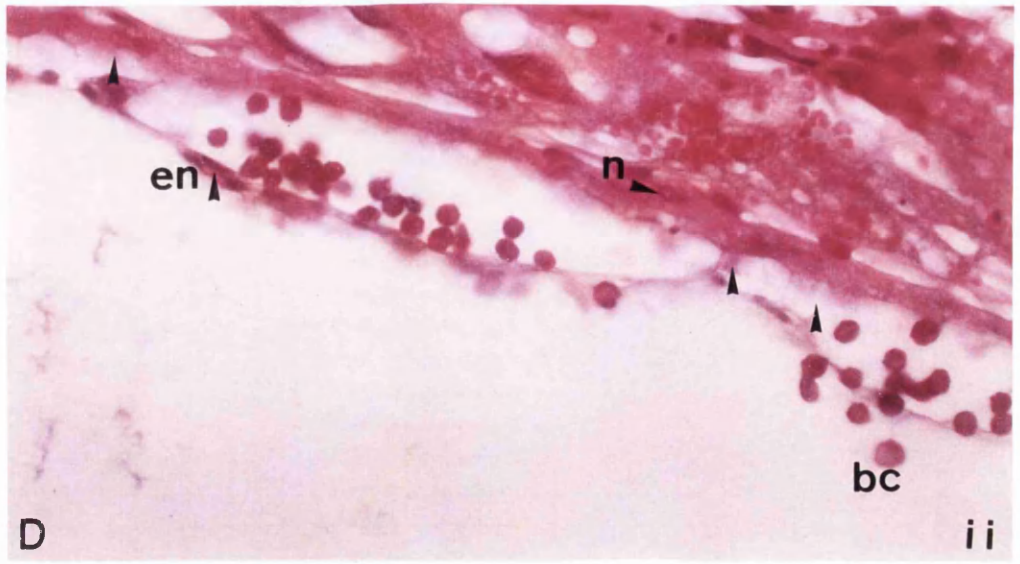
en
n
bc
D
ii

Figure 20 - Histological Assessment of Intact TGFβ1 Knockout Conceptuses at 9.5dpc (3).

Conceptuses (A) and (B) (Figure 18) were scored for defects of the extra-embryonic vasculature including placental defects. A normal placenta has organised tissue layers clearly visible (A). Conceptus (B) which was classified class (i), exhibited a disorganised, less dense placenta in which the spongiotrophoblast layer appeared underdeveloped. Photograph (C) is a higher magnification of developmentally delayed conceptus (C) (Figure 18). The arrowhead indicates an area of infiltration in the head fold mesenchyme. The tissue appear less dense, and suggests the onset of necrosis.

Scale bar = 50μm.
hf = head folds, gi = giant cells, la = labyrinthine spongiotrophoblast, sp = spongiotrophoblast.

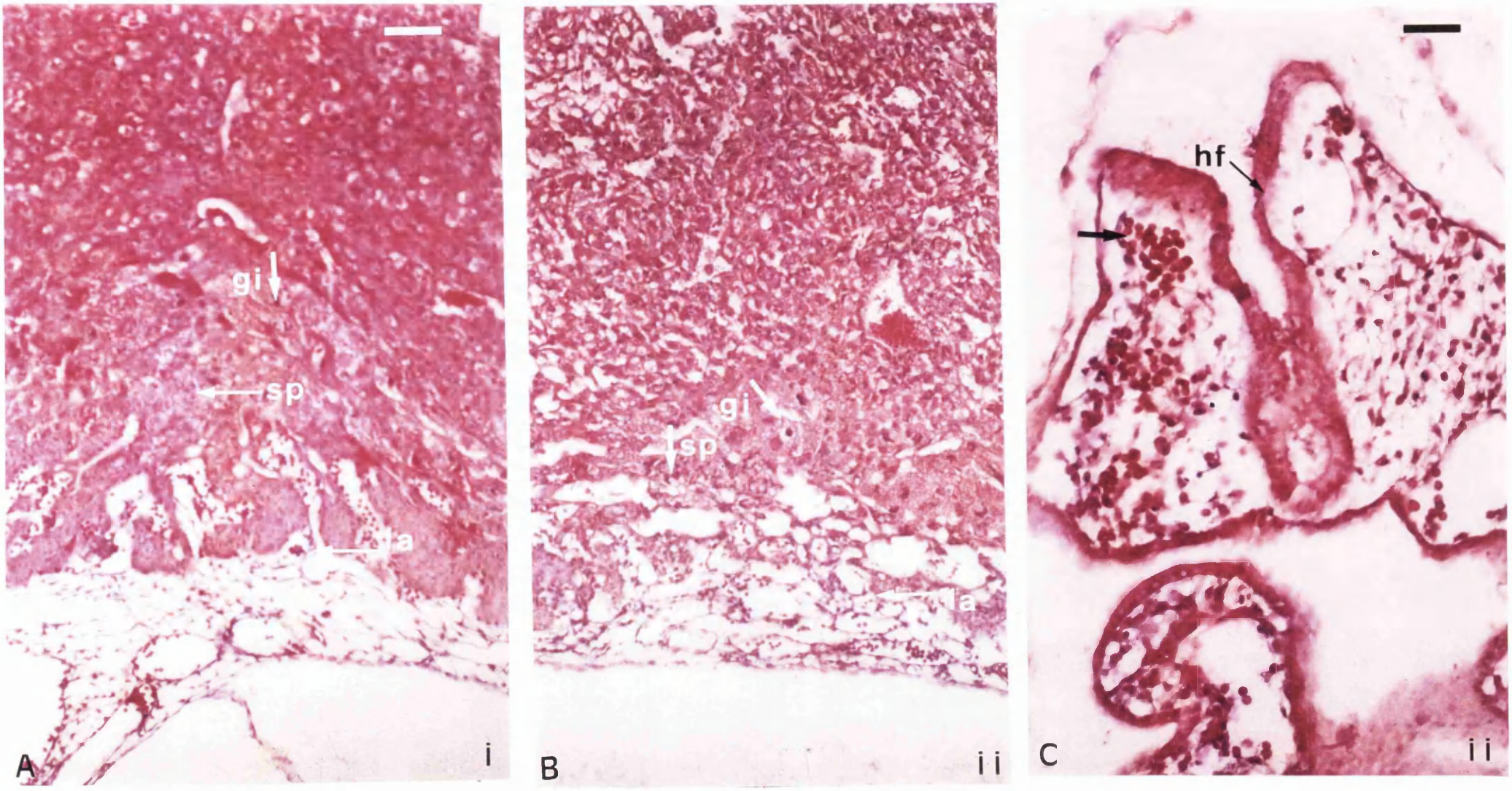
gi
sp
a
A
i
gi
sp
a
B
ii
hf
C
ii

3.7 Reduced α Smooth-Muscle Actin Expression in TGFβ1-/- Yolk Sacs.

Pericyte cells are found in close contact with endothelial cells in the developing vessel wall and are thought to play a regulatory role in microvascular integrity and endothelial cell function during angiogenesis. There have been a number of reports suggesting a connection between pericytes and TGFβ (Sato & Rifkin, 1989 & Antonelli-Orlidge *et al.*, 1989). α smooth-muscle actin is known to be a marker for pericytes (Herman *et al.*, 1985). TGFβ1 is reported to induce the expression of α smooth-muscle actin in 2D microvascular culture systems (Madri et al., 1992) and to induce the expression of α smooth-muscle actin in pericytes in culture (Verbeek *et al.*, 1994). Hence, an investigation of α smooth-muscle actin protein expression was undertaken in conceptuses from TGFβ1+/- intercrosses and is described below.

3.7.1 Opened F1 Yolk Sacs.

The dissected, opened yolk sac, half-embryo and chorion from F1 conceptuses were sectioned and examined histologically in Results 3.5.3. Genomic DNA was isolated from the removed half-embryo and used to genotype the conceptus by PCR. In this experiment, neighbouring sections of tissue to those used in Results 3.5.2 which contained both of large and small vessels were subjected to immunohistochemistry using an antibody for α smooth-muscle actin (see Materials and Methods). Five slides prepared from normal TGFβ1+/+ conceptuses and seven slides prepared from TGFβ1+/- and -/- conceptuses judged to have abnormal yolk sac vasculature were used. Sections of a 14.5dpc embryos were used also as a positive experimental control.

α smooth-muscle actin positive vessels were counted in 3 sections per conceptus. It was found that 5/ 5 of the TGFβ1+/+ yolk sacs contained α smooth-muscle actin positive cells, as did 3/ 7 of the phenotypic yolk sacs. However, 4/ 7 TGFβ1+/- and -/- abnormal yolk sacs were completely devoid of α smooth-muscle actin positive vessels (see Table 20).

3.7.2 Unperturbed NIH and F1 Yolk Sacs.

Undisrupted F1 and NIH conceptuses were sectioned and examined histologically in Results 3.6. The embryos were classified as either Class (i) (TGFβ1+/+ / +/-) or Class (ii) (TGFβ1-/-) by radioactive in-situ hybridisation. In this experiment, neighbouring sections of tissue to those used in Results 3.6.2 were subjected to immunohistochemistry using an antibody for α smooth-muscle actin (see Materials and Methods). Six slides prepared from normal Class (i) conceptuses and seven slides prepared from conceptuses judged to have a vascular phenotype which also failed to, or which hybridised very weakly with the TGFβ1 radioactive in-situ probe were utilised. The tissue used in this experiment facilitated the use of the embryonic heart as an internal positive control on each slide. The heart provides a strong positive signal for α smooth-muscle actin. Sections of a 14.5dpc embryos were used also as a positive experimental control.

α smooth-muscle actin positive vessels were counted in 3 sections per conceptus. Since it is known that α smooth-muscle actin positive cells are found in the wall of developing major vessels, particular attention was paid to the umbilical and vitelline vessels. It was found that 5/ 6 of the Class (i) yolk sacs and major vessels contained α smooth-muscle actin positive cells, as did 2/ 7 of the phenotypic yolk sacs. 1/ 6 of the Class (i) extra-embryonic tissue and 1/ 7 of the phenotypic yolk sacs examined showed an intermediate number of positive cells. That is some positive cells were visible in the smaller yolk sac vessels, but none were seen in the major vessels. 4/ 7 abnormal yolk sacs had no α smooth-muscle actin positive vessels (see Table 20).

3.7.3 The Vascular Defects Observed at 9.5dpc in TGFβ1-/- Yolk Sacs May Be Due to a Reduced Number of Perivascular Pericytes.

In both of the above experiments the level of α smooth-muscle actin expression in the yolk sac and major vessels of normal conceptuses and those judged to have the TGFβ1 knockout phenotype were compared. Sections from a non-transgenic 14.5dpc embryo were used in both experiments as a positive control for the antibody. In the unpertubed yolk sacs, the embryonic heart could also used as an intrinsic positive control for α smooth-muscle actin staining.

	Summary of α smooth-muscle actin staining in opened yolk sacs.	**Summary of α smooth-muscle actin staining in unperturbed yolk sacs.**
TGFβ1+/+, normal yolk sacs	5/ 5 strongly positive 0/ 5 negative	5/ 6 strongly positive 1/ 6 weakly positive 0/ 6 negative
TGFβ1+/- and-/-, abnormal yolk sacs	3/ 7 strongly positive 4/ 7 negative	2/ 7 strongly positive 1/ 7 weakly positive 4/ 7 negative

Table 20. α Smooth-Muscle Actin Staining in Opened and Unperturbed Yolk Sacs from Normal and Abnormal TGFβ1 Knockout Conceptuses at 9.5dpc.

Normal and abnormal, dissected and unperturbed yolk sacs from TGFβ1+/- intercross litters were stained with an antibody for α smooth-muscle actin and the number of positive staining extra-embryonic vessels counted in three sections from each conceptus. Yolk sacs which did not appear to have any major vessels were not included in the study.

Figure 21 - Expression of α Smooth-Muscle Actin Protein in TGFβ1 Knockout Conceptuses at 9.5dpc (1).

α smooth-muscle actin is a marker for perivascular pericytes, cells involved in maintaining vascular integrity. Intact and dissected yolk sacs were incubated with an α smooth-muscle actin antibody and the number of positive-staining major vessels calculated. In all experiments sections from a 14.5dpc embryo were included as a positive control (A). (B) shows an example of positive α smooth-muscle actin staining in the heart, and (C) is an example of positive α smooth-muscle actin staining in the allantois.

Scale bar = (A) (B) 125μm (C) 50μm.
al = allantois, ht = heart, lu = lung, nt = neural tube, ve = vessel.

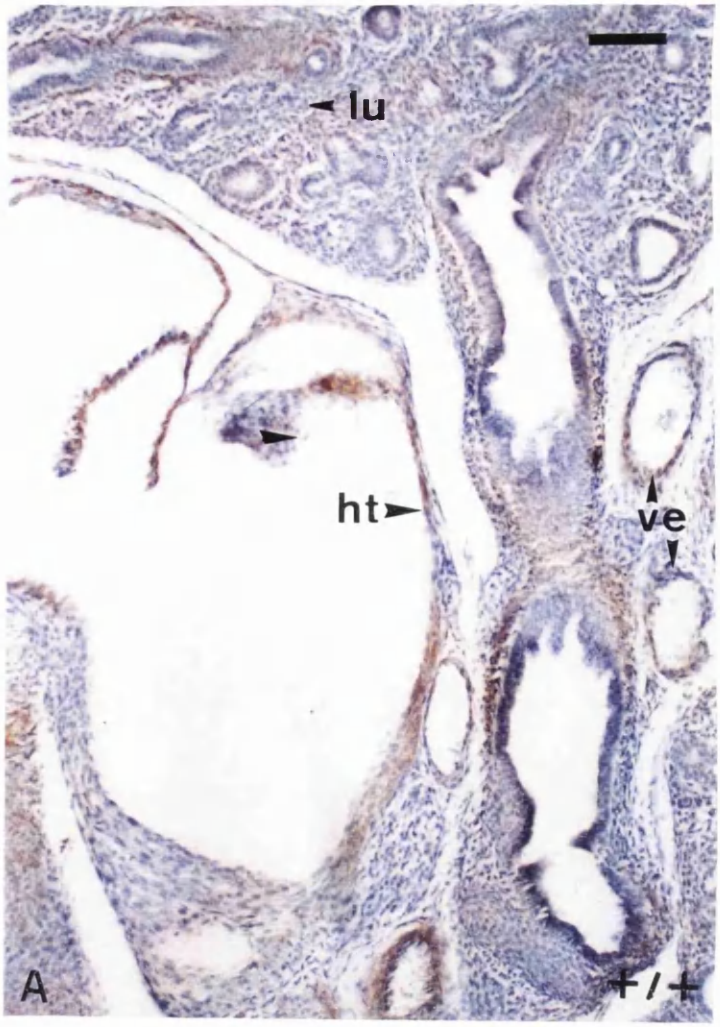
lu
ht
ve
A
+/+

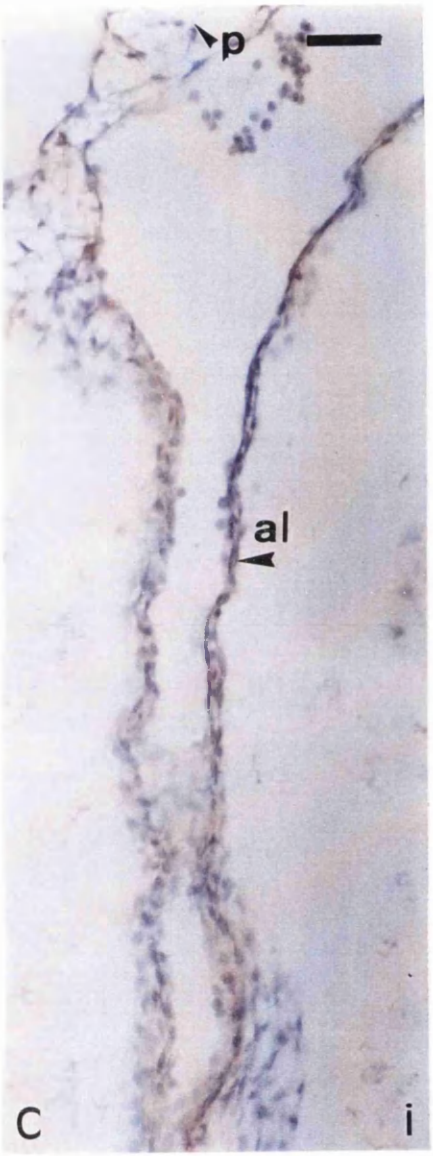
p
al
C
i

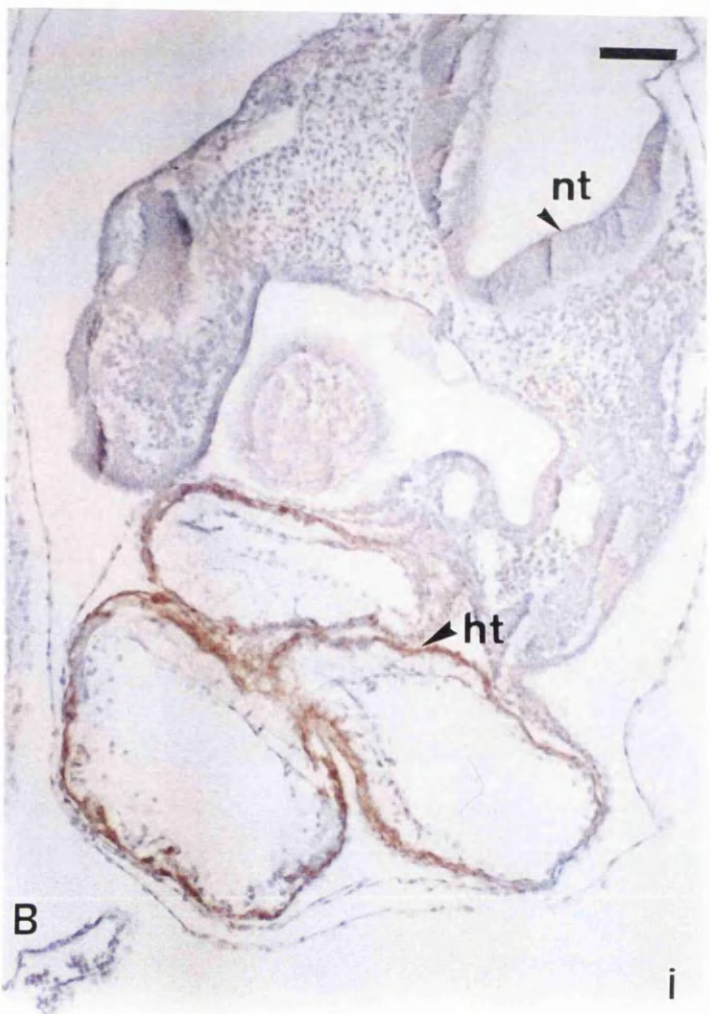
nt
ht
B
i

Figure 22 - Expression of α Smooth-Muscle Actin Protein in TGFβ1 Knockout Conceptuses at 9.5dpc (2).

This panel shows an example of major vessels from class (i) and class (ii) conceptuses showing contrasting levels of α smooth-muscle actin staining. (A) and (B) are photos of vitelline vessels, (C) and (D) show large yolk sac vessels. Note that (B) and (D) are class (ii) conceptuses - and both are negative for α smooth-muscle actin staining compared to (A) and (C), class (i) littermates.

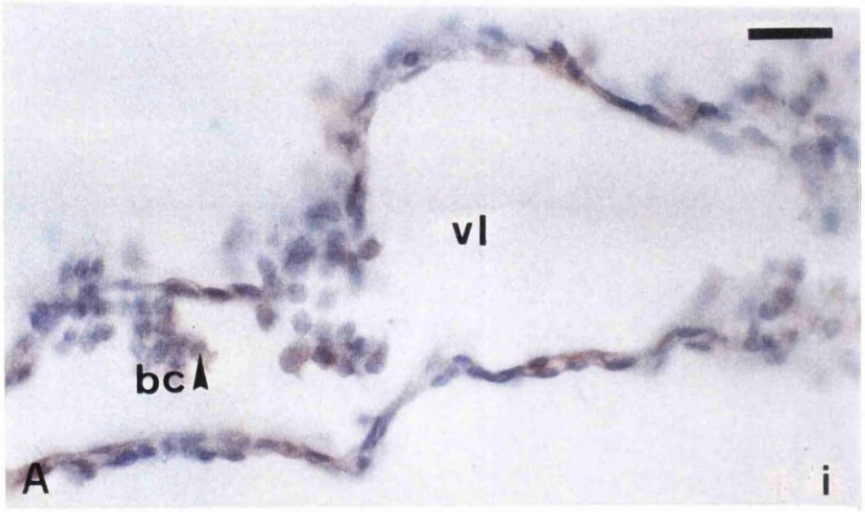
vl
bc
A
i

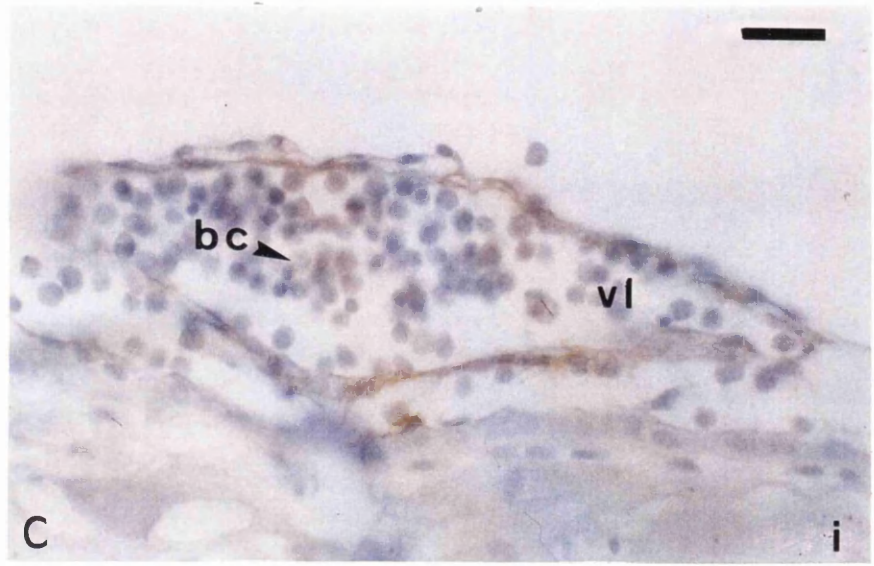
bc
vl
C
i

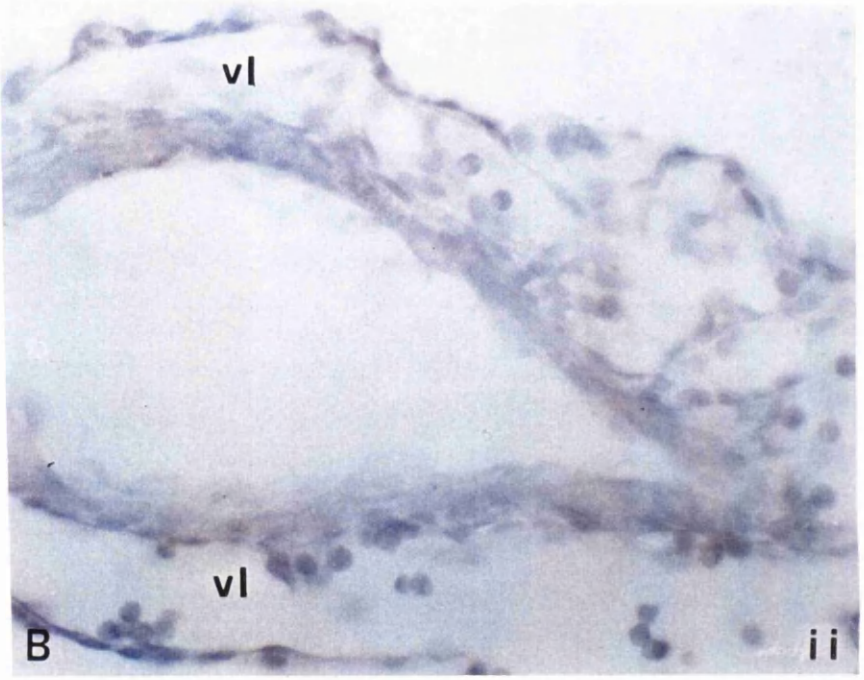
vl
vl
B
ii

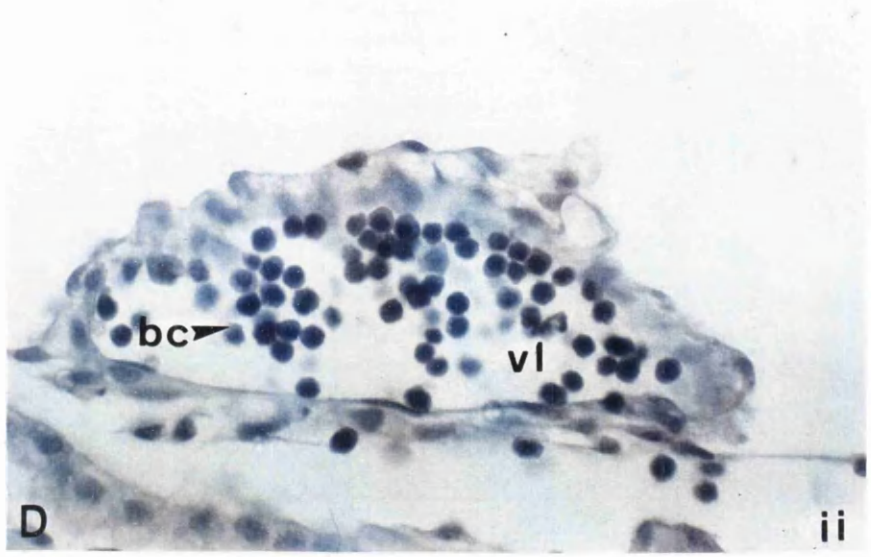
bc
vl
D
ii

In both cases, the only conceptuses found to be devoid of any α smooth-muscle actin positive cells in the extra-embryonic vasculature were TGFβ1-/- or TGFβ1+/- and severely abnormal. However, 4/ 14 TGFβ1-/- or TGFβ1+/- severely abnormal conceptuses scored had α smooth-muscle actin positive cells in the yolk sac and/ or major vessels. This finding may be explained by the range of severity of the TGFβ1 knockout phenotype at mid-gestation, the influence of maternal TGFβ1 on the developing conceptus and a possible requirement of a threshold number of pericytes for vessel intergrity.

Thus, the defects in the murine yolk sac vasculature observed at mid-gestation in TGFβ1 knockout conceptuses may be due in part to the effects caused by an absence of, or defect in, the normal differentiation of pericytes. Photographic examples of α smooth-muscle actin positive and negative TGFβ1 knockout embryos and yolk sacs are shown in Figures 21 and 22).

3.8 The Possible Involvement of a Genetic Modifier Linked to *D5Mit268* in Determining Embryonic Phenotype.

3.8.1 Screening Scored F2 TGFβ1+/- and -/- Conceptuses from TGFβ1+/- Intercrosses.

Concomitant work by this group has shown that a strain-specific polymorphism in a modifier gene exists between NIH and C57 strains of mice. This modifier polymorphism is estimated to be responsible for 80% of the variance in genetic effect of the pre-natal lethal phenotype of mice carrying 2 copies of the C57 polymorphism. *D5Mit268* is genetically linked to this modifier, and therefore an excellent marker for this gene (Bonyadi *et al.*, 1997).

By 3 weeks of age a significant number of C57 TGFβ1+/- animals have died due to an unknown cause; this is not the case with NIH TGFβ1+/- animals. 89% of C57 TGFβ1-/- embryos die before 9.5dpc whereas 80% of NIH TGFβ1-/- conceptuses survive to birth (Bonyadi *et al.*, 1997). The majority of F1 TGFβ1-/- conceptuses die at 10.5-12.0dpc with yolk sac insufficiency. Since there is an obvious disparity in the onset and penetrance of the TGFβ1 knockout phenotype on the different genetic backgrounds studied in this project, the association between phenotype, TGFβ1

genotype and strain-specific alleles of the modifier gene at 9.5dpc was studied in an attempt to dissect the role of the modifier gene in prenatal lethality.

On an F1 genetic background, all embryos should be heterozygous at *D5Mit268*, with one allele from the NIH strain (N) and one from the C57 strain (C). Likewise every embryo on an NIH genetic background should be homozygous NN at *D5Mit268*, and C57 conceptuses should all be homozygous CC at *D5Mit268* (see Discussion 4.4.2). The effect of this polymorphism on the distribution of the TGFβ1 knockout phenotypes was investigated in >260, 9.5dpc F2 embryos from TGFβ1+/- intercrosses. The F2 genetic background was chosen for this study because each embryo has a 1 : 2 : 1 chance of being either NN : CN : CC at *D5Mit268*. Therefore, using *D5Mit268*, it was possible to follow non-random segregation of alleles of the modifier gene.

The F2 conceptuses were dissected free of maternal tissue and scored using an objective morphological scoring system. Genomic DNA was isolated from the whole, cleaned conceptus and used to genotype and screen the embryo by PCR (Materials and Methods). The observed TGFβ1 genotype distribution and ratio of normal and abnormal conceptuses are shown in Table 21 and Graphs 16 and 17. All of the defects identified by morphological scoring were comparable to any seen at mid-gestation on the other genetic backgrounds studied, i.e. inadequate yolk sac vasculature, an abnormal allantois and/ or yolk sac anaemia. These defects occurred solely in TGFβ1+/- and -/- conceptuses.

It is estimated that 65% of the TGFβ1-/- animals die *in utero* (M. Bonyadi, pers. comm.). No significant loss of F2 embryos had occured prior to 9.5dpc. However, when the TGFβ1+/+ : +/- : -/- 1 : 2 : 1 genotype ratio for phenotypically normal conceptuses was calculated; $p=<0.01$. The number of normal conceptuses was calculated by subtracting those classified as severely abnormal from the total in each genotypic class (see Table 22). Therefore, F2 TGFβ1-/- conceptuses die at mid-gestation, in similar proportions to those on an F1 genetic background.

Tables 21, 22 and 23. Correlation of TGFβ1 Knockout Phenotype, Genotype and Screening Class in 9.5dpc F2 Conceptuses.

>260 embryos from TGFβ1+/- intercrosses on an F2 genetic background were morphologically scored and genotyped by PCR. All of the TGFβ1+/- and -/- conceptuses were screened for a strain-specific polymorphism at *D5Mit268,* the locus of a strain-specific TGFβ1 modifier gene. The screening and scoring data are correlated here in an attempt to provide an accurate picture of the role of the modifier gene in the developmental onset of TGFβ1 phenotype. Numbers in parenthesis represent the number of conceptuses from each genotypic or screening class (NN/ CN/ CC) scored as severely abnormal. The observed results were analysed using a χ^2 'goodness of fit' statistical test. The number of normal embryos was calculated by subtracting the number of severely abnormal conceptuses from the total in each genotypic/ screening class.

Table 21. Genotype and Abnormal Phenotype Ratios of F2 Conceptuses at 9.5dpc from TGFβ1+/- Intercrosses.

Strain	+/+	+/-	-/-	Dead	Total
F2	62 (0)	129 (22=17%)	53 (28=53%)	18	262

Strain	Ratio TGFβ1 +/+ :+/- : -/-	1 : 2 : 1 TGFβ1 +/+ :+/- : -/- Total embryos	1 : 1 TGFβ1 +/+ : -/- Total embryos	1 : 2 : 1 TGFβ1 +/+ :+/- : -/- Normal embryos
F2	1 : 2.1 : 0.8	p=0.28	p=0.35	p=<0.01

Table 22. Incidence of Phenotype with a TGFβ1 Strain-Specific Polymorphism in F2 TGFβ1+/- and -/- Embryos at 9.5dpc.

Genotype	NN at *D5Mit268*	CN at *D5Mit268*	CC at *D5Mit268*	Total	NN : NC : CC Ratio
F2+/-	30 (2=7%)	66 (9=14%)	33 (11=33%)	129 (22= 17%)	1 : 2 : 0.9
F2-/-	14 (2=14%)	31 (19=61%)	8 (7=88%)	53 (28= 53%)	1 : 2.2 : 0.6

Table 23. χ^2 Analysis of the Incidence of a Marker for a TGFβ1 Strain-Specific Modifier Gene and Phenotype in F2 TGFβ1-/- Embryos at 9.5dpc.

	Total Embryos 1 : 2 : 1 NN : CN : CC	Severely Abnormal Embryos 1 : 2 : 1 NN : CN : CC	Normal Embryos 1 : 2 : 1 NN : CN : CC
F2 TGFβ1+/-	p=0.78	p=0.02	p=0.61
F2 TGFβ1-/-	p=0.23	p=0.07	p=0.01

Graph 16. F2 TGFβ1 +/+ : +/- : -/- 1 : 2 : 1 Ratios at 9.5dpc.

The expected ratio of TGFβ1+/+ : +/- : -/- animals generated by TGFβ1+/- intercrosses at any developmental stage is 1 : 2 : 1. Graph 16 shows the observed genotype ratios of F2 conceptuses at 9.5dpc. In the calculation of ratios, the number of TGFβ1+/+ conceptuses in each genotypic class was taken as '1'. There is no significant loss of TGFβ1+/- or -/- animals prior to 9.5dpc.

Graph 17. Observed Percentage of Severely Abnormal F2 TGFβ1 Knockout Conceptuses at 9.5dpc in Each Genotypic Class.

Upon dissection each TGFβ1 knockout conceptus was morphologically scored. Graph 17 shows the percentage of F2 conceptuses which were scored as being severely abnormal in each genotypic class. Only a proportion of the total TGFβ1+/- and -/- embryos scored in each genotypic class were scored as severely abnormal.

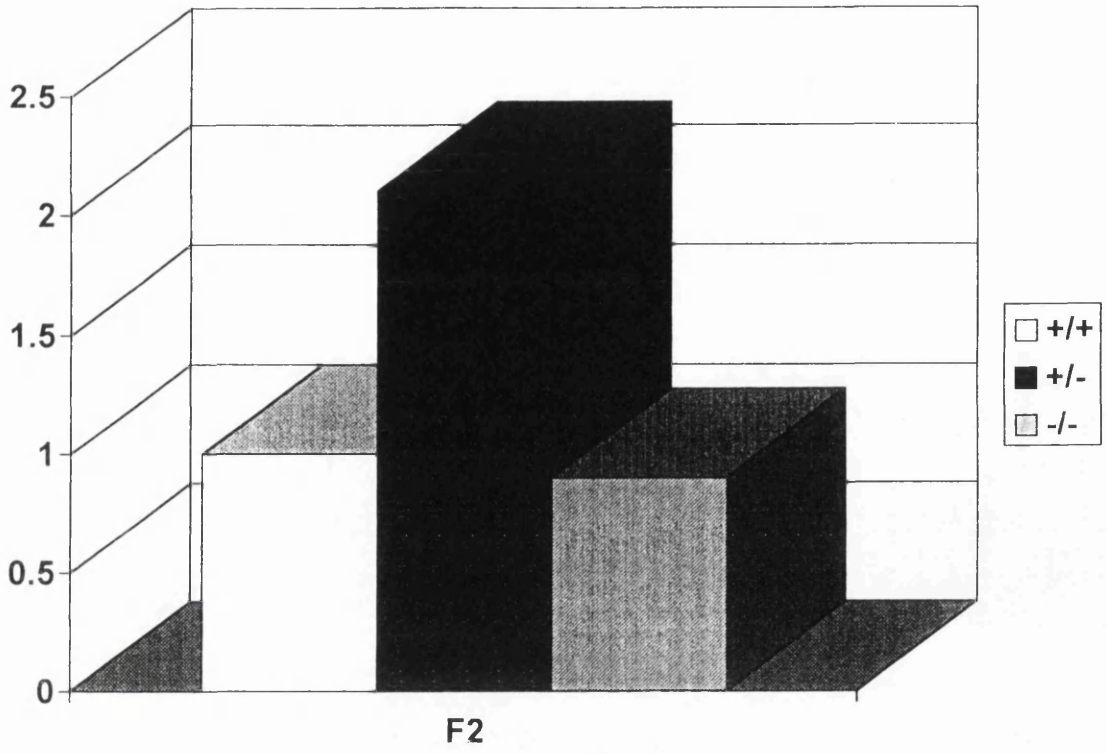
2.5
2
1.5
1
0.5
0
+/+
+/-
-/-
F2

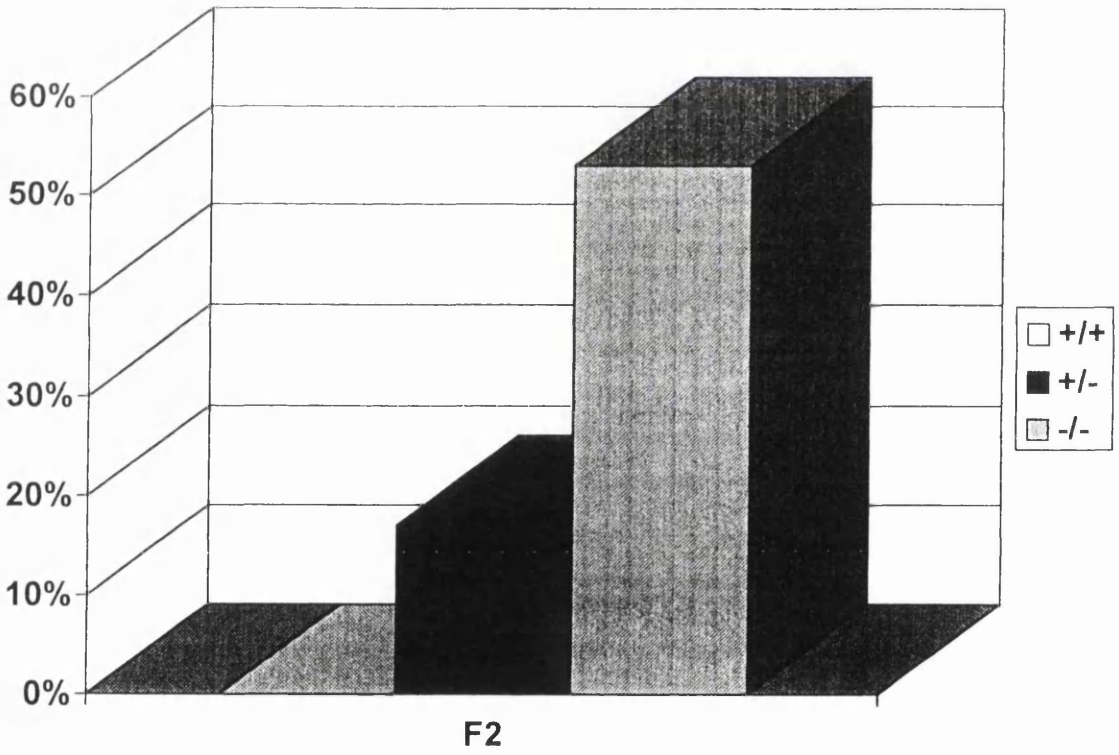
60%
50%
40%
30%
20%
10%
0%
+/+
+/-
-/-
F2

Graph 18. 1 : 2 : 1 NN : CN : CC Ratios in F2 TGFβ1+/- and -/- Conceptuses at 9.5dpc.

The role of the parental origin of the strain-specific modifier gene in prenatal lethality of animals generated by TGFβ1+/- intercrosses was investigated. >260 F2 conceptuses were dissected, morphologically scored and genotyped for TGFβ1. All TGF1+/- and -/- conceptuses were further screened for alleles of the strain-specific modifier gene. Using a polymorphism, it was possible to tell by PCR if a conceptus had two NIH-derived alleles (NN), two C57-derived alleles (CC), or was heterozygous (CN) at the modifier gene chromosomal location *D5Mit268*. The expected ratio of was 1 : 2 : 1 NN : CN : CC in both genotypic classes. In the calculation of ratios, the number of NN conceptuses in each genotypic class was taken as '1'. The apparent loss of TGFβ1-/- CC conceptuses prior to 9.5dpc is not significant.

Graph 19. Observed Percentage of Severely Abnormal F2 TGFβ1+/- and -/- Conceptuses at 9.5dpc in Each Screening Class.

Upon dissection each TGFβ1 knockout conceptus was morphologically scored. All TGFβ1+/- and -/- conceptuses were further screened for the origin of their alleles of the strain-specific modifier gene. Graph 19 shows the percentage of TGFβ1+/- and -/- F2 conceptuses which were scored as being severely abnormal in each screening class. A proportion of the total TGFβ1+/- and -/- embryos in each screening class were scored as severely abnormal.

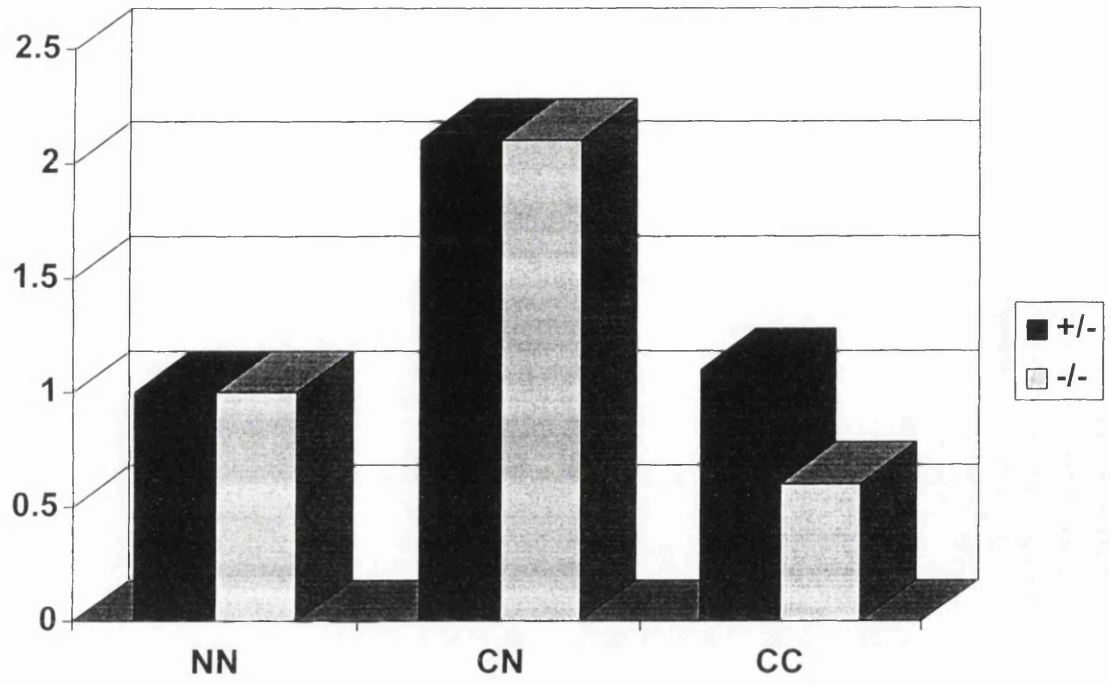
2.5
2
1.5
1
0.5
0
NN
CN
CC
+/-
-/-

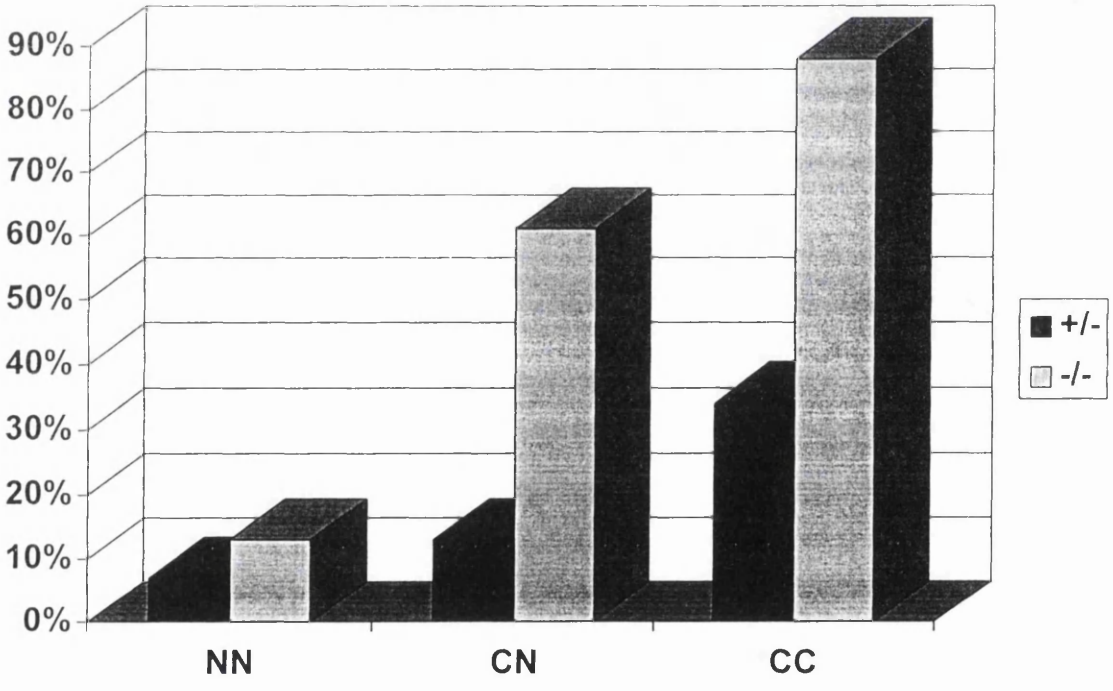
90%
80%
70%
60%
50%
40%
30%
20%
10%
0%
NN
CN
CC
+/-
-/-

All of the TGFβ1+/- and -/- conceptuses were screened by PCR for the presence of the C and/ or N polymorphism at *D5Mit268* (see Materials and Methods and Figure 7) and the phenotype, TGFβ1 genotype and screening data for each conceptus correlated (see Table 22; Graphs 18 and 19).

χ^2 'goodness of fit' tests were used in both TGFβ1+/- and -/- genotypes in order to clarify if there was a either a significant loss of conceptuses from a specific screening class prior to 9.5dpc, or if the TGFβ1 mid-gestation phenotype was segregating randomly with respect to the genotype at *D5Mit268*. If this were the case, then neither of the calculations would result in a significant p value. In all of the above-mentioned χ^2 tests a ratio of 1 : 2 : 1 NN : CN : CC was expected. The data shows that there is no loss of F2 TGFβ1+/- embryos at 9.5dpc, regardless of which polymorphic marker is present at *D5Mit268*. However, the incidence of a severe phenotype in F2 TGFβ1+/- embryos may segregate with C57 homozygosity, or C57/ NIH heterozygosity at *D5Mit268*: However, there was a disparity in the significance of the statistical data - whereas there was a high probability that the proportion of normal F2 TGFβ1+/- conceptuses was unrelated to the strain-specific polymorphism (p=0.61), the probability of the variation seen in the ratios of observed and expected abnormal conceptuses in each screening class was p=0.02. This effect was caused by insufficient sample size. The number of normal conceptuses was calculated by subtracting those scored as severely abnormal from the total in each screening class. All statistical data is shown in Table 23.

The same statistical tests were applied to the F2 TGFβ1-/- data. Although there was a 43% loss of CC conceptuses prior to 9.5dpc, this loss was not significant, due to the relatively low number of animals examined (p=0.23). The p values for both the 1 : 2 : 1 NN : CN : CC segregation of normal and abnormal conceptuses were low; p=0.01 and p=0.07 respectively. Throughout this project, a p value of <0.05 was interpreted as significant.

Thus, F2 TGFβ1-/- conceptuses are more likely to have a mid-gestation phenotype if they are CC or CN at *D5Mit268*.; 87.5% of CC F2 TGFβ1-/- conceptuses and 61% of CN F2 TGFβ1-/- conceptuses were scored as severely phenotypic compared to 14% NN F2 TGFβ1-/- conceptuses. It is possible that a proportion of CC TGFβ1-/- conceptuses may die before 9.5dpc, however, a much larger sample size would be required to prove this. In the F2 TGFβ1+/- embryos, there is no significant loss from any screening class prior to 9.5dpc, however, 33% of CC F2 TGFβ1+/- conceptuses

and 14% of CN F2 TGFβ1+/- conceptuses were scored as severely phenotypic compared to 7% NN F2 TGFβ1+/- conceptuses.

Therefore, it is probable that the presence of a C57-derived polymorphism at D5Mit268 may contribute to the onset and penetrance of phenotypes in F2 TGFβ1+/- and -/- embryos (see Discussion 4.2.2).

3.8.2 An NIH-Derived Allele for the Modifier Gene May Enable C57 Conceptuses to Survive to 9.5dpc.

During the investigation of the onset and manifestation of the TGFβ1 knockout phenotype (Results 3.3.2), a large preorganogenesis loss of C57 TGFβ1-/- conceptuses was observed. The data showed that, compared to 42 C57 TGFβ1+/+ embryos, only 5 homozygous null embryos survived to 9.5dpc. 4/ 5 of these conceptuses were scored as having a severe mid-gestation TGFβ1 knockout phenotype.

It was noted that three of the five surviving TGFβ1-/- 9.5dpc conceptuses came from the same litter. It was also notable that this litter was abnormally large in comparison to the average C57 litter size at 9.5dpc i.e. 11 conceptuses compared to 8. It was possible therefore, that one (or both) of the parents of this litter, although 93.75% C57 throughout the genome, had an NIH-derived allele at the modifier locus. Unfortunately, parental genomic DNA samples were no longer available for analysis and the TGFβ1-/- conceptus DNA had been used in repeated genotyping. However, if any of the littermates screened were CN rather than CC at *D5Mit268*, it could be concluded that one of the parents of this litter was CN at D5Mit268. If this were the case, then using Mendelian rules of inheritance, the N allele would be transmitted to approximately 50% of offspring, resulting in a 1 : 1 CN : CC ratio.

The results show that out of 4 informative littermates screened, one was CC at *D5Mit268* and three were CN at this locus, therefore showing that at least one of the parents of this litter was heterozygous for the strain-specific modifier gene polymorphism. Twenty other C57 TGFβ1+/- embryo DNAs from the initial study representing eight different TGFβ1+/- intercross litters (Results 3.3.2) were also screened as a control; no N alleles were detected. Present among the control sample were ten embryos from two litters also sired by the same stud mouse which fathered 3/ 5 of the C57 TGFβ1-/- embryos, thus, the N allele was probably transmitted by the

dam. Therefore, it is possible that the CN maternal environment was also a contributory factor in the survival of these possible CN C57 TGFβ1-/- embryos to 9.5dpc.

3.9 A Summary of Results.

1. There are three periods of lethality in the TGFβ1 knockout mice: Firstly, prior to 9.5dpc; secondly, mid-gestation; thirdly, 3 weeks post-partum. 89% of C57 TGFβ1-/- embryos die before 9.5dpc for an unknown reason. The majority of F1, F2 and 129 TGFβ1-/- embryos die at 10.5-12.0dpc with defects of the extra-embryonic tissue. The majority of NIH animals die at around 3 weeks of age due to a multi-focal inflammatory response. Thus, there is strain-dependent expressivity and penetrance of the TGFβ1 knockout phenotype.

2. A strain-specific proportion of TGFβ1+/- animals die prior to 3 weeks of age.

3. A small proportion of the observed lethality of TGFβ1+/- and -/- embryos may be due to the maternal environment.

4. The mid-gestation phenotype in the TGFβ1+/- and -/- conceptuses was typified by a combination of any of the following defects; inefficient formation of the yolk sac vasculature; abnormalities in the allantois and chorion; haemorrhages in the yolk sac or embryo; swelling of the pericardium; and yolk sac anaemia.

5. Histological examination of yolk sacs from TGFβ1+/- intercross littermates with defective vasculature dissected at 9.5dpc, revealed separation of the tissue layers along the plane of the endothelial cells, dilation of the endothelial tubes and exovasation of erythroid cells.

6. There is no difference in the abundance of ζ-globin mRNA at 8.5dpc in TGFβ1+/- intercross littermates. However, there was a significant downregulation in the number of haemoglobinised cells counted in blood smears taken from anaemic yolk sacs at 9.5dpc, as assayed using May-Grunwald Geimsa staining.

7. Yolk sacs with the TGFβ1 knockout vascular phenotype have a lower number of α smooth-muscle actin staining cells around the large vessels compared to normal littermates. α smooth-muscle actin is known to be a marker for perivascular pericytes.

8. Possession of a C57-derived allele (C) at the chromosomal location *D5Mit268* may compromise F2 TGFβ1+/- and -/- conceptuses at crucial stages during development. *D5Mit268* has been shown to be linked to the locus of a TGFβ1 modifier gene in C57 and NIH mice (Bonyadi *et al.*, 1997). Three 93.75% pure, inbred C57 TGFβ1-/- littermates which survived to 9.5dpc, albeit with severe abnormalities, were shown to have a one parent with an NIH-derived allele at *D5Mit268*. DNA from the embryos themselves was unavailabe for screening.

Chapter 4

DISCUSSION.

4.1 Introduction.

This thesis presents evidence of a strain-dependent variation in the penetrance and expressivity of phenotypes in TGFβ1 knockout mice (Kulkarni *et al.*, 1993). The data was generated by a study of the TGFβ1 knockout phenotype at 9.5 and 11.5dpc, at birth, and at 3 weeks post partum. Previously, the phenotypic effects of the TGFβ1 knockout allele were characterised in detail by Dickson *et al.* (1995) working on a mixed genetic background (12.5% 129/Sv/Ola (129), 37.5% C57BL/6J/Ola (C57), 50% NIH/Ola (NIH)). Dickson *et al.*, reported a 50% loss of TGFβ1-/- embryos and a 25% loss of TGFβ1+/- embryos at around 10.5dpc caused by defective haematopoiesis and vasculogenesis in the extra-embryonic tissue. The surviving TGFβ1-/- conceptuses died at approximately 3 weeks post partum due to the previously characterised multi-focal inflammatory reaction (Shull *et al.*, 1992; Kulkarni *et al.*, 1993 & Dickson *et al.*, 1995). However, because of conflicting reports regarding the penetrance of this phenotype (Shull *et al.*, 1992; Kulkarni *et al.*, 1993; Dickson *et al.*, 1995 & T. Doetchsmann, unpublished), the TGFβ1 knockout allele was bred to 93.75% purity on NIH, C57 and 129 genetic backgrounds (F. Cousins) for further investigation.

In this project, the onset and cause of lethality were studied in these three strains and defined intercrosses, i.e reciprocal C57 x NIH (F1) and F1 x F1 (F2). It was found that 89% of C57 TGFβ1-/- embryos died for an unknown reason prior to 9.5dpc, whereas NIH TGFβ1-/- animals tended to die at around 3 weeks post-partum from a massive inflammatory reaction, as did all the other surviving TGFβ1-/- animals. Differing numbers of F1, F2 and 129 TGFβ1-/- conceptuses died between 10.5 and 12.0dpc all due to severe defects of the extra-embryonic vasculature and anaemia. Thus, the defects seen at mid-gestation in the TGFβ1-/- and +/- conceptuses tended to be a combination of abnormalities of the extra-embryonic tissue; i.e. inadequacy/

complete failure of yolk sac vasculogenesis; haemorrhages in the yolk sac; blockage or blood clots in the allantois; swelling of the chorion and/ or yolk sac anaemia. Occassional defects of the embryo were seen; typically, slight developmental retardation, necrosis, and swelling of the pericardiac membrane and/ or haemmorhage around the heart. These observations coincide with reports that the first detection of TGFβ1 by *in-situ* hybridisation is at 7.5dpc within the blood islands of the yolk sac, the mesoderm of the allantois and the pro-angiogenic progenitors in the cardiac mesoderm (Akhurst *et al.*, 1990).

Thus, there is a strain-specific difference in the expressivity of the TGFβ1 knockout phenotype and in the penetrance of the mid-gestation phenotype, but no strain-specific variation in the manifestation of the latter. Therefore, it appears that there are three key stages where TGFβ1 is vital for normal development: Prior to 9.5dpc, mid-gestation and 2-3 weeks post-partum.

4.2 Identification of the Strain-Dependent Expressivity and Penetrance of the TGFβ1 Knockout Phenotype.

4.2.1 Prenatal Assessment of the TGFβ1 Knockout Phenotype and Genotype Ratios.

4.2.1.1 Scoring 9.5dpc Conceptuses.

>100, 9.5dpc conceptuses from TGFβ1+/- intercrosses from each of the NIH, C57, 129, F2 and F1 (both directions of the reciprocal NIH x C57 cross) genetic backgrounds were dissected free from maternal tissue with the yolk sac intact, morphologically scored then genotyped by PCR using genomic DNA. The observed Mendelian ratios of embryos in each genotypic class were compared to the expected ratios using a χ^2 'goodness of fit' statistical test.

In order to objectively assess the more subtle morphological effects of the TGFβ1 knockout phenotype at 9.5dpc a two-part scoring system was used. The first part used a number of landmark characteristics to identify the precise developmental stage of the conceptus in question and gave 'score 1'. The second part formed a detailed assessment of any abnormalities observed in the embryo or yolk sac, and gave 'score 2'. Comparison of score 1s for the genotypic classes of each strain revealed that there are

no striking differences of the developmental stage of the conceptus between the different genotypes or strains at 9.5dpc. However, comparison of score 2s showed a striking relationship between the genotype of the embryo and the severity of the observed defects i.e. in general; a few minor defects were observed in TGFβ1+/+ conceptuses. A wider range of defects, from the very minor to the more severe were seen in TGFβ1+/- conceptuses whereas, the greatest incidence of more severe abnormalities were observed on the TGFβ1-/- conceptuses.

The scoring system devised for use in this project gives an objective, quick, easy and accurate routine assessment of the gross morphology of murine 8.5-10.5dpc yolk sacs and embryos. Comparison of the numbers of conceptuses scored at 9.5dpc as severely abnormal with phenotype and genotype results from a similar study at 11.5dpc and at birth (Bonyadi *et al.*, 1997) shows that this system can be used to reliably identify conceptuses with the lethal TGFβ1 mid-gestation phenotype. This approach in the study of post-implantation conceptuses is supported by evidence that a routine histological study reveals little more information than a detailed assessment of gross morphology (Langenfeld *et al.*, 1988). Throughout this project, the use of this scoring system minimised subjective variation in the assessment of the litters studied, and standardised the classification of the abnormalities typically seen in TGFβ1 knockout conceptuses at 9.5dpc. Thus, the individual scores produced for each embryo and yolk sac could be reliably compared between genotypes and across strains to give an accurate picture of the effects of the TGFβ1 knockout at 9.5dpc. This led us to conclude that there was a strain-dependent difference in the penetrance in the TGFβ1 knockout mid-gestation phenotype, but the effects of the knockout at 9.5dpc did not differ between strains (see Discussion 4.2.2).

4.2.1.2 Assessment of the TGFβ1 Knockout Phenotype at 11.5dpc.

<100 11.5dpc conceptuses generated by TGFβ1+/- intercrosses from each of the NIH, 129 and F1 genetic backgrounds were dissected free from maternal tissue, scored and genotyped by PCR using genomic DNA. The observed Mendelian ratios of embryos in each genotypic class were compared to the expected ratios using a χ^2 'goodness of fit' statistical test. By identifying the number of conceptuses which had died, and those which appeared to be severely phenotypic in each genotypic class, it was clear that there was a strain-specific difference in penetrance of the TGFβ1 knockout phenotype at mid-gestation (see Discussion 4.2.2).

Scoring undertaken at this developmental stage was less rigorous since an obvious segregation of the normal and abnormal phenotypic classes had occurred by 11.5dpc. Due to the time of onset of the TGFβ1 knockout phenotype, affected conceptuses were either dead, or dying by this age and therefore easily recognisable. The results obtained at 11.5dpc bore out those obtained at 9.5dpc using the objective scoring system, and mirrored those obtained from neonates (Bonyadi *et al.*, 1997). The dead embryos recovered at 11.5dpc had reached a developmental stage parallel to that of a 9.5-10.0dpc embryo before death (see Figure 12). Unfortunately, due to the onset of necrosis in these conceptuses it was impossible to study an intact yolk sac. The cause of death was yolk sac insufficiency, and typically occurred between 10.5 and 12.0dpc.

It was notable that there had been distinct variations in the influence of the TGFβ1 knockout allele(s) by 11.5dpc: Some conceptuses were completely normal, some yolk sacs with delicate vessels contained a normal embryo, whereas some contained an obviously dead or dying embryo. Thus, there may be a threshold requirement for TGFβ1 in compromised conceptuses, for example; certain TGFβ1+/- and -/- embryos may need to form a fully-functional chorio-allantoic connection, or express a sufficient number of TGFβ1 receptors prior to 11.5dpc to ensure survival. The essential function of the extra-embryonic tissues in development will be discussed in detail below.

4.2.2 Strain-Specific Differences in Knockout Mice.

Classic Mendelian dominant or recessive traits are attributable to a single locus, and can override other genetic or non-genetic factors. However, as in the TGFβ1 knockouts, there is not always a simple relationship between genotype and phenotype. Complex traits do not override the effects of other factors, hence - interactions with other loci, or the environment can result in a heterogeneous phenotype. There have been a number of examples of other knockout mice which exhibit variation in phenotype on different genetic backgrounds; for example, the TGFβ3 (Proetzel *et al.*, 1996), keratin 8 (Baribault *et al.*, 1994), epidermal growth factor receptor (EGF-R) (Threadgill*et al.*, 1995 & Sibilia & Wagner 1995), BMP-4 (Winnier *et al.*, 1995) and the cystic fibrosis transmembrane regulator (CTFR) (Rozmahel *et al.*, 1996) mice.

The most striking of these is the EGF-R knockouts; where, as in the TGFβ1 knockouts, there were three definite lethal phenotypes. Lethality occured during the peri-implantation period due to degeneration of the inner cell mass in the CF-1 strain, at

mid-gestation due to a reduced placental spongiotrophoblast layer in the 129/ Sv strain, and at three weeks post-partum due to multiple defects of the epithelium in the CD-1 strain. All of the phenotypes were fully penetrant and non-overlapping. Embryo transfer experiments showed that maternal effects were not involved and examination of chimeras generated from EGF-R-/- ES cells suggested that the effects were intrinsic to the cell or tissue involved rather than due to variations in other factors. The observed strain-specific variations were postulated to be caused by the action of unidentified strain-specific modifier gene(s) (Threadgill *et al.*, 1995 & Sibilia & Wagner, 1995).

Modifier genes are defined as allelic variants at loci other than the one being modified which can act directly or indirectly on a phenotype; directly, by supressing or enhancing any of the genes involved in the patho-physiological pathway affected by the knockout, or indirectly, by facilitating an the use of an alternative pathway or gene product (Erickson, 1996). By intercrossing TGFβ1+/- C57 and NIH animals, Bonyadi et al., (1997) used microsatellite polymorphisms between the two strains, linkage data and statistical analysis to identify the location of one strain-specific modifier gene responsible in part for the death/ survival of C57 and NIH TGFβ1 knockout animals (Bonyadi *et al.*, 1997) (see Discussion 4.4). The identity and function of this modifier gene remain unknown, but IL-6 and FGF-R3 map closely to its location (Bonyadi *et al.*, 1997).

Mapping and identifying modifier genes has become a natural extension of the characterisation of knockout mice. Thus, the use of different, polymorphic inbred strains, and defined intercrosses of those strains in the characterisation of knockouts can provide information regarding the function of the gene *in vivo*, as well as the other gene products which may modify the knockout phenotype.

4.3 Analysis of the TGFβ1 Knockout Phenotype.

4.3.1 Death Prior to 9.5dpc in the C57 TGFβ1-/- Embryos.

During the course of this project, an 89% loss of C57 TGFβ1-/- conceptuses prior to 9.5dpc was identified. No C57 TGFβ1-/- survived to birth (Bonyadi *et al.*, 1997). Ongoing work has found that a ratio of approximately 1 : 2 : 0.3 TGFβ1+/+ : +/- : -/- C57 embryos exists at 8.5dpc (48 conceptuses studied) (Dr. J. Quinn pers.comm.). Dr. Quinn has not noted an excessive number of resorptions/ dead or dying conceptuses in the litters analysed nor any striking abnormalities in the surviving

TGFβ1-/- conceptuses. These observations suggest that death occurs in the period prior to 7.5dpc. This group has shown that one unknown modifier gene is responsible for around 80% of this effect, and that the different expressivity of the knockout phenotype in C57 animals is not due to selective failure or low transmission of the TGFβ1 null allele through the parental gametes (Bonyadi *et al.*, 1997); however, we have been unable to categorically exclude any other reason for the early loss of C57 TGFβ1-/- embryos or pinpoint the time of death.

There is conflicting evidence for the role of TGFβ1 in the pre/ peri implantation period. It is known that the maternal decidual and uterine tissue can respond to TGFβ1 in an autocrine fashion from 4.5dpc (Roelen *et al.*, 1994); however, researchers disagree as to whether TGFβ1 or its receptors are switched on in embryonic tissue before 7.5dpc (see Introduction 1.4.1). The observation that TβR-II-/- embryos die at the same developmental stage, and with strikingly similar defects to the abnormal TGFβ1+/- and -/- embryos (Oshima *et al.*, 1996) would suggest that if TGFβ is vital for pre/ peri implantation; it either signals via another receptor II, or a separate, compensatory pathway is invoked - indeed, this may be the root of the difference in expressivity of the TGFβ1 knockout phenotype between NIH and C57 inbred strains (see Discussion 4.2.2).

During pregnancy, a complex series of events including maternal immunosupression and modulation of the extra-cellular matrix (ECM) must take place to permit the foetus to develop in the uterus. It has been suggested that some cytokines such as TGFβ1, IL-4 and IL-10 favour embryonic survival and growth (Jokhi *et al.*, 1994). Studies have shown that in mice, the number of gamma-delta T cells - regulators of the maternal anti-foetal immune response at the maternal-foetal interface, increase in a strain-specific manner during pregnancy. The immunosuppressive ability of gamma-delta T cells can be blocked by the addition of an anti-TGFβ1 monoclonal antibody (Suzuki *et al.*, 1995). Thus, TGFβ1 may act in the deciduum either in a paracrine or autocrine fashion as an immunosupressor, permitting the embryo to develop without rejection.

In order to become capable of implanting into the uterine epithelium, the embryo must convert its external surface from a quiescent, non-adhesive state to an adhesive phenotype (Sutherland *et al.*, 1988 & Sutherland *et al.*, 1993). This activation is poorly understood, but the implantation process involves the blastocyst binding to fibronectin, collagen and laminin in the uterine stroma (Sutherland *et al.*, 1988) and the invasion of the trophoblast tissue into the uterine stroma via interactions with laminin (Sutherland *et*

al., 1993). TGFβ is known to regulate the expression levels of the integrins which bind fibronectin, collagen and laminin *in vitro* (Ignotz *et al.*, 1989 & Heino & Massague, 1989). ECM molecules are also involved in essential morphogenetic movements of tissue. For example, E-Cadherin knockouts (Larue *et al.*, 1994) die in a developmentally delayed state at 4.5dpc having failed to form a trophectoderm epithelium, whereas β1 integrin knockouts (Stephens *et al.*, 1995) die at 5.5dpc with defective morphogenesis of the primitive endoderm. TGFβ1 is known to upregulate β1 integrin *in vitro* (Heino & Massague, 1989). However, to more adequately discuss the cause of early loss in the C57 TGFβ1-/- embryos, the developmental stage of death must be identified. This could be done by genotyping blastocysts and early-implantation embryos from TGFβ1+/- intercrosses, then comparing the gross morphology and histology of littermates in the period immediately prior to lethality. The observed phenotype and stage of death should suggest further molecular investigations to the researcher.

The incomplete penetrance of the phenotype observed in C57 TGFβ1-/- embryos may be due to a combination of two factors; the maternal environment and the genetic contribution of the remaining regions of the genome which are not homozygous pure C57 i.e. the genome of each C57 mouse is still approximately 3.0% NIH and 0.75% 129 (see Discussion 4.4).

4.3.2 Molecular Aspects of the Formation of the Extra-Embryonic Vascular System.

The TGFβ1 knockout mid-gestation phenotype is typified by severe defects in the extra-embryonic vasculature and inefficient haematopoiesis. Both the endothelial and primitive erythroid cell lineages arise from the haemangioblasts located in the blood-islands of the yolk sac. TGFβ1 is expressed in haemangioblasts and its descendant lineages throughout development (Akhurst *et al.*, 1990). The formation of the vascular plexus of the murine yolk sac is a complex process, involving both vasculogenesis and angiogenesis. The former is the *de novo* formation of blood vessels from differentiating mesodermally-derived endothelial cell precursors, whereas the latter is the sprouting of new capilliaries from pre-existing blood vessels thus refining the vascular network. Both vasculogenesis and angiogenesis require the differentiation, maturation, migration and proliferation of endothelial cells and the remodelling of the ECM to facilitate the formation and stabilisation of lumenised vessels.

Both these processes involve a variety of molecular factors.

4.3.2.1 Regulation of Endothelial Cell Function.

Five receptor tyrosine kinases (RTK) have been identified; *flk*-1, *flt*-1, *flt*-4, *tie*-1 and *tie*-2 (also known as tek) (reviewed by Breier & Risau, 1996). Each has a specific role in blood vessel formation and are of fundamental importance in the transmission of angiogenic and differentiation signals in endothelial cells. The ligand of *tie*-1 is unknown, but *tie*-2 is the receptor of angiopoietin-1 which is expressed on vascular endothelial cells, and *flk*-1 and *flt*-1 are the receptors of vascular endothelial growth factor (VEGF), a candidate regulator of angiogenesis. All have been knocked-out *in vivo*. *flk*-1 is required for the blood-island formation, and *flk*-1-/- embryos die without yolk sac vessel formation, blood formation and with incomplete endothelial cell differentiation (Shalaby *et al.*, 1995). *flt*-1 knockout embryos die at 9.0-10.0dpc with dilated embryonic blood vessels and a disorganised assembly of endothelial cells (Fong *et al.*, 1995). The *tie*-1 homozygous null embryos died at 1dpp with widespread oedema due to reduced vascular integrity, whereas *tie*-2 homozygous nulls died at around 10.0dpc with a greatly reduced number of endothelial cells and distended and leaky yolk sac and embryonic vasculature (Sato *et al.*, 1995 & Dumont *et al.*, 1994).

Expression studies of these knockouts show that different RTKs can be used to indicate the differentiation state of endothelial cells. In the *flk*-1-/- conceptuses, the markers of endothelial precursors, *flt*-1 and *flt*-4 were detectable. However, *tie*-2, a marker of angiogenesis expressed at the terminal differentiation of the enothelial cells, was not found (Shalaby *et al.*, 1995). *tie*-1 and *flk*-1 are markers of endothelial cell maturity - in the *tie*-2 homozygous mutants both *tie*-1 and *flk*-1 were present, but at a much lower level than normal (Dumont *et al.*, 1994). Thus, a complete comparison of the expression levels of the RTKs of the endothelial cells in normal and abnormal TGFβ1 knockout yolk sacs and *vice versa* could be used to pinpoint the precise differentiation stage of these cells, and the processes which are affected by each gene knockout. TGFβ1 is known to inhibit endothelial cell proliferation in 2D-culture and to elicit the formation of microvascular tubes in 3D culture (Madri *et al.*, 1988). Martin (1996) has excluded any effects in the TGFβ1 knockout conceptuses on the proliferation rate of the endothelial cells, and excluded an overall downregulation of the number of endothelial cells in the abnormal TGFβ1 knockout yolk sac (Martin *et al*, 1996). *in vitro*, TGFβ1 can mediate the expression levels of *flk*-1 not *flt*-1 in endothelial cells (Mandriota *et al.*, 1996). These results imply that TGFβ1 is involved in the maturation of endothelial cells

rather than commitment to the endothelial lineage. It has already been reported that, similar to the *tie*-2 knockouts, *flk*-1 mRNA expression is down-regulated in abnormal TGFβ1 knockout yolk sacs (Dumont *et al.*, 1994 & Dickson *et al.*, 1995).

Recently, mutations in two genes involved in TGFβ1 signalling have been cited as the cause of hereditary human telangieactasia (HHT). The symptoms of HHT include vascular dysplasia and recurrent haemmorhage. Mutations in two genes have been identified for HHT, firstly, truncations in endoglin, the TGFβ type III receptor found on endothelial cells (McAllister *et al.*, 1994) and secondly, mutations in ALK-1 (Johnson *et al.*, 1996), a type one receptor shared by activin and TGFβ which is also thought to be located on endothelial cells (J. Quinn & E. Duffie pers. comm.). These finding support a role for TGFβ1 in vascularisation, and maintenance of vascular integrity.

Tissue factor (TF) is the primary cellular initiator of blood coagulation, but is also involved in angiogenesis, inflammation, atherosclerosis and cancer. It is unknown whether TF exerts its role in vessel development directly or indirectly. TF knockout homozygous null conceptuses display a remarkably similar phenotype to that seen in the abnormal TGFβ1 knockout mice, namely; a grossly normal embryo but incomplete development of the yolk sac vitelline artery and vien, areas of aberrant capilliary development in areas of the yolk sac, blood lakes between the tissue layers of the yolk sac and exovasation of erythroid cells into the yolk sac cavity due to defective formation of the contacts between the endodermal and mesothelial layers of the yolk sac (Cameliet *et al.*, 1996). The defects were attributed to a defect in pericyte accumulation and function. This was proposed to have compromised vascular development at a critical time when vessels needed to develop a 'muscular' wall in response to physiological changes in blood pressure. This effect was postulated to be poorly accommodated by the yolk sac compared to the embryo, which is a more rigid structure. A down-regulation of a number of ECM markers diagnostic of mesenchymal cells was also noted (Cameliet *et al.*, 1996).

This thesis presents evidence that α smooth-muscle actin expression is downregulated in the yolk sac vasculature of abnormal TGFβ1 knockout conceptuses. α smooth-muscle actin is a marker for perivascular pericyte cells. The precise function of perivascular pericytes is unknown, but they are thought to regulate endothelial cell differentiation, function and vascular integrity. For example, an absence of perivascular pericytes has been cited as the cause of micro-aneurysms in diabetic retinopathy (Nehls

& Drenckhahn, 1993). As the developing vessel matures, pericytes migrate along the microvascular sprout and reach a maximal concentration as the new vessel is completed and its secondary branches are formed (Nicosia & Villaschi, 1995). TGFβ1 is known to induce α smooth-muscle actin expression in pericytes (Verbeek *et al.*, 1994), and cocultures of pericytes and endothelial cells can activate TGFβ1 possibly using it in cell-cell communication (Sato *et al.*, 1989); thus, it is possible that the lack of vascular integrity observed in the abnormal TGFβ1 knockout conceptuses was due to the number of pericytes around the developing extra-embryonic vessels being below a critical level.

The apparent absence of pericytes (or mature pericytes) in the abnormal TGFβ1 knockout yolk sacs could be a function of abnormal or delayed differentiation of endothelial cells. In the abnormal TGFβ1 mutant yolk sacs *flk*-1 expression was downregulated, however in the TF-/- yolk sacs *flk*-1 expression was unaffected. It is possible that intrinsic defects of mesenchymal differentiation are responsible for the lack of pericytes in abnormal TGFβ1 mutant yolk sacs.

Very recently, it has been shown that embryos and yolk sacs which are homozygous null for the angiopoietin-1 gene exhibit an abnormal vascular architecture and die at around 12.5dpc. The vasculature of these knockouts is reported to be less complex, with fewer branches and more homogenously-sized vessels (Suri *et al.*, 1996). Using electron-microscopy, Suri *et al.* (1996) found that the principle defect was a failure to recruit pericyte precursors to the developing vascular system; and concluded that angiopoietin-1 played a crucial role in mediating reciprocal interactions between the vascular endothelium, the surrounding matrix and mesenchyme. In light of these findings, a complex model for vascular formation has been proposed (Folkman & D'Amore, 1996): Angiopoietin-1 produced by mesenchymal cells activates its receptor, *tie*-2 on endothelial cells. This leads to the production of a recruiting signal for mesenchymal cells. TGFβ1 is activated as the mesenchymal cells contact the endothelium (Antonelli-Orlidge *et al.*, 1989); and induces the differentiation of the mesenchymal cells to pericytes (Rohovsky *et al.*, 1996). Then, TGFβ1 inhibits proliferation of the endothelial cells and stimulates matrix deposition, permitting endothelial migration and facilitating vessel formation. Thus, the poor vascular integriy and reduced remodelling seen in both the *tie*-2 and angiopoietin-1 null conceptuses may be secondary effects caused by insufficient active TGFβ1.

4.3.2.2 The Regulation of the ECM in Formation of the Yolk Sac Vascular Plexus.

The correct formation of the extra-cellular matrix (ECM) is crucial for normal development of the murine vasculature. The ECM is important in the formation of vessels, the migration of endothelial cells, the formation of cohesive tubes and the maintainance of vessel integrity. TGFβ1 is involved in the modulation of degradation and remodelling of the ECM, and both processes are required for endothelial cell migration (Roberts and Sporn, 1990). For example, long-term overproduction of TGFβ1 may be the cause of several human fibrotic disorders. In pig arteries, direct transfer of the TGFβ1 gene leads to a massive increase in ECM deposition (Nabel *et al.*, 1993). Also, antagonists of TGFβ1 prevent restenosis in rat artery walls after angioplasty (Wolf *et al.*, 1994). Thus, the ability of TGFβ1 to induce deposition of the ECM following injury may be developed to form the basis of a clinical therapy.

TGFβ1 can regulate the expression of a number of integrins. Integrins are the promiscuous molecules which control cell-adhesion to the ECM; for example, certain collagen, vitronectin and fibronectin (FN) receptors are upregulated in response to TGFβ1 (Heino & Massague, 1989; Ignotz *et al.*, 1989). Interestingly, a number of ECM knockouts exhibit similar mid-gestation defects to those seen in abnormal TGFβ1+/- and -/- conceptuses; suggesting that the TGFβ1 knockout phenotype might be mediated via effects on the ECM. Hence, ECM knockouts pertinent to TGFβ1 are reviewed below.

in vitro, TGFβ1 has been reported to induce the expression of FN and thus modulate the migration and adhesion of large vessel endothelial cells (Madri *et al.*, 1989 & Hauser *et al.*, 1993). The cause of death in the fibronectin (FN)-/- embryos is a failure in the formation of the extra-embryonic vasculature at the blood island stage. (George *et al.*, 1993) Similar to the abnormal TGFβ1 knockout yolk sacs, shearing takes place between the tissue layers of the yolk sac, however - unlike the TGFβ1 knockouts; abnormal vessel formation and gross defects are also seen in the embryo *per se*. Disruption of α5 integrin, part of the FN receptor leads to a slightly later lethality: The yolk sac develops weak vessels comprised of distended endothelial tubes which leak erythroid cells into the yolk sac cavity similar to the TGFβ1 knockout phenotype. However, gross defects of the embryo were also observed (Yang *et al.*, 1993).

Antagonists of αv integrin, part of the vitronectin receptor, have been studied and also found to block vascular development and angiogenesis in normal animals. A preliminary report of the αv knockout phenotype reveals a split phenotype: A proportion of αv-/- animals die during embryogenesis and a proportion survive to birth, whereupon they die post-natally due to extensive brain haemmorhages. No other organs were affected suggesting a tissue specific role for αv integrin in blood vessel development (Stromblad & Cheresh, 1996).

TGFβ1 is thought to have an influence on collagen synthesis and proteolysis (Cui & Akhurst, 1996). Both processes are co-ordinated in the migration and assembly of large vessel endothelial cells in culture (Iruela-Arispe *et al.*, 1991). Ablation of the murine collagen I gene leads to embryonic death betwen 12 and 14dpc due to degeneration of developing erythroid cells and the liver, as well as the rupture of the great vessels. The phenotype of the yolk sac in mutant conceptuses was not commented upon (Lohler *et al.*, 1984).

To date there has been no analysis of differential expression levels of any components of the ECM or their receptors in TGFβ1 knockout conceptuses, nor any reported studies of the expression level of TGFβ1 in the knockouts described above. A study of this nature would help to clarify the role of TGFβ1 in the modulation of the ECM, and the role of the latter in the formation of the extra-embryonic vasculature.

4.3.3 Haematopoiesis in the Yolk Sac.

A proportion of the abnormal TGFβ1 knockout yolk sacs assessed at 9.5dpc were scored as anaemic. In some cases, there were no blood cells visible in the yolk sac vessels; in others, blood cells which appeared to be non-haemoglobinised were present in the yolk sac vasculature. Yolk sac anaemia was frequently, but not always accompanied by abnormalities of the extra-embryonic vasculature. Embryonic anaemia was infrequently observed at 9.5dpc, and did not necessarily accompany yolk sac anaemia.

Haematopoiesis in the developing mouse involves two spatially distinct phases under separate molecular controls, producing morphologically and biochemically distinct cell lineages (Medinsky *et al.*, 1993; Godin et al., 1995 & Nakano *et al.*, 1996): Primitive haematopoiesis commences in the blood islands of the yolk sac at 8.0-8.5dpc and definitive haematopoiesis begins in the AGM region of the embryo at around 9.5dpc.

Haematopoietic activity begins in the foetal liver slightly later. Haematopoietic stem cells (HSC) from the yolk sac may contribute transiently to definitive haematopoiesis, but their exact role is unclear (Godin *et al.*, 1995). By 14.0dpc the majority of circulating erythroid cells are derived from definitive precursors (Nakano *et al.*, 1996). In the TGFβ1 knockouts, a very small proportion of embryos were scored as anaemic at 9.5dpc; however, we have made no attempts to assess the progress of definitive haematopoiesis in these embryos.

A number of other knockouts of genes involved in haematopoiesis have been generated, identifying molecular involvement in specific cell lineages in either primitive or definitive haematopoiesis, or both. However, since ablation of a gene crucial for primitive haematopoiesis typically leads to death at around 10.5dpc, it is hard to gauge fully the influence of the mutation on definitive haematopoiesis without *in vitro* experiments. For example, TAL-1/ SCL null mice lack primitive erythroid cells and explants *in vitro* fail to develop definitive erythroid and myeloid precursors (Shivdasani *et al.*, 1995). GATA-2-/- embryos also die due to failure of primitive haematopoiesis, and chimaeric mice generated with GATA-2 null ES cells have a markedly reduced number of definitive HSC or progenitor cells (Tsai, *et al.*, 1994). There are a number of knockouts which die at around 15.0dpc due to defective definitive haematopoiesis, but undergo normal primitive haemtopoiesis; this occurs for example, in the c-myb-/- embryos (Mucenski, *et al.*, 1991). Thus, it would be informative to assay the ability of the AGM region and foetal liver of anaemic from TGFβ1+/- and -/- embryos to commence and sustain definitive haematopoiesis.

The combination of vascular and haematopoietic abnormalities observed in defective TGFβ1 knockout conceptuses, makes the anaemic phenotype harder to analyse. ζ-globin is a marker for haemoglobinisation. In situ hybridisation using an antisense mRNA ζ-globin probe showed that normal TGFβ1 knockout conceptuses are indistinguishable at 8.5dpc i.e. all have an anastomosing corona of blood islands highlighted by an abundant, positive ζ-globin signal. By 9.5dpc, on a mixed genetic background, the ζ-globin signal is strikingly lower in some TGFβ1+/- and -/- compared to TGFβ1+/+ yolk sacs (Dickson *et al.*, 1995). Using this data, Dickson *et al.*, (1995) attributed the anaemic phenotype of TGFβ1+/- and -/- yolk sacs to a downregulation of the total number of circulating erythroid cells caused by a decrease in the number of blood cells differentiating from haemangioblasts. This assessment was made after whole-mount in situ hybridisation on torn yolk sacs. In this thesis, data is presented to show that a degree of exovasation occurs in mutant yolk sacs, which may

account for a loss of blood cells. However, no assessment was made in this project to compare the total number of mature/ immature blood cells in phenotypic and normal yolk sacs. This could be performed by comparing either standardised, total blood counts, or the expression levels of early haematopoietic markers in TGFβ1+/+ and TGFβ1-/- 9.5dpc yolk sacs such as GATAs 1 and 2. These are transcription factors involved in the proliferation and maintainance of early haematopoietic precursors (Tsai *et al.*, 1994).

As mentioned above, the anaemic appearance of mutant yolk sacs could be due to exovasation of erythroid cells, or it could be due directly either to a defect in haemoglobinisation, or to a delay in the maturation process of the erythroid cells, or (most probable) to a combination of these defects. TGFβ1 can promote the haemoglobinisation process in certain cell lines (Chen *et al.*, 1989). Indeed, in this project, a significant difference in the haemoglobinisation process (as monitored via the degree of May-Grunwald Geimsa staining) was seen between yolk sac blood smears taken from anaemic and non-anaemic TGFβ1 knockout conceptuses. However, the process of differentiation of haemangioblasts to descendant endothelial and erythroid lineages requires a normal ECM and normal stromal-cell interactions in the blood-islands. β1 integrin forms part of the heteromeric receptor for a number of ECM molecules including FN. Both β1 integrin and FN expression are thought to be modulated by TGFβ1 (Heino *et al.*, 1989 & Basson *et al.*, 1992). Yolk sac explants from chimaeric embryos generated with β1 integrin deficient stem cells are reported to undergo yolk sac haematopoiesis, but at a drastically reduced level. They also have impaired HSC migration and cannot colonise the foetal liver (Hirsch *et al.*, 1996). Both the FN and α5 integrin-/- yolk sacs contain primitive erythroid cells while similtaneously exhibiting abnormal yolk sac vasculature and a gross amount of exovasation, similar to the defective TGFβ1 knockout yolk sacs: However, in these mutants the question of inefficient primitive haematopoiesis has not been addressed, although FN has long been thought to contribute to the process of erythropoiesis (Patel & Lodish, 1987 & 1994).

Interactions within the developing blood islands create the required microenvironment for the correct differentiation of haemangioblasts to endothelial and primitive erythroid cells in the blood islands. The completely anaemic phenotype of *flk*-1-/- conceptuses suggests that erythroid precursors do not form in the blood islands until the endothelial cells lining the blood island mature fully (Shalaby *et al.*, 1995). Notably, the recent VEGF knockouts were reported to express *flt*-1, f*lk*-1, *tie*-1 and *tie*-2, but at very low

levels, and to have a normal density of endothelial cells i.e. the endothelial cells were present but their development was severely delayed. The defects seen in VEGF+/- and -/- conceptuses involved impaired vasculogenesis and angiogenesis in the yolk sac and embryo, as well as a substantially reduced number of blood cells in the yolk sac. Leakage from the blood vessels was not mentioned (Ferrara *et al.*, 1996 & Carmeliet *et al.*, 1996).

The observed BMP-4 -/- phenotype underlines the requirement for correct interactions in the induction and development of the yolk sac blood islands for normal haematopoietic and vascular development. The BMP-4 knockout mice, like the TGFβ1 knockouts, die at a range of embryonic stages - depending on the genetic background. Death occurs between 6.5 and 9.5dpc with a variable phenotype. Conceptuses which develop to 8.5dpc and beyond are developmentally retarded, have truncated posterior structures and a reduction in the amount of embryonic and extra-embryonic mesoderm. The latter defect is postulated to lead to an overall reduction in blood islands and circulating erythroid cells; the blood islands arise as distinct areas of mesodermal proliferation induced by the yolk sac endoderm (see Figure 3). However, histological analysis of dissected yolk sacs from BMP-4 -/- embryos shows shearing of the tissue layers along the plane of the endothelial cells. This appears to result in the observed leakage of red blood cells and dilation of the endothelial tubes, as seen in abnormal TGFβ1 knockout yolk sacs. Therefore, it would have been interesting to have assayed expression levels of markers of the ECM and/ or endothelial maturity, or to have performed a total blood count in the BMP-4 knockouts, in an attempt to clarify the effects of this knockout on the induction and development of the primitive circulatory system.

Thus a contributory factor to the anaemic phenotype of the TGFβ1 mutant yolk sacs could be the failure of a proportion of the blood islands to develop into a suitable environment for complete haematopoietic differentiation.

4.3.4 Formation of the Chorio-Allantoic Connection.

The fusion of the allantois with the chorion is crucial for embryonic survival and begins at around 8.5dpc. By 9.5dpc the primitive vasculature of the allantois has connected to the chorionic vasculature and the umbilical vessels have formed. Thus, the developing placenta supercedes the yolk sac as the main materno-foetal interface. A variety of chorio-allantoic defects were observed in the TGFβ1 knockout conceptuses; most

commonly an empty umbilical artery and/ or vein, or the appearance of 'lumps' or blood clots in the umbilical vessels. This was sometimes accompanied by chorionic swelling.

As mentioned above, TGFβ1 is able to modulate the expression of a number of integrins, for example; increase the expression of β1 integrin *in vitro* (Heino & Massague, 1989; Ignotz *et al.*, 1989). β1 integrin binds with α4 integrin to form the heteromeric receptor for VCAM-1 as well as forming part of the receptor for FN, collagen and laminin. Prior to, and during chorio-allantoic fusion, α4 integrin is expressed in the chorion and VCAM-1 is expressed in the allantois. Interestingly, both the homozygous null α4 integrin and VCAM-1 knockout mice die at around 12.0dpc with varying degrees of failure of chorio-allantoic fusion and cardiac defects which culminate in pericardiac haemmorrhage. Also; the reported phenotype of the extra-embryonic tissues in the *csk* knockout embryos is very similar to that seen in abnormal TGFβ1 knockout conceptuses, i.e. inadequate circulation in the yolk sac and a disorganised allantois which does not form an adequate junction with the chorion (Imamato *et al.*, 1993). There is a striking similarity between the abnormalities seen in the *csk*-/- embryos and those reported in FN-/- embryos (Imamato *et al.*, 1993 & George *et al.*, 1993). Thus, the absence of blood in the abnormal TGFβ1 knockout chorio-allantoic connections may be due to inefficient fusion of the chorion and allantois caused directly or indirectly by an incomplete expression of ECM molecules or their receptors.

The blood pools observed in the chorion of the TGFβ1 knockout conceptuses could be due to the inability of the compromised embryo to set up a fully functional circulation. The same distended chorion phenotype was also observed in the *tie*-2-/- conceptuses and attributed to a decrease in embryonic blood pressure due to haemorrhages throughout the yolk sac and embryo (Dumont *et al.*, 1994). These haemorrhages were similar to those seen in the phenotypic TGFβ1 knockouts. The appearance of lumps in the allantois may be caused by a disorganised vascular endothelium, similar to that reported in the *flt*-1-/- embryos (Fong *et al.*, 1995). A decrease in blood pressure in the conceptus due to leaks or to inadequately lumenised vessels would simultaneously slow down blood flow and contribute to the formation of these clots. A combination of these effects would result in a discontinuous connection between the embryo and primitive placenta and contribute to the described TGFβ1 knockout phenotype. However, a detailed comparative histological and molecular study of the allantois and chorion of

normal and abnormal TGFβ1 knockout littermates is required to fully characterise the observed defects.

4.3.5 Defects Observed in the Embryo *per se.*

Throughout this project, very few defects of the embryo itself were observed. In the main these abnormalities comprised any combination of the following: Developmental retardation of the embryo by >0.5dpc, necrosis, the swelling of the pericardiac membrane and haemmorhage around the heart. All of these defects are attributable to the cessastion of blood flow throughout the yolk sac plexus. Pericardiac swelling is an indicator of osmotic imbalance in the embryo (Copp, 1995) and has been reported in a number of knockouts involving the circulatory system, for example, GATA-2-/- embryos die before 11.5dpc with marked anaemia and swollen pericardia. GATA-2 is a transcription factor crucial for haematopoiesis in mice (Tsai et al., 1994). However, the incidence of pericardiac haemmorhage may be another manifestation of defects of the ECM. Notably, collagen I homozygous null embryos die with ruptured great vessels, resulting in bleeding into the pericardiac space (Lohler *et al.*, 1984). However, no gross cardiac abnormalities have been identified in the TGFβ1 knockout mice from TGFβ1+/- intercrosses.

Dickson *et al* (1995) noted that the endothelial marker *flk*-1 was downregulated in abnormal TGFβ1 knockout yolk sacs, whereas levels of signal were comparable between embryos regardless of phenotype or genotype. TGFβ1 may only exert an effect on discrete subsets of endothelial cells. For example; zebrafish *cloche* mutants lack a large proportion of blood cells, but the sole effect on endothelial cells is the absence of an endocardium (Stanier *et al.*, 1995). There is also evidence that although yolk sac-derived angioblasts may migrate into the embryo to contribute to the vascularisation of the developing embryo, *de novo* differentiation of early endothelial cells occurs within the lateral splanchnic mesoderm of the embryo (Augustin *et al.*, 1994). Also, the proportion of αv integrin-/- animals which survive to birth, die due to extensive brain haemmorhages. No other organs were affected suggesting a tissue specific role for αv integrin in blood vessel development (Stromblad & Cheresh, 1996). Thus, tissue specific subsets of endothelial cells and ECM molecules may explain why no gross defects of the intra-embryonic vasculature have been noted in embryos from abnormal TGFβ1 knockout yolk sacs. However, Carmeliet *et al.*, (1996) asserted that the reason that vascular defects were observed in the TF-/- yolk

sacs, not the TF-/- embryos was because the embryo was a more rigid structure, and therefore better for supporting vessels.

4.4. Genetic and Epigenetic Factors Acting in the Onset and Manifestation of the TGFβ1 Knockout Phenotype.

4.4.1 Maternal Rescue of Phenotypic Embryos.

The mid-gestation phenotype in TGFβ1-/- conceptuses has a strain-dependent penetrance: Conceptuses could be normal and survive to birth, or have single or multiple defects of the yolk sac of differing severity and die between 10.5 and 12.0dpc. It is probable that maternal rescue of affected embryos could be influencing the range of defects seen at 9.5dpc. Letterio *et al.*, (1994) demonstrated that maternal radio-iodinated TGFβ1 could be transferred between the maternal and embryonic circulations, and two groups have shown that a greater proportion of TGFβ1+/- and -/- conceptuses are abnormal when born to a TGFβ1-/- mother (Letterio *et al.*, 1994 & Dickson *et al.*, 1995). It would have been interesting to compare the expression levels of markers like *flk*-1, α smooth-muscle actin or markers of the ECM between litters from genetically identical TGFβ1+/- and TGFβ1-/- mothers, in an attempt to assess the effect of the maternal environment on the severity of the mid-gestation TGFβ1 knockout phenotype.

Additional cardiac defects were seen in embryos from TGFβ1-/- mothers (Letterio *et al.*, 1994). However, it is unknown whether these were directly due to a complete lack of TGFβ1, or a secondary effect of decreased pressure in the yolk sac and embryonic circulation. There are strain-specific differences in the levels of circulating TGFβ1; i.e. NIH and C57 have comparable amounts (around 5ng ml^{-1}), but 129 animals have an undetectable level (<1ng ml^{-1}) (R. Akhurst & D. Grainger, unpublished). This finding may explain why there is no maternal effect seen in the reciprocal C57 x NIH crosses used to produce the F1 genetic background (see Table 12). Other studies by this group show that there is a significantly greater loss of TGFβ1+/- and -/- conceptuses in reciprocal C57 x 129 TGFβ1+/- intercrosses when the mother is 129 (Dr. L-M Leong, pers. comm.). Thus, the greater penetrance of the mid-gestation phenotype in 129 embryos may be due to a lesser capability for maternal rescue. Notably, there was no evidence for any directional loss of TGFβ1+/- offspring from reciprocal 129 TGFβ1+/- x TGFβ1+/+ crosses at 3 weeks post-partum. Studies have shown that there are no

gross inter-strain differences in the expression of ALKs 1 and 5, or TβR-II mRNA in TGFβ1+/+ embryos of each strain (J. Quinn and E. Duffie, pers. comm). However, we have not investigated the possible compensatory upregulation of any of the TGFβ1 receptors in TGFβ1+/- or -/- animals.

The TGFβ1+/- mothers used in this study are thought to have 50% of the normal level of circulating TGFβ1 (A. Kulkarni pers.comm.). Dickson *et al.*, (1995) showed that their observed 25% loss of TGFβ1+/- embryos was rectified by transfer into a TGFβ1+/+ mother. If a proportion of TGFβ1+/- embryos are as similarly compromised as their TGFβ1-/- littermates over a crucial developmental period, for example; the transition between yolk-sac and placental nutrition; they may compete with each other for the limited amount of maternal TGFβ1 for survival. As mentioned in Discussion 4.2.1.2, at 11.5dpc, a number of TGFβ1+/- and -/- yolk sacs were observed to be mildly phenotypic but containing a dead/ dying embryo, whereas some mildly phenotypic yolk sacs contained a normal embryo, this dichotomy could be due to maternal rescue facilitated by the timely and efficient formation of a chorio-allantoic junction.

Other examples of heterozygous loss have been characterised. Most recently, the fully penetrant lethal phenotype of VEGF+/- embryos. In this case the effect was proposed to be due to a tightly-controlled ligand-dose effect of VEGF during development (Ferrara *et al.*, 1996 & Carmeliet *et al.*, 1996). The loss of TGFβ1+/- embryos due to both the mid-gestation and the post-natal phenotype may be due to a number of other factors; environmental factors, such as the level of maternal TGFβ1 and competition between littermates for certain resources; or the genetic predisposition to lethality of a subset of TGFβ1+/- conceptuses (see Discussion 4.4.2).

Significant lethality was also observed post-natally during this project in the C57 and 129 TGFβ1+/- mice. This data suggests that a 50% loss of circulating TGFβ1 can be lethal. However, this phenotype was not fully penetrant either. TGFβ1+/- loss and the disparity of the penetrance and expressivity of the TGFβ1-/- phenotype may be due in part to genetic effects.

4.4.2 The Role of a Strain-Specific Modifier Gene.

This group has shown that around 80% of the difference in expressivity of the TGFβ1 knockout phenotype in C57 and NIH is due to one co-dominant modifier

gene (Bonyadi *et al.*, 1997). Using linkage analysis, a region of the genome was pinpointed that predisposed TGFβ1-/- pups to embryonic survival or death, depending on the parental origin of the alleles at that point. That is, working on an F2 genetic background; there was a significant dearth of pups with homozygous C57 (C) alleles at *D5Mit268* at birth, but the expected numbers of pups were born which were homozygous NIH (N) and heterozygous CN at *D5Mit268* (Bonyadi *et al.*, 1997).

A modifier gene is defined as one that can act directly or indirectly at any point in patho-physiological pathway to supress or enhance the expression or activity of the genes (or related genes) involved in the expressivity or penetrance of a phenotype (Erickson, 1996). For example, it is thought that the higher activity of an alternative cyclic AMP-dependent, colonic chloride channel in C57 mice ameliorates the phenotype of the ΔF508 cystic fibrosis model when it is bred onto this genetic background (Rozmahel *et al.*, 1996 & Erickson, 1996). In the case of the TGFβ1 knockouts, several candidate genes have already been excluded including TGFβ2, TGFβ3, TβR-II, Endoglin and IGFR2. IL-6 and FGF-R3 map close to this locus and have not yet been investigated (Bonyadi *et al.*, 1997). Positional cloning is now required to identify the TGFβ1 modifier gene and characterise its role in the TGFβ1 knockout phenotype.

In order to further examine the influence of *D5Mit268* on TGFβ1 knockout mice, the ratio of NN : NC : CC conceptuses on each of the three genotypic classes was examined at 9.5dpc on the F2 genetic background. The expected ratio of screening classes was 1 : 2 : 1 NN : CN : CC, in each genotypic class. Each conceptus was morphologically scored (Discussion 4.2.1); and the prevalence of severe defects interpreted in TGFβ1+/- and -/- conceptuses in terms of each screening class. The findings suggested a role for the modifier in both the early loss of CC TGFβ1-/- conceptuses and in the ability of TGFβ1+/- and -/- conceptuses to survive through the transition from yolk-sac to placental nutrition. It is possible that the C allele confers a higher requirement for TGFβ1 during development - consequently more CC TGFβ1-/- embryos die before 9.5dpc than CN or NN TGFβ1-/- embryos. The finding that 3/ 5 surviving C57 TGFβ1-/- conceptuses at 9.5dpc, had a parent with an N allele at *D5Mit268*, also lends credence to the postulate that TGFβ1+/- and -/- embryos which are CC at *D5Mit268* are in some way compromised compared to NN or CN embryos of the same genotype. TGFβ1+/- embryos with a C allele may

also have a greater requirement for TGFβ1 compared to littermates; however, their higher level of embryonic TGFβ1 may facilitate their survival to mid-gestation.

Thus,the presence of an N allele at *D5Mit268* may reduce the embryo's dependence on TGFβ1, permitting embryos to survive to mid-gestation, at which stage all surviving TGFβ1-/- conceptuses and TGFβ1+/- CC conceptuses compete with each other and their littermates for maternal TGFβ1. The modifier gene may however somehow permit redundancy, or the commencement of a different, compensatory developmental pathway.

There are a number of caveats for the work done on *D5Mit268* in this study: Firstly, larger data sets would have better clarified the results - however, this would have involved many hundreds more mice and secondly, the mice used in this project to create the F2 genetic background were only 93.75% purebred. That is, in each C57, NIH (and 129) mouse used, the remaining 6.25% of the genome comprised 0.75% 129, 3.0% NIH and 2.25% C57 genetic material. Unfortunately, wholesale retrospective screening at *D5Mit268* was made difficult by the small amount of DNA yielded by embryos and the length of time the DNA samples had been in storage. Also, although we could discern between C57 and NIH contributions at *D5Mit268*, we have not yet identified a specific marker for 129 in this region of the genome (A. Condie, pers. comm.), so we have no means of determining the role of the modifier gene in the 129 strain. Preliminary work done on reciprocal C57 x 129, and NIH x 129 TGFβ1+/- intercrosses by Dr. L-M. Leong shows a loss of TGFβ1-/- and +/- pups in the C57 x 129 crosses when a 129 animal is the mother; but no similar effect in the NIH x 129 crosses. These results were unexpected. Previous work has shown that 129 mice have a much lower level of circulating TGFβ1 than compared to both C57 and NIH strains (D. Grainger & R. Akhurst, unpublished), and it was expected that this experiment would have shown a comparative rescue of TGFβ1+/- and -/- pups in each cross when the mother was <u>not</u> 129.

Thus, there appear to be other factors contributing to the survival or death of TGFβ1+/- and -/- embryos. In certain strains, maternal rescue may be a factor, but it is possible that other genetic effects are occurring which may not be as obvious on the genetic backgrounds used in Bonyadi *et al.* (1997). The modifier gene at *D5Mit268* is only responsible for around 80% of the difference in expressivity of the TGFβ1 knockout between C57 and NIH mice. The remaining 20% could comprise a combination of environmental and other, lesser genetic effects.

Unfortunately, to clarify these effects a further screening study would be required involving a massive number of animals, and possibly breeding the TGFβ1 knockout allele to more diverse inbred strains of mice.

4.5 Summary of Suggestions for Future Work.

1. The cause of early death in C57 TGFβ1-/- embryos:

i) 6.5 and 7.5dpc embryos from TGFβ1+/- intercrosses should be dissected, morphologically scored and genotyped. If a significant loss of TGFβ1-/- embryos has occured prior to 6.5dpc, then blastocysts from TGFβ1+/- intercrosses could be harvested and cultured, their progress monitored, then genotyped by PCR. Histological analysis of littermates from the period up to and including lethality should suggest suitable molecular investigations to pinpoint the cause of death.

2. The abnormal vascular phenotype:

i) The relative expression levels of *flk*-1, *flt*-1, VEGF, *tie*-1 angiopoietin-1 and *tie*-2 in TGFβ1+/+ and abnormal TGFβ1-/- conceptuses could be used to assess the effect that the ablation of the TGFβ1 gene has on the differentiation state and proliferation and location of endothelial cells at mid-gestation.

ii) Examination of markers of the ECM, such as fibronectin, collagen, vitronectin, laminin, VCAM-1, β1 integrin, α4 integrin, α5 integrin, αv integrin in 9.0-11.5dpc TGFβ1+/+ and abnormal TGFβ1-/- conceptuses would clarify the relationship between the ECM, TGFβ1 and vascular dysplasia.

iii) A detailed inspection of mutant yolk sac ultrastructure by electron microscopy would lead to a precise characterisation of any defects in the cellular composition and integrity of yolk sac vessels.

3. The anaemic phenotype:

i) The relative number and differentiation state of developing primitive erythroid cells in the yolk sac could be analysed using haematopoietic markers such as GATAs 1 and 2 in normal and abnormal TGFβ1 knockout yolk sacs.

ii) A comparison between the abundance of ζ-globin protein and mRNA expression may help in the characterisation of a specific defect in haematopoiesis. Performing in situ hybridisation/ immunohistochemistry on sections of conceptuses embedded intact may restrict the number of blood cells lost through exovasation.

iii) Comparative total blood cell counts as well as a detailed morphological assesment of blood cells from TGFβ1+/+ and anaemic littermates at 9.5dpc would

be informative. This could be achieved by complete yolk sac bleeding into a standard volume of a suitable medium, then histological analysis of a defined aliquot.

iv) Culture of AGM explants would reveal whether abnormal TGFβ1-/- conceptuses also had impaired definitive haematopoiesis.

4. Chorio-allantoic defects:

i) The markers of the ECM and endothelial maturity mentioned above, would be informative in an asessment of defects of the chorio-allantoic connection. *Mash2* could also be used as a marker of the placental spongiotrophoblast layer (McLaughlin *et al.*, 1996).

ii) Most importantly, a detailed, standardised histological study of the allantois and developing placenta should be undertaken. Parallel sections could be used for molecular investigations.

5. Maternal effects on the TGFβ1 knockout phenotype:

i) If there is any effect on compromised TGFβ1 knockout mice due to the maternal environment, it is relatively small. Thus, in order to refute or prove such an effect in all of the strains studied, far larger TGFβ1+/- intercross and reciprocal TGFβ1+/- x TGFβ1+/- sample sizes are necessary at birth and/ or at 3 weeks of age.

ii) A comparison of the expression levels of markers like *flk*-1 and α smooth-muscle between litters from genetically identical TGFβ1+/- and TGFβ1-/- mothers, would help to dissect the effect of the maternal environment on the severity of the mid-gestation TGFβ1 knockout phenotype.

6. TβR-II Knockouts:

ii) Breeding the TβR-II knockout allele onto different defined inbred strains of mice and characterising the phenotypes observed on each genetic background may lead to the discovery of more modifier genes pertinent to the action of TGFβ1. Characterisation of the observed phenotypes and any modifiers would greatly enhance our understanding of the interaction between the TGFβ isoforms, their receptors and other developmental pathways.

ii) A comparative study performed on the published TβR-II+/+ and -/- knockouts (Oshima *et al.*, 1996) of the endothelial markers, ECM markers, clarification of the anaemic phenotype and yolk sac ultrastructure, at different developmental stages - as detailed above, may help to clarify the role of TGFβ1 and its receptors in the onset and severity of vascular dysplasia.

7. Genetic effects on the TGFβ1 knockout phenotype:

i) Postional cloning of the C57/ NIH TGFβ1 modifier gene would enable full characterisation of the gene and dissection of its role in the differential expressivity of the TGFβ1 knockout phenotype.

ii) A marker for the equivalent 129 allele of the TGFβ1 modifier gene would help to further clarify the genetic effects of the TGFβ1 knockout.

iii) Other genetic effects may be occurring in the TGFβ1 knockout mice which may not be obvious on the genetic backgrounds used in the identification of the C57/ NIH modifier gene. Clarification of these would require a further screening study and possibly breeding the TGFβ1 knockout allele to different, more diverse inbred strains of mice.

Mapping of a major genetic modifier of embryonic lethality in TGFβ1 knockout mice

Mortaza Bonyadi[1], Sarah A. B. Rusholme[1,4], Frances M. Cousins[1], Helen C. Su[2], Christine A. Biron[2], Martin Farrall[3] & Rosemary J. Akhurst[1,5]

The transforming growth factor β1 (TGFβ1) signalling pathway[1,2] is important in embryogenesis[3] and has been implicated in hereditary haemorrhagic telangiectasia (HHT)[4,5], atherosclerosis[6,7], tumorigenesis[8,9] and immunomodulation[10,11]. Therefore, identification of factors which modulate TGFβ1 bioactivity *in vivo* is important. On a mixed genetic background, ~50% *Tgfb1*$^{-/-}$ conceptuses die mid-gestation from defective yolk sac vasculogenesis[3]. The other half are developmentally normal but die three weeks *postpartum* [3,10,11]. Intriguingly, the vascular defects of *Tgfb1*$^{-/-}$ mice share histological similarities to lesions seen in HHT patients[3–5]. It has been suggested that dichotomy in *Tgfb1*$^{-/-}$ lethal phenotypes is due to maternal TGFβ1 rescue of some, but not all, *Tgfb1*$^{-/-}$ embryos[12]. Here we show that the *Tgfb1*$^{-/-}$ phenotype depends on the genetic background of the conceptus. In NIH/Ola, C57BL/6J/Ola and F1 conceptuses, *Tgfb1*$^{-/-}$ lethality can be categorized into three developmental classes. A major codominant modifier gene of embryo lethality was mapped to proximal mouse chromosome 5, using a genome scan for non-mendelian distribution of alleles in *Tgfb1*$^{-/-}$ neonatal animals which survive prenatal lethality. This gene accounts for around three quarters of the genetic effect between mouse strains and can, in part, explain the distribution of the three lethal phenotypes. This approach, using neonatal DNA samples, is generally applicable to identification of loci that influence the effect of early embryonic lethal mutations, thus furthering knowledge of genetic interactions that occur during early mammalian development *in vivo*.

In an earlier study, *Tgfb1*$^{-/-}$ conceptuses of a mixed genetic background (see Methods) were found to have one of two lethal phenotypes; mid-gestation loss due to defects in yolk sac vasculogenesis and haematopoiesis[3] or death at three weeks *postpartum* due to multisystemic inflammation[3,10,11]. To investigate the effects that genetic background might have on prenatal lethality, the *Tgfb1* null allele was bred onto C57BL/6J/Ola and NIH/Ola backgrounds (see Methods). Our analysis of the neonatal TGFβ1 genotype ratios from *Tgfb1*$^{+/-}$ intercrosses demonstrated that genetic factors clearly influence the frequency of prenatal lethality of *Tgfb1*$^{-/-}$ mice (Fig. 1), with C57BL/6J/Ola alleles predisposing to prenatal lethality.

We set up *Tgfb1*$^{+/-}$ × *Tgfb1*$^{+/-}$ intercrosses between various combinations of NIH/Ola, C57BL/6J/Ola and C57BL/6J/Ola × NIH/Ola (F1) mice, to investigate whether there was a maternal effect[12], whether the modifier gene(s) were dominant or recessive and to make a crude estimate of the number of genetic modifiers (Fig. 1). Reciprocal crosses of NIH/Ola × C57BL/6J/Ola, and F1 NIH/Ola or F1 × C57BL/6J/Ola demonstrated that there were no significant germ cell or maternal effects (Fig. 1), ruling out the possibility that NIH/Ola and C57BL/6J/Ola *Tgfb1*$^{+/-}$ mothers differed in their ability to rescue *Tgfb1*$^{-/-}$ conceptuses (*via* maternal TGFβ1)[12] or to support intra-uterine development of *Tgfb1*$^{-/-}$ conceptuses. Additionally, we excluded the existence of X-linked modifier loci by these reciprocal crosses, and from the observation of equal numbers of male and female *Tgfb1*$^{-/-}$ mice at birth. The inferred ~70% prenatal loss of *Tgfb1*$^{-/-}$ conceptuses in the NIH/Ola × C57BL/6J/Ola crosses (Fig. 1) was intermediate between the levels of prenatal loss observed within the two inbred strains, suggesting codominance. The frequencies of surviving neonates on the NIH/Ola and C57BL/6J/Ola backgrounds and F1 can be used to assess the goodness-of-fit of a simple mendelian model to the frequencies of survival found in the two backcross and F2 generations (Fig.1). There was no significant difference between the observed and expected frequencies ($P>0.05$) which indicates that the simplest genetic model consistent with the data is a single codominant modifier.

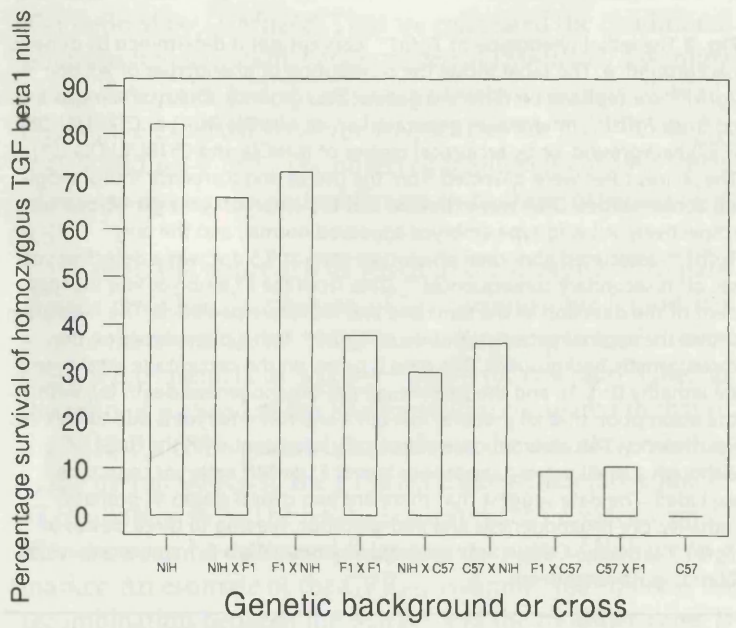

Fig. 1 Genetic background determines incidence of *Tgfb1*$^{-/-}$ prenatal lethality. The percentage survival of *Tgfb1*$^{-/-}$ animals to birth was estimated as 100 × (number of *Tgfb1*$^{-/-}$/number of *Tgfb1*$^{+/+}$). The data were obtained from screening (*n*) newborn offspring of *Tgfb1*$^{+/-}$ intercrosses. C57BL/6J/Ola, *n* = 190; C57BL/6J/Ola × F1, *n* = 82; F1 × C57BL/6J/Ola, *n* = 245; C57BL/6J/Ola × NIH/Ola, *n* = 84; NIH/Ola × C57BL/6J/Ola, *n* = 155; F1 × F1, *n* = 630; F1 × NIH/Ola, *n* = 438; NIH/Ola × F1, *n* = 87; and NIH/Ola, *n* = 241.

To investigate the effect that genetic background has on the yolk sac phenotype[3], conceptuses derived from *Tgfb1*$^{+/-}$ intercrosses on different genetic backgrounds were examined at 9.5 days *postcoitum* (dpc) (Fig 2*a*). The majority of C57BL/6J/Ola *Tgfb1*$^{-/-}$ embryos had died prior to 9.5 dpc. The single embryo which survived to 9.5 dpc had a defective yolk sac. In contrast, there was no statistically significant loss of F1 or NIH/Ola *Tgfb1*$^{-/-}$ embryos

Department of Medical Genetics, Glasgow University, Duncan Guthrie Institute, Yorkhill, Glasgow G3 8SJ, UK. [2]Division of Biology and Medicine, Box G-B618, Brown University, Providence, Rhode Island 02912, USA. [3]Nuffield Department of Medicine, Oxford University, Wellcome Trust Centre for Humans Genetics, Headington Road, Oxford, OX3 7BN, UK. [4]Current address: Department of Genetics, Oxford University, South Parks Road, Oxford, UK. [5]Current address: Onyx Pharmaceuticals, 3031, Research Drive, Richmond California 94806, USA. Correspondence should be addressed to R.J.A. e-mail: Rosemary@onyx-pharm.com

a

Genetic Background	TGFβ1$^{+/+}$	TGFβ1$^{-/-}$		
	All Phenotypically Normal	Total	Phenotypically Normal	Defective yolk sac
C57BL/6J/Ola	39	1	0	1
F1	57	50	22	28
NIH	29	23	15	8

b

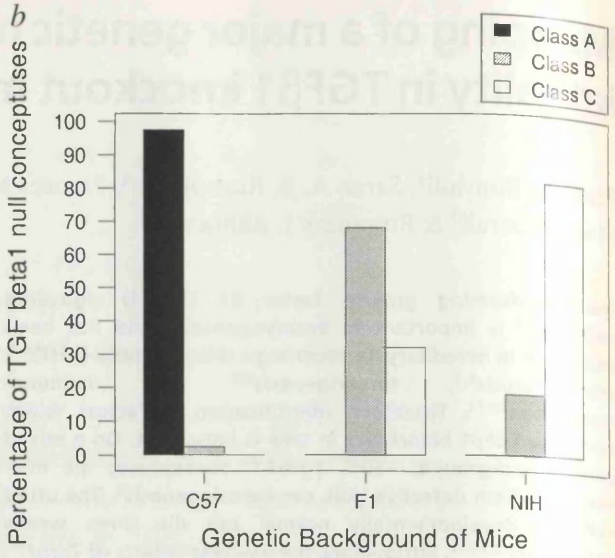

Fig. 2 The lethal phenotype of *Tgfb1*$^{-/-}$ conceptuses is determined by genetic background. ***a***, The table shows the distribution of phenotypes of 9.5-dpc *Tgfb1*$^{-/-}$ conceptuses on different genetic backgrounds. Embryos were collected from *Tgfb1*$^{+/-}$ intercrosses generated on an NIH/Ola (NIH) or C57BL/6J/Ola (C57) background, or by reciprocal crosses of NIH/Ola and C57BL/6J/Ola (F1). The conceptuses were dissected from the uterus and scored for morphological abnormalities. DNA was extracted and the embryos were genotyped retrospectively. All wild-type embryos appeared normal, and the only *Tgfb1*$^{-/-}$-associated abnormal phenotype seen at 9.5 dpc was a defective yolk sac or its secondary consequences[10]. Data from the F1 embryos was independent of the direction of the cross and was therefore pooled. ***b***, The histogram shows the approximate distribution of *Tgfb1*$^{-/-}$ lethal phenotypes on the three genetic backgrounds. The data is based on the percentage total prenatal lethality (Fig. 1), and the percentage pre-organogenesis death (*a*), with the assumption that all prenatal loss of F1 and NIH embryos is due to yolk sac insufficiency. This assumption is statistically consistent with the data, although a small pre-organogenesis loss of F1 or NIH embryos cannot be excluded. The data suggest that there are two critical stages of prenatal lethality, pre-organogenesis and mid-gestation, leading to three classes of *Tgfb1*$^{-/-}$ lethality; Class A, loss pre-organogenesis; Class B, mid-gestation loss; Class C, post-natal death.

prior to 9.5 dpc, but both backgrounds displayed lethal yolk sac defects in a portion of the *Tgfb1*$^{-/-}$ conceptuses (Fig. 2). On each background, the estimate of prenatal loss made at birth (Fig.1) was consistent with the sum of embryos having lethal yolk sac defects or estimated to have died before 9.5 dpc (Fig. 2*a*). Therefore, *Tgfb1*$^{-/-}$ lethality could be categorized into three distinct classes: i) pre-organogenesis loss (Class A, on a C57BL/6J/Ola background), ii) postnatal death (Class C, predominantly on an NIH/Ola background) and iii) mid-gestation yolk sac failure (Class B, predominantly in F1(NIH/Ola × C57BL/6J/Ola) conceptuses). Each phenotype is determined by genetic background, but the three genetic backgrounds studied (NIH/Ola, C57BL/6J/Ola and F1) show some overlap of phenotypes (Fig. 2*b*). This data would be consistent with a single codominant modifier gene, with threshold effects[13] or incomplete penetrance, determining the *Tgfb1*$^{-/-}$ lethal phenotype. It is also consistent with our previous findings of ~50% prenatal lethality on a mixed genetic background[3] (see Methods).

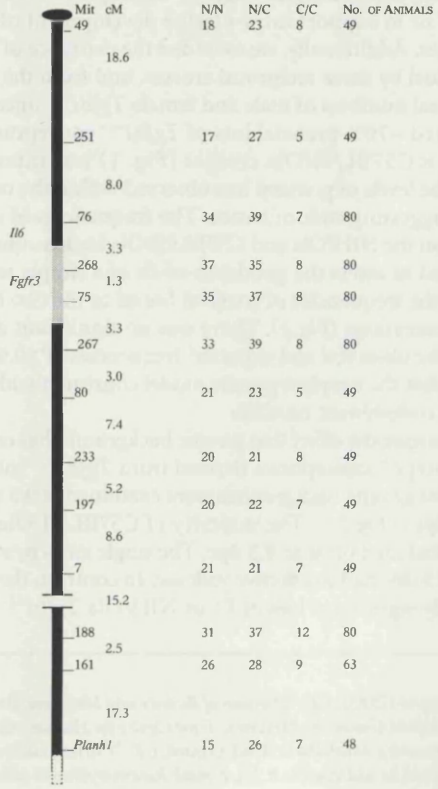

Due to the codominant behaviour of the modifier gene(s), the most informative cross for genetic linkage analysis was considered to be an F1 intercross. With the premise that C57BL/6J/Ola alleles would be underrepresented in class C animals, a primary genome-wide search for major modifier genes that influence *Tgfb1*$^{-/-}$ embryonic survival was initiated using 50 polymorphic DNA markers on 50 *Tgfb1*$^{-/-}$ neonates from an F1 intercross (equivalent to 100 meioses). Survival to birth was utilised as the criterion for linkage analysis, as this was an unambiguous phenotype, and provided large amounts of DNA for genome analysis. The quantities of DNA available from class A and B embryos were considered impractical for genome scanning purposes. These considerations outweighed the fact that ~60% of F2 *Tgfb1*$^{-/-}$ conceptuses were lost *in utero*, and therefore not available for genotype analysis (Fig. 1).

It has been estimated that a simple monogenic trait can easily be mapped with 40 informative meioses using markers at 20 cM intervals[14]. In the current study, we estimate that we have scanned 75% of the autosomal genome for a major modifier gene with power = 80% using a stringent significance test ($P = 0.001$). Modifier genes located in proximal mouse chromosome 7 would not be identified during our search, as *Tgfb1* maps to this region[15] and most mice were homozygous 129/Sv here[11] (data not shown).

Four regions of the genome showed suggestive linkage ($P < 0.05$; ref. 16) in the first screen (*D3Mit6*, *D5Mit267/268*, *D5Mit188* and

Fig. 3 Map of chromosome 5 showing the location of the major modifier gene and the proximity of *Fgfr3* and *Il6*. The position of the informative Mit markers used for mapping are shown to the right of the chromosome, and the map distances (cM) are indicated between each pair of markers (not drawn to scale). Map distances were calculated from the data using MAPMAKER[32]. Note that *D5Mit268* was previously incorrectly mapped (Research Genetics), its true map location being between *D5Mit76* and *D5Mit267*. The genotype numbers (CC : CN : NN) of the F2 neonates for each Mit marker is shown to the right of the figure. Note that 8/80 *Tgfb1*$^{-/-}$ mice are homozygous CC over the region containing the major modifier gene.

Table 1 • Genome screen for modifiers of the *Tgfb1*$^{-/-}$ phenotype

Ch.	Marker	cM	$P_{value\ (d.f.\ 2)}$	
			n = 47–50	n = 80
1	Mit 318	17		
	Mit 76	33		
	Mit 387	66		
	Mit 403	98		
2	Mit 83	17		
	Mit 38	45		
3	Mit 6	18	0.021	0.056
	Mit 106	41		
4	Mit 192	9		
	Mit 178	27		
	Mit 175	42		
	Mit 170	63		
5	Mit 49		0.1185	
	Mit 251	18.6[a]	0.0445	
	Mit 76	8.0[a]	0.0100	0.00011
	Mit 268	3.3[a]	0.0021	0.000014
	Mit 75	1.3[a]		0.000088
	Mit 267	3.3[a]	0.0021	0.00039
	Mit 80	3.0[a]	0.0048	
	Mit 233	7.4[a]	0.0264	
	Mit 197	5.2[a]	0.0246	
	Mit 7	8.6[a]	0.0111	
	Mit 188	15.2[a]	0.0084	0.0088
	Mit 161	2.5[a]	0.015	0.0088
	[a]Pai1	17.3[a]	0.12	
6	Mit 74	11		
	Mit 213	30		
	Mit 25	50		
7	Mit 284	44		
8	Mit 190	22		
	Mit 9	36		
	Mit 166	57		
9	Mit 286	17		
	Mit 16	57		
	Mit 150	59		
	[a]TβRII	62		
	Mit 18	67		
10	Mit 20	23		
	Mit 95	50		
11	Mit 5	37		
	Mit 258	67		
12	NDS 11	7	0.0069	0.052
	Mit 46	17	0.0069	0.052
	Mit 68	28	0.47	
	Mit 8	60	0.47	
13	Mit 63	20		
	Mit 290	46		
14	Mit 140	16		
	Mit 141	19		
	Mit 239	46		
	Mit 35	49		
15	Mit 220	17		
	Mit 159	46		
16	Mit 181	4		
	Mit 59	26		
	Mit 114	35		
17	Mit 43	1		
	Mit 16	7		
	Mit 21	20		
	Mit 93	41		
18	Mit 150	17		
19	Mit 31	13		
	Mit 19	28		
	Mit 103	40		

A list of the dinucleotide repeat markers and restriction fragment length polymorphism (RFLPs) used in the primary genome screen. In total, 60 of 150 dinucleotide repeat markers were found to be informative between C57BL/6J/Ola and NIH/Ola. 49 of these, together with a RFLP in *Tgfbr2* (ref. 19) were used for the first round genome screen. The most significant linkage was observed using a single marker on chromosome 5, *D5Mit80* (P = 0.0048), with two further loci on chromosomes 3 and 12 also showing suggestive linkage (P<0.05). An additional 11 dinucleotide repeat markers and an RFLP for *Planh1* (M.B., unpublished) were used to provide a more detailed linkage map on chromosome 5 (see also Fig. 3). This gave strongest linkage with *D5Mit268* (P = 0.002). A further 30 *Tgfb1*$^{-/-}$ F2 mice were genotyped for selected markers on chromosomes 3, 5 and 12, to confirm or dismiss linkage. Column 3 denotes chromosomal position (cM) of each Mit marker (Research Genetics), with the exception of chromosome 5*, where markers were reassigned positions according to our own data using MAPMAKER[32]. Column 4 lists P values <0.05 in the first round genome screen. All markers were used to screen all 50 mice, but only those with P < 0.05 are listed. Column 5 lists P values of selected markers which were used to screen 80 animals. n, number of animals.

D12Mit46; Table 1). To confirm or dismiss linkage at each of these four loci, an additional 30 neonatal *Tgfb1*$^{-/-}$ intercross DNA samples were analysed for markers on chromosome 3, 5 and 12. P values at the loci on chromosomes 3 and 12 remained only suggestive (~0.05). It is most likely that these are false positives. In contrast, the support for linkage was strengthened at *D5Mit268*, surpassing the stringent linkage criteria proposed by Lander and Kruglyak[16] ($P < 5 \times 10^{-5}$). To evaluate the independent support for a second modifier gene on chromosome 5 (*D5Mit188*), it is necessary to account for the linked major modifier defined by *D5Mit268*. Thus we calculated the conditional genotype frequencies that are expected at *D5Mit188*. Assuming a map distance of 43.4 cM separating the two markers (Table 1, Fig. 3), the expected genotype frequencies are f_{NN} = 33%, f_{NC} = 49% and f_{CC} = 18%. The observed frequencies of 39% : 46% : 15% are not significantly different from those expected (P = 0.5).

We used the approach of Risch and colleagues[17] to gain insight into the contribution of the chromosome 5 modifier gene to the overall genetic variability segregating in the F1 intercross. It is convenient to define the genotypic risk ratio (GRR) as the ratio of survival in the F2 generation, compared to that of the NIH/Ola (NN) parental strain. From the data shown in Fig. 1, the overall GRR_{F2} in the F2 generation is therefore equal to 37.6%/82% = 46%. The GRR_{F2} contributed by a specific modifier gene can be estimated from the strength of linkage to a marker. An estimate of the GRR_{F2}, assuming that there is no recombination between the marker and the modifier gene, is equal to $(1+f_{CC}/f_{NN}+f_{CN}/f_{NN})/4$ (ref. 17; M.F. unpublished). By substituting the observed genotype frequencies for *D5Mit268*, we estimate the GRR_{F2} for the chromosome 5 major modifier gene to be 54%. Risch *et al.*[17] proposed two multilocus genetic models, an additive model in which the effects at one modifier gene may substitute for another and a multiplicative, epistatic model of gene interaction. Under an additive model, where the overall GRR_{F2} (expressed as $1/GRR_{F2}-1$) is a sum of contributions from individual modifier genes, the chromosome 5 modifer gene explains 72% of the overall GRR_{F2}. Under a multiplicative model, where the overall GRR_{F2} is the product of contributions from modifier genes, the chromosome 5 modifier explains 79% of the overall GRR_{F2}. We therefore conclude that the chromosome 5 modifier locus accounts for about three-quarters of the variability in the lethal embryonic phenotype and that one or more minor loci account for the rest.

The nature of the gene product encoded by the chromosome 5 modifier locus remains to be identified. From the distribution of prenatal lethal phenotypes, it would appear that there are two prenatal events (pre-organogenesis and mid-gestation) which are critically dependent on both TGFβ1 and the modifier gene. The modifier locus (which accounts for 3/4 of the genetic effect), when homozygous for C57BL6/J/Ola, confers a higher requirement for TGFβ1 during development and thus TGFβ1-deficient embryos die pre-organogenesis. The NIH/Ola allele reduces the embryo's dependence on TGFβ1, thus heterozygous animals survive until mid-gestation and animals homozygous NIH/Ola at the modifier locus even survive beyond birth (Figs 1, 2). Polymorphic forms of the gene product might determine the embryo's ability to respond to limiting quantitites of maternal TGFβ1 (ref. 12) or might permit redundancy by utilization of other TGFβ ligands of alternative developmental pathways. Many obvious candidate genes have been excluded by this study, including *Tgfb2* (ref. 14), *Tgfb3* (ref. 14), *Igf2r*[17], *Tgfbr2* (ref. 18), *Eng*[20], *Planh1* (M.B. unpublished), although two good candidates *Fgfr3* (refs 21–23) and *Il6* (refs. 24, 25) map close to this modifier (Fig. 3).

The existence of modifier genes which influence the phenotypic outcome of gene knock out mice is now well established[26–30]. Several studies have demonstrated variable prenatal lethal phenotypes which are genetic background-dependent[26–29]. Furthermore, localization of genetic modifiers of postnatal phenotypes of spontaneous and targeted mutations have been reported[29,31]. However, the current study demonstrates the feasibility of using genetic material from postnatal animals to investigate genetic interactions which occur during very early mammalian embryogenesis. This approach overcomes the constraints of working with small amounts of embryonic DNA, which could be contaminated by maternal tissue. The genetic approach to the identification and eventual cloning of genetic modifiers adds another dimension to the analysis of prenatal lethal knock outs, thus advancing knowledge of genetic interactions which occur during early mammalian development *in vivo*.

Methods

Animals. The *Tgfb1* null allele was originally generated on a 129/Sv genetic background[11]. In an earlier study from our laboratory, the mice were bred through two generations onto a C57BL/6J genetic background and crossed once to NIH/Ola. *Tgfb1*$^{-/-}$ conceptuses derived from intercrossing these *Tgfb1*$^{+/-}$ mice were found to have one of two lethal phenotypes; midgestation loss due to defects in yolk sac vasculogenesis and haematopoiesis[3], or death at three weeks *postpartum* due to multisystemic inflammation[10,11]. For the purposes of this study, the null allele was bred through four generations onto either inbred NIH/Ola or inbred C57BL/6J/Ola, obtained from Harlan Olac Ltd., UK. Thus the animals were, on average, 93.75% pure.

For genomic screening purposes, F1 intercrosses between essentially genetically identical mice were set up ((*Tgfb1*$^{+/-}$; NIH/Ola × C57BL/6J/Ola) × (*Tgfb1*$^{+/-}$; NIH/Ola × C57BL/6J/Ola)) and the F2 pups culled soon after birth (see below). As the mice were 6.25% impure, each parental pair was genotyped with each microsatellite to ensure that both parents were heterozygous at that locus prior to genotyping the offspring. This analysis confirmed the expectation[11,15] that proximal chromosome 7 would be predominantly homozygous 129/Sv in the *Tgfb1*$^{-/-}$ animals.

Analysis of embryos. Embryos were collected from natural timed matings of *Tgfb1*$^{+/-}$ animals of different genetic backgrounds. Noon on the day of the vaginal plug was regarded as 0.5 dpc. Embryos were dissected from the uterus into PB1 medium (Gibco BRL) and scored for morphological abnormalities. DNA was then extracted and the embryos were genotyped retrospectively.

Genotyping and microsatellite analysis. For the purpose of breeding, genomic DNA was extracted from tail biopsies of anaesthetised 3-week-old mice. For screening purposes, genomic DNA was isolated from the tails of neonates culled prior to the stage of postnatal death which results from lack of TGFβ1[10,11]. Animals were screened for *Tgfb1* genotype as described[3], using, simultaneously the three oligonucleotide primer sets in a 20 μl reaction volume containing 1× PCR buffer (Cambio); 1.5 mM $MgCl_2$; 5 mM dNTPs; 150–200 ng DNA and 1 U *Tfl* polymerase (Cambio).

Dinucleotide repeat primers for genomic mapping were either a gift from John Todd, purchased from Research Genetics, or synthesized on an Applied Biosystems 391 DNA synthesiser. The polymerase chain reaction (PCR) was performed according to manufacturer's recommendations. Primer sets (150) were screened to search for polymorphisms between C57BL/6J/Ola and NIH/Ola. Only 60 primer sets were polymorphic, and most size differentials were so small (1–8 nucleotides) that the polymorphisms could only be resolved by 8% acrylamide gel electrophoresis. DNA was visualized by silver staining; the gel was fixed in 10% ethanol, 0.5% acetic acid for 15 min; stained in 0.1% silver nitrate; washed in H_2O; and developed for 20 min in 1.5% NaOH, 0.1% formaldehyde.

Southern blot analysis. Southern blotting was performed as described[19], using Quikhyb™ (Stratagene).

Genome screen. A genome wide screen was undertaken on newborn *Tgfb1*$^{-/-}$ pups (class C) from an F1 *Tgfb1*$^{+/-}$ intercross, to search for modifier genes which determine the likelihood of prenatal lethality on the different genetic backgrounds. The decision to use *Tgfb1*$^{-/-}$ neonates (class C) was due to the limiting quantities of DNA which could be obtained from class A or B embryos. The premise was that the C57BL/6J/Ola allele of the modifier gene(s) predisposes to prenatal lethality, and would thus be underrepresented in class C animals, based on the observation that there is complete prenatal loss of C57BL/6J/Ola embryos, ~70% prenatal loss of F1 embryos, but only ~20 % loss of NIH/Ola embryos (Fig. 1). If a single codominant gene was entirely responsible for this genetic effect, one would expect that, by birth, the genotype frequency at that locus would deviate from mendelian expectations and would be 0 CC: 0.75 CN : 1.0 NN ($0 \times 1 : 0.3 \times 2 : 0.8 \times 1$, see Fig. 1). The frequencies of the three genotypes f_{CC}, f_{CN} and f_{NN} detected by each marker were compared with those expected for an independently segregating locus (0.25 : 0.5 : 0.25); the significance of any difference was assessed by using a χ^2 test (with 2 degrees of freedom).

As there was no control group for genotype analysis (class A and B embryos were not genotyped) the possibility existed that linkage (at *D5Mit268*) could be artefactual due, for example, to strain-specific segregation distortion on chromosome 5. This possibility was excluded by analysis of 50 *Tgfb1*$^{+/+}$ animals born from the same F2 litters. The distribution of *D5Mit268* alleles in these wild-type mice was the expected 1 : 2 : 1.

Calculation of conditional genotype frequencies. $f_{CC} = g_{CC}(1-2r+r^2)+g_{CN}(r-r^2)+g_{NN}r^2$. $f_{CN} = 2g_{CC}(r-r^2)+g_{CN}(1-2r+2r^2)+2g_{NN}(r-r^2)$. $f_{NN} = g_{CC}r^2+g_{CN}(r-r^2)+g_{NN}(1-2r+r^2)$ where f_{CC}, f_{CN} and f_{NN} are the expected genotype frequencies at a linked locus (*D5Mit188*) and g_{CC}, g_{CN} and g_{NN} are the observed genotype frequencies at the modifier gene (*D5Mit268*). r = recombination fraction between the two modifier genes. Note that when r = 0, $f_{CC} = g_{CC}$, $f_{CN} = g_{CN}$, $f_{NN} = g_{NN}$; when r = 0.5, $f_{CC} = 1/4$, $f_{CN} = 1/2$, $f_{NN} = 1/4$.

Estimation of genotype frequencies on the mixed genetic background. In our earlier study[3], the mixed genetic background was roughly 1/8 129/Sv; 3/8 C57BL/6J; 1/2 NIH/Ola. Of the *Tgfb1*$^{-/-}$ embryos examined, only ~1/7 ($(3/8)^2$) would have been homozygous C57BL/6J at any single locus, that is, 1/28 (1/7 × 1/4) of each litter. Thus class A conceptuses would easily have gone undetected in the analysis. The majority of embryos would have been heterozygous CN (~50%) or homozygous NN (~25%) at any one locus, thus accounting for the observation of ~50% prenatal lethality due to yolk sac deficiencies[3].

Acknowledgements

We thank D. Duggan and B. O'Hare for technical assistance, J. Todd for advice and for supplying some oligonucleotide primers, A. Kulkarni and S. Karlsson for supplying the original Tgfb1 null mice and A. Balmain for critical reading of the manuscript. All animal experiments were performed under Home Office Licence. The work was supported by the CRC, MRC, NIH and Wellcome Trust. M.B. was the recipient of a predoctoral scholarship from the Ministry of Culture, Iran. S.A.B.R. was the recipient of an MRC graduate studentship, H.C.S. was the recipient of an HHMI predoctoral fellowship.

Received 19 July; accepted 26 November 1996.

Cui,W. & Akhurst, R.J. Transforming growth factor βs: biochemistry and biology *in vitro* and *in vivo*. in *Growth factors and cytokines in health and disease*. (eds. D. LeRoith and C. Brody) 357–394 (JAI Press, London, 1996).
Massague, J. TGFβ signaling, receptors, transducers and Mad proteins. *Cell* **85**, 947–950 (1996).
Dickson, M.C. *et al.* Transforming growth factor-β 1 is essential for hematopoiesis and endothelial differentiation *in vivo*. *Development* **121**, 1845–1854 (1995).
McAllister, K. A. *et al.* Endoglin, a TGF-β binding protein of endothelial cells, is the gene for hereditary haemorrhagic telangiectasia type 1. *Nature Genet.* **8**, 345–351 (1994).
Johnson, D. W. *et al.* Mutations in the activin receptor-like kinase 1 gene in hereditary haemorrhagic telangiectasia type 2. *Nature Genet.* **13**, 189–195 (1996).
Grainger, D.J., Kemp, P.R., Liu, A.C., Lawn, R.M. & Metcalfe, J.C. Activation of transforming growth factor-β is inhibited in transgenic apolipoprotein(a) mice. *Nature* **370**, 460–462 (1994).
Grainger, D.J. *et al.* The serum concentration of active transforming growth factor-β is severely depressed in advanced atherosclerosis. *Nature Med.* **1**, 74–79 (1995).
Markowitz, S. *et al.* Inactivation of the type II TGF-β receptor in colon cancer cells with microsatellite instability. *Science* **268**, 1276–1277 (1995).
Cui, W. *et al.* TGFβ1 inhibits the formation of benign skin tumours but enhances progression to invasive spindle cell carcinomas in transgenic mice. *Cell* **86** 531–546 (1996).
Shull, M.M. *et al.* Targeted disruption of the mouse transforming growth factor-β1 gene results in multifocal inflammatory disease. *Nature* **359**, 693–699 (1992).
Kulkarni, A.B. *et al.* Transforming growth factor-β1 null mutation in mice causes excessive inflammatory response and early death. *Proc. Natl. Acad. Sci. USA* **90**, 770–774 (1993).
Letterio, J.J. *et al.* Maternal rescue of the transforming growth factor β knockout. *Science* **264**, 1936–1938 (1994).
Green J.B.A. & Smith, J.C. Graded changes in dose of *Xenopus* activin A homologue elicit stepwise transitions in embryonic cell fate. *Nature* **347**, 391–394 (1990).
Lander, E.S. & Schork, N.J. Genetic dissection of complex traits. *Science* **265**, 2037–2048 (1994).
Dickinson, M.E. *et al.* Chromosomal localization of seven members of the murine TGF-β superfamily suggests close linkage to several morphogenetic mutant loci. *Genomics* **6**, 505–520 (1990).
Lander, E. & Kruglyak, L. Genetic dissection of complex traits: guidelines for interpreting and reporting results. *Nature Genet.* **11**, 241–247 (1995).
Risch, N., Ghosh, S. & Todd, J.A. Statistical evaluation of multiple-locus linkage data in experimental species and its relevance to human studies: application to nonobese diabetic (NOD) mouse and human insulin-dependent Diabetes Mellitus. *Am. J. Hum. Genet.* **53**, 702–714 (1993).
18. Laurey, S.G., Barton, D.E., Ullrich, A. & Franke, U. Chromosome mapping of the gene for type II insulin like growth factor receptor/cation-independent mannose-6-phosphate receptor in man and mouse. *Genomics* **3**, 224–229 (1988).
19. Bonyadi, M., Cui, W., Nagase, H. & Akhurst, R. J. The TGFβ type II receptor, *Tgfbr2*, maps to distal mouse chromosome 9. *Genomics* **33**, 328–329 (1996).
20. Qureshi, S. T., Gros, P., Letarte, M. & Malo, D. The murine endoglin gene (*Eng*) maps to chromosome 2. *Genomics* **26**, 165–166 (1995).
21. Avraham, K.B. *et al.* Mapping of murine fibroblast growth factor receptors refines regions of homology between mouse and human chromosomes. *Genomics* **21**, 656–658 (1994).
22. Kimelman, D. & Kirschner, M. Synergistic induction of mesoderm by FGF and TGF-β and the identification of an mRNA coding for FGF in the early *Xenopus* embryo. *Cell* **51**, 869–877 (1987).
23. Saunders, K.B. & D'Amore, P.A. FGF and TGF-β: Actions and interactions in biological systems. *Eukaryot. Gene Expr.* **1**, 157–172 (1991).
24. Mock, B.A. *et al.* The murine interleukin 6 gene maps to the proximal region of chromosome 5. *J. Immunol.* **142**, 1372–1376 (1989).
25. Gautum, S.C. *et al.* Transforming growth factor beta1 (TGFβ1) potentiates IL1 alpha-induced IL6 mRNA and cytokine protein production in a human astrocytoma cell line. *Oncol. Res.* **5**, 423–432 (1993).
26. Liu, J., Baker, J., Perkins, A. S., Robertson, E. J. & Efstradiatis, A. Mice carrying null mutations of the genes encoding insulin-like growth factor I (*Igf-1*) and type 1 IGF receptor (*Igf1r*). *Cell* **75**, 59–72 (1993).
27. George, E. L., Georges-Labouesse, E. N., Patel-King, R. S., Rayburn, H. & Hynes, R. O. Defects in mesoderm, neural tube and vascular development in mouse embryos lacking fibronectin. *Development* **119**, 1079–1091 (1993).
28. Threadgill, D.W. *et al.* Targeted disruption of mouse EGF receptor: effect of genetic background on mutant phenotype. *Science* **269**, 230–234 (1995).
29. Rozmahel, R. *et al.* Modulation of disease severity in cystic fibrosis transmembrane conductance regulator deficient mice by a secondary genetic factor. *Nature Genet.* **12**, 280–287 (1996).
30. Proetzel, M. *et al.* Transforming growth factor-β3 is required for secondary palate fusion. *Nature Genet.* **11**, 409–414 (1995).
31. Neumann, P.E. *et al.* Multifactorial inheritance of neural tube defects: localization of the major gene and recognition of modifiers in *ct* mutant mice. *Nature Genet.* **6**, 357–362 (1994).
32. Lander, E.S. *et al.* MAPMAKER: An interactive computer package for constructing primary genetic linkage maps of experimental and natural populations. *Genomics* **1**, 174–181 (1987).

BIBLIOGRAPHY.

Akhurst, RJ. (1994) The Transforming Growth Factor β Family in Vertebrate Embryogenesis . Growth Factors and Signal Transduction Development: 97-122.

Akhurst, RJ., Lenhert, SA., Faissner, AJ. & Duffie, E. (1990) TGFβ in Murine Morphogenetic Processes: The Early Embryo and Cardiogenesis . Development 108, 645-656.

Albano, RM., Groome, N. & Smith, JC. (1993) Activins are Expressed in Preimplantation Mouse Embryos and in ES and EC Cells and are Regulated on their Differentiation. Development 117, 711-733.

Altman, Pl. & Katz, DD. (1979) Inbred and Genetically Defined Strains of Laboratory Animals (Rat and Mouse). FASEB.

Anderson, DM., Lyman, SD., Baird, A., Wignall, JM., Eisenman, J., Rauch, C., March, CJ., Boswell, HS., Gimpel, SD., Cosman, D. & Williams, DE. (1990) Molecular Cloning of Mast Cell Growth Factor, a Haematopoietin That is Active in Both Membrane Bond and Active Forms. Cell 63, 235-243.

Antonelli-Orlidge, A., Saunders, KB., Smith, SR. & D'Amore, PA. (1989) An Activated Form of TGFβ is Produced by Cocultures of Endothelial Cells and Pericytes. Proc. Natl. Sci. USA 86, 4544-4548.

Arora, K., Dai, H., Kazuko, SG., Jamal, J., O'Connor, MB., Letsou, A. & Warrior, R. (1995) The Drosophila Gene *schnurri* Acts in the *dpp*/ TGFβ Signalling Pathway and Encodes a Transcription Factor Homologous to the Human MBP Family. Cell 81: 781-790.

Assoian, RK., Komoriya, A., Meyers, CA., Miller, DM. & Sporn., MB (1983) Transforming Growth Factor β in Human Platelets. Identification of a Major Storage Site. Purification and Characterisation. J. Biol. Chem. 258, 7155-7160.

Augustin, HG., Kozian, DH. & Johnson, RC. (1994) Differentiation of Endothelial Cells: Analysis of the Constitutive and Activated Endothelial Cell Phenotypes. BioEssays 16, 901-906.

Baird, A. & Durkin, T. (1994) Inhibition of Endothelial Cell Proliferation by TGFβ1: Interactions with Acidic and Basic Fibroblast Growth Factors. Biochem. & Biophys. Res. Comms. 138, 476-482.

Baribault, H., Penner, J., Iozzo, RV. & Wilson-Heiner, M. (1994) Colorectal Hyperplasia and Inflammation in Keratin 8-Deficient FVB/ N Mice. Genes Dev. 8, 2964-2973.

Barinager, M. (1994) Knockout Mice: Round Two. Science 265, 25-28.

Bassing, CH., Yingling, JM., Howe, DJ., Wang, T., He, WH., Gustafson, ML., Shah, P., Donahoe, PK. & Wang, X-F. (1994) A Type I Transforming Growth Factor β Receptor That Signals to Activate Gene Expression. Nature 263, 87-89.

Bassler, K., Edlund, T., Jessell, TM. & Yamada, T. (1993) Control of Cell Pattern in the Neural Tube: Regulation of Cell Differentiation by *dorsalin-1* a novel TGFβ Family Member. Cell 73, 687-702.

Basson, CT., Kocher, O., Basson, MD., Assis, A. & Madri, JA. (1992) Differential Modulation of Vascular Cell Integrin and ECM Expression *in vitro* by TGFβ1 Correlates with Reciprocal Effects on Cell Migration. J. Cell. Physiol. 153, 118-128.

Bhambi, B. & Eghbali, M (1991) Effects of Norepinephrine on Myocardial Collagen Gene Expression and Response of Cardiac Fibroblasts After Norepinephrine Treatment. Am. J. Path. 139, 1131-1142.

Bonyadi, M., Rusholme, SAB., Cousins, F., Farrall, M. & Akhurst, RJ. (1997) Mapping of a Major Modifier of Embryonic Lethality in TGFβ1 Knockout Mice. Nature Genetics 15, 207-210.

Breier, G & Risau, W. (1997) The Role of VEGF in Blood Vessel Formation. Trends in Cell Biol. 6, 454-456.

Brown, NA. & Fabro, S. (1981) Quantiation of Rat Embryonic Development *in vitro* : A Morphological Scoring System. Teratology 24, 65-78.

Brown, SDM. & Peters, J. (1996) Combining Mutagenesis and Genomics in the Mouse-Closing the Phenotype Gap. Trends in Genetics 12, 433-435.

Brunet, CL., Sharpe, PM. & Ferguson, MWJ. (1995) Inhibition of TGFβ1 (but not TGFβ2 or β3) Activity Prevents Normal Mouse Embryonic Palate Formation. J. Dev. Biol. 39, 345-355.

Buhring, CH., Muller, CA., Letarte, M., Gougos, A., Saalmuller, A., van Agthoven, AJ. & Busch, FW. (1991) Endoglin is Expressed in a Sub-Population of Immature Erythroid Cells of Normal Human Bone Marrow. Leukaemia. 5, 841-847.

Campbell, G., Weaver, T. & Tomilinson, A. (1993) Axis-Specification in the Developing *Drosophila* Appendage: the Role of *wingless, dpp* and the Homeobox gene *aristaless* . Cell 74, 1113-1123.

Carcamo, J., Weis, FM., Ventura, F., Weiser, R., Wrana, JL., Attisano, L. & Massague, J. (1994) Type I Receptors Specify Growth-Inhibitory and Transcriptional Responses to Transforming Growth Factor β and Activins: Mol. Cell. Biol. 14, 3810-3821.

Carcamo, J., Zentrella, A. & Massague, J. (1995) Disruption of Transforming Growth Factor β Signalling by a Mutation That Prevents Transphosphorylation within the Receptor Complex. Mol. Cell. Biol. 15, 1573-1581.

Carlino, JA., Higley, HR., Creson, JR., Avis, PD., Ogawa, Y. & Ellingsworth, LR. (1992) TGFβ1 Systematically Modulates Granuloid, Erythroid, Lymphoid and Thrombocytic Cells in Mice. Exp. Haematol. 20, 943-950.

Carmeliet, P., Mackman, N., Moons, L., Luther, T., Gressens, P., van Vlaenderen, I., Dermunck, H., Kasper, M., Breier, G., Evrard, P., Muller, M., Risau, W., Edginton, T. & Collen, D. (1996a) Role of Tissue Factor in Embryonic Blood Vessel Development. Nature 383, 73-75.

Carmeliet, P., Ferreira, V., Breier, G., Pollefeyt, S., Kieckens, L., Gertsenstein, M., Fahrig, M., Vandenhoek, A., Harpal, K., Eberhardt, C., Declercq, C., Pawling, J., Moons, L., Collen, D., Risau, W. & Nagy, A. (1996b) Abnormal Blood Vessel Development and Lethality in Embryos Lacking a Single VEGF Allele. Nature 380, 435-438.

Chabot, B., Stephenson, DA., Chapman, VM., Besmer, P. & Bernstein, A. (1988) The Proto-Oncogene *c-kit* Encoding a Transmembrane Tyrosine Kinase Maps to the Mouse *W* Locus . Nature 335, 88-89.

Cheiftez, S., Bassols, A., Stanley, K., Ohta, M., Greenberger, J. & Massague, J. (1988) Heterodimeric Transforming Growth Factor β. Biological properties and Interaction with 3 Types of Cell Surface Receptors. J. Biol. Chem. 263, 16984-16991.

Cheifetz, S., Bellon, T., Cales, C., Vera, A., Bernabeu, C., Massague, J. & Letarte, M. (1992) Endoglin is a Component of the Transforming Growth Factor β Receptor System in Human Endothelial Cells. J. Biol. Chem. 267, 19027-19034.

Chen, LL., Dean, A., Jenkinson, T. & Mendelsohn, J. (1992) Effect of TGFβ1 on Proliferation and Induction of Haemoglobin Accumulation in K-562 Cells. Blood 74, 2368-2375.

Chen, R-H., Meittinen, PJ., Maruka, EM., Choy, L.& Derynck, R. (1995) A WD-Domain Protein that is Associated with and Phosphorylated by the type II TGFβ Receptor. Nature 377, 548-552.

Chiquet-Ehirismann, R., Kalla, P., Pearson, CA., Beck, K. & Chiquet, M. (1995) Tenascin Interferes with Fibronectin Action. Cell 53, 383-390.

Clarke, AR., Mandag, ER., van Roon, M., van der Lugt, NM., van der Valk, M., Hooper, ML (1992). Requirement for a Functional Rb-1 Gene in Murine Development Nature 359, 328-330.

Collignon, J., Varlet, I. & Robertson, EJ. (1996) Relationship Between Asymmetric *nodal* Expression and the Direction of Embryonic Turning. Nature 381, 155-158.

Copp, AJ. (1996) Death Before Birth: Clues from Gene Knockouts and Mutations. Trends in Genetics 11, 87-93.

Cui, W. & Akhurst, RJ. (1996) Transforming Growth Factor βs: Biochemistry and Biological Activities *in vitro* and *in vivo* . Growth Factors and Cytokines in Health and Disease Volume 1B, 318-356.

Dallas, L., Miyazono, K., Skerry, TM., Mundy, GR. & Bonewald, LF. (1995) A Role for Latent Transforming Growth Factor β Binding Proten in Storage of Latent TGFβ in the ECM and as a Structural Matrix Protein. J. Cell. Biol. 131, 539-549.

Das, V. (1992) Modulation of TGFβ1 Anti-Proliferative Effects on Endothelial Cells By Cysteine, Cystine and N-acetylcysteine. J. Clinical Invest. 90, 1649-1656.

de Celis, JF., Barrio, R.& Kafatos., FC. (1996) A Gene Complex Acting Downstream of *dpp* in Drosphila Wing Morphogenesis. Nature 1996, 421-424.

de Martin, R., Haendler, E., Hoferwarbinck, R., Gaugitsch, H., Wrana, M., Schlosener, H., Seifert, SM., Bodmer, S., Fontana, A. & Hofer, E. (1987) Complementary DNA for Human Glioblastoma-Derived T Cell Supressor Factor, A Novel Member of the TGFβ Gene Family . EMBO. J. 6, 3673-3677.

Derynck, R., Jarrett, JA., Chen, EY., Eaton, DH., Bell, JR., Assoian, RK., Roberts, AB., Sporn, MB. & Goeddel, DV. (1985) Human Transforming Growth Factor β cDNA Sequence and Expression in Tumour Cell Lines. Nature 316, 701-705.

Derynck, R., Jarrett, JA., Chen, EY. & Goeddel, DV. (1987) The Murine TGFβ Precursor. J. Biol. Chem. 261, 4377-4379.

Derynck, R., Rhee, L., Chen, EY. & Van Tilburg, A. (1987) Intron-Exon Structure of the Human TGFβ Precursor Gene. Nuc. Acids. Res. 15, 3188.

Dickson, M., Slager, H., Duffie, E. & Akhurst RJ. (1993) TGFβ2 RNA and Proten Localisation in the Early Embryo Suggest a Role in Cardiac Development and Myogenesis. Development. 117, 625-639.

Dickson, MC., Martin, JS., Cousins, FM., Kulkarni, AB., Karlsson, S. & Akhurst, RJ. (1995) Defective Haematopoiesis and Vasculogenesis in TGFβ1 Knockout Mice. Development. 121, 1845-1854.

Doctor, JS., Jackson, D., Rashka, KE., Visalli, M., Hoffmann, M. (1992) Sequence, Biochemical Characterisation, and Developmental Expression of a New Member of the Transforming Growth Factor β Superfamily in Drosophila melangoster .Dev. Biol. 151, 491-505.

Dudley, AT., Lyons, KM. & Robertson, EJ. (1995) A Requirement for Bone Morphogenetic Protein-7 During Development of the Mammalian Kidney and Eye. Genes Dev. 9, 2795-2807.

Dumont, DJ., Gradwohl, G., Fong, G-H., Puri, MC., Gertsenstein, M., Auerbach, A., Breitman, ML. (1994) Dominant-Negative and Targeted Null Mutations in the Endothelial Receptor Tyrosine-Kinase, *tek*, Reveal a Critical Role in Vasculogenesis of the Embryo. Genes Dev. 8, 1897-1909.

Dzierzak, E. & Medvinsky, A. (1995) Mouse Embryonic Haematopoiesis. Trends in Genetics 11, 359-366.

Ecohard, V., Cayrol, C., Foulquiet, F., A Zaraisky, & Duprat, AM. (1995) A Novel TGFβ-Like Gene *fugacin*, Specifically Expressed in the Spemann Organiser of *Xenopus*.. Dev. Biol. 172, 699-703.

Erickson, RP. (1996) Mouse Models of Human Genetic Disease: Which is More Like a Man?. BioEssays 18, 993-998.

Estevez, M., Attisano, L., Wrana, JL., Albert, PS., Massague, J. & Riddel., DL. (1993) The *daf-4* Gene Encodes a Bone Morphogenetic Protein Receptor Controlling *C. elegans* Dauer Larva Development. Nature 365, 644-649.

Feijen, A., Goumans, MJ. & van den Eijnden-van Raaij, A. (1994) Expression of Activin Subunits, Activin Receptors and Follistatin in Post-implantation Mouse Embryos Suggests Specific Developmental Functions for Different Activins. Development 120, 3621-3637.

Ferguson, MWJ. (1988) Palate Development. Development 103. Supplement., 41-60.

Festing, MFW (1993) Origins and Characteristics of Inbred Strains of Mice. Mouse Genome 91: 393-509.

Fitzpatrick., DR., Denhez, F., Kondaiah, P. & Akhurst, RJ. (1990) Differential Expression of TGFβ Isoforms in Murine Palatogenesis. Development 109, 585-595.

Folkman, J. & D'Amore, P. (1996) Blood Vessel Formation: What is its Molecular Basis? Cell 87, 1153-1155.

Fong, G-H, Rossant, J., Gertsenstein, M. & Breitman, ML (1995) Role of *flt*-1 RTK in Regulating the Assembly of the Vascular Endothelium. Nature 376, 66-70.

Franzen, P, ten Dijke, P., Ichijo, H., Yamashita, H., Schulz, P., Heldin, C-H. & Miyazono, K. (1993) Cloning of a TGFβ Type I Receptor That Forms a Heteromeric Complex with the TGFβ Type II Receptor . Cell 75, 681-692.

Frolick, CA.,Dart, LL., Meyer, CA., Smith, DM. &Sporn., MB. (1983) Purification and Initial Characterisation of a Type β Transforming Growth Factor from Human Placenta. Proc. Natl. Acad. Sci. USA 80, 3676-3680.

Frohmann, MA. & Martin, GR. (1989) Cut, Paste, and Save: New Approaches to Altering Specific Genes in Mice. Cell 56, 1245-147.

Furth, PA., St. Onge, L., Boger, H., Gruss, P., Gossen, M., Kistner, A., Bujard, H. & Hennighausen, L. (1994). Proc. Acad. Natl. Sci. USA 91, 9302-9306.

Geiser, AG., Letterio, JL., Kulkarni, AB., Karlsson, S., Roberts, AB. & Sporn, MB. (1993) TGFβ1 Controls Exprssion of Major Histocompatability Genes in the Postnatal Mouse: Aberrant Histocompatability Antigen Expression in the Pathogenesis of the TGFβ1 Null Mouse Phenotype. Proc. Acad. Natl. Sci. USA. 90, 9944-9948.

Geissler, EN., Ryan, MA. & Housman, DE. (1988) The *Dominant White Spotting (W)* Locus of the Mouse Encodes the c-kit Proto-oncogene. Cell 55, 185-192.

George, EL., Georges Lobouesse, EN., Patel-King, RS., Rayburn, H. & Hynes, RO. (1993) Defects in the Mesoderm, Neural Tube, and Vascular Development in Mouse Embryos Lacking Fibronectin. Development 119, 1079-1091.

Ghosh, S: & Brauer, PK. (1996) Latent Transforming Growth Factor β is Present in the ECM of Embryonic Hearts In Situ. Dev. Dynam. 205, 126-134.

Godin, I., Dieterlen-Lievre, F. & Cumano, A. (1995) Emergence of Multipotent Haematopoietic Cells in the Yolk Sac and Paraaortic Splanchnopleura in Mouse Embryos, Beginning at 8.5dpc. Proc. Natl. Acad. Sci. USA 92, 773-777.

Graff, JM., Bansal, A.& Melton, DA. (1996) Xenopus mad Proteins Transduce Distinct Subsets of Signals for the TGFβ Superfamily. Cell 85, 479-487.

Grieder, NC., Nellen, D., Burke, R., Basler, K.& Affolter, M. (1995) *schnurri* is Required for *Drosophila dpp* Signalling and Encodes a Zinc Finger Protein Similar to the Mammalian Transcription Factor PRDII-BF1. Cell 81, 791-800.

Gu, Z., Oh, S., Yu, L., Raynolds, E., Simpson, B., Lei, H., Goss, K., Donahoe, P., Gridley, T, Nomamura, M. & Li. E. (1996) Role of Activin Receptors in Mammalian Gastrulation. Proceedings of Mouse Molecular Genetics Meeting, Cold Spring Harbour, 1996.

Hauser, IA., Setter, E., Bell, L. & Madri, JA. (1993) Fibronectin Expression Correlates with U937 Cell Adhesion to Migrating Bovine Aortic Endothelial Cells *in vitro* . Am. J. Path. 143, 173-180.

Heimark, RL., Twardzik, DR. & Schwartz, SM. (1986) Inhibition of Endothelial Regeneration by TGFβ from Platelets. Science 233, 1078-1080.

Heino, J. & Massague, J. (1989) TGFβ Switches Off the Pattern of Integrins Expressed in MG-63 Human Osteosarcoma Cells and Causes a Selective Loss of Cell Adhesion to Laminin. J. Biol. Chem. 36, 21806-21811.

Heino, J., Ignotz, RA., Hemier, ME., Crouse, C. & Massague, J. (1989) Regulation of Cell Adhesion Receptors by TGFβ. J. Biol. Chem. 264, 380-388.

Herman, IM. & D'Amore. PA. (1985) Microvascular Pericytes Contain Muscle and Non-Muscle Actins. J.Cell.Biol. 101, 43-52.

Hirsch, E., Iglesias, A., Potocnik, AJ., Hartmann, U. & Fassler, R. (1996) Impaired Migration but not Differentiation of Haematopoietic Stem Cells in the Absence of β1 Integrins. Nature 380, 171-175.

Hogan, B., Beddington, R., Costantini, F. & Lacy, E. (1994) Manipulating the Mouse Embryo: A Laboratory Manual 2nd Edition . Cold Spring Harbor Laboratory Press.

Ignotz, RA. & Massague, J. (1987) Cell Adhesion Protein Receptors as Targets for TGFβ Action. Cell 51, 189-197.

Ignotz, RA., Heino, J. & Massague, J. (1989) Regulation of Cell-Adhesion Receptors by TGFβ). J. Biol. Chem. 264, 4337-4345.

Imamato, A. & Sorlano, P. (1993) Disruption of the *csk* Gene, Encoding a Negative Regulator of the Src Family Tyrosine Kinases, Leads to Neural Tube Defects and Embryonic Lethality in Mice. Cell 73, 117-1124.

Jakowlew, SB., Dillard, PJ., Sporn, MB. & Roberts, AB. (1988) Nucleotide Sequence of Chicken TGFβ1. Nuc. Acids. Res. 16, 8730.

Jennings, JC., Mohan, S., Linkhart, TA., Widstrom, R. & Baylink, DJ. (1988) Comparison of the Biological Actions of TGFβ1 and TGFβ2: Differential Activity in Endothelial Cellsx. J. Cell. Physiol. 137, 167-172.

Jokhi, PP., King, A., Sharkey, AM., Smith, SK. & Loke, YW. (1994) Screening for Cytokine Messenger Ribonucleic Acids in Purified Human Decidual Lymphocyte Populations by RT-PCR. J. Immunol. 153, 4427-4435.

Kanzaki, T., Olofsson, A., Moren, A., Wernstedt, C., Hellman, U., Miyazono, K., Claesson-Welsh, L. & Heldin, C. (1990) TGFβ1 Binding Protein: A Component of the Large Latent Complex of TGFβ1 with Muliple Repeat Sequences. Cell 61, 1051-1061.

Kawabata, M., Imamura, T., Miyazono, K., Engel., ME. & Moses, HL. (1990) Interaction of the TGFβ Type I Receptor with Faresyl Transferase-α (1995). J. Biol. Chem. 270, 29628-29631.

Keller, JR., Jaconsen, SEW., Sill, K., Ellingsworth, L. & Ruscetti, FW. (1991) Stimulation of Granulopoiesis by TGFβ. Synergy with GM-CSF . Proc. Acad. Natl. Sci. USA 88, 7190-7193.

Keller, JR., McNeice, IK., Sill, KT., Ellingsworth, LR., Quesenberry, PJ., Sing, GK. & Ruscetti, FW. (1990) TGFβ Directly Regulates Primitive Murine Haematopoietic Cell Proliferation. Blood 75, 596-600.

Kim, S., Glick, A., Sporn, MB. & Roberts, AB. (1989) Characterisation of the Promoter Region of the Transforming Growth Factor β1 Gene . J. Biol. Chem. 264, 402-408.

Kingsley, DM. (1994) The TGFβ Superfamily New Members, New Receptors, and New Genetic Tests of Function in Different Organisms. Genes Dev. 8, 133-146.

Kulkarni, AB., Huh, C., Becker, D., Geiser, A., Lyght, M., Flanders, KC., Roberts, AB., Sporn, MB., Ward, JM. & Karlsson, S. (1993) TGFβ1 Null Mutation in Mice Causes Excessive Inflammatory Response and Early Death. Proc. Acad. Natl. Sci. USA. 90, 770-774.

Kwee, L., Baldwin, HS., Shen, HM., Stewart, CL., Buck, C., Buck, CA. & Labow, MA. (1995) Defective Development of the Embryonic and Extra-Embryonic Circulatory Systems in VCAM-1 Deficient Mice. Development 121, 489-503.

Lafyatis, R., Lechleider, R., Kim, S., Jakolew, S., Roberts, AB. & Sporn MB. (1990) Structural and Functional Characterisation of the Transforming Growth Factor β3 Promoter. J. Biol. Chem. 265, 19128-19136.

Langenfeld, KB., Garbis-Berkvens, JM., Verhoef, A. & Peters, PWJ. (1988). Histology of the Rat Embryo, Cultured *in vitro* Toxicol. *in vitro* 2, 149.

Larue, AA., Ohsugi, M., Hirchenhain, J. & Kemler, R. (1994) E-Cadherin Null Mutant Embryos Fail To Form a Trophectoderm Epithelium. Proc. Acad. Natl. Sci. USA 91, 8263-8267.

Lasko, M., Sauer, B., Mosinger, BJ., Lee, EJ., Manning, RW., Yu, SH., Mulder, KL. & Westphal, H. (1992) Targeted Oncogene Activation by Site-Specific Recombination in Transgenic Mice. Proc. Acad. Natl. Sci. USA 89, 6232-6236.

Lastres, A., Letamendia, A., Zhang, H., Rius, C., Almendro, N., Raab, U., Lopez, LA., Larga, C., Fabra, A., Letarte, M. & Bernabeu, C. (1996) Endoglin Modulates Cellular Responses to TGFβ1. J. Cell. Biol. 133, 1109-1121.

Lenhert, SA. & Akhurst, RJ. (1988) Embryonic Expression Pattern of TGFβ1 RNA Suggests Both Paracrine and Autocrine Mechanisms of Action. Development 104, 263-273.

Letterio, JJ., Geiser, AG., Kulkarni, AB., Roche, NS., Sporn, MB. & Roberts, AB. (1994) Maternal Rescue of the Transforming Growth Factor β1 Knockout. Science 264, 1936-1938.

Lin, HY., Wang, XF., Ng-Eaton, E., Weinberg, RA. & Lodish, H. (1992) Expression Cloning of a Transforming Growth Factor β Type II Receptor, a Functional Transmembrane Serine/ Theronine Kinase. Cell 68, 775-785.

Lin, HY., Moustakas, A., Knaus, P., Wells, RG., Henis, YI. & Lodish, HF. (1995) The Soluble Exoplasmic Domain of the Type II Transforming Growth Factor β Receptor. J. Biol. Chem. 270, 2747-2754.

Lohler, K., Timpl, R., Jaenisch, R. (1984) Embryonic Lethal Mutation in Mouse Collagen I Gene Causes Rupture of the Great Vessels and Is Associated with Erythropoietic and Mesenchymal Cell Death . Cell 38, 597-607.

Lopez-Casillas, F., Wrana, JL. & Massague, J. (1993) Betaglycan Presents Ligand to the TGFβ Signalling Receptor. Cell 73, 1435-1444.

Lopez-Casillas, F., Cheifetz, S., Doody, J., Andres, JL., Lane, WL. & Massague, J. (1991) Structure and Expression of the Membrane Proteoglycan Betaglycan, a Component of the TGFβ Receptor System. Cell 67, 785-795.

Lopez-Casillas, F., Payne, HM., Andres, JL. & Massague, J. (1994) Betaglycan can act as a Dual Modulator of TGFβ Access to Signalling Receptors, Ligand binding and GAG Attatchment Sites. J. Cell. Biol. 124, 557-568.

Lui, F., Hata, A., Baker, JC., Doody, J., Carcamo, J., Harland, RM, & Massague, J. (1996) A Human *mad* Protein Acting as a BMP-Regulated Transcriptional Activator. Nature 381, 620-623.

McCartney-Francis, N., Mizel, D., Wong, H., Wahl, L. & Wahl, S. (1988) TGFβ as an Immunoregulatory Molecule. Abstract FASEB J. 2, A875.

McDonald, NQ and Henrickson, WA. (1992) A Structural Superfamily of Growth Factors Containing a Cysteine Knot . Cell 73, 421-424.

McLaughlin, J., Szabo, P., Haegel, H. & Mann, JR. (1996) Mouse Embryos with Parental Duplication of an Imprinted Chromosome 7 Region Die at Midgestation and Lack Placental Spongiotrophoblast. Development 122, 265-270.

Ma, C., Zhou, Y., Beachy, PA. & Moses, K. (1993) The Segment Polarity Gene *hedgehog* is Required for the Progression of the Morphogenetic Wave in the *Drosophila* Eye. Cell 75, 927-938.

Madri, JA., Pratt, BM., Tucker, AM. (1988) Phenotypic Modulation of Endothelial Cells By TGFβ Depends Upon the Composition and Organisaton of the Extra-Cellular Matrix. J. Cell. Biol. 106, 1375-1384.

Madri, JA., Reidy, MA., Kocher, O. & Bell, L. (1989) Endothelial Cell Behaviour After Denudation Injury is Modulated by TGFβ1 and Fibronectin. Lab. Invest. 60, 755-765.

Madri, JA., Bell, L. & Merwin, JA. (1992) Modualtion of Vascular Cell Behaviour by TGFβ. Mol. Reprod. Dev. 32, 121-126.

Martin, JS. (1996) *in vivo* and *in vitro* Characterisation of the TGFβ1 Knockout Phenotype. Thesis Submitted for the Degree of PhD (University of Glasgow).

Mandriotta, SJ., Menoud, P-A., Pepper, MS. (1996) TGFβ1 Down-Regulates VEGF Receptor 2/ *flk*-1 Expression in Vascular Endothelial Cells. J. Biol. Chem. 271, 11500-11505.

Massague, J. (1992) Receptors for the TGFβ Family. Cell 69, 1067-1070.

Matthews, LS. & Vale, WW. (1993) Characterisation of Type II Activin Receptors, Binding, Processing and Phosphorylation. J. Biol. Chem. 268, 19013-19018.

Matzuk, MM., Rajendra Kumar, T., Vassali, A., Bickenbach, JR., Roop, DR, Jaenisch R, & Bradley, A. (1995a) Functional Analysis of Activins during Mammalian Development. Nature 374, 354-356.

Matzuk, MM., Rajendra Kumar, T, & Bradley, A (1995a) Different phenotypes for Mice Deficient in either Activins or Activin Receptor Type II. Nature 374, 356-359.

Medvinsky, AL., Samoylina, NL., Muller, AM. & Dzierzak, EA. (1993) An early Pre-Liver Intra-Embryonic Source of CFU-S in the Developing Mouse. Nature 364, 64-66.

Melton, DW. (1994) Gene Targeting in the Mouse. BioEssays 16, 633-638.

Meno, C., Saijoh, Y., Fujii, H., Ikeda, M., Yokohama, T., Yokohama, M., Toyoda, Y. & Hamada, H. (1996) Left-Right Asymmetric Expression of the TGFβ Family Member *lefty* in Mouse Embryos. Nature 381, 151-155.

Merwin, JR., Anderson, J., Kocher, O., van Itallie, C. & Madri, JA. (1996) TGFβ1 Modulates Extracellular Marix Organisation and Cell-Cell Junctional Complex Formation During *in vitro* Angiogenesis. J. Cell. Physiol. 142, 117-128.

Merwin, JR., Newman, W., Beall, LD., Tucker, A. & Madri, J. (1991) Vascular Cells Respond Differently to TGFβ1 and TGFβ2 *in vitro* . Am. J. Path. 138, 37-51.

Millan, FA., Kondaiah, P., Denhez, F. & Akhurst, RJ. (1991) Embryonic Gene Expression Patterns of TGFβs 1, 2 and 3 Suggest Different Developmental Roles *in vivo*. Development. 111, 131-144.

Mishina, Y., Susuki, A., Ueno, N.& Behringer, RR. (1995) BMPR Encodes a Type 1 Bone Morphogenetic Protein Receptor which is Essential for Gastrulation in Mouse Embryogenesis. Genes Dev. 9, 3027-3037.

Miura, Y. & Wilt, FH. (1969) Tissue Interaction and the Formation of the First Erythroblasts of the Chick Embryo: Dev. Biol. 19, 201-211.

Miyazono, K., Hellman, U., Wernstedt, C. & Heldin, CH. (1988) Latent High Molecular Weight Complex of Transforming Growth Factor β1: Purification from Human Platelets and Structural Characterisation. J. Biol. Chem. 263, 6407-6415.

Miyazono, K., Ichijo, H. & Heldin, C. (1988) Transforming Growth Factor β: Latent Forms, Binding Proteins and Receptors. Growth Factors 8, 11-22.

Moore, MSA. & Metcalf, D. (1988) Ontogeny of the Haematopoietic System: Yolk Sac Origin of *in vivo* and *in vitro* Colony Forming Units in The Developing Mouse Embryo. British. J. Haemat. 18, 279-296.

Moren, AA., Olofsson, G., Stenman, P., Sahlin, T., Kanzaki, L., Claesson, P., ten Dijke, P., Miyazono, K. & Heldin, C. (1994) Identification and Characterisation of LTBP-2, a Novel Latent Transforming Growth Factor β Protein. J. Biol. Chem. 269, 32469-32478.

Morse, HC. (1978) Origins of Inbred Mice. Academic Press, New York.

Mucenski, ML., McLain, K., Kier, AB., Swerdlow, SH., Schreiner, CM., Miller, TA., Pietryga, DW., Scott, WJ. & Potter, SS. (1991) A Functional *c-myb* Gene is Required for Normal Murine Fetal Hepatic Haematopoiesis. Cell 65, 677-689.

Muller, G., Behrens, J., Nussbaumer, U., Bohlen, P. & Birchmeier, W. (1987) Inhibitory Action of TGFβ on Endothelial Cells. Proc. Acad. Natl. Sci. USA 84, 5600-5604.

Muslin, AJ. & Williams, LT. (1991) Well-Defined Growth Factors Promote Cardiac Development in Axolotl Mesoderm Explant. Development 112, 1095-1101.

Nabel., EG. (1994) Direct Transfer of TGFβ1 Gene into Arteries Stimulates Fibrocellular Hyperplasia. Proc. Natl. Acad. Sci. USA 90, 10759-10763.

Nakamura, T., Asashima, M., Eto, Y., Takio, K., Uchiyama, H., Moriya, N., Ariizumi, T., Yashiro, T., Sugino, K., Titani, K & Sugino, H. (1992) Isolation and Characterisation of Native Activin B. J. Biol. Chem. 267, 16385-16389.

Nakano, T., Kodama, H. & Honjo, T. (1996) In vitro Development of Primitive and Definitive Erythrocytes from Different Precursors. Nature 272, 722-724.

Nieuwkoop, PD. (1969) The Formation of Mesoderm in Urodelan Amphibians.I. Induction by the Endodermx. Wilhelm Roux's Arch. Entwicklungmech. 162, 341-373.

Nehls, V. & Drenckhahn, D. (1993). The Versatility of the Perivascular Pericyte: From Mesenchyme to Smooth Muscle Histochem. 99, 1-12.

Neuhaus, H., Rosen, V. & Theis, S. (1996) T-ALK, a BMP Type II Receptor, binds with High Affinity to BMP-9. Proc. Mouse Molecular Genetics Meeting 1996. CSHL.

Nicosia, RF. & Villaschi, S. (1995) Rat Aortic Smooth Muscle Cells Become Pericytes during Angiogenesis *in vitro* . Lab. Invest. 73, 658-665.

Noma, T., Glick, AB., O'Reilly, MA., Miller, J., Roberts, AB. & Sporn, MB. (1991) Molecular Cloning and Structure of the Human Transforming Growth Factor β2 Gene Promoter. Growth Factors 4, 247-255.

O'Gorman, S., Fox, DT. & Wahl, GM. (1991) Recombinase-Mediated Gene Activation and Site-Specific Integration in Mammalian Cells. Science 251, 1351-1355.

Ogawa, Y., Schmidt, DK., Dasch, JR., Chang, RJ. & Glaser, CB. (1992) Purification and Characterisation of TGFβ 2 and 3; and 1 and 2 Heterodimers from Bovine Bone. J. Biol. Chem 267, 2325-2328.

Oh, S., Schrewe, H., Goss, K., Gridley, T., Lei, H. & Li, E. (1996) Essential Function for the Type II Activin Receptors in Axial Patterning and Organogenesis. Proceedings of Mouse Molecular Genetics Meeting, Cold Spring Harbour, 1996.

Ohta, M., Greenberger, JS., Anklesaria, P., Bassols, A. & Massague, J. (1987) Two Forms of TGFβ Distinguished by Multipotential Haematopoietic Progenitor Cells. Nature 329, 539-541.

Orkin, SH. (1995) Haematpoiesis: How Does it Happen?: Curr. Opin. Cell. Biol. 7, 870-877.

Oshima, M., Oshima, H. & Taketo, MM. (1996) TGFβ Receptor Type II Deficiency Results in Defects of Yolk Sac Haematopoiesis and Vasculogenesis. Dev. Biol. 179, 297-302.

Ottman, O. & Pelus, LM. (1988) Differential Proliferative Effects of TGFβ on Human Haematopoietic Precursor Cells. J. Immunol. 140, 2661-2665.

Padgett, RW, Wozney, JM. & Gelbart WM. (1993) Human BMP Sequences can Confer Normal Dorsal-Ventral Patterning in the *Drosophila* Embryox. Proc. Acad. Natl. Sci. USA. 90, 2905-2909.

Pardanaud, L., Yassine, F. & Dieterlen-Lievre, F. (1989) Relationship Between Vasculogenesis, Angiogenesis and Haematopoiesis During Avian Ontogeny. Development 105, 473-485.

Paria, BC. & Dey, SK. (1990) Preimplantation Embryo Development *in vitro*: Cooperative Interactions Among Embryos and Role of Growth Factors. Proc. Acad. Natl. Sci. USA 87, 4756-4760.

Paria, BC., Jones, KL., Flanders, KC. & Dey, SK. (1992) Localisation and Binding of TGFβ Isoforms in Mouse Preimplantation Embryos and in Delayed and Activated Blastocysts. Dev. Biol. 151, 91-104.

Parker, TG. & Schneider, MD. (1991) Growth Factors, Proto-Oncogenes and Plasticity of the Cardiac Phenotype. Ann. Review. Physiol. 53, 179-200.

Patel, VP. & Lodish, HF. (1994) A Fibronectin Matrix is Required for the Differentiation of Murine Erythroleukemia Cells into Reticulocytes. J. Cell. Biol. 105, 3105-3118.

Pelton, RW., Hogan, BML., Miller, DA. & Moses, HL. (1990) Differential Expression of Genes Encoding TGFβs 1, 2 and 3 During Mouse Embryonic Palate Formation. Dev. Biol. 141, 456-460.

Pelton, RW., Saxena, B., Jones, M., Moses, HL. & Gold, LI. (1991) Immunohistochemical Localisation of TGFβ1, TGFβ2 and TGFβ3 in the Mouse Embryo: Expression Patterns Suggest Multiple Roles During Embryonic Development. J. Cell. Biol. 115, 1091-1105.

Qian, SW., Burmester, JK., Merwin, JR., Madri, JR., Sporn, MB. & Roberts, AB. (1992) Identification of a Structural Domain that Distinguishes the Actions of Type 1 and 2 Isoforms of Transforming Growth Factor β on Endothelial Cells. Proc. Natl. Acad. Sci. USA 89, 6290-6294.

Racke, MK., Dhib-Jalbut, S., Cannella, B., Albert, PS., Raine, CS. & McFarlin, DE. (1991) Prevention and Treatment of Chronic Relapsing Experimental Encephalomyelitis by TGFβ1. J. Immunol. 146, 3012-3017.

Raftery, LA., Twombly, V., Wharton, K.& Gelbart, WM. (1995) Genetic Screens to Identify Elements of the *dpp* Signalling Pathway in Drosophila. Genetics 139, 241-254.

Rappolee, DA., Brenner, CA., Schultz, R., Mark, D. & Werb, Z. (1988) Developmental Expression of PDGF, TGFβ and TGFα Genes in Preimplantation Mouse Embryos. Science 241, 1823-1825.

Reddi, H. (1992) Regulation of Cartilage and Bone Differentiation by Bone Morphogenetic Proteins. Curr. Opin. Cell. Biol. 4, 850-855.

Roberts, AB., Anzano, MA., Meyer, CA., Wideman, J., Blacher, R., Pan, Y., Stein, S., Lehrman, SR., Smith, JM., Lamb, LC. & Sporn, MB. (1983) Purification and Properties of a Type β Transforming Growth Factor from Bovine Kidney. Biochem. 22, 5692-5698.

Roberts, MB., Birkenmeier, TM., McQuillan, JJ., Akiyama, SK., Yamada, SS., Chen, W-T, Yamada, KM.& McDonald, JA. (1988) TGFβ Stimulates the Expression of Fibronectin and of Both Subunits of the Human Fibronectin Receptor by Cultured Human Lung Fibroblasts. J. Biol. Chem. 263, 4586-4592.

Roberts, AB & Sporn, MB. (1990) The Transforming Growth Factor βs. Peptide Growth Factors and their Receptors-Handbook of Experimental Pharmacology 419-472.

Roelen, BAJ., Yin, HL., Knezevic, V., Freund, E. & Mummery, CL. (1994) Expression of TGFβs and their Receptors During Implantation and Organogenesis of the Mouse Embryo. Dev. Biol. 166, 716-728.

Rosenweig, BL., Imamura, T., Okadome, T., Cox, GN., Yamashita, H., ten Dijke, P., Heldin, C-H. & Miyazono, K. (1995) Cloning and Characterisation of a Human Type II Receptor for Bone Morphogenetic Proteins. Proc. Natl. Acad. Sci. USA. 92, 7632-7636.

Rozmahel, R. (1996) Modulation of Disease Severity in Cystic Fibrosis Transmembrane Conductance Regulator Deficient Mice by a Secondary Genetic Factor. Nature Genetics 12, 280-287.

Ruberte, E., Marty, T., Nellen, D., Affolter, M. & Basler, K. (1995) An Absolute Requirement for Both the Type II and Type I Receptors, *punt* and *thick veins*, for *dpp* Signalling *in vivo* . Cell 80, 889-897.

Runyan, RB. & Markwald, RR. (1983) Invasion of Mesenchyme into 3D-Collagen Gels: A Regional and Temporal Analysis of Interaction in Embryonic Heart Tissue. Dev. Biol. 95, 108-114.

Runyan, RB., Potts, JD. & Weeks, DL.(1992) TGFβ3 Mediated Tissue Interaction During Embryonic Heart Development. Mol. Reprod. Dev. 32, 152-159.

Sabin, FR. (1920) Studies on the Origin of the Blood Vessels and of the Red Blood Corpusles as Seen in the Living Blastoderm of the Chick During the Second Day of Incubation. Contrib. Embryol. 9, 215-262.

Sambrook, J., Fritsch, EF. & Maniatis, T. (1989) Molecular Cloning: A Laboratory Manual. Second Edition, Cold Spring Harbour. Cold Spring Harbour Laboratories

Sampath, TK., Rashka, KE., Doctor JS., Tucker RF. & Hoffmann FM. (1993) *Drosophila* Transforming Growth Factor Beta Superfamily Proteins Induce Endochondral Bone Formation in Mammals. Proc. Acad. Natl. Sci. USA. 90, 6004-6008.

Sankar, S., Mahooti-Brooks, N., Bensen, L., McCarthy., Centrella, M. & Madri, JA. (1996) Modulation of TGFβ Receptor Levels on Microvascular Endothelial Cells During *in vitro* Angiogenesis. J. Clin. Invest. 97, 1436-1446.

Sato, Y. & Rifkin, DB. (1989) Inhibition of Endothelial Cell Movement by Pericytes and Smooth Muscle Cells: Activation of a Latent TGFβ1-Like Molecule by Plasmin During Co-Culturex. J. Cell. Biol. 109, 309-315.

Sato, TN., Tozawa, Y., Deutsch, U., Wolburg-Buchholz, K., Fujiwara, Y., Gendron-Maguire, M., Gridley, T., Wolburg, H., Risau, W. & Qin, Y. (1995) Distinct Roles for the RTKs *tie*-1 and *tie*-2 in Blood Vessel Formation. Nature 376, 70-74.

Savage, C., Das, P., Finelli, AL., Townsend, SR., Sun, CY., Baird, SE. & Padgett, RW. (1996) *C. elegans* Genes *sma*-2, *sma*-3 *and sma*-4 Define a Conserved Family of TGFβ Pathway Components. Proc. Acad. Natl. Sci. USA. 93, 790-794.

Sekelsky, JJ., Newfeld, SJ., Raftery, LA., Chartoff, EH. & Gelbart WM. (1995) Genetic Characterisation and Cloning of *mothers against decaplentaplegic*, a Gene Required for *dpp* Function in *Drosophila* Genetics 139, 1347-1358.

Shalaby, F., Rossant, J., Yamaguchi, TP., Gertsenstein, M, Wu, W-F., Breitman, ML. & Schuh, AC. (1995) Failure of Blood Island Formation and Vasculogenesis in *flk*-1 Deficient Mice. Nature 376, 62-66.

Sharples, J. (1987) Cloning and Sequence Analysis of Simian TGFβ DNA. DNA 6, 3239-3244.

Shivdasani, RA., Mayer, EL. & Orkin, SH. (1995) Absence of Blood Formation in Mice Lacking the T-cell Leukaemia Oncoprotein tal-1/ SCL. Nature 373, 432-434.

Shull, MM., Ormsby, I., Kier, AB., Pawlowski, S., Diebold, RJ., Yin, M., Allen, R., Sidman, C., Proetzel, G., Calvin, G., Annunziata, N. & Doetschman, T. (1992) Targeted Disruption of the Mouse TGFβ1 Gene Results in Multifocal Inflammatory Disease. Nature 359, 693-699.

Sibilia, M. & Wagner, EF. (1996) Strain-Dependent Epithelial Defects in Mice Lacking the EGF Receptor. Nature 269, 234-238

Sing, GK., Keller, JR., Ellingsworth, LR. & Ruscetti, FW.(1988) TGFβ Selectively Inhibits Normal and Leukemic Human Bone Marrow Cell Growth *in vitro*. Blood 72, 1504-1511.

Slack, JMW.(1983) From Egg to Embryo. 1st Edition. Cambridge University Press.

Slager, HG., Lawson, KA., van den Eijnden-van Raaij, AJ., de Laat, SW. Mummery, CL. (1991) Differential Localisation of TGFβ2 in Mouse Preimplantation and Early Post-Implantataion Development. Dev. Biol. 145, 205-218.

Smith, J. (1995) Angles on Activin's Absence. Nature 374, 311-312.

Stanier, DYR., Weinstein, BM., Detrich III, HW., Zon, LI. & Fishman, MC. (1995) *cloche*, an Early Acting Zebrafish Gene is Required by Both the Endothelial and Haematopoietic Lineages. Development 121, 3141-3150.

Stephens, L., Sutherland, AE., Klimanskaya, IV., Andrieux, A., Meneses, J., Pedersen, RA. & Damsky, CH. (1995) Deletion of β1 Integrin in Mice Results in Inner Cell Mass Failure and Peri-Implantation Lethality. Genes. Dev. 9, 1883-1895.

Stromblad, S. & Cheresh, DA. (1996) Cell Adhesion and Angiogenesis. Trends in Cell Biology 6, 462-467.

Suri, C., Jones, PF., Patan, S., Bartunkova, S., Maisonpierre, PC, Davis, S., Sato, TN & Yancopoulos, GD. (1996) Requisite Role of Angiopoietin-1, a Ligand for the TIE2 Receptor, During Embryonic Angiogenesis. Cell 87, 1171-1180.

Sutherland, AE., Calarco, PG. & Damsky, CH. (1988) Expression and Function of Cell Surface Extra-Cellular Matrix Receptors in Blastocyst Attatchment and Outgrowth. J. Cell. Biol. 106, 1331-1348.

Sutherland, AE., Calarco, PG. & Damsky, CH. (1993) Developmental Regulation of Integrin Expression at the Time of Implantation in the Mouse Embryo. Development 119, 1175-1186.

Taipale, J., Miyazono, K., Heldin, C-H. & Keski-Oja, J. (1994) Latent Transforming Growth Factor β1 Associates to Fibroblast ECM via Latent TGFβ Binding Protein. J. Cell. Biol. 124, 171-181.

Takahashi, JS., Pinto, LH. & Hotz Vitaterna, M. (1994) Forward and Reverse Approaches to Behaviour in the Mouse. Science 264, 1724-1732.

Tamada, H., McMaster, MT., Flanders, KC., Andrews, GK. Dey, SK. (1990) Cell-Type Specific Expression of TGFβ1 in the Mouse Uterus During the Preimplantation Period. Mol. Endocrinol. 4, 965-972.

ten Dijke, P., Yamashita, H., Sampath, TK., Reddi, AH., Estevez, M., Riddle, DL., Ichijo, H., Heldin, C-H. & Miyazono, K. (1994) Identification of Type 1 Receptors for Osteogenic Protein-1 and Bone Morphogenetic Protein-4. J. Biol. Chem. 269, 16985-16988.

ten Dijke, P., Miyazono, K. & Heldin, C-H. (1996) Signalling via Hetero-Oligomeric Complexes of Type I and Type II Serine/ Threonine Kinase Receptors. Curr. Op. Cell Biol. 8, 139-145.

Thompson, NL., Bazoberry, F., Spier, EH., Casscells, W., Ferrans, VJ., Flanders, KC., Kondaiah, P., Geiser, AG. & Sporn, MB. (1988) TGFβ1 in Acute Myocardial Infarction in Rats. Growth Factors 1, 91-99.

Thompson, NL., Flanders, KC., Smith, JM., Ellingsworth, LR., Roberts, AB. & Sporn, MB. (1989) Expression of TGFβ1 in Specific Cells and Tissues of Adult and Neonatal Mice. J. Cell. Biol. 108, 661-669.

Thomsen, GH., (1996) Xenopus *mothers against deceplentaplegic* is an Embryonic Ventralizing Agent that Acts Downstream of the BMP-2, 4 Receptor . Development

Threadgill. DW., Dlugosz, AA., Hansen, LA., Tennenbaum, T., Lichti, U., Yee, D., LaMantia, C., Mourton, T., Herrup, K., Harris, RC., Barnard, JA., Yuspa, SH., Coffey, RJ. & Magnuson, T. (1995) Targeted Disruption of the Mouse EGF Receptor: Effect of Genetic Background on Mutant Phenotype. Science 269, 230-233.

Treisman, JE., Lai, Z-C. & Rubin, GM. (1995) *shortsighted* acts in the *dpp* pathway in *Drosophila* Eye Development and has Homology to a Mouse TGFβ-Responsive Gene. Development 121, 2835-2845.

Tremml, G. & Bienz, M. (1992) Induction of *labial* Expression in the *Drosophila* Endoderm: Response Elements for *dpp* Signalling and for Autoregulation. Development 116, 447-456.

Tsai, F-Y., Keller, G., Kuo, FC., Weiss, M., Chen, J., Rosenblatt, M., Alt, FW. & Orkin, SH. (1994) An Early Haematopoietic Defect in Mice Lacking the Transcription Factor GATA-2. Nature 371, 221-226.

Tsunawaki, S., Sporn, M., Ding, A.& Nathan, C. (1988) Deactivation of Macrophages by TGFβ. Nature 334, 260-262.

van-Obberghen-Schiling, E., Kondaiah, P., Ludwig, RL., Sporn, MB. & Baker, CC. (1987) Complementary DNA Clone of Bovine TGFβ1. Mol. Endocrinol. 1, 693-698.

Vassali, A., Matzuk, MM., Gardner, HAR., Lee, K-F. & Jaenisch, R. (1994) Activin/ Inhibin βb Subunit Disruption Leads to Defects in Eyelid Formation and Female Reproduction.Genes Dev. 8, 414-427.

Verbeek, MM., Otte-Holler, I., Wesseling, P., Ruiter, DJ. & de Waal, RMW. (1994) Induction of α Smooth- Muscle Actin in Cultured Human Brain Pericytes by TGFβ1. Am. J. Path. 144, 372-382.

Vitaterna, MH., King, DP., Chang, A-M., Kornhauser, JM., Lowrey, PL., McDonald, JD., Dove, WF., Pinto, LH., Turek, FW. & Takahashi, JS. (1994) Mutagenesis and Mapping of a Mouse Gene, *Clock*, Essential for Circadian Behaviour. Science 264, 719-725.

Wahl, SM., Hunt, DA., Wakefield, LM., McCartney-Francis, N., Wahl, LM., Roberts, AB. & Sporn MB. (1987) TGFβ Induces Monocyte Chemotaxis and Growth Factor Production. Proc. Acad. Natl. Sci. USA 84, 5788-5792.

Wang, T., Donahoe, PK.& Zervos, AS. (1994) Specific Interaction of Type I Receptors of the TGFβ Family with the Immunophilin FKBP-12. Science 265, 674-676.

Wang, XF., Lin, HY., Ng-Eaton, E., Downward, J., Lodish, HF.& Weinberg, RA. (1991) Expression, Cloning and Characterisation of the TGFβ Type III Receptor. Cell 67, 797-805.

Watabe, T., Kim, S., Candia, A., Rothbacher, U., Hashimoto, C., Inoue, K. & Cho, KWY. (1995) Molecular Mechanisms of Spemann's Organiser Formation: Conserved Growth factor Synergy between Xenopus and Mouse. Genes Dev. 9, 3038-3050.

Weis-Garcia, F. & Massague, J. (1996) Complementation between Kinase-Defective and Activation-Defective TGFβ Receptors Reveals a Novel Form of Receptor Cooperativity Essential for Signalling. EMBO 15, 276-289.

Weiss, MJ., Keller, G. & Orkin, SH. (1994) Novel Insights into Erythroid Development Revealed Through *in vitro* Differentiation of GATA-1 Embryonic Stem Cells. Genes Dev. 8, 1184-1197.

Weeks, DL. & Melton, DA. (1987) A Maternal mRNA Localised to the Vegetal Hemisphere in Xenopus Eggs Codes for a Growth Factor Related to TGFβ. Proc. Acad. Natl. Sci. USA 51, 861-867.

Wieczorek, Z., Sion, J., Kluczyk, A., Zbozien, R., Stafanowicz, P. & Siemion, IZ. (1995)The Immunomodulatory Diversity of the Proteins of the TGFβ Family. J. Protein. Peptide. Res. 46, 113-118.

Wilt, FH. (1965) Erythropoiesis in the Chick Embryo: The Role of Endoderm. Science 147, 1588-1590.

Wharton, KA., Ray, RP. & Gelbart, WM. (1993) An Activity Gradient of *decaplentaplegic* is Necessary for the Specification of Dorsal Pattern Elements in the *Drosophila* Embryo. Development 117, 807-822.

Winnier, G., Blessing, M., Labosky, PA. & Hogan, BLM. (1995) Bone Morphogenetic Protein 4 is Required for Mesoderm Formation and Patterning in the Mouse. Genes Dev. 9, 2795-2805.

Wolf, YG., Rasmussen, LM., Ruoslahti, E. (1994) Antibodies Against TGFβ1 Supress Intimal Hyperplasia in a Rat Model. J. Clinical Invest. 93, 1172-1178.

Wrana, JL., Attisano, L., Caracomo, J., Zentrella, A., Doody, J., Laiho, M., Wang, X-F. & Massague, J. (1992) TGFβ Signals Through a Heteromeric Protein Kinase Receptor Complex. Cell 71, 1003-1014.

Wrana, JL., Attisano, L., Weiser, R., Ventura, F. & Massague, J. (1994a) Mechanism of Activation of the TGFβ Receptor. Nature 370, 341-347.

Wrana, JL., Tran, H., Attisano, L., Arora, K., Childs, SR, Massague, J. & O' Connor, MB. (1994b) Two Distinct Transmembrane Serine/ Threonine Kinases form an Activin Receptor Complex. Mol. Cell. Biol. 14, 944-950.

Yang, JT, Rayburn, H. & Hynes, RO. (1993) Embryonic Mesodermal Defects in α5 Integrin Deficient Mice. Development 119, 1093-1105.

Yang, JT., Rayburn, H. & Hynes, RO. (1995) Cell Adhesion Events Mediated by α4 Integrins are Essential in Placental and Cardiac Development. Development 121, 549-560.

Zhang, H. & Bradley, A.(1996) Mice Deficient in BMP-2 are Non-Viable and have Defects in Amnion/ Chorion and Cardiac Development. Development 122, 2977-2986.

Zhang, H. Shaw, ARE., Mak, A. & Letarte, M. (1996) Endoglin is a Component of the TGFβ Receptor Complex of Human Pre-B Leukemic Cells. J. Immol. 156, 565-573.

Zhang, Y., Feng, X-H., Wu, R-Y. & Derynck, R. (1996) Receptor Associated *mad* Homologues as Effectors of the TGFβ Response. Nature 383, 168-172.

Zhou, X., Sasaki, H., Lowe, E., Hogan, BML. & Kuehn, MR. (1993) *nodal* is a Novel TGFβ -Like Gene Expressed in the Mouse Node During Gastrulation. Nature 361, 543-547.

Zhou, G., Sechrist, GL., Periyasamy, S., Brattain, MG., Mulder, KM. (1995) Transforming Growth Factor Beta Isoform-Specific Differences with Type I and II Receptors. Cancer Res. 55, 2056-2062.

Zsebo, KM., Wypych, IK., McNiece, IK., Lu, HS., Smith, KA., Karkare, SB., Sachdev, RK., Yuschenkoff, VN., Birkett, NC., Williams, LR., Satyagal, VN., Tung, W., Bosselman, RA., Mendiaz, EA. & Langley, KE. (1990) Identification, Purification

and Biological Characterisation of Haematopoietic Stem Cell Factor from Buffalo Rat Liver-Conditioned Medium. Cell 63, 195-201.

APPENDIX 1.

Graphs 6a-10b - Morphological Scores of TGFβ1+/- Intercross Litters at 9.5dpc.

At 9.5dpc >100 TGFβ1 knockout conceptuses from the NIH, C57, 129 and reciprocal F1 genetic backgrounds were dissected free from the maternal tissue, morphologically scored and genotyped for TGFβ1 by PCR of genomic DNA. The morphological scoring was based on two scores: Score 1 was an additive score giving a precise developmental staging of the conceptus using landmarks, whereas score 2 was a quantitative and qualitative assessment of the specific abnormalities suffered by the conceptus. Both scores, for each TGFβ1 genotypic class, on each genetic background studied are presented in the following box and whisker graphs. The data is laid out as follows; the box represents the 1st to 3rd quartiles, the line in the centre of the box is the median value and the whiskers cover the remaining data. Stars represent individual pieces of outlying data.

It is clear that on each genetic background score 1 does not vary greatly between genotypic class or genetic backgrounds. However, the magnitiude of score 2 is clearly related to the genotype of the concepus; i.e. little or no defects were seen in TGFβ1+/+ conceptuses; any abnormalities observed were typically non-specific, for example - slight developmental retardation rather than defects characteristic of the TGFβ1 knockout mid-gestation phenotype. A large range of severity of defects were observed in TGFβ1+/- conceptuses. This is in concordance with the disparity of onset and severity of the mid-gestation phenotype in the heterozygotes. As expected, on each genetic background, the largest proportion of severe defects befell the TGFβ1-/- conceptuses. These defects mainly comprised abnormalities of the extra-embryonic vasculature and haematopoiesis.

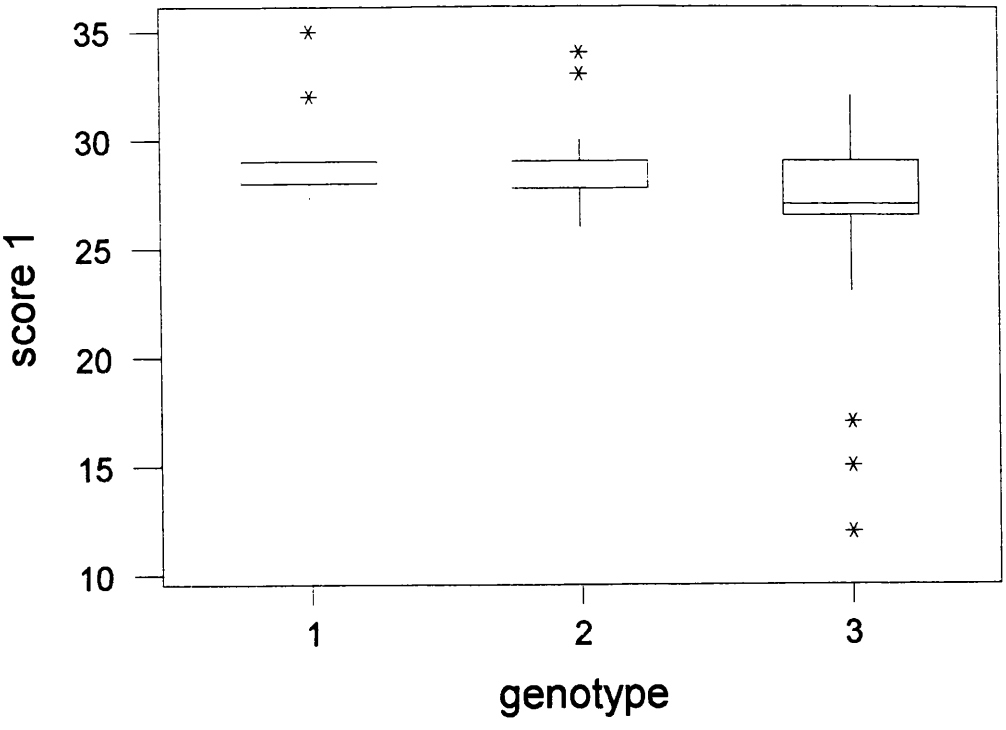

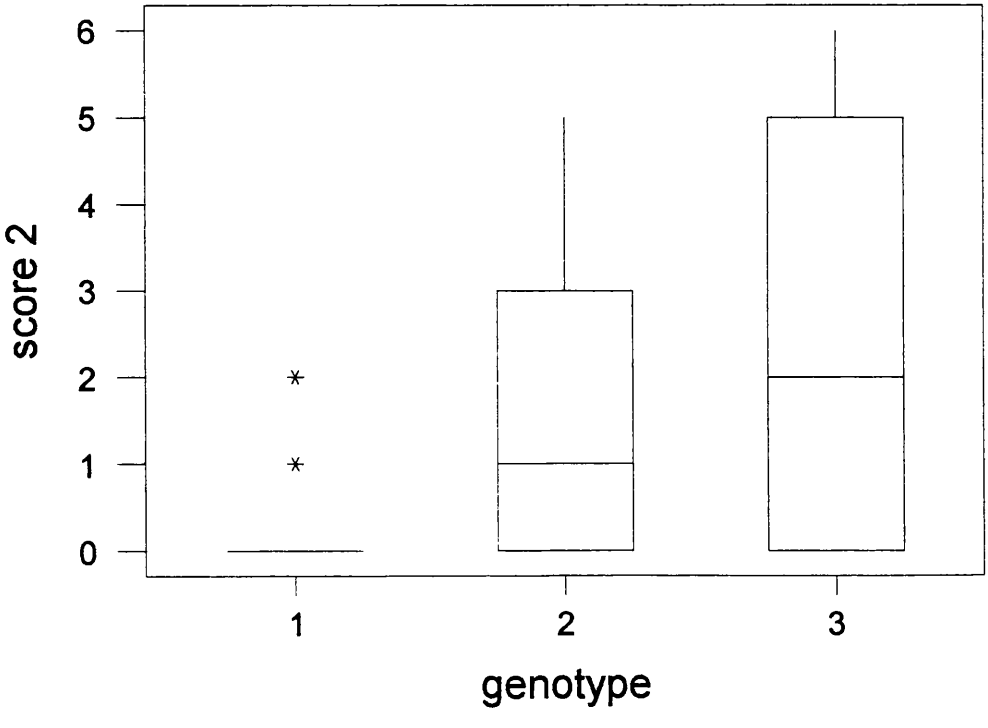

Graphs 6a and b. Box and Whisker Plots of Morphological Scores 1 and 2 in NIH Conceptuses of Each Genotypic Class at 9.5dpc.

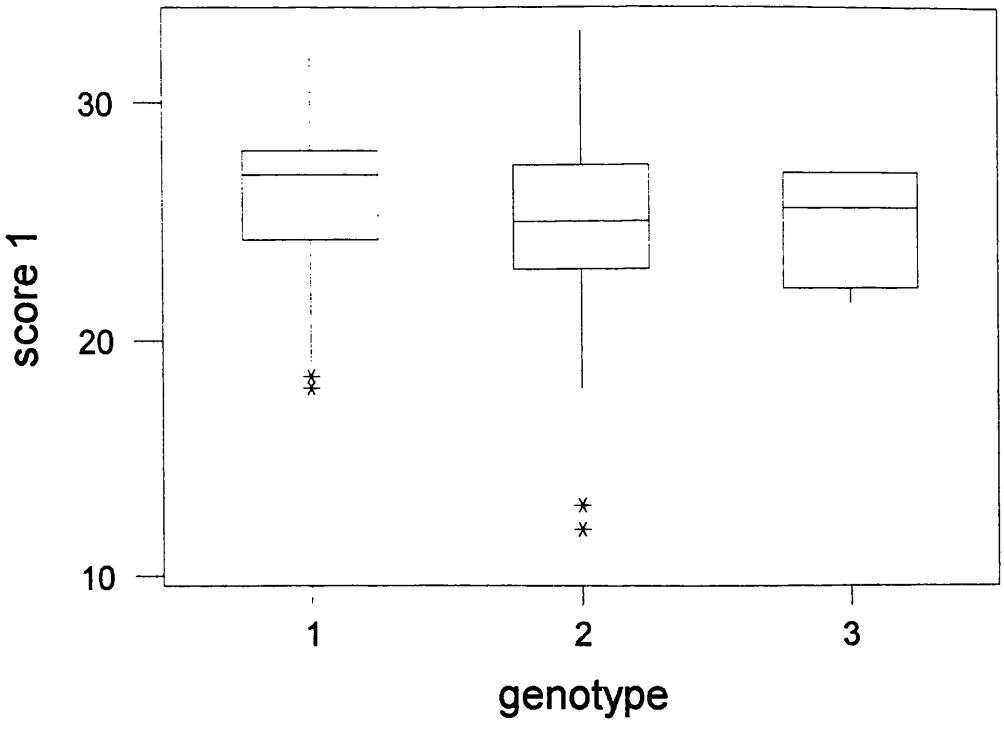

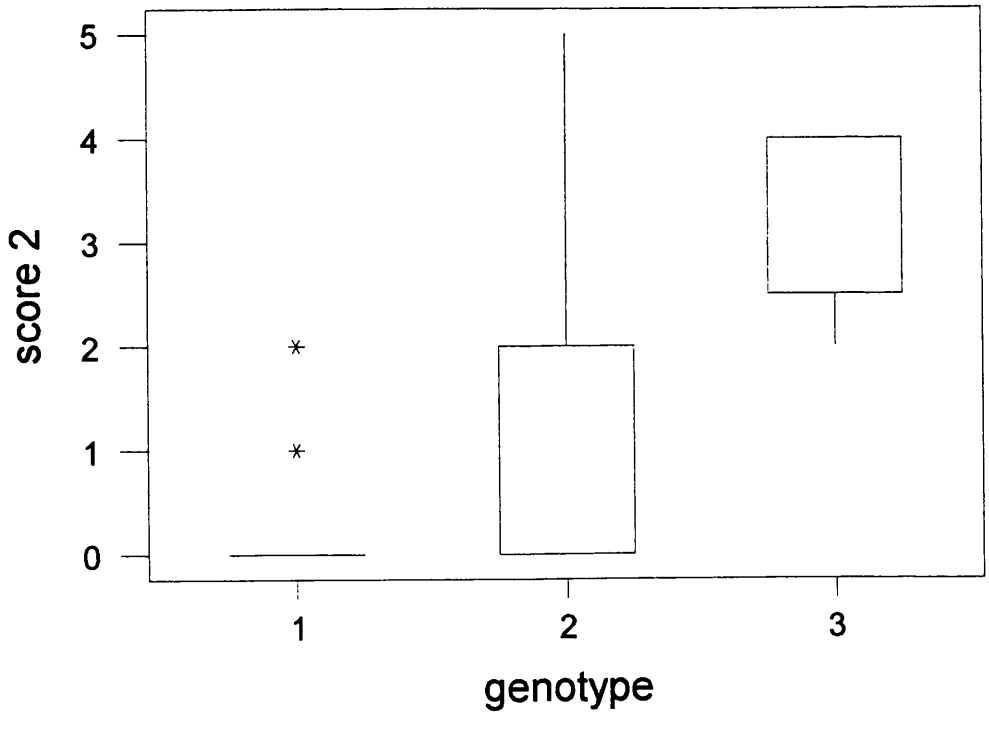

Graphs 7a and b. Box and Whisker Plots of Morphological Scores 1 and 2 in C57 Conceptuses of Each Genotypic Class at 9.5dpc.

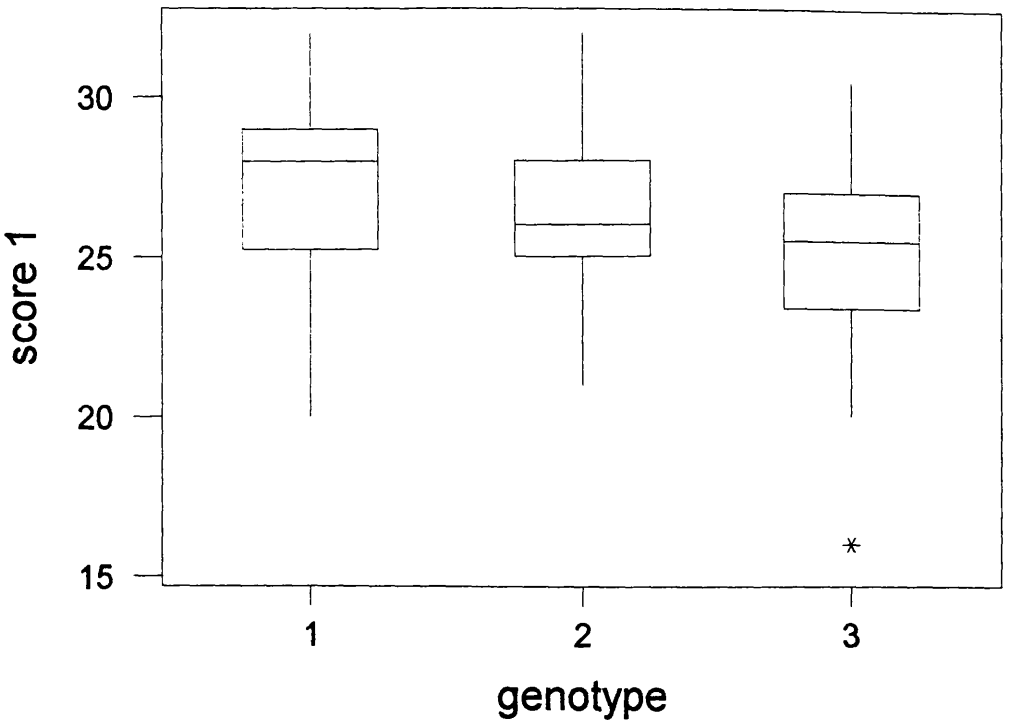

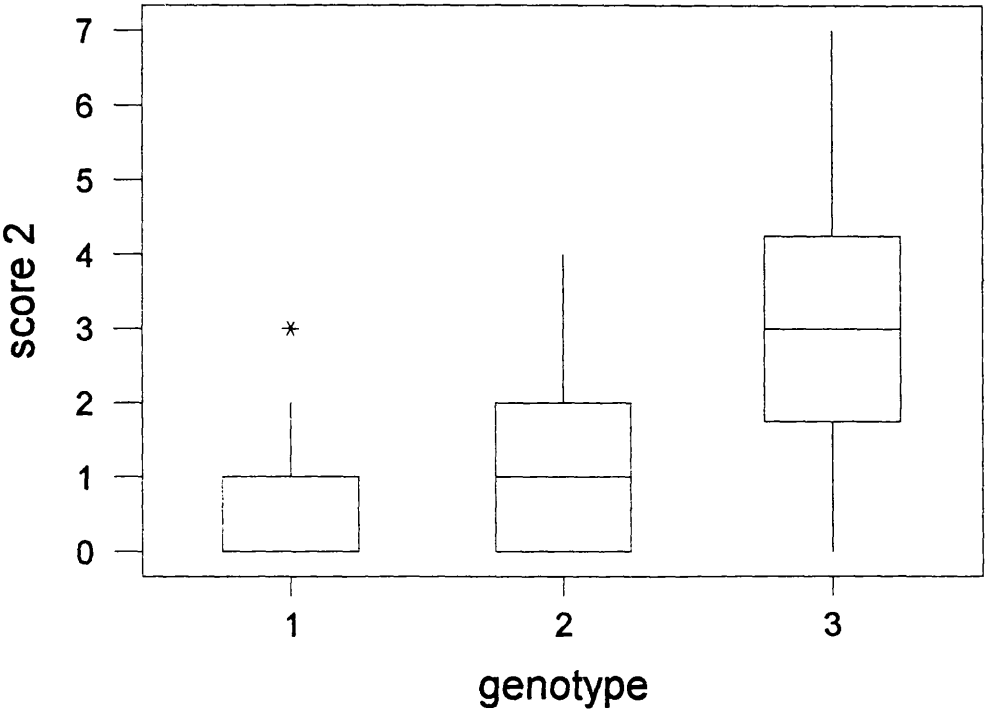

Graphs 8a and b. Box and Whisker Plots of Morphological Scores 1 and 2 in 129 Conceptuses of Each Genotypic Class at 9.5dpc.

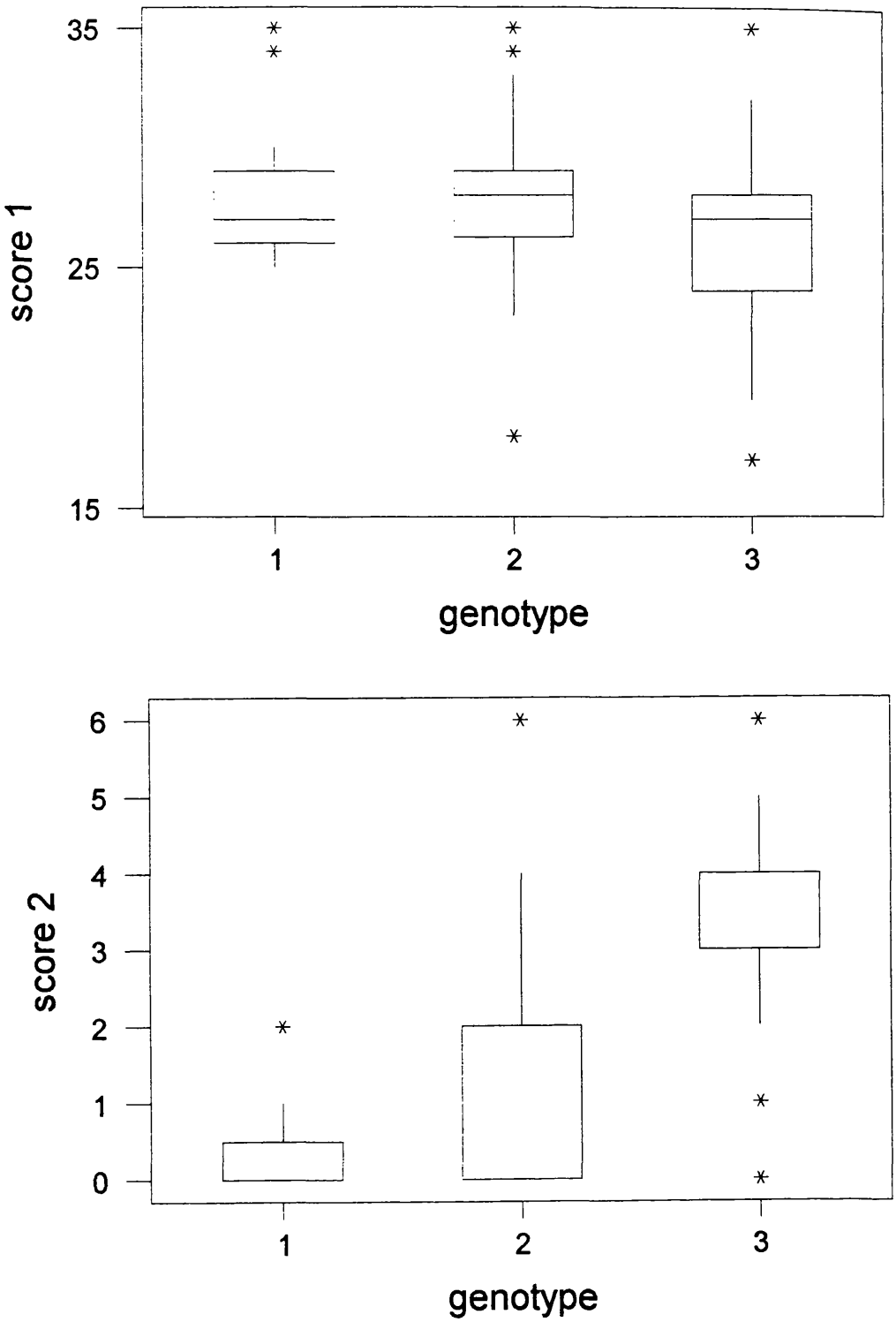

Graphs 9a and b. Box and Whisker Plots of Morphological Scores 1 and 2 in NIH x C57 Conceptuses of Each Genotypic Class at 9.5dpc.

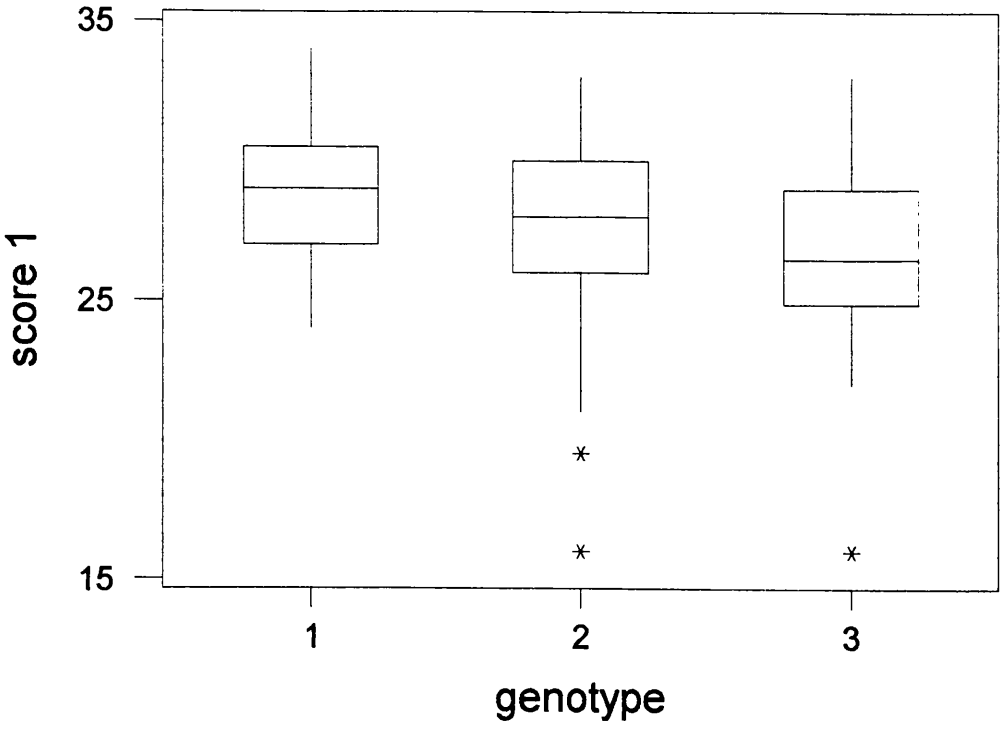

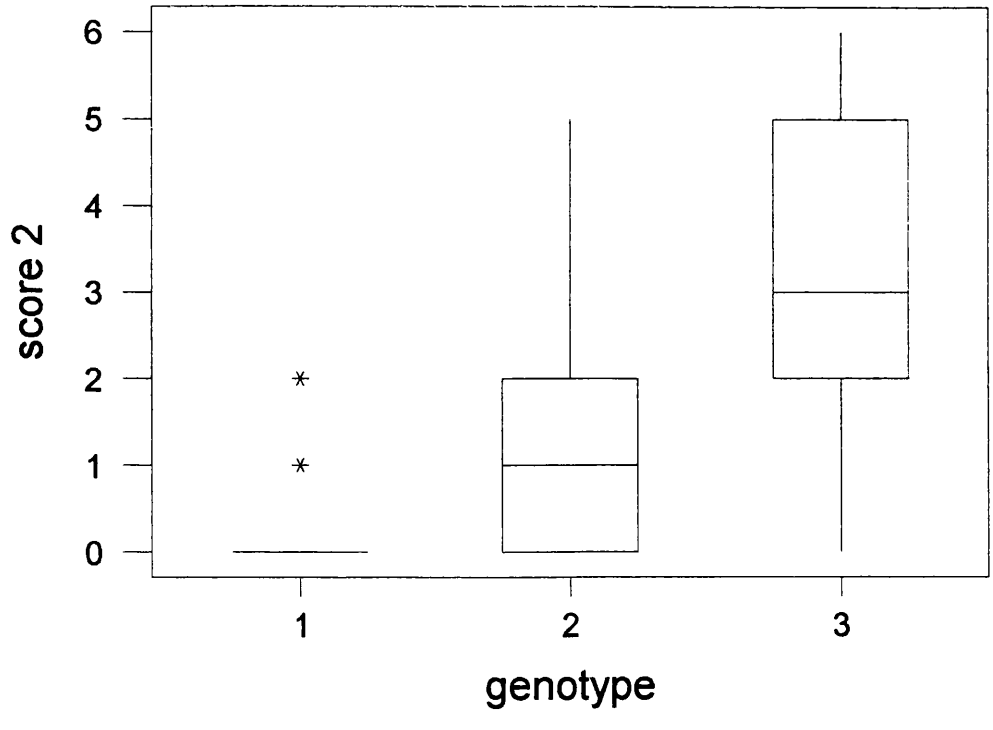

Graphs 10a and b. Box and Whisker Plots of Morphological Scores 1 and 2 in C57 x NIH Conceptuses of Each Genotypic Class at 9.5dpc.